BEHAVIOR OF CONCRETE SPECIMENS REINFORCED WITH COMPOSITE MATERIALS – LABORATORY STUDY

Final Report

SPR 387

Oregon Department of Transportation

BEHAVIOR OF CONCRETE SPECIMENS REINFORCED WITH COMPOSITE MATERIALS – LABORATORY STUDY

Final Report

SPR 387

by

Damian I. Kachlakev, PhD , Bryan K. Green, and William A. Barnes
Department of Civil, Construction and Environmental Engineering
Oregon State University
Corvallis, Oregon 97331

for

The Oregon Department of Transportation
Research Group
200 Hawthorne Ave. SE, Suite B-240
Salem, Oregon 97301-5192

and

Federal Highway Administration
400 Seventh Street SW
Washington D.C. 20590

February 2000

1. Report No.	2. Government Accession No.	3. Recipient's Catalog No.
FHWA-OR-RD-00-10		

4. Title and Subtitle	5. Report Date
Behavior of Concrete Specimens Reinforced with Composite Materials – Laboratory Study	February 2000
	6. Performing Organization Code

7. Author(s)	8. Performing Organization Report No.
Damian I. Kachlakev, PhD , Bryan K. Green, and William A. Barnes Department of Civil, Construction and Environmental Engineering Oregon State University, Corvallis, OR 97331	

9. Performing Organization Name and Address	10. Work Unit No. (TRAIS)
Oregon Department of Transportation Research Group 200 Hawthorne SE, Suite B-240 Salem, Oregon 97301-5192	11. Contract or Grant No. SPR 387

12. Sponsoring Agency Name and Address	13. Type of Report and Period Covered
Oregon Department of Transportation Research Group 200 Hawthorne SE, Suite B-240 Salem, Oregon 97301-5192 and Federal Highway Administration 400 Seventh Street SW Washington, D.C. 20590	Final Report
	14. Sponsoring Agency Code

15. Supplementary Notes

16. Abstract

The world's infrastructure continues to age and deteriorate. Forty percent of the nation's 575,000 bridges are structurally deficient or structurally obsolete, and 25 percent are over 50 years old. Many older bridges were designed for lower traffic volumes and lighter loads than what are common today. External post-tensioning and epoxy-bonded steel plates are the strategies commonly used to upgrade deficient structures. However, fiber reinforced polymer (FRP) composites are also starting to be used for strengthening.

The main objective of this study was to investigate the interaction between FRP composite and concrete by addressing the most important variables in terms of FRP properties. Type of fibers, thickness of the laminates, fiber orientation and FRP strengthening configuration were studied while keeping the type of concrete, steel reinforcement and geometry of the samples constant.

The intent of the data collection and analysis was to gather extensive information on the performance of FRP-reinforced concrete, rather than to investigate the structural behavior of FRP-reinforced members. Appearance of first crack on the concrete, ultimate loads and the corresponding strains and deflection, and the failure modes were of main interest.

The FRP systems included in this study were most of those known to be currently available. In addition, two customized FRP systems were developed using only domestically available materials. All systems were tested under nearly identical conditions with respect to concrete strength, specimen dimensions, reinforcement, surface preparation, test methods, and analysis.

The ultimate strength increase at failure ranged from 18 to 545 percent, depending upon the FRP-application scheme. The specimens showed no significant increase in stiffness prior to initial cracking of the concrete. The FRP-strengthened specimens exhibited greater deflections prior to initial cracking of the concrete. Following initial cracking, the behavior of the specimens was mostly influenced by the properties of the FRP laminate. The results showed that the increase of the load-carrying capacity and the performance of the FRP-reinforced beams were strongly dependent on the FRP configuration. The failure modes showed dependency on the stiffness and strength of the FRP reinforcement and scheme used to strengthen them. The study suggested that the effectiveness of the FRP composite decreases as the rigidity (elastic modulus x FRP thickness) of the laminates increases.

17. Key Words	18. Distribution Statement
fiber reinforced polymers, FRP, composites, concrete strengthening, concrete beam behavior, cracking	Copies available from NTIS

19. Security Classification (of this report)	20. Security Classification (of this page)	21. No. of Pages	22. Price
unclassified	unclassified	180	

Technical Report Form DOT F 1700.7 (8-72) Reproduction of completed page authorized

SI* (MODERN METRIC) CONVERSION FACTORS

APPROXIMATE CONVERSIONS TO SI UNITS

Symbol	When You Know	Multiply By	To Find	Symbol
		LENGTH		
In	Inches	25.4	millimeters	mm
Ft	Feet	0.305	meters	m
yd	Yards	0.914	meters	m
mi	Miles	1.61	kilometers	km
		AREA		
in^2	square inches	645.2	millimeters squared	mm^2
ft^2	square feet	0.093	meters squared	m^2
yd^2	square yards	0.836	meters squared	m^2
ac	Acres	0.405	hectares	ha
mi^2	square miles	2.59	kilometers squared	km^2
		VOLUME		
fl oz	fluid ounces	29.57	milliliters	mL
gal	gallons	3.785	liters	L
ft^3	cubic feet	0.028	meters cubed	m^3
yd^3	cubic yards	0.765	meters cubed	m^3
NOTE: Volumes greater than 1000 L shall be shown in m^3.				
		MASS		
oz	ounces	28.35	grams	g
lb	pounds	0.454	kilograms	kg
T	short tons (2000 lb)	0.907	megagrams	Mg
		TEMPERATURE (exact)		
°F	Fahrenheit temperature	5(F-32)/9	Celsius temperature	°C

APPROXIMATE CONVERSIONS FROM SI UNITS

Symbol	When You Know	Multiply By	To Find	Symbol
		LENGTH		
mm	millimeters	0.039	inches	in
m	meters	3.28	feet	ft
m	meters	1.09	yards	yd
km	kilometers	0.621	miles	mi
		AREA		
mm^2	millimeters squared	0.0016	square inches	in^2
m^2	meters squared	10.764	square feet	ft^2
ha	hectares	2.47	acres	ac
km^2	kilometers squared	0.386	square miles	mi^2
		VOLUME		
mL	milliliters	0.034	fluid ounces	fl oz
L	liters	0.264	gallons	gal
m^3	meters cubed	35.315	cubic feet	ft^3
m^3	meters cubed	1.308	cubic yards	yd^3
		MASS		
g	grams	0.035	ounces	oz
kg	kilograms	2.205	pounds	lb
Mg	megagrams	1.102	short tons (2000 lb)	T
		TEMPERATURE (exact)		
°C	Celsius temperature	1.8 + 32	Fahrenheit	°F

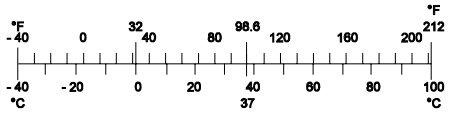

***** SI is the symbol for the International System of Measurement (4-7-94 jbp)

ACKNOWLEDGMENTS

The authors wish to express their appreciation to Mr. Marty Laylor, Mr. Steven Soltesz, Project Managers at the Research Unit of the Oregon Department of Transportation, Salem, Oregon for their valuable suggestions and many contributions to this project. We would like to thank Dr. Barnie Jones, Research Manager at the Research Unit of the Oregon Department of Transportation for his support and encouragement during this study. The authors also gratefully acknowledge the rest of the technical advisory committee for their direction and review of this work.

The authors wish to extend their special gratitude to Dr. Ali Ganjelou, Sumitomo Corporation of America; Mr. Kensuke Yagi, Mitsubishi Chemical Corporation, Japan; Dr. Howard Kliger, Master Builders; Mr. Edward Fyfe and Mr. Duane Gee, Fyfe Corporation, LLC; Mr. Joe Mockapetris, Sika Corporation; Mrs. Jaime Mack, Hexcel Ventures; Mr. Richard Pauer, formerly Reichhold Chemicals, Inc.; Mr. Theodore Humphrey, formerly Owens Corning World Headquarters; Mr. John Walling, Owens Corning; Mr. Gordon Brown, Clark Schwebel Tech-Fab Company; and Mr. Thomas Ohnstad, Composite Retrofit Systems, LLC for donations of FRP materials and technical support, without which this study would not have been possible.

The authors would like to thank Dr. Solomon Yim and Dr. Thomas Miller, professors at the Civil, Construction and Environmental Engineering Department at the Oregon State University for the many valuable suggestions during this study. In addition, we would like to acknowledge Mr. Andy Brickman for his valuable help and time during the experimental part of this research.

DISCLAIMER

BEHAVIOR OF CONCRETE SPECIMENS REINFORCED WITH COMPOSITE MATERIALS – LABORATORY STUDY

TABLE OF CONTENTS

APPENDICES

APPENDIX A: BEAM DESIGNATION LEGEND
APPENDIX B: TYPICAL FAILURE MODES

List of Tables

List of Figures

1.0 INTRODUCTION

1.1 BACKGROUND

The world's infrastructure continues to age and deteriorate. Many bridges across the United States are deteriorating due to problems associated with reinforced concrete. Factors contributing to deterioration include environmental effects, de-icing salts, seismic activity, and increases in both the number and weight of vehicles. Forty percent of the Nation's 575,000 bridges are structurally deficient or structurally obsolete, and 25 percent are over 50 years old (*Marshall and Busel 1996*). Approximately 75 percent of the bridges in Oregon are over 50 years old. Many older bridges were designed for lower traffic volumes and lighter loads than those which are common today; hence they are under-designed for current or projected traffic needs. Therefore, rehabilitation to original standards will not bring them up to the current standards. Additional strengthening must be considered.

The retrofit and strengthening of existing, reinforced concrete structures has become one of the most important challenges in civil engineering. Civil engineers are frequently faced with the problems associated with rehabilitation and structural enhancement of existing structures. The need for such actions are due to increased traffic loads, corrosion of the reinforcing steel and deterioration of the concrete.

Restoring the structural integrity and enhancing the strength and stiffness of older structures is a major challenge. The selection of proper retrofit strategies is a complex task. Until recently, external post-tensioning and epoxy-bonded steel plates were the two strategies commonly used to upgrade deficient structures.

External post-tensioning has been used successfully to increase the strength of girders in bridges and buildings *(Klaiber et al. 1982; Saadatmanesh et al. 1989).* This method, however, has several practical difficulties such as providing anchorage for the post-tensioning strands, maintaining the lateral stability of the girders during post-tensioning, and protecting the strands against corrosion *(Saadatmanesh and Ehsani 1996).* Additionally, post-tensioning requires considerable force to stress the concrete effectively, and may significantly reduce overhead clearance *(Dussek 1980).*

Epoxy-bonded steel plates have been used successfully in Europe, Japan, Australia, and South Africa for the last 25 years to increase the load-carrying capacity of existing reinforced concrete bridges *(Dussek 1980; Chan and Tan 1996; Yong et al. 1996).* This strengthening technique has been found economical and efficient to apply. However, its application in the United States has been extremely rare *(Saadatmanesh et al. 1996).*

Fiber Reinforced Polymer (FRP) composites are being researched worldwide as a promising solution for rehabilitation of aging facilities. FRP composites, initially developed and used in the defense and aerospace industries, offer unique advantages where conventional materials cannot provide satisfactory service. The high strength-to-weight ratio, excellent resistance to corrosion, durability, relative ease of application, minimum disruption of traffic during repairs, and low maintenance requirements make the FRP composites an excellent candidate for rehabilitation and strengthening of reinforced concrete structures.

Three approaches for strengthening concrete structures with FRP composites have been developed:

1. Pre-impregnation (prepreg) materials are dry sheets of fiber and resin that are cold laminated onto the concrete structure. A resin-fiber sheet-resin lay-up technique is used to build up the desired thickness of the composite reinforcement.

2. With wet lay-up systems, the fiber sheet is impregnated with the resin either immediately before applying it to the structure or as part of the placement procedure when it put on the structure. A variation of the wet lay-up technique used on cylindrical columns wraps the column with a continuous, resin-wetted fiber.

3. In pultruded systems, a fully cured FRP composite preform is epoxy-bonded to the concrete structure. All of the approaches can be applied to conventional reinforced or prestressed concrete elements to take advantage of the high strength offered by FRP materials.

FRP composites have the potential for tremendous impact on the construction industry internationally. Recent earthquakes in Southern California demonstrated the need for civil engineering structures with enhanced seismic protection. Applications of composite material systems to repair and/or upgrade structures may save billions of dollars, as well as many human lives.

Many concrete bridge columns designed before the new seismic design provisions were adopted in 1970 have low shear strength and low flexural strength and ductility. These problems, combined with environmental deterioration, have contributed to catastrophic bridge failures in resent earthquakes *(Cercone and Korff 1997).* Post earthquake analysis of the seven freeway bridges that collapsed during the Northridge earthquake revealed that they could have survived if they had been retrofitted to withstand seismic forces.

The work of some researchers has indicated that increasing the confinement in the potential plastic hinge regions of the column will increase the apparent concrete compressive strength and ductility *(Saadatmanesh and Ehsani 1994).* Therefore, strengthening techniques typically involve methods for increasing the confining forces either in the potential plastic hinge regions or over the entire column.

An unwrapped concrete column loaded in compression will fail by developing a crack network and shear cones in the column. In order to visualize the failure mechanism associated with confined concrete columns, it is important to think of the wrapped column as a system of

concrete cores loaded in compression and concentrically wrapped with a tensile-loaded jacket. The existence of the jacket, which provides a high degree of confinement, can prevent or delay the initiation and propagation of the internal cracking mechanism.

Until recently, the steel jacketing of bridge columns was the only widely approved retrofitting method. This technique is effective in preventing columns from collapsing due to shear or flexural failure. However, installation is labor intensive, time consuming, and requires heavy equipment to handle the steel. Another problem is that the installation requirements rather than the confinement requirements determine the thickness and weight of the steel jackets. In order to prevent buckling under its own weight during lifting, the steel jacket has to be extremely heavy and strong. Thus, the resulting retrofit projects are typically expensive and use an excessive amount of material *(Cercone and Korff 1997).*

Advanced composite materials have unique mechanical and durability characteristics that complement column strengthening. Research by the Advanced Composites Technology Transfer Consortium (ACTT) at the University of California, San Diego (UCSD) has shown that seismically deficient bridge columns can be wrapped with FRP materials in an automated fashion, further reducing the time requirements as compared to equivalent steel jacket installations. Recent developments in automated manufacturing and application processes for FRP column wrapping has shown that this type of structural enhancement is cost effective *(Seible, et al. 1995).*

While the advantages and limitations of conventional materials are well established, the advanced composite science and industry must clearly answer many questions such as: What is a composite? How much will it cost? How long will it last? Properly designed and manufactured composite material systems offer superior structural performance while being compatible with existing construction industry practices. Consensus is needed on standards and design guidelines, so that composite materials can enter the construction market on a large scale in the near future *(McConnell 1995).* Most importantly, selection and application of FRP materials for repair of structures should be used where the benefits of composites can be best realized.

1.2 SCOPE AND OBJECTIVES

While the advantages and limitations of conventional materials are well established, the performance of FRP composites in civil engineering applications needs further investigation. Properly designed and manufactured composite systems can provide superior structural enhancement while complementing existing construction industry practices.

Unlike conventional materials, FRP composite performance depends on the orientation of the fibers. Selection and application schemes for structural enhancement must maximize the benefits that can be realized with composites without compromising the design of the structure.

The objectives of this research project were:

1) Demonstrate the effectiveness of FRP reinforcement on small beams and columns.

2) Determine the effect of fiber type, fiber orientation and composite thickness on the flexure and shear response for the small beams.

3) Determine the effect of fiber type and thickness on the compressive strength of FRP reinforced concrete cylinders.

4) Develop recommendations for strengthening concrete beams using FRP.

5) Develop a database that will assist in future model verification.

The FRP systems included in this study were most of those known to be currently available. In addition, two customized FRP systems, one based on glass fibers and one based on carbon fibers, were developed using only domestically available materials. All systems were tested under nearly identical conditions with respect to concrete strength, specimen dimensions, reinforcement, surface preparation, test methods, and analysis. This type of comparative study had never been done by any academic or research institution in the world.

1.3 LITERATURE REVIEW

While the use of fiber reinforced polymer composites in civil engineering is a fairly new topic, a significant amount of research has been performed in this area. Testing performed thus far shows that significant strength and stiffness gains can be achieved both for flexural strengthening (*Challal et al. 1998; Demers et al. 1996; Hutchinson and Rahimi 1996; Limberger and Vielhaber 1996; Rostasy et al. 1992; Saadatmanesh and Ehsani 1991; Sharif et al. 1994; Swamy et al. 1996; Triantafillou and Plevris 1991*), and shear strengthening (*Al-Sulaimani et al. 1994; Chajes et al. 1995; Challal et al. 1998, Dolan et al. 1992; Limberger and Vielhaber 1996; Sato et al. 1996; Triantafillou 1998*). Most of these studies used either glass (GFRP) or carbon (CFRP) reinforcement; however, research has shown that similar results can be achieved with aramid FRP composites as well (*Demers et al. 1996; Dolan et al. 1992*)

It is generally assumed that gains in strength and stiffness are usually associated with a decrease in ductility. Additional research has shown that GFRP reinforced concrete can actually behave with more ductility than regular reinforced concrete (*Swamy et al. 1996*). This study showed that, in addition to strength and stiffness, the strain at failure was also higher.

Several researchers have come up with techniques for attempting to predict flexural capacities and failure modes for FRP reinforced structural elements. Results of research performed by Hamid Saadatmanesh and Mohammed Ehsani (*1991*) suggested that reasonably accurate strength predictions of FRP reinforced beams could be made using simple force equilibrium equations. Work done by Thanasis Triantafillou and Nikolaos Plevris (*1991*) indicated that the failure mode of FRP reinforced beams was highly influenced by the reinforcement ratios of the FRP and steel. Their research also offers equations for strength based on the various modes of FRP reinforced beam failure.

Other research has identified a relationship between FRP reinforced beam stiffness and the strain that can be achieved in the composite (*Kachlakev et al. 1998; Rostasy et al. 1992*).

Practices of strength predictions recommended by the Canadian Standards Association are presented in another research effort (*Chaalal et al. 1998*). This work suggests that the maximum allowable strain in the FRP composite be limited to fifty percent of the strain at failure of the composite.

As with flexural strength predictions, there are nearly as many methods for shear prediction as there are researchers in the area. Methods for determining shear capacity of FRP reinforced concrete use three main variables, concrete contribution (V_c), steel stirrup contribution (V_s), and FRP contribution (V_{frp}). The first two (V_c and V_s) can be treated in a straightforward manner using common equations such as those suggested by the ACI. V_{frp} is the confounding variable for shear design with composites.

Shear design was addressed by Al-Sulaimani, et al. (*1994*). Their test results suggested that the maximum shear stresses be limited to 3.5 MPa. This was suggested since this appeared to be the maximum shear stress that could be developed in the FRP-concrete interface without plate separation.

Another researcher reported that a limiting vertical strain of 0.5% in the FRP should be used in predicting the shear capacity of composite strengthened reinforced concrete elements (*Chajes et al. 1995*). This assumed that a glass fiber fabric with a $0^o/90^o$ fiber orientation with respect to the longitudinal axis was used as the shear reinforcement.

Research that is more recent has indicated that FRP stiffness may be used to limit the strain that can be developed in the FRP composite (*Kachlakev et al. 1998; Triantafillou 1998*). Triantafillou's work also used an empirical formula to suggest a maximum strain value that can be developed in the FRP material.

Perhaps the most accurate method of predicting strength of FRP reinforced beams, both flexural and shear, is through the use of finite element modeling programs as suggested by some researchers (*Hutchinson and Rahimi 1996*).

A critical factor for both flexural and shear capacity design is the adhesion between the concrete and the composite. For shear reinforced beams, the primary mode of failure is not cohesive failure in the laminate or concrete, but adhesive failure between the composite and the concrete. Research has shown that this occurs most often with relatively thick, stiff laminates (*Kachlakev et al. 1998; Sato et al. 1996*).

The work of Triantafillou and Plevris (*1991*) addresses interfacial stress issues. Shear research by Dolan et al (*1992*) on beams with no surface preparation showed that adhesive failure was a major problem. The work of Finch, et al (*1995*), suggests that proper surface preparation and priming results in sufficient adhesion to fully develop the fiber elongation. Other research has shown that through the use of proper surface preparation or some type of anchoring system, adequate development of the FRP reinforcement can occur without debonding (*Juvandes et al. 1998*). Blaschko et al. (*1998*) studied the different modes of bond failures, especially the most common failure mechanisms.

To insure proper bonding of FRP materials to concrete surfaces, some researchers suggest non-destructive testing techniques as a means of quality control for FRP reinforcement (*Limberger and Vielhaber 1996*).

2.0 SAMPLE PREPARATION, INSTRUMENTATION, AND TEST PROCEDURE

2.1 BEAM SPECIMEN FABRICATION

Two hundred fifty six 15 cm x 15 cm x 53 cm (6 in. x 6 in. x 21 in.) reinforced concrete specimens were fabricated for the study. Molds for the specimens were made out of plywood and steel plates. One number 3 (3/8 inch diameter), grade 40 rebar was centered 51 mm (2 in.) from the bottom along the longitudinal axis of each mold. The rebar sections extended to within 38 mm (1.5 in.) of each end and were held in place with 51 mm (2 in.) concrete spacer blocks, Figure 2.1.

The terms "beam", "specimen", and "sample" are used interchangeably in this report. The term "beam" complies with the ASTM C78-84, according to which the specimens were tested. The term "beam" as used in this study does not comply with the ACI defined ratios of beam height and span. As previously mentioned, this study intended to investigate the performance of various FRP strengthening systems, externally bonded to concrete, under similar conditions, rather than to explain the structural behavior of FRP-reinforced members.

Ready-mix concrete with a 28-day design compressive strength of 32 MPa was poured into each mold, which were subsequently vibrated and finished. The specimens were covered with plastic sheeting for one day and then placed in a water bath to cure for at least 28 days in accordance with ASTM C192.

In order to document the compressive strength of the concrete, six standard cylinders were tested at the time of the beam tests. The results ranged from 27 MPa to 34 MPa, in good agreement with the nominal strength.

Figure 2.1: Molds used for preparation of reinforced concrete beam specimens.

All specimens were sand blasted on three longitudinal faces to prepare the surface for application of FRP laminates. Ten of the specimens were used as control specimens and tested without FRP reinforcement. The composite application procedures are discussed in Chapter 3 of this report.

2.2 BEAM STRENGTHENING SCHEMES

A total of 241 specimens were strengthened with FRP composites using 80 different sets of reinforcement conditions as shown in Table 2.1. In the table F refers to flexural strengthening and S refers to shear strengthening. The orientation of the shear strengthening fibers is in parentheses following each S. The 45^o orientation was in the expected direction of the maximum principal strain that would result from the loading configuration used in the tests. For the 90^o orientation, some beams had composite that extended across the middle portion of the shear faces while other beams had no reinforcement in this area. This difference was considered insignificant because third-point loading does not produce macro shear stresses in the middle third of the beam.

Table 2.1: Strengthening schemes for this study

SIKA CARBODUR - Nominal thickness 1.2 mm (0.047 inches)				
Type of Retrofit	**No. of Plies**	**Orientation**	**No. of specimens**	**Application**
Flexure	1	0	3	CFRP on the tensile face only
Shear	1	0	3	CFRP on each side of the beam
Total			6	

SIKA CARBODUR/HEXCEL - Nominal thickness 1.2 mm (0.047 inches)				
Type of Retrofit	**No. of Plies**	**Orientation**	**No. of specimens**	**Application**
F + S(45)	1	0- F / 45 - S	5	Combination of Sika and Hexcel GFRP on face and sides
F + S(90)	1	0- F / 90 - S	3	Combination of Sika and Hexcel CFRP on face and sides
F + S(90)	2	0- F / 90 - S	3	
Total			11	

HEX-WRAP 103 CFRP- Nominal thickness 1 mm (0.040 inches)				
Type of Retrofit	**No. of Plies**	**Orientation**	**No. of specimens**	**Application**
Flexure	1	0	3	CFRP on the tensile face only
Flexure	2	0	3	
F + S(90)	1	0- F / 90 - S	3	CFRP on the tensile face and sides
F + S(90)	2	0- F / 90 - S	3	
Total			12	

Table 2.1: Strengthening schemes for this study (continued)

Replark 30 - Nominal thickness 0.17 mm (0.0066 inches)

Type of Retrofit	No. of Plies	Orientation	No. of specimens	Application
Flexure	1	0	3	CFRP on the Tensile Face Only
Flexure	2	0	3	
Flexure	3	0	3	
Shear	1	90	3	CFRP on Each Side of the Beam
Shear	2	90	3	
Shear	3	90	3	
Shear	1	45	3	CFRP on Each Side of the Beam/Crossed on the face
Shear	2	45	3	
Shear	3	45	3	
F + S(90)	1	0- F / 90 - S	3	CFRP on the Bottom and Each Side of the Beam
F + S(90)	2	0- F / 90 - S	3	
F + S(90)	3	0- F / 90 - S	3	
Total			36	

MBrace Cl-30 - Nominal thickness 1.65 mm (0.065 inches)

Type of Retrofit	No. of Plies	Orientation	No. of specimens	Application
Flexure	1	0	3	CFRP on the Tensile Face Only
Flexure	2	0	3	
Flexure	3	0	3	
F + S(90)	1	0- F / 90 - S	3	CFRP on the Bottom and Each Side of the Beam
F + S(90)	2	0- F / 90 - S	3	
F + S(90)	3	0- F / 90 - S	3	
Total			18	

MBrace GE-30 - Nominal thickness 1.65 mm (0.065 inches)

Type of Retrofit	No. of Plies	Orientation	No. of specimens	Application
Flexure	1	0	3	GFRP on the Tensile Face Only
Flexure	2	0	3	
Flexure	3	0	3	
F + S(90)	1	0- F / 90 - S	3	GFRP on the Bottom and Each Side of the Beam
F + S(90)	2	0- F / 90 - S	3	
F + S(90)	3	0- F / 90 - S	3	
F + S(90)	2F: 1S @ 90	0- F / 90 - S	1	
Total			19	

Table 2.1: Strengthening schemes for this study (continued)

Fyfe Co. SEH-51 - Nominal thickness 1.3 mm (0.051 inches)

Type of Retrofit	No. of Plies	Orientation	No. of specimens	Application
Flexure	1	0	3	GFRP on the Tensile Face Only
Flexure	2	0	3	
Flexure	3	0	3	
Shear	1	45	3	GFRP on the Each Side/Crossed on the Face
Shear	2	45	3	
Shear	3	45	3	
F + S(90)	1	0- F / 90 - S	3	GFRP on the Bottom and Each Side of the Beam
F + S(90)	2	0- F / 90 - S	3	
F + S(90)	3	0- F / 90 - S	3	
Total			27	

Fyfe Co. SCH-41 - Nominal thickness 1.2 mm (0.047 inches)

Type of Retrofit	No. of Plies	Orientation	No. of specimens	Application
Flexure	1	0	3	CFRP on the Tensile Face Only
Flexure	2	0	3	
Flexure	3	0	3	
Shear	1	45	3	CFRP on the Each Side/Crossed on the Face
Shear	2	45	3	
Shear	3	45	3	
F + S(90)	1	0- F / 90 - S	3	CFRP on the Bottom and Each Side of the Beam
F + S(90)	2	0- F / 90 - S	3	
F + S(90)	3	0- F / 90 - S	3	
Total			27	

CMI/Reichold - Nominal thickness 0.25 mm (0.010 inches)

Type of Retrofit	No. of Plies	Orientation	No. of specimens	Application
Flexure	1	0	3	CFRP on the Tensile Face Only
Flexure	2	0	3	
Flexure	3	0	3	
Shear	1	45	3	CFRP on the Each Side/Crossed on the Face
Shear	2	45	3	
Shear	3	45	3	
Shear	1	90	1	CFRP on Each Side/ Face – no FRP contribution
F + S(45)	1	0- F / 45 - S	3	CFRP on the Bottom and Each Side of the Beam
F + S(45)	2	0- F / 45 - S	3	
F + S(45)	3	0- F / 45 - S	3	
F + S(90)	1	0- F / 90 - S	3	CFRP on the Bottom and Each Side of the Beam
F + S(90)	2	0- F / 90 - S	3	
F + S(90)	3	0- F / 90 - S	4	
Total			38	

Table 2.1: Strengthening schemes for this study (continued)

Owens-Corning/Reichold - Nominal thickness 0.25 mm (0.010 inches)

Type of Retrofit	No. of Plies	Orientation	No. of specimens	Application
Flexure	1	0	3	GFRP on the Tensile Face Only
Flexure	2	0	4	
Flexure	3	0	4	
Shear	1	45	3	GFRP on the Each Side/Crossed on the Face
Shear	2	45	3	
Shear	3	45	3	
F + S(45)	1	0- F / 45 - S	3	GFRP on the Bottom and Each Side of the Beam
F + S(45)	2	0- F / 45 - S	3	
F + S(45)	3	0- F / 45 - S	3	
F + S(90)	1	0- F / 90 - S	3	GFRP on the Bottom and Each Side of the Beam
F + S(90)	2	0- F / 90 - S	3	
F + S(90)	3	0- F / 90 - S	3	
Total			38	

CS – T – 1012/RC/Reichold - Nominal thickness 0.5 mm (0.0206 inches)

Type of Retrofit	No. of Plies	Orientation	No. of specimens	Application
Flexure	1	0	3	GFRP on the Tensile Face Only
Shear	1	0	3	GFRP on Each Side
F + S	1	0	3	GFRP on Each Side and Bottom
Total			9	

For flexural strengthening, the composite was applied to the tensile face of the specimens with the strengthening fibers oriented in the longitudinal direction, Figure 2.2.

Figure 2.2: Flexural reinforcement at a zero degree orientation. Flexural face is shown.

For shear strengthening, the composite was applied to one side, wrapped around the tensile face, and applied to the opposite shear face. The strengthening fibers were oriented either 0^o, 45^o, or 90^o to the longitudinal axis, Figures 2.3 and 2.4.

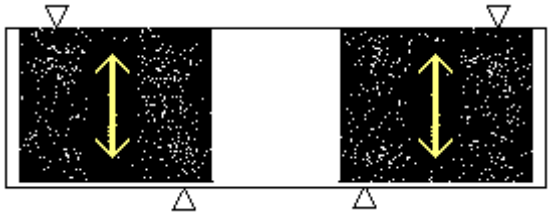

Figure 2.3: Shear reinforcement at a 90-degree orientation. Shear face is shown.

Figure 2.4: Shear reinforcement at a 45-degree orientation. Shear face is shown.

2.3 BEAM TEST PROCEDURE AND SETUP

The specimens were tested using third-point loading according to ASTM C78 (Figures 2.5 and 2.6) on either a 60 kip Baldwin universal testing machine or a 200 kip Satec 200HVL universal testing machine. The rate of loading was 8.9 kN per minute, which resulted in a 1.15 MPa per minute increase in stress in the extreme tension fiber.

Beam deflection was measured with an Electro Sense Linear Variable Differential Transformer (LVDT), shown in Figure 2.7. Outer-fiber strain was measured with one 60mm-long strain gage centered in the longitudinal direction on the tensile face of each beam (Figure 2.8). Load, strain, and deflection data were collected using a data acquisition system consisting of a personal computer equipped with Easy Sense software and a Validyne UPC 607 data acquisition card.

Load, strain, and deflection data was recorded at both first crack and failure. The first crack was determined from data and graphs of load versus strain and load versus deflection. For the purposes of this study, first crack was defined as the point where the stiffness or beam modulus changed abruptly. Some specimens did not show an abrupt change but rather a gradual one. For these cases, an estimate of the point of transition was made. Failure was defined as the point of ultimate load.

Figure 2.5: Beam test setup (Satec 200HVL universal testing machine).

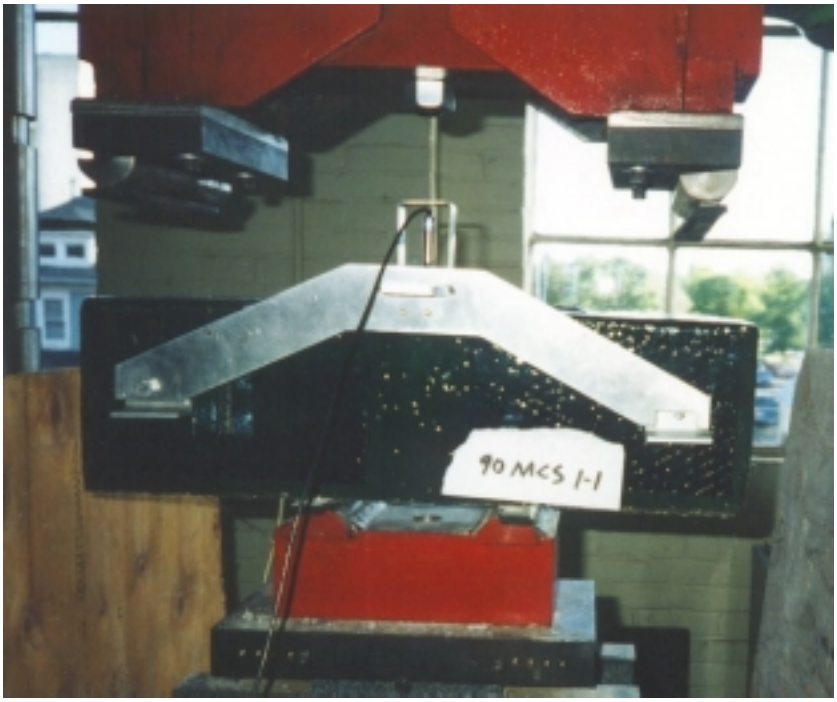

Figure 2.6: Third point loading frame.

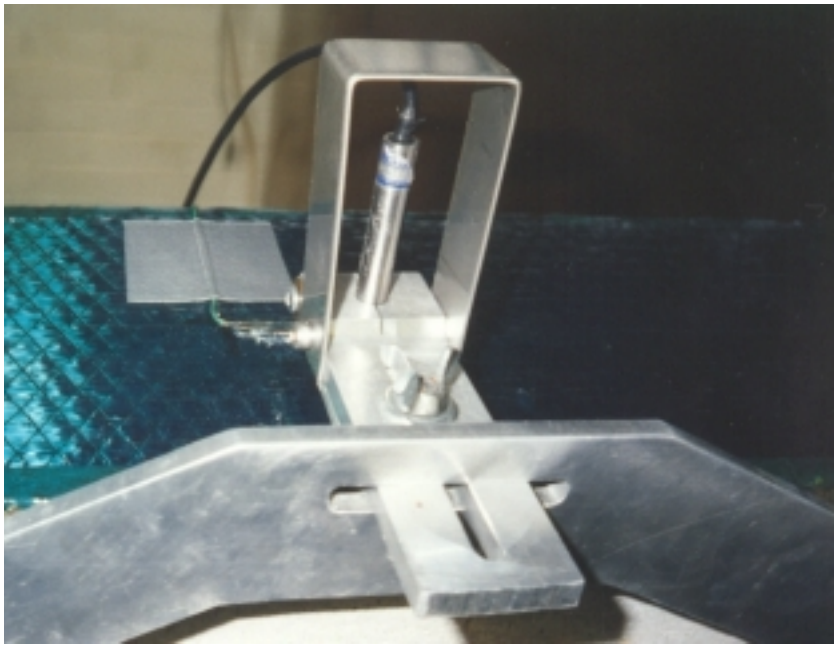

Figure 2.7: Typical LVDT setup.

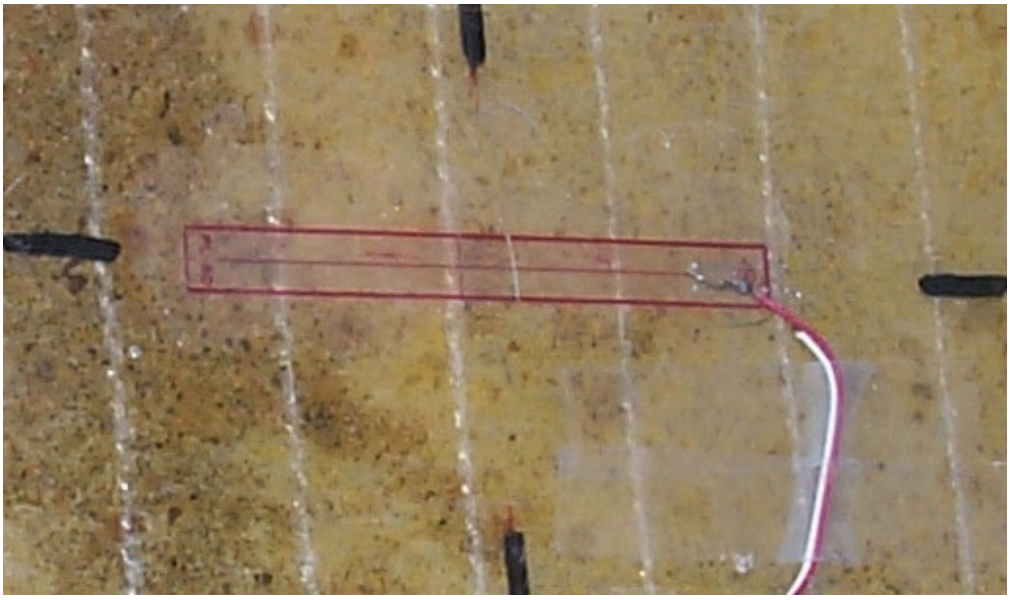

Figure 2.8: 60-mm strain gage.

2.4 CYLINDER FABRICATION AND STRENGTHENING

Twenty concrete cylinders used for the pilot FRP composite reinforced columns study were prepared in accordance with ASTM C31-91 using ready-mix concrete with a 28-day compressive strength of 32 MPa. These cylinders were standard compressive strength specimens with a diameter of 152-mm and a height of 305-mm. Compressive strength tests of six control specimens produced results ranging from 27 MPa to 34 MPa with an average of 32 MPa. Table 2.2 shows the experiment matrix.

Table 2.2: FRP strengthening for cylinder specimens.

FRP Material	Thickness, in.	Number of Specimens
GFRP		
Owens Corning 111A-AD-25	0.022	3
Owens Corning 111A-AD-25	0.044	3
Owens Corning 111A-AD-25	0.066	3
Owens Corning 111A-AD-25	0.088	3
Owens Corning 111A-AD-25	0.11	3
Total:		**15**
CFRP		
Fortafil 556	0.067	3
Fortafil 556	0.11	2
Total:		**5**
Total Specimens		**20**

Composite Retrofit Systems, LLC of Salem, Oregon built a machine to apply the FRP composites to the cylinders, shown in Figure 2.9. Each cylinder was placed between eight rubber wheels, two of which were driven by a motor that rotated the cylinder at a constant rate. The fiber was pulled through a resin pan by the action of the rotating cylinder and fed through an application arm. A separate, variable-speed motor moved the application arm back and forth along the length of the cylinder while the cylinder rotated providing consistent, one-layer, circumferential fiber application for each pass of the application arm.

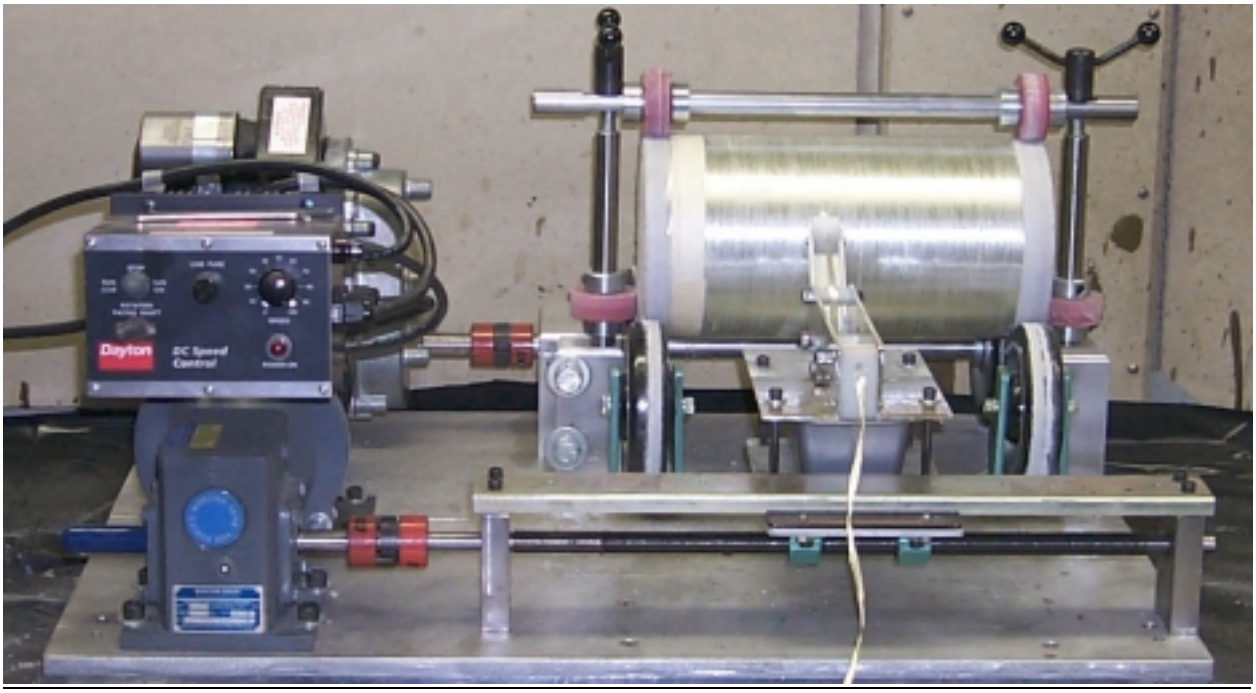

Figure 2.9: Wrapping machine for applying FRP to cylinder specimens.

2.5 CYLINDER TESTING

The ultimate compressive strength of the reinforced cylinders was the only data generated for the column pilot study. Tests and measurements were in accordance with ASTM C39 using a Tinius-Olsen Super L compression test machine with a maximum loading range of 400 kips.

3.0 FRP STRENGTHENING FOR REINFORCED CONCRETE BEAMS AND COLUMNS

FRP strengthening systems typically consist of two or more constituents whose mechanical properties and performance when combined are superior to those of the two materials acting independently. The mechanical properties of these systems vary based on position, orientation, and volume percentage of fiber reinforcement. The material behavior of these systems can, therefore, be controlled by the properties of the system's constituents (*Kachlakev, 1998*).

The backbone of FRP strengthening systems is reinforcing fibers made of high-strength, high-stiffness, low-density materials. Quite often, bundles of fibers pre-impregnated with resin (prepreg fibers), called "tows," are assembled into thin sheets producing what are referred to as "tow sheets." The terms fiber sheet, tow sheet, and fabric are used interchangeably throughout this report. Common materials used for reinforcement are carbon (CFRP), aramid (AFRP), and glass (GFRP). Typical fiber material properties can be seen in Table 3.1. Each fiber type has its own advantages and disadvantages (*Kachlakev, 1998*). In this study, only glass and carbon fibers were used.

Table 3.1: Typical Fiber Properties

	Fiber Type			
	E-Glass	S-Glass	Kevlar™ 49	Carbon (HS)
Density (g/cm^3)	2.54	2.49	1.45	1.8
Tensile Strength (GPa)	1.72 - 3.45	2.53 - 4.48	2.27 - 3.80	2.80 - 5.10
Elastic Modulus (GPa)	72.5	87	117	227
Elongation at Failure (%)	2.5	2.9	1.8	1.1

(*Kachlakev, 1998*)

The other constituent of an FRP system is the polymer matrix that encapsulates the fibers and bonds them to the concrete. The matrix is used to transfer stresses among the fibers so that when one fiber breaks the entire load carrying capacity of the system is not lost. Shear strength and transverse strength are also greatly influenced by the resin matrix (*Kachlakev, 1998*). The matrix also plays an important role by providing a barrier to the environment including protection from moisture and elevated temperatures. The type of matrix also affects the cost of the composite system (*Swanson, 1997*). Some typical matrix properties can be seen in Table 3.2.

Table 3.2: Typical Matrix Properties

	Matrix Type			
	Polyester	Phenolic	Vinylester	Epoxy
Density (g/cm^3)	1.20	1.20	1.15	1.10 - 1.40
Tensile Strength (MPa)	50 - 60	40 - 50	70 - 80	50 - 90
Elastic Modulus (GPa)	3.0	3.0	3.5	3.0
Elongation at Failure (%)	2.0 - 3.0	1.0 - 2.0	4.0 - 6.0	2.0 - 8.0

(*Kachlakev, 1998*)

The polymeric resins used in composite materials are usually divided into two general types: thermosets, and thermoplastics. Of the two, thermosets are most often used and preferred in structural applications (*Kachlakev, 1998*).

Commonly used thermosets are two-part epoxies, polyesters, and polyamides. The properties of thermosets are dependent on the composition of the resin and the extent of cross-linking and polymerization that take place during exothermic chemical reactions that occur while curing (*Kachlakev, 1998*). Polyester and vinyl ester are two lower-cost thermosets with very good solvent resistance; however, epoxy resins are more commonly used even though they are more costly then typical polyesters (*Swanson, 1997*).

Thermoplastics are one-component resins that soften and fuse together when heated and solidify on cooling. Thermoplastics, unlike thermosets, do not exhibit cross-linking, are typically softer than the thermosets, and do not cure by chemical reactions. The use of thermoplastics is quite uncommon with continuous fiber systems primarily due to high costs and a general lack of experience in the area (*Swanson, 1997*).

Typical laminate properties of fiber reinforced composites are in Table 3.3.

Table 3.3: Typical Laminate Properties (assumed 40 % fibers 60 % resin by volume)

	Composite Type			
	E-glass/Epoxy	S-glass/Epoxy	Aramid/Epoxy	Carbon/Epoxy
Density (g/cm^3)	2.10	2.00	1.38	1.58
Tensile Strength (MPa)	1080	1280	1280	2280
Elastic Modulus (GPa)	39.0	43.0	87.0	142.0
Fiber Volume (%)	55	50	60	63

(*Kachlakev, 1998*)

3.1 CARBON FIBER REINFORCED POLYMERS

Carbon fibers are divided into three categories: high strength, high modulus, and ultra-high modulus. Approximate elastic moduli for the three classifications are, respectively, 227 GPa, 370 GPa, and 350 to 520 GPa. Typical tensile strengths for the three grades are 2.8 to 5.1 GPa,

1.8 GPa, and 1.0 to 1.75 GPa. It is clear that any gains achieved in stiffness, from one grade to the next, are lost in strength, and vice versa (*Kachlakev, 1998*).

In this study, six different carbon systems, from five different manufacturers, were used. A brief description of each of the systems with application procedures follows.

3.1.1 MBrace™

The MBrace™ carbon system is a dry layup system consisting of unidirectional carbon fibers, and a two-part epoxy matrix, MBrace™ Saturant. The Tonen Corporation (Japan) produces the carbon fiber sheet, and Master Builders (Cleveland, OH, USA) provides the epoxy matrix. The fibers are manufactured with a paper backing and are held together by a $\pm 60^{o}$ single fiber grid woven through the main fibers every 1 to 2 centimeters. The design thickness of the fiber "tow sheet" is 0.165 mm (6.5 mils) and is manufactured in 50 cm (20 in.) wide rolls. Material properties reported by the manufacturer for the carbon fiber sheets are shown in Table 3.4.

Table 3.4: MBrace™ Carbon Fiber Sheet Properties

	Tow Sheet Type		
	FTS C1-20	FTS C1-30	FTS5-30
Fiber Type	High Tension Carbon	High Tension Carbon	High Modulus Carbon
Fiber Density (g/cm3)	1.82	1.82	1.82
Tensile Strength Kg/cm of sheet width	390	590	500
Tensile Modulus Kg/cm of sheet width	25900	38800	62700
Design Thickness (cm)	0.011	0.0165	0.0165
Design Tensile Strength (kg/cm^2)	35500	35500	30000
Design Tensile Modulus ($kg/cm^2 \times 10^6$)	2.35	2.35	3.8
Elongation at Failure (%)	1.5	1.5	0.8

(Forca Tow Sheet Manual, 1996)

Installation of the MBrace™ system requires several steps as recommended by the manufacturer:

- The concrete surface is abraded and cleaned.
- MBrace™ Primer is rolled onto the concrete and allowed to reach a tack-free condition. This primer is a low-viscosity, high-solids epoxy that seals the concrete and provides a moisture barrier between the concrete and fiber sheet.
- Irregularities in the surface of the beam are filled using MBrace™ Putty, which is allowed to become tack-free. This putty is also a high-solids epoxy but far more viscous than MBrace™ Primer.

- MBrace™ Saturant is rolled onto the primed concrete. The standard formulation of this epoxy has a pot life of 40 minutes at 20°C; the summer and winter versions have 110-minute and 20-minute pot lives at 20°C, respectively.

- The fiber sheet is smoothed out over the area that has been prepared with MBrace Saturant while the epoxy is uncured.

- MBrace™ Saturant is rolled over the fiber sheet.

This application procedure is illustrated in Figure 3.1.

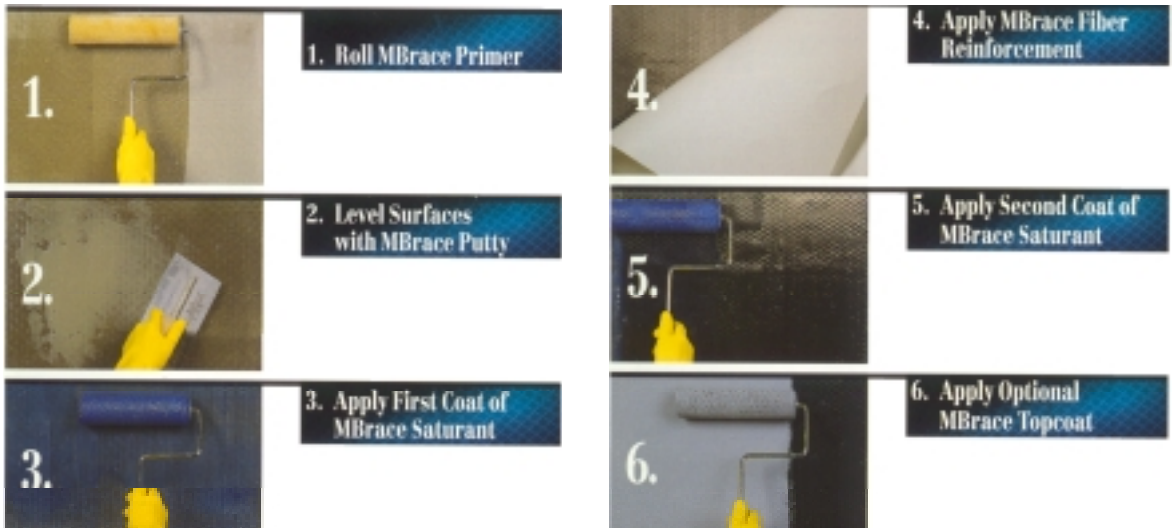

Figure 3.1: MBrace™ Application Procedure *(Master Builders, 1997)*

In this study, the MBrace™ system was prepared and applied according to the manufacturer's guidelines. First, the beams were sandblasted and blown clean with compressed air. Next, MBrace™ Primer was applied and allowed to cure for approximately 16 hours at room temperature. After the curing, the primed beams had reached a tack-free state, and irregularities in the concrete surface were repaired with putty. The putty was allowed to cure for several hours until it became tack-free as well. While the putty cured, the carbon fiber tow sheets were cut to size using a sharp box knife and cutting on top of a piece of stiff cardboard. It was found that this was the easiest way to successfully cut the fibers, without disturbing or damaging them, with the tools that were available.

After all of the fiber sheets were cut and the putty had cured, the MBrace™ Saturant was prepared and applied to the beams. Within 10 to 15 minutes, one fiber sheet was applied, carbon side down, to each beam. The tow sheet was smoothed by hand in the direction of the fibers in order to remove any air that had been trapped during application. The paper backing was removed, and the fibers were rolled in the fiber direction with a grooved plastic roller to remove any remaining entrapped air. The beams were left undisturbed for 30 minutes to 1 hour so that

the epoxy could fully impregnate the fibers. Next, a layer of MBrace™ Saturant was rolled on over the fiber sheet. For beams reinforced with multiple layers of fiber, a slightly thicker layer was applied to serve as the under coat for the subsequent tow sheet. This procedure was repeated until the desired number of fiber layers was reached. At the end of each day, regardless of whether or not the required number of layers of reinforcement had been applied, all applied carbon fiber sheets were coated with a layer of MBrace™ Saturant to protect them from damage. Following application of all fiber and epoxy layers, the beams were allowed to cure for at least seven days prior to testing. Figure 3.2 shows the typical appearance of a MBrace™ carbon fiber reinforced beam from this study.

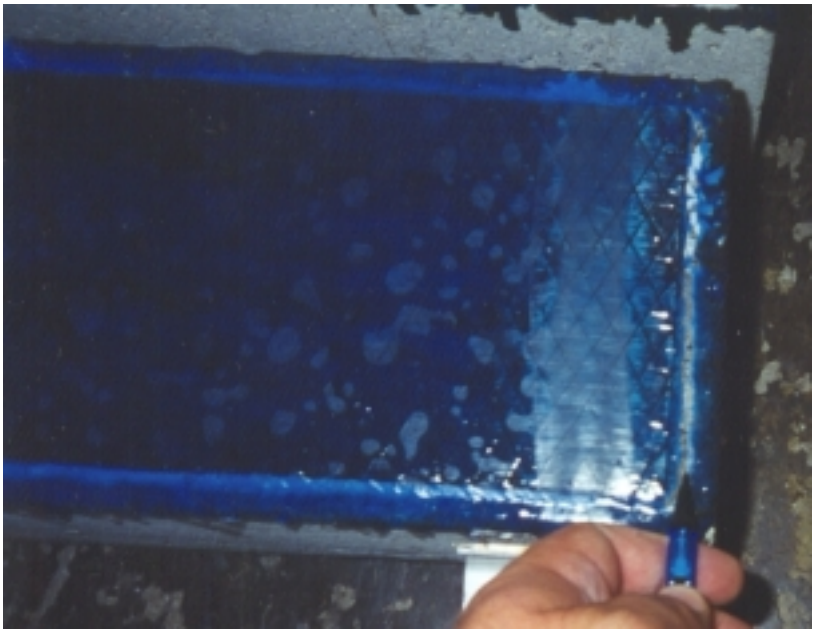

Figure 3.2: Typical appearance of MBrace™ carbon fiber reinforced beam.

3.1.2 Replark®

Replark®, manufactured by the Mitsubishi Chemical Corporation, and marketed in the U.S. by the Sumitomo Corporation of America, is another dry layup carbon system. Replark® 30 carbon fibers were used in this study; however, other Replark® fibers are available as seen in Table 3.5. The Replark® 30 fibers are typically supplied in 100 meter-long rolls, and come in both 25 cm and 33 cm widths, with a standard thickness of 0.167 mm (6.57 mils). Like the MBrace® material, these fibers are unidirectional with a single fiber woven through, at $\pm 60^{o}$ every 1 to 2 centimeters to hold the tows together. The Replark sheets also have a removable paper backing to help maintain fiber position during handling.

Table 3.5: Replark® Fiber Sheet Properties

	Tow Sheet Type		
	Replark 20	Replark 30	Replark HM
Fiber Color	White	Black	Green
Design Tensile Strength (kg/cm^2)	35000	35000	20000
Design Tensile Modulus ($kg/cm^2 \times 10^6$)	2.35	2.35	6.5
Design Thickness (mm)	0.111	0.167	0.143

(*Mitsubishi Chemical Corporation, 1997*)

The Replark® 30 system is applied in a manner similar to that of the MBrace™ system. A typical application procedure for the Replark® system is as follows *(Mitsubishi Chemical Corporation, 1997)*:

- Concrete surface is roughened and cleaned.
- Primer coat of resin is applied to the concrete to seal the surface.
- Irregularities in the concrete surface, larger than 1 mm, are smoothed with putty.
- An under coat layer of saturating resin is applied to prepared beam surface.
- The fiber sheet is placed in position and paper backing is removed.
- The fibers are rolled to remove entrapped air.
- An over coat layer of saturating resin is applied to protect the fibers.
- The FRP system is allowed to cure for approximately seven days, depending on site conditions.

In this study, the beams were sandblasted and blown clean with compressed air. Epotherm® PS401 primer (Table 3.6) was prepared according to the manufacturer's recommendation and slowly mixed for several minutes to avoid creating air bubbles in the epoxy. The primer was applied to the beams at a rate of 0.1 to 0.35 kg/m^2 (0.02 to 0.07 lb/ft^2) and allowed to cure at room temperature approximately 20 hours. According to application procedures supplied by the manufacturer, the time required for the necessary tack-free condition is approximately 7 hours, but actual length of time is not critical as long as the next step of the process takes place within 7 days. When the next step could not be continued in the seven day period, the primer coat was roughened with sandpaper, and cleaned prior to proceeding with the next step, as recommended by the manufacturer (*Mitsubishi Chemical Corporation, 1997*).

After priming, Mitsubishi Epotherm® L525 epoxy putty was used to smooth out all irregularities and sharp edges. Care was exercised to use as little putty as possible to correct the deficiencies. The putty became tack-free in approximately 4 hours at room temperature. If a beam was not processed 7 days after putty application, the puttied areas were sanded and cleaned before proceeding to the next step according to the manufacturer's recommendation.

Table 3.6: Properties of Epotherm® Putty and Primer

	Epotherm Putty	Epotherm Primer	
	L525	PS301	PS401
Conditions for use	All	Cool Season	Warm Season
Specific Gravity (hardened @ 25°C)	1.4 - 1.5	.85 -1.25	.85 - 1.25
Adhesive Strength (kg/cm^2 @ 23°C)	15+	15+	15+
Standard Pot Life (min. @ 23°C)	50	40	240
Tack-Free time (hours @ 23°C)	3.5	3.5	7.0
Standard Quantity Used (kg/m^2)	0.5	0.25	0.25

(*Mitsubishi Chemical Corporation, 1997*)

While the putty was becoming tack-free, all of the fiber sheets were cut to the correct size. The fiber sheets were stored and transported per the manufacturer's recommendation by wrapping them around a cardboard cylinder with a radius of 15 cm (approx. 6") to prevent damage to the fibers.

After applying the putty and cutting the fiber sheets, Mitsubishi Epotherm® L700S epoxy undercoat (Table 3.1.2.3) was applied at a rate of 0.4 to 0.5 kg/m^2 (0.008 to 0.01 lb/ft^2) as recommended by the manufacturer. Immediately after coating each beam, a fiber sheet was placed fiber side down on the beam. Working from the center of the beam to each end, the fiber sheet was pressed carefully into the resin by hand following the direction of the fibers to keep from separating or damaging them. This step removed much of the trapped air from under the fiber sheet.

After the fiber sheet was attached to the surface of the beam, the paper backing was very carefully removed. Next, the fiber sheet was rolled with a special "air removal roller" that was supplied by the manufacturer. The grooved roller was rolled in the direction of the fibers to remove any entrapped air. No rolling was done in the transverse direction as this could have caused separation of or damage to the fibers. Once the rolling was completed, the beam was left undisturbed for thirty minutes to one hour to allow the resin to impregnate the fibers.

An over coating layer of Epotherm L700S was applied in the same manner as the undercoat; however, the thickness of this coat was approximately half that of the undercoat. For multiple layer fiber sheet applications, the overcoat also served as the undercoat layer for the subsequent fiber sheet layer; consequently, 0.6 to 0.8 kg/m^2 (0.012 to 0.016 lb/ft^2) of Epotherm L700S was used between the layers of fiber sheets. An overcoat was applied at the end of each workday regardless of whether or not more fiber layers were to be added to the beam. Following application of the final overcoat, the beams were allowed to cure for at least seven days at room temperature prior to testing. Figure 3.3 shows the typical appearance of the Replark® reinforced concrete beams used in this study.

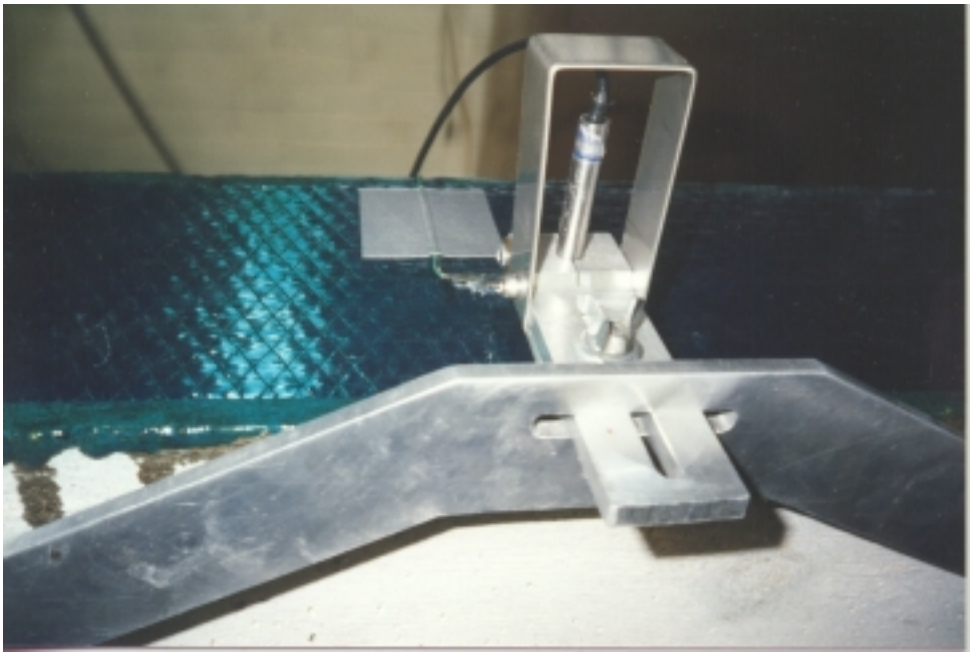

Figure 3.3: Typical appearance of Replark® FRP composite.

3.1.3 Carbodur®

Unlike the MBrace™ and Replark® dry lay-up systems, Sika Carbodur® is a pultruded carbon fiber laminate consisting of at least 68 percent carbon fibers by volume. This is relatively high compared to 40 to 60 percent for most other CFRP systems. Carbodur® is available from the manufacturer in 50 mm, 80 mm, and 100-mm (2", 3.125", and 4") widths and is made with a standard thickness of 1.2 mm (47.2 mils). The laminate is bonded to the exterior of concrete beams with a high modulus, high strength epoxy, Sikadur® 30. The prepared epoxy has a 70-minute pot life at 73^{o}F, which was more than sufficient for this study (*Sika Product Guide, 1997*). Table 3.7 shows material properties for both Sikadur® 30 and Carbodur®.

Table 3.7: Properties of Sika Carbodur® and Sikadur® 30

	Carbodur	**Sikadur 30**	**Test Method**
Color	Black	Light Grey	(Applies to
Shelf Life	Unlimited	2 years	Sikadur Only)
Tensile Strength	2,400 N/mm^2	24.8 MPa	ASTM D638
Tensile Modulus of Elasticity	155,000 N/mm^2	4478 MPa	ASTM D638
Elongation at Failure (%)	1.9	1.0	ASTM D638
Flexural Strength (Modulus of Rupture)	NA	46.8 MPa	ASTM D790
Bond Strength (2 day - dry cure)	NA	22.0 MPa	ASTM C882
Water Absorption (24 Hour)	NA	0.03%	ASTM D570
Modulus of Elasticity (7 day)	NA	2687 MPa	NA

(*Sika Product Guide, 1997*)

Typical application of the Carbodur® system is as follows:

- The concrete beam is abraded (the manufacturer recommends shot blasting) and cleaned.
- The Carbodur® strip is cut to length, and the exposed carbon side is cleaned with acetone.
- Epoxy is applied separately to the surface of the concrete beam and the exposed carbon surface of the laminate.
- The laminate is positioned on the concrete surface and rolled with a rubber roller to remove entrapped air.
- The system is cured for seven days at room temperature to reach full strength.

In this study, the beams were first sandblasted and cleaned. The Carbodur® strip was cut to length using a large shear, and the exposed carbon side of the strip was wiped clean with acetone on a white rag until no black carbon particles could be seen on the rag. Sikadur 30 epoxy was prepared and applied to the concrete surface with a wide putty knife. This was continued until an even surface approximately 1.5 mm (1/16”) thick covered the entire area over which the laminate was to be applied. The same method was used to apply epoxy to the laminate. The laminate was then placed onto the prepared concrete surface and was rolled with a hard rubber roller until the adhesive began to come out from under the laminate edges. This excess epoxy was removed, and small weights were placed on top of the laminate to prevent it from lifting out of the epoxy. All of the specimens were allowed to cure for at least 7 days at room temperature prior to testing. Figure 3.4 shows a typical Sika Carbodur® reinforced beam used in this study.

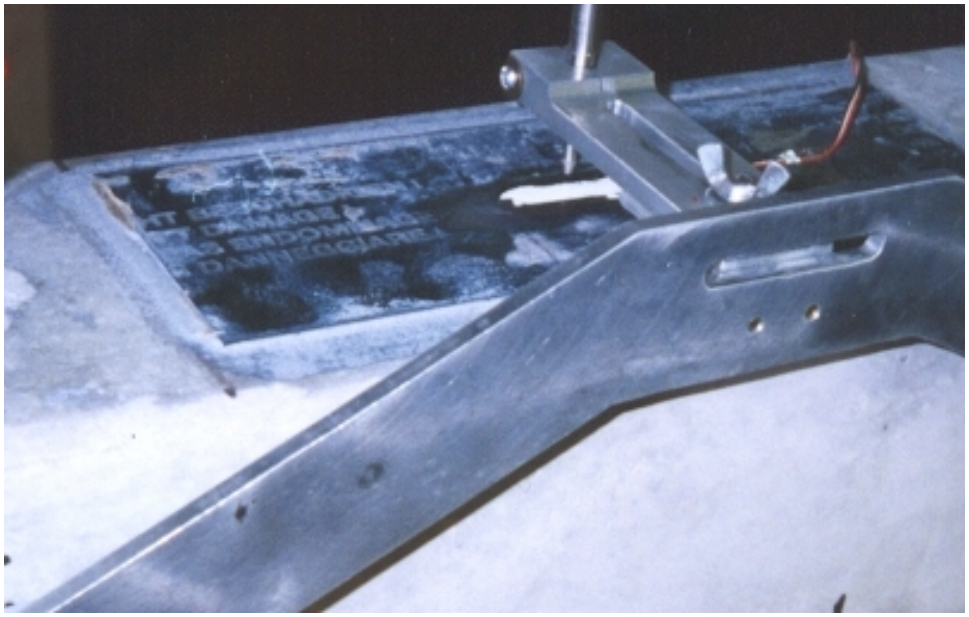

Figure 3.4: Typical appearance of the Sika Carbodur® system.

3.1.4 SikaWrap® Hex

Another Sika® product that was used in this study was SikaWrap® Hex 103C. The SikaWrap® Hex system is part of a collaborative development and manufacturing effort between the Sika Corporation and the Hexcel Corporation. This product is a unidirectional, high strength, high modulus carbon fiber fabric that employs a wet layup application process. Unlike Carbodur®, SikaWrap® is flexible prior to application, and therefore, has a wider range of structural applications for which it can be used.

The standard width of the SikaWrap® carbon fabric is 63.5 cm (25 in.) with a standard thickness of 1 mm (0.04 in). The unidirectional carbon fibers are held together with glass fibers woven through approximately every centimeter perpendicular to the primary fiber direction. The SikaWrap® Hex 103C fibers are saturated and applied to concrete beams with Sikadur® Hex 300 resin. A thixotropic version of the epoxy, Sikadur® Hex 306 is available for overhead applications as well. Table 3.8 shows the reported properties of the Sikadur® Hex products used in this study (*Sika Corporation, 1998*).

Table 3.8: Properties of SikaWrap® Hex Carbon System and Constituents

	Hex 103C Fibers	**Hex 300 Resin**	**Cured Laminate**
Color	Black	Clear/Amber	Black
Tensile Strength (N/mm^2)	3450	72.45	960
Tensile Modulus of Elasticity (N/mm^2)	234500	3167	73100
Elongation at Failure (%)	1.5	4.8	1.33
Flexural Strength (N/mm^2)	NA	123.5	NA
Flexural Modulus (N/mm^2)	NA	3118	NA

(*Sika Product Guide, 1998*)

Sikadur® Hex 300 is a high modulus, high strength, impregnating epoxy with a 4-hour pot life, which was found to be more than adequate for this study. Unlike the previously mentioned fiber sheet based systems, there is no primer used with the SikaWrap® system. Instead, a light coating of the impregnating epoxy is used to seal and prepare the concrete prior to application of the fibers (*Sika Corporation, 1998*).

Application of the SikaWrap® system is typical of most wet layup systems and is accomplished in the following way:

- After the concrete surface is abraded and cleaned, the beam surface on which the fiber fabric is to be applied is coated with Sikadur® Hex 300 epoxy. This primer coat is allowed to cure for approximately 10 minutes.

- The fiber fabric is saturated using either hand or mechanical methods. Figure 3.5 shows a typical fiber saturation machine. Saturated fiber sheets are cut to length using a sharp razor knife, or scissors.

- The saturated fabric is applied to the prepared concrete surface.

- Once the fabric is placed in the proper position, voids, gaps, and creases are smoothed out by hand.

- The reinforced beam is allowed to cure for 10 to 14 days prior to testing.

Figure 3.5: Fiber saturation machine. Glass fibers shown. (*Sika Corporation, 1998*)

Because of the small size of the beams used in this study, the limited workspace, and the available tools, the application method was modified slightly, as suggested by a representative of the manufacturer. After thorough cleaning of the sandblasted beams with compressed air, Sikadur® 300 epoxy was prepared and applied to the beams with a short nap roller. Next, the SikaWrap® Hex 103C carbon fiber fabric was unrolled on a piece of plywood and cut with a sharp box knife. Individual fiber sheets were placed in a plastic lined wooden box that was made on site. Hex 300 epoxy was poured over each fiber sheet until it was covered with approximately 0.5 cm of the epoxy. The fiber sheet was left undisturbed for 5 to 10 minutes to allow the epoxy to thoroughly impregnate the fabric. Then the excess epoxy was removed and discarded.

After a sheet was saturated, it was positioned on the beam and smoothed out by hand. Excess epoxy and any remaining entrapped air was removed with a plastic putty knife by pressing firmly and dragging the knife in the direction of the fibers. Care was taken to assure that the fibers were not disturbed or damaged during this procedure. The process was repeated for beams with multiple layers of fiber reinforcement. The strengthened beams were allowed to cure for at least 14 days prior to testing. Appearance of the SikaWrap® Hex system used in this study is shown in Figure 3.6.

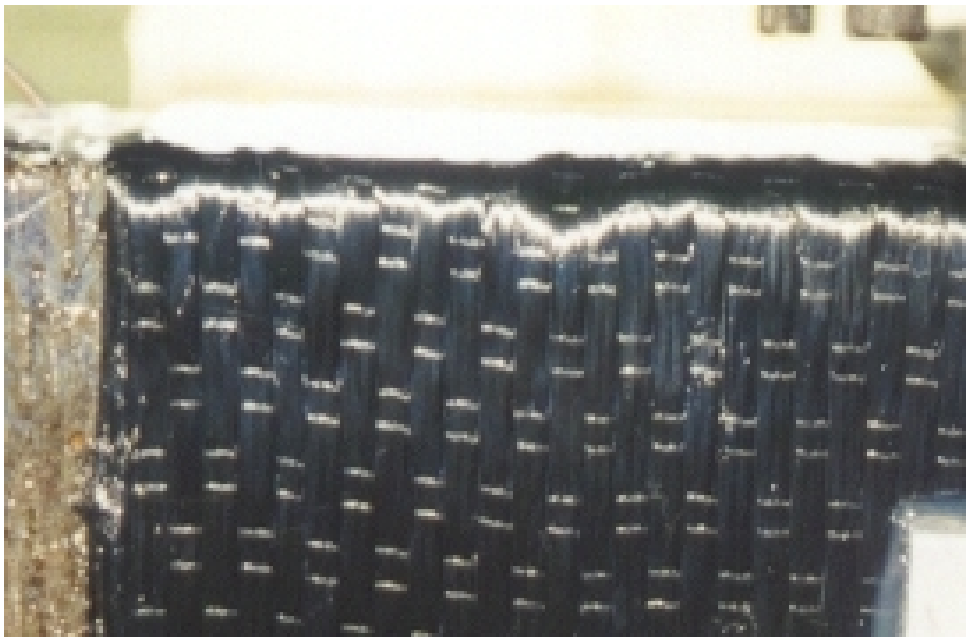

Figure 3.6: Typical appearance of SikaWrap® Hex FRP system.

3.1.5 Tyfo® Carbon

The Tyfo® system, developed by the Fyfe Corporation of San Diego, CA, is another wet lay-up carbon system that was used in this study. Although various epoxies and fiber fabrics are available from the company, the system used in this study consisted of SCH-41 carbon fiber fabric and Tyfo® S epoxy, Table 3.9. The 1 mm (0.04 in) thick SCH-41 fabric consists of unidirectional carbon fibers with Kevlar fibers woven perpendicular to the main fibers approximately every 1cm to hold the carbon fibers in place (*Fyfe Company, 1998*).

Tyfo® S epoxy, which is used both as a primer and a saturating epoxy, has a pot life of approximately 2 hours at 21^{o}C (70^{o}F), which was more than adequate for this study. Another epoxy available from Fyfe Corporation, Tyfo® TC, is more viscous than Tyfo® S, and has better adhesion properties. Tyfo® TC is generally used in limited amounts for overhead and vertical applications. (*Fyfe Company, 1998).*

Table 3.9: Properties of Tyfo® SCH-41 Fibers and Tyfo® S Resin Composite System

Tensile Strength in fiber direction (N/mm^2)	**Tensile Strength** @ 90o to fiber direction (N/mm^2)	**Tensile Modulus** based on fiber area (N/mm^2)	**Maximum Elongation** Percent
690	1.55	55200	1.5

(*Fyfe Company, 1998*)

The Fyfe Company's Tyfo® system has one unique feature that none of the other systems has. Glass fiber anchors are used in full size beam applications to help develop stresses in the fibers

with less possibility of debonding. The anchors, shown in Figure 3.7, are glass fiber loops that are inserted into predrilled holes, loop-end in, and held in place with injected epoxy. The cut ends of the fiber anchors, which are left hanging out of the concrete, are passed through a hole in the fabric and are spread out in different radial directions against the impregnated fabric. This can be seen in the picture on the right side of Figure 3.7. In order to make fair comparisons of all of the systems, and because of the small size of the beams, no anchors were use on any of the Tyfo® reinforced beams in this study.

Figure 3.7: Typical Tyfo® system glass anchors (left), and typical appearance of applied anchor in concrete beam (right).

Application of the Tyfo® system is similar to that of the SikaWrap® system. The process is as follows:

- After roughening and cleaning the concrete, any defects in the concrete surface are repaired with thickened Tyfo® S epoxy. The epoxy is thickened with fumed silica until the desired viscosity is attained.
- Non-thickened Tyfo® S is mixed and applied to the concrete surface in liberal amounts to serve as a primer. The applied resin is allowed to tack, which takes approximately 30 minutes.
- Minimal amounts of Tyfo® TC are applied in areas where needed to assure proper bonding.
- While the applied epoxy is reaching a tacky state, the fiber sheet is saturated with Tyfo® S either by hand or with a fiber saturation machine.
- The saturated fabric is placed in position and smoothed by hand to remove any entrapped air.

- When the application is complete, the surface is coated with Tyfo® S, thickened with fumed silica, to protect the FRP from possible damage.

- The FRP system is allowed to cure for at least 4 days prior to testing.

In this study, the beams were abraded and cleaned, the fiber sheets cut and impregnated, and the lay up conducted similar to the Sika Wrap Hex system discussed in Section 3.1.4. For multi-layer applications, the first impregnated fiber sheet was allowed to reach the tacky condition, another thin layer of Tyfo® TC was applied and allowed to tack, and the subsequent impregnated fiber sheet was placed in position and smoothed out. This procedure was followed until the desired number of layers was applied. Finally, a thin layer of Tyfo® S epoxy thickened with Cab-o-Sil fumed silica was spread over the surface to protect the composite reinforcement The composite reinforcement was allowed to cure for at least 14 days prior to testing. Figure 3.8 shows one of the beams reinforced with the Tyfo® carbon fiber system.

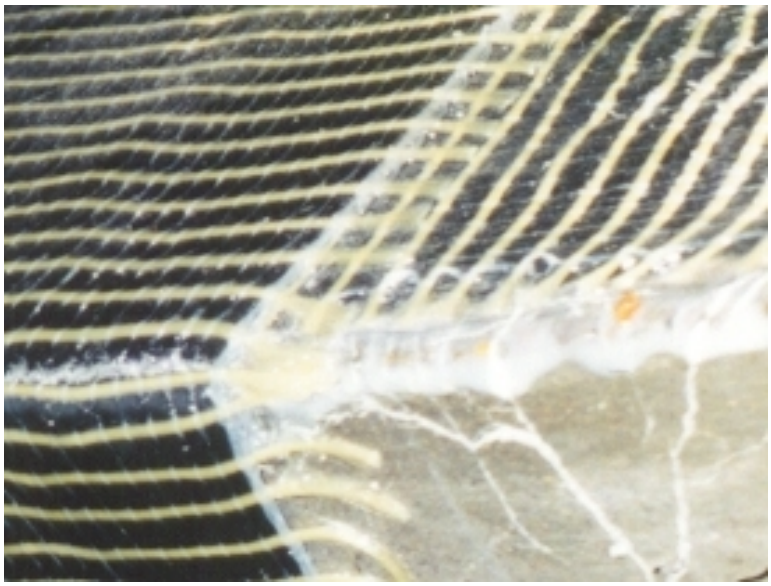

Figure 3.8: Typical appearance of Tyfo® carbon fiber composite system.

3.1.6 Composite Materials, Inc./Reichhold Chemicals

The Composite Materials, Inc. (CMI)/Reichhold Chemicals, Inc. carbon FRP system is currently under development by Composite Retrofit Systems (CRS), Salem, Oregon. CMI is the manufacturer of the carbon fiber sheets and Reichhold is the supplier of the resin and primer.

Three different weights of CMI fiber sheet were used in this study. The sheets had 4oz., 8oz., and 12oz. of carbon fibers per square yard. These are later referred to as one, two, and three layers respectively. The unidirectional fibers in the sheets are held in place by a thin veil on each side

of the sheet. The veil dissolves during application of the resin. The properties of the carbon fiber sheets are shown in Table 3.10, and a picture of the unimpregnated sheet is shown in Figure 3.9.

Table 3.10: CMI Carbon Fiber Sheet Properties

	CMI 4 oz.	CMI 8 oz.	CMI 12 oz.
Tensile Strength (N/mm^2)	3795	3795	3795
Tensile Modulus (N/mm^2)	227700	227700	227700
Elongation at Failure (%)	1.7	1.7	1.7
Design Thickness (mm)	0.254	0.508	0.762

(*Composite Materials, Inc., 1998*)

Figure 3.9: CMI carbon fiber sheet.

The general application process for the CMI/Reichhold system is as follows:

- The concrete surface is abraded and cleaned.
- Irregularities and voids in the concrete surface larger than 1 mm are filled with an epoxy putty.
- The primer, ATPRIME® 2, is applied to the concrete and permitted to cure. ATPRIME® 2 is a two-component urethane system. After mixing, the primer is left undisturbed for a 30-minute induction period. It is then applied to the concrete at a rate of one pound per

50-100 square feet. The primer is allowed to cure from 2 to 24 hours. When a curing time of 24 hours is exceeded, re- application is necessary.

- The fiber sheets are applied using dry or wet lay-up, depending on thickness.
- The sheets are rolled to remove entrapped air.
- A topcoat of matrix resin is applied for additional protection of the fibers.
- The reinforcement system is allowed to cure for at least seven days.

For the beams in this study, commercially available epoxy putty was used to fill voids and irregularities larger than 1mm. Irregularities were filled, and sharp edges were smoothed using as little putty as possible to correct the deficiency. After the putty became tack-free in about 4 hours, the beams were ready for priming. If priming was not started within seven days of applying the putty, the puttied areas were sanded and cleaned prior to the priming step. The ATPRIME® 2 primer was rolled on using a paint roller. Properties of the putty and primer are in Table 3.11.

Table 3.11: Properties of Putty and ATPRIME® 2 Primer

	Putty	**ATPRIME® 2 Primer**
Specific Gravity @ 25^{o}C	1.4 - 1.5 (hardened)	1.05 (Liquid)
Adhesive Strength (kg/cm^2 @ 23^{o}C)	15+	Not Given
Standard Pot Life @ 23^{o}C (minutes)	50	720 @ 50% rel. humidity
Tack-Free time (hours @ 23^{o}C)	3.5	NA
Standard Quantity Used	0.5 (kg/m^2)	0.01 - 0.02 (lb/ft^2)

(*Reichhold Chemicals, Inc., 1996)*

The matrix for the fiber was Atlac® 580-10 vinyl ester resin that was catalyzed with methyl-ethyl-ketone peroxide (MEKP) at 1.25% by weight. In this study, Superox® MEKP by Reichhold, was used. The 4-ounce fiber sheets were applied using dry lay-up methods while the 8 and 12-ounce fiber sheets utilized wet lay-up methods. Properties of the resin are in Table 3.12. Figure 3.10 shows a portion of a beam strengthened with the CMI/Reichhold system in this study.

Table 3.12: Atlac® 580-10 Material Properties

Tensile Strength (N/mm^2)	**Tensile Modulus** (N/mm^2)	**Flexural Strength** (N/mm^2)	**Flexural Modulus** (N/mm^2)	**Elongation at Failure (%)**
90.4	3174	155.9	3381	4.2

(*Reichhold Chemicals, 1993*)

Figure 3.10: Typical appearance of CMI/Reichhold FRP composite.

3.2 GLASS FIBER REINFORCED POLYMERS

Glass fibers are the most commonly used fiber type. The mechanical characteristics of glass fibers make them suitable for most civil engineering applications; however, they have lower stiffness, less strength, and higher elongation than carbon fibers. Glass fibers are produced by an efficient manufacturing process which makes them available at a relatively low cost (*Swanson, 1997*).

E-glass and S-glass are the two most common types of glass fibers although several others exist. S-glass possesses higher strength and stiffness than E-glass, and is typically more expensive. E-glass fibers typically have a tensile strength of 1.72 to 3.45 GPa, while S-glass fibers have a tensile strength of 2.53 to 4.48 GPa depending on the manufacturer. The elastic modulus of the two glass fibers, E-glass and S-glass, are commonly around 72.5 GPa and 87 Gpa respectively. The difference between the two is primarily the result of quality control during the manufacturing process. Typical glass fiber reinforced polymer (GFRP) systems consist of E-glass and a thermoset resin (*Kachlakev, 1998*).

3.2.1 MBrace™

The MBrace™ glass system is a dry lay-up system consisting of unidirectional glass fibers in an epoxy matrix. The dry glass fibers are available as a tow sheet with a paper backing similar to the MBrace™ carbon fibers. The glass fibers are held together with a single fiber woven at $\pm 60^{o}$ to the longitudinal fiber at approximately 1cm intervals. Like the carbon fibers, MBrace™ glass

fibers are manufactured in 50cm (20 in) wide rolls (*Forca Tow Sheet Manual, 1996*). Material properties for the MBrace™ glass fibers are shown in Table 3.13.

Table 3.13: MBrace™ FTS GE-30 Glass Fiber Sheet Material Properties

Design Thickness (cm/ply)	**Tensile Strength** (kg/cm^2)	**Tensile Modulus** (kg/cm^2)	**Max. Elongation** Percent
0.0118	15500	740000	2.1

(*Forca Tow Sheet Manual, 1996*)

The application procedures for the MBrace™ glass system are identical to those for the carbon system except for the type of fibers used. Typical application procedures can be seen in Figure 3.1. A detailed description of the application procedures used in this study can be found in Section 3.1.1. Typical appearance of the MBrace™ GFRP system can be seen in Figure 3.11.

Figure 3.11: Typical appearance of MBrace™ GFRP system.

3.2.2 SikaWrap® Hex 101G

SikaWrap® Hex 101G is another product that is the result of a collaborative effort between the Sika Corporation and the Hexcel Corporation. Unlike the previously mentioned products, it is not unidirectional. It is a fabric consisting of E-glass fibers at $\pm 45^{o}$ angles to the length of the sheet and is used primarily for enhancing the shear strength of beams. Because of the fiber orientation, installation time for shear reinforcement is shortened since there are no angles to layout. The fabric is manufactured in 127 cm (50 in) wide rolls with a standard thickness of 1 mm (0.04 in). Mechanical properties of the laminate formed by combining the fibers with SikaWrap® Hex 300 resin, as was done in this study, are in Table 3.14 (*Hexcel Corporation, 1998*).

Table 3.14: SikaWrap® Hex 101G / SikaWrap® Hex 300 - Laminate Material Properties

Thickness (cm/ply)	Tensile Strength (N/mm^2)	Tensile Modulus (N/mm^2)	Shear Strength (N/mm^2)	Poisson's Ratio	Maximum Elongation (%)
0.1016	304	15663	62.1	0.189	2.37

(*Hexcel Corporation, 1998*)

For this study, the SikaWrap® Hex 101G fabric was used only as shear reinforcement with Sika Carbodur® used to reinforce the beam for flexure. Part of a beam reinforced with these two systems can be seen in Figure 3.12. Application is identical to the other SikaWrap® Hex products and was performed as described in Section 3.1.4.

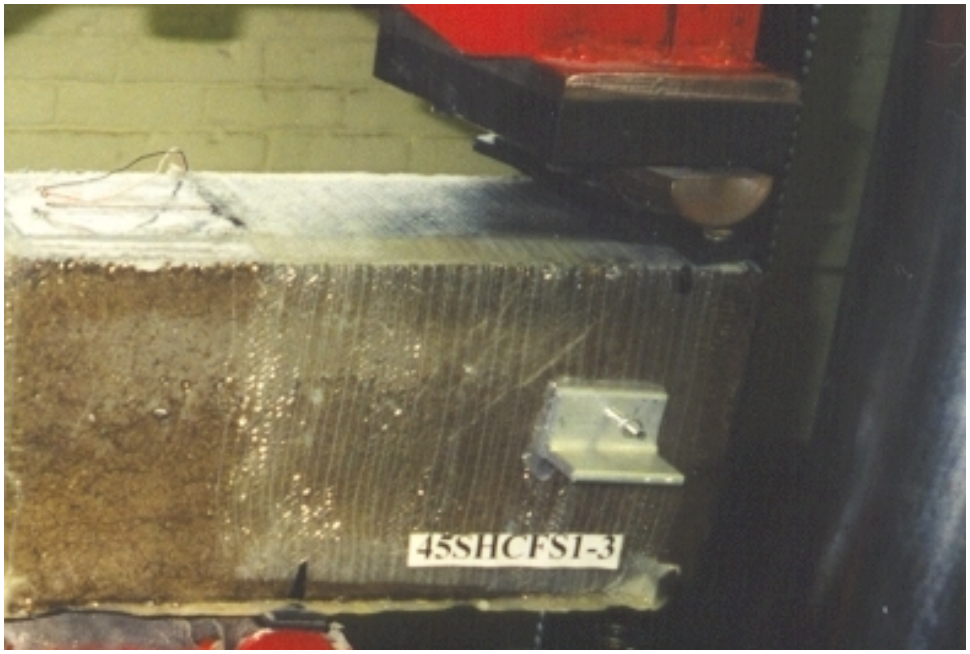

Figure 3.12: Typical appearance of SikaWrap® Hex 101G.

3.2.3 Tyfo® Glass

The Tyfo® SHE-51 Glass system was developed by the Fyfe Corporation of San Diego, California. The system consists of unidirectional E-glass fabric and Tyfo® S epoxy. The fibers, which make up the fabric, have Kevlar™ fibers woven through them perpendicular to the main fiber at approximately 1cm intervals for stability. Typical material properties for this system are in Table 3.15.

The Tyfo® glass fabric is slightly thicker than the Tyfo® carbon fabric with a thickness of 1.3 mm (0.051 in). As with the carbon system, Tyfo® TC epoxy is used on large vertical and overhead surfaces. A detailed description of the resins, the use of their glass fiber anchors, and application procedures are in Section 3.1.5.

Table 3.15: Properties of Tyfo® SEH-51 Fibers and Tyfo® S Resin Composite System

Tensile Strength in fiber direction (N/mm^2)	**Tensile Strength** @ 90o to fiber direction (N/mm^2)	**Tensile Modulus** based on fiber area (N/mm^2)	**Maximum Elongation** Percent
552	37.95	27580	2.0

(*Fyfe Company, 1998*)

Typical appearance of the Tyfo® E-glass system can be seen in Figure 3.13.

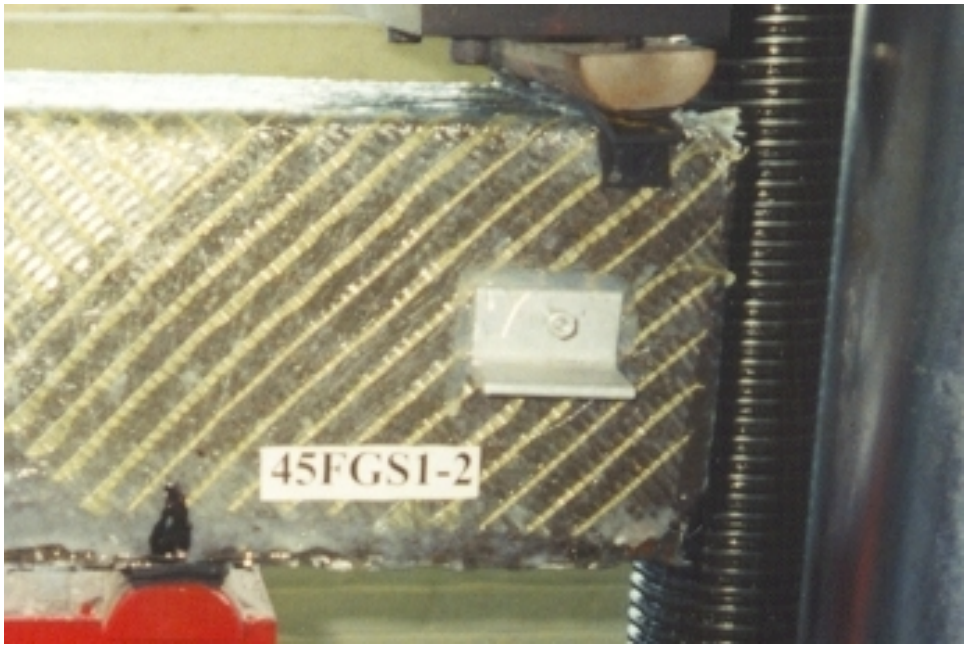

Figure 3.13: Typical appearance of Tyfo® E-glass system.

3.2.4 Clark Schwebel Structural Grid

The Clark Schwebel Structural Grid system is unique. According to the manufacturer, it can be used in a variety of reinforcement applications including reinforcing wood, asphalt overlays, and as external reinforcement for concrete. The grid is a non-woven glass fiber and epoxy composite. During the manufacturing process of the grid, the epoxy matrix is allowed to cure while the fibers are under uniform tension. This results in a grid that has a slight curve to it, but its thinness allows it to lie flat so that it is excellent for roadbed and concrete reinforcement applications. The company manufactures a variety of grid products with different grid spacing, but for this study only the T-1012 grid was used (*Clark Schwebel, 1997*). Typical material properties for the structural grid used in this study are in Table 3.16. The structural grid was attached to the concrete beams using Reichhold Chemicals' Atlac® 580-10 vinyl ester resin discussed in Section 3.1.6.

Table 3.16: Clark Schwebel Structural Grid Material Properties

Thickness (cm/ply)	**Tensile Strength** (N/mm^2)	**Tensile Modulus** (N/mm^2)	**Grid Openings** (cm)	**Standard Grid Width (cm)**
0.055	690	34500	.15 - .48	122

(*Clark Schwebel, 1997*)

Typical application procedures for the structural grid system are as follows:

- Following cleaning of roughened concrete surfaces, a light coating of Atlac® 580-10 resin is applied to the surface that is to receive the structural grid. This coating serves as a primer layer and is allowed to cure overnight.

- After curing of the initial layer, another, slightly thicker, layer of resin is applied to the prepared concrete beam surface.

- The resin coating is allowed to sit for approximately 5 minutes before the precut structural grid is applied.

- The structural grid is positioned on the resin coated concrete surface while the resin is still tacky.

- Evenly distributed pressure is applied over the structural grid, using small weights, while the resin cures for approximately 8 hours.

- After curing, an additional light coat of resin is applied to the grid to give it a smooth finish, and the reinforcement system is allowed to cure for at least 14 days.

The Reichhold Atlac® resin was prepared using 1.2 percent by weight of the Superox® catalyst. It was found that for the conditions in the laboratory, this ratio provided the pot life that was needed for installation of the structural grid. Once the catalyst was added, the two parts were mixed for approximately 3 minutes to assure thorough mixing. The resin was then applied to the beam using a short nap paint roller.

The Clark Schwebel Structural Grid was cut to size with a pair of heavy-duty scissors and was applied as described above. Typical appearance of a Clark Schwebel Structural Grid reinforced beam is shown in Figure 3.14

Figure 3.14: Typical appearance of Clark Schwebel Structural Grid.

3.2.5 Owens-Corning/Reichhold Chemicals

The Owens-Corning/Reichhold Chemicals, Inc. system is a glass FRP system currently under development by Composite Retrofit Systems (CRS), Salem, Oregon. The glass fiber sheets are manufactured by Owens Corning; the resin and primer are products of Reichhold Chemicals, Inc and are discussed in Section 3.1.6. The glass fibers are unidirectional and are held together by woven cross-fibers that are about 2.5 cm apart. The fiber rolls do not contain any pre-impregnating resins. The properties of the glass fibers are shown in Table 3.17. Application is accomplished by using a dry lay-up method.

Table 3.17: Owens-Corning Glass Fiber Properties

	A060	A130
Tensile Strength (kg/cm^2)	3450	3450
Tensile Modulus ($kg/cm^2 \times 10^6$)	72450	72450
Elongation at Failure (%)	4.8	4.8
Design Thickness (mm)	0.25	0.53

(*Owens-Corning, 1998*)

The typical application process for the Owens Corning/Reichhold Chemicals system was very similar to the CMI/Reichhold Chemicals system described in Section 3.1.6. The only significant difference in the application procedure was that no wet layup was done when placing the glass

fibers. Figure 3.15 shows the typical appearance of the Owens-Corning/Reichhold glass FRP reinforced concrete beams used in this study.

Figure 3.15: Typical appearance of Owens-Corning/Reichhold FRP composite beam reinforced at 45 degrees for shear.

3.3 FRP FOR COLUMN WRAPPING

In this study, two types of FRP were used to wrap concrete cylinders: carbon and E-glass. The carbon used was supplied by Fortafil Fiber, Inc. of Rockwood, Tennesee and the E-glass was supplied by Owens Corning. Both types of fibers were supplied as continuous multiple filament tows. Properties of the Fortafil® 556 fibers are shown in Table 3.18. Except for thickness, properties for the Owens Corning E-glass fibers are identical to those of the fibers used for beam reinforcing found in Table 3.17. Reichhold resin, discussed in Section 3.1.6, was used in the application of both types of fibers.

Table 3.18: Fortafil® 556 Continuous Carbon Fiber Properties

	Fiber Properties	Tow Properties
Tensile Strength (MPa)	3800	1930
Tensile Modulus (GPa)	230	130
Elongation at Failure (%)	1.65	NA
Flexural Strength (MPa)	NA	2280
Flexural Modulus (GPa)	NA	130
Shear Strength (Mpa)	NA	97

(*Fortafil Fibers, Inc., 1993*)

Fibers were applied to the specimens with the cylinder-wrapping machine described in Section 2.4.1. Following application of the FRP, all wrapped cylinders were allowed to cure for at least 14 days before testing. Figure 3.16 shows the typical appearance of the carbon wrapped cylinders and the E-glass wrapped cylinders used in this study.

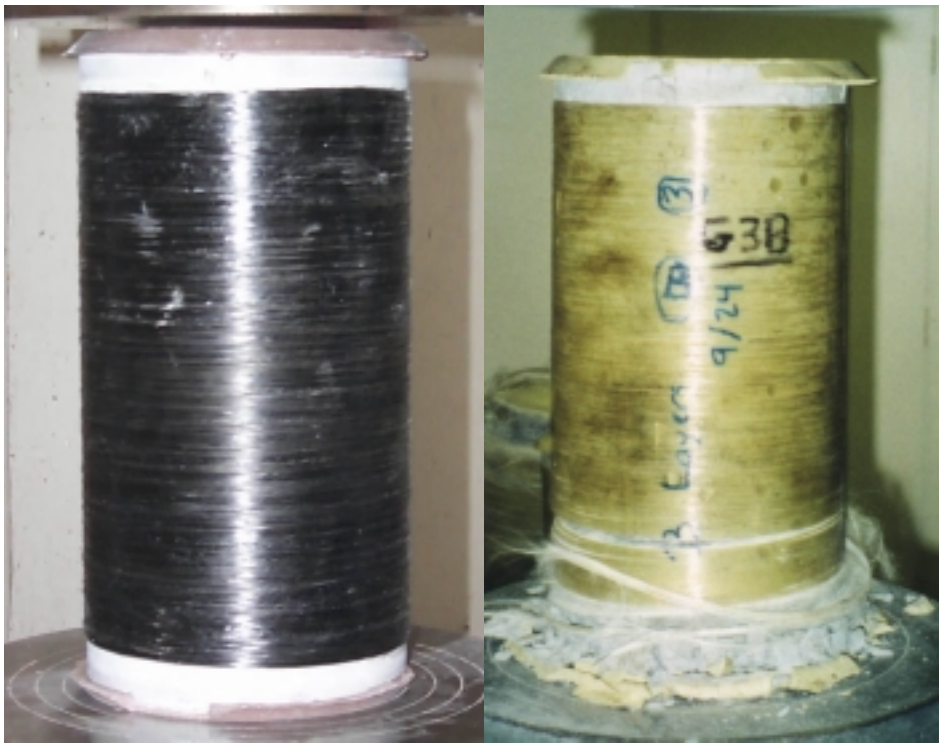

Figure 3.16: Typical appearance of CFRP (left) and GFRP reinforced cylinder, broken (right).

4.0 TEST RESULTS AND ANALYSIS

All of the FRP strengthened specimens showed significant gains in strength. Gains in sustained load at first crack were 20 to 200 percent above the control specimens. Increases in load at failure ranged from 18 to 545 percent.

Two hundred fifty-six reinforced concrete specimens were tested in this study, and the results are presented in the following sections. For each strengthening scheme, a representative specimen was chosen. The load-versus-deflection and load-versus-flexural strain graphs are presented for each of these specimens, as well as some discussion of the results. Complete results for all of the specimens tested are presented in Appendix A. Appendix B contains figures illustrating typical crack patterns and failure modes for each of the systems.

The specimens in this study exhibited a variety of failure modes. The governing failure mode was determined by the mechanical properties of the materials and the reinforcement scheme. The most typical failure mechanisms were: flexural failure of the beam and the laminate due to tension; shear (diagonal tension) failure of the beam; failure due to local stresses developed at the ends of the FRP laminate; and debonding (separation of concrete and laminate). Combinations of these failure modes were also observed.

The FRP-reinforced specimens showed significant increases in stiffness after initial cracking. The deflections at failure, however, were typically similar to or greater than those of the control samples. It is believed that the increased deflection was a result of the greater energy absorption capacity of the specimens provided by the FRP composites. These results contradict the general belief that application of high stiffness composites to a reinforced concrete member promotes brittle failure. It seems that the classical definition of ductility, the ratio of ultimate deformation (deflection or strain) to the deformation at yield, is not applicable to composites because of their linear stress-strain curves. We believe that adoption of energy principles provides a better approach for explaining the ductility of FRP-reinforced structural members. Ductility comparisons based on energy considerations require calculating a ratio incorporating inelastic energy and total energy expended in a beam test. The energy values are determined from analysis of the area under the load-deformation curves. For this study, qualitative ductility comparisons were made by comparing the area under the load-deformation curves after first crack.

Some of the results indicate that the effectiveness of the FRP composite decreases significantly in beams that are reinforced with very stiff laminates. It has been shown that the effectiveness of FRP strengthening varies greatly and is proportional to the axial rigidity of a particular laminate as expressed by the product $t_{frp}E_{frp}$, where t_{frp} is the FRP thickness, and E_{frp} is the FRP elastic modulus (*Triantafillou 1997, Kachlakev et al. 1998, Kachlakev and Barnes 1999*). As the FRP relative stiffness increases, so does the required bond development length. The effective strain developed in the composite laminate decreases, leading to a premature failure by debonding

rather than FRP tensile failure as shown in this study. The governing mode of failure for these specimens was typically in shear, thus reducing the ultimate load at failure and diminishing the effectiveness of the FRP. These results also indicate that over-reinforcement of the beams is possible and is detrimental to the behavior of the specimen.

The average results for each group of specimens are presented in Tables 4.1 and 4.2. Table 4.1 gives results at first crack while 4.2 gives results at failure.

Table 4.1: Average Results for FRP Systems at First Crack

Beam	Load (N)	Deflection (mm)	Flexural Strain (x 10-4)	E-Modulus (GPa)
Control	22895	0.0353	1.396	22.76
CSGF	36080	0.0568	2.815	16.56
CSGFS	39281	0.0738	2.299	22.70
CSGS	27864	0.0510	2.329	16.26
FCF1	43185	0.0619	3.222	17.36
FCF2	47633	0.0699	2.807	21.94
FCF3	46150	0.0661	2.775	21.56
FCFS1	48745	0.0871	3.158	19.93
FCFS2	53193	0.0779	2.750	25.13
FCFS3	59495	0.0638	3.011	25.70
45FCS1	45780	0.0476	2.469	23.96
45FCS2	47818	0.0604	2.705	22.85
45FCS3	56344	0.0567	3.075	23.67
FGF1	44668	0.1094	3.203	17.96
FGF2	44482	0.0624	3.509	16.41
FGF3	50042	0.0783	3.075	21.04
FGFS1	44853	0.0784	3.649	16.44
FGFS2	45780	0.0657	3.394	17.42
FGFS3	52637	0.0640	3.451	19.71
45FGS1	49301	0.0995	2.858	22.79
45FGS2	48189	0.0236	2.833	22.61
45FGS3	53749	0.0681	2.820	24.68
MBCF1	30659	0.0514	1.940	22.61
MBCF2	33848	0.0514	0.959	53.55
MBCF3	33067	0.0502	1.317	32.29
MBCFS1	34269	0.0466	2.059	21.67
MBCFS2	41874	0.0564	1.729	31.90
MBCFS3	43557	0.0756	1.137	49.48
MBGF1	32629	0.0439	1.937	21.04
MBGF2	36010	0.0492	2.234	21.48
MBGF3	38305	0.0459	2.543	19.70
MBGFS1	43793	0.0528	2.522	22.77
MBGFS2	39460	0.0578	2.644	19.75
MBGFS3	35964	0.0344	2.224	20.89
MBG2F1S	38215	0.0466	2.230	22.13
MCF1	37810	0.0808	2.680	18.33
MCF2	42984	0.0610	2.733	20.42
MCF3	43162	0.0627	2.462	22.66
MCFS1	42912	0.0609	2.792	19.98
MCFS2	44260	0.0695	2.724	20.97
MCFS3	48245	0.0579	2.520	24.76
45MCS1	36167	0.0619	NA	NA
45MCS2	38482	0.0486	NA	NA
45MCS3	45562	0.0599	NA	NA
90MCS1	35629	0.0542	NA	NA
90MCS2	37727	0.0449	NA	NA
90MCS3	39921	0.0423	NA	NA

Table 4.1 (continued): Average Results for FRP Systems at First Crack

Beam	Load (N)	Deflection (mm)	Flexural Strain (x 10-4)	E-Modulus (GPa)
SCF	52992	0.0752	3.12533	22.09
SHCF1	41173	0.0545	2.60900	20.48
SHCF2	41575	0.0562	2.51533	21.41
SHCFS1	46388	0.0739	2.61300	22.96
SHCFS2	46706	0.0637	2.57733	23.31
SCFS1	53193	0.0728	2.54533	27.02
SCFS2	51711	0.0580	2.74333	24.49
45SHCFS1	51664	0.0605	2.599	26.05
CMIRF1	39044	0.0590	2.98	17.23
CMIRF2	38271	0.0550	3.00	16.50
CMIRF3	37949	0.0357	2.65	17.56
CMIRFS1-90	32396	0.0524	2.77	15.32
CMIRFS2-90	43568	0.0937	3.38	16.75
CMIRFS3-90	40853	0.071	2.63	20.20
CMIRFS1-45	37936	0.0611	2.35	20.86
CMIRFS2-45	44877	0.0583	2.78	20.97
CMIRFS3-45	43196	0.0519	2.58	21.65
CMIRS1-45	31431	0.0788	NA	NA
CMIRS2-45	36034	0.0986	NA	NA
CMIRS3-45	42935	0.0973	NA	NA
OCRF1	35473	0.0890	3.14	14.95
OCRF2	35151	0.0577	2.97	15.42
OCRF3	35092	0.0750	2.44	18.89
OCRFS1-90	26741	0.0544	1.90	18.70
OCRFS2-90	36169	0.0542	1.92	27.64
OCRFS3-90	35709	0.0310	2.04	23.50
OCRFS1-45	39830	0.0611	1.85	27.91
OCRFS2-45	40153	0.0583	2.06	26.80
OCRFS3-45	44651	0.0519	2.32	21.30
OCRS1-45	30850	0.0657	NA	NA
OCRS2-45	36739	0.0495	NA	NA
OCRS3-45	34321	0.0685	NA	NA

Table 4.2: Average Results for FRP Systems at Failure (Ultimate Load).

Beam	Load (N)	Deflection (mm)	Flexural Strain (x 10-3)	Strain in Shear Laminate(x10-4)	Cracked Stiffness (N/mm)
Control	45851	1.617	NA	NA	NA
CSGF	84974	3.885	10.173	NA	40335
CSGFS	73870	3.532	18.644	NA	43102
CSGS	54151	3.396	18.493	NA	31969
FCF1	196092	2.893	8.210	NA	58603
FCF2	172925	1.586	3.995	NA	144105
FCF3	181080	1.343	3.008	NA	119807
FCFS1	217592	2.805	9.074	7.477	78311
FCFS2	264855	2.615	6.286	12.077	160252
FCFS3	295621	1.690	4.966	8.255	192249
45FCS1	168291	1.159	5.689	3.006	106177
45FCS2	189049	0.984	3.799	1.872	202648
45FCS3	216295	0.736	3.192	1.209	231110
FGF1	148274	3.749	13.975	NA	42747
FGF2	172554	2.787	9.110	NA	68188
FGF3	170144	1.854	5.340	NA	91858
FGFS1	155688	3.050	13.915	NA	52798
FGFS2	228898	2.989	11.677	NA	86628
FGFS3	265225	2.182	9.248	NA	115680
45FGS1	138822	1.779	7.824	4.801	70773
45FGS2	197761	1.482	6.509	2.971	124170
45FGS3	184231	0.936	4.140	1.995	163697
MBCF1	91936	1.877	5.053	NA	102965
MBCF2	107752	1.718	2.775	NA	174997
MBCF3	101362	1.153	2.551	NA	133781
MBCFS1	130415	1.809	7.318	NA	86700
MBCFS2	143058	1.730	3.936	NA	147546
MBCFS3	169557	3.614	3.198	NA	107097
MBGF1	66201	1.519	6.306	NA	116982
MBGF2	99009	2.704	8.694	NA	141999
MBGF3	103297	2.212	9.249	NA	43536
MBGFS1	66561	0.989	9.048	NA	75621
MBGFS2	101889	2.490	9.366	NA	70833
MBGFS3	120324	2.245	9.867	NA	59185
MBG2F1S	100846	3.618	9.645	NA	NA
MCF1	134984	2.687	8.38850	NA	63105
MCF2	189754	2.240	6.572	NA	89120
MCF3	164665	1.493	4.004	NA	151464
MCFS1	175499	2.490	9.650	10.959	80133
MCFS2	227906	2.570	7.848	10.501	92304
MCFS3	201096	1.179	4.767	8.376	139819
45MCS1	129182	1.909	NA	38.088	75075
45MCS2	160628	1.389	NA	25.435	92304
45MCS3	170152	0.969	NA	18.947	152925
90MCS1	38792	0.457	NA	NA	NA
90MCS2	59397	0.450	NA	NA	NA
90MCS3	58610	0.489	NA	NA	NA

Table 4.2 (continued): Average Results for FRP Systems at Failure (Ultimate Load).

Beam	Load (N)	Deflection (mm)	Flexural Strain (x 10-3)	Strain in Shear Laminate(x10-4)	Cracked Stiffness (N/mm)
SCF	175743	1.145	2.724	NA	139993
SHCF1	141313	1.665	5.289	NA	66985
SHCF2	143360	1.183	3.206	NA	107064
SHCFS1	174794	1.717	6.575	NA	73970
SHCFS2	247432	2.103	5.622	NA	119369
SCFS1	206286	1.216	3.652	NA	145095
SCFS2	233532	1.335	4.129	NA	160361
45SHCFS1	226966	1.704	4.063	111.675	152459
CMIRF1	69290	0.897	5.246	NA	40400
CMIRF2	121723	2.689	9.13	NA	48607
CMIRF3	123918	1.757	5.798	NA	63420
CMIRFS1-90	72952	1.328	5.35	NA	39773
CMIRFS2-90	99090	1.570	6.343	NA	45939
CMIRFS3-90	138551	2.133	7.277	NA	58881
CMIRFS1-45	117827	1.509	6.055	47.26	56541
CMIRFS2-45	154768	1.267	5.249	32.71	86494
CMIRFS3-45	175554	1.366	4.988	25.27	121322
CMIRS1-45	80047	1.353	NA	28.91	44569
CMIRS2-45	114592	1.926	NA	29.20	62626
CMIRS3-45	123639	1.383	NA	26.92	78969
OCRF1	61341	1.529	8.39	NA	33338
OCRF2	100006	4.03	12.03	NA	44297
OCRF3	127821	4.06	15.35	NA	48723
OCRFS1-90	60368	1.400	8.52	NA	35460
OCRFS2-90	111873	3.70	9.49	NA	50815
OCRFS3-90	128810	3.793	9.58	NA	45151
OCRFS1-45	100278	2.349	8.787	98.44	41052
OCRFS2-45	134451	2.545	6.176	35.12	68698
OCRFS3-45	167954	1.829	5.898	35.46	86077
OCRS1-45	74765	1.738	NA	28.91	39020
OCRS2-45	105424	2.637	NA	29.20	57172
OCRS3-45	108637	1.619	NA	26.92	64760

4.1 CONTROL SPECIMENS

Five control specimens were tested without FRP reinforcement. The control specimens were designed to fail in flexure. Four of the five beams failed in flexure as expected. The fifth control specimen failed in shear at a significantly lower load than the others did. The behavior of this specimen was not typical of the other control specimens and the results were excluded from the averages of the control beam data.

Figure 4.1, and Figure 4.2 show the load-versus-deflection and load-versus-strain curves, respectively, for a representative sample from the group of control specimens.

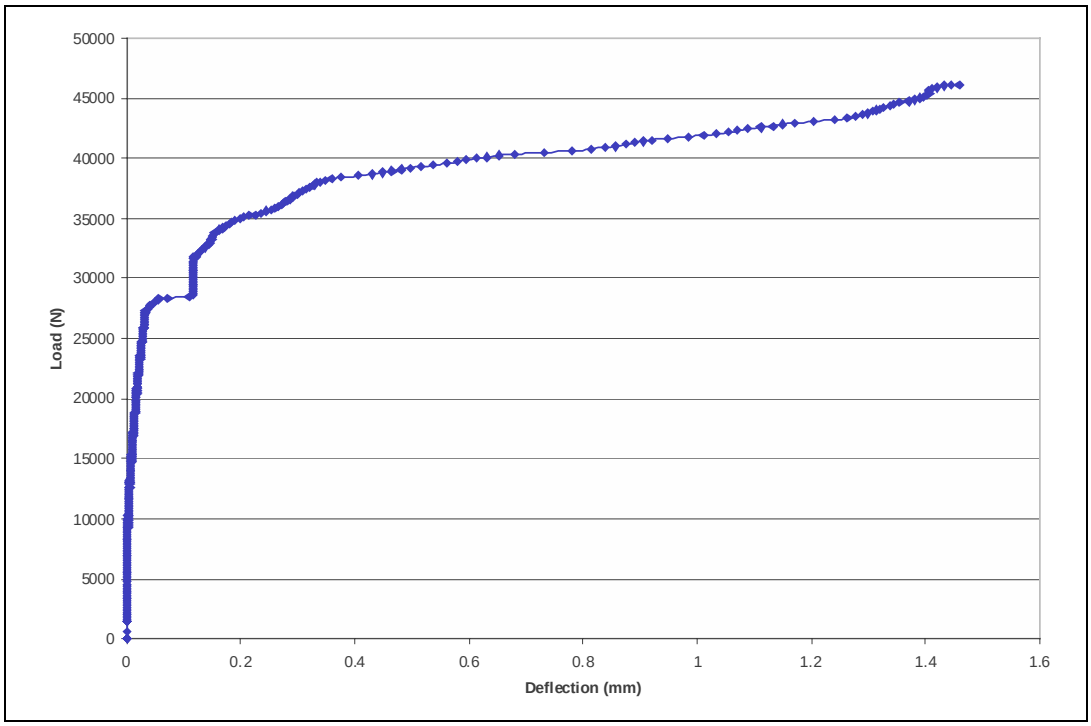

Figure 4.1: Typical load-versus-deflection behavior of control specimens

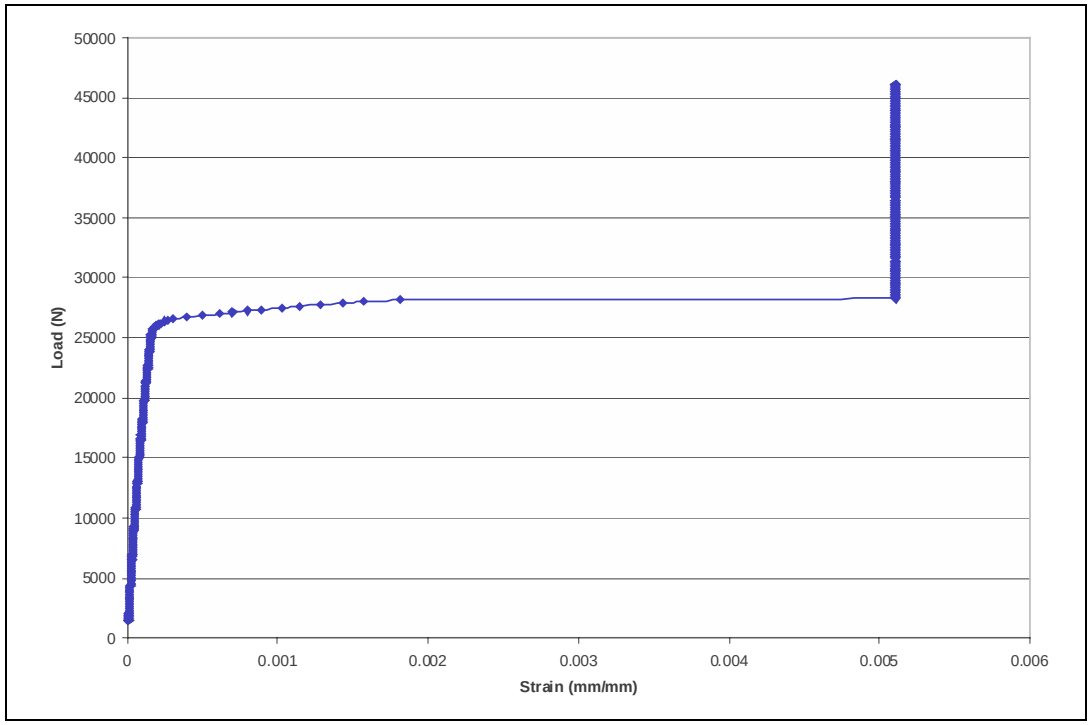

Figure 4.2: Typical stress-versus-strain behavior for control specimens

Of the four initial control specimens that failed in flexure, the average load at failure was 46,000 N. Average deflection at failure was approximately 1.5 mm. Initial cracking occurred at approximately 26,000 N.

Strain measurements of three additional control beams were recorded using fiber optic sensors. A Bragg grating sensor on standard telecom optical fiber was used in the center of the tensile face of each specimen. This fiber optic gauge was attached to the specimen with a high modulus epoxy. During testing, a broadband light source was directed into the optical fiber. A portion of the light traveled through the sensor and a narrow-band wavelength of light was reflected to the detector. The system converted the input at the detectors into two voltages. The ratio of the two voltages was used to determine a change in wavelength of the light, and the change in wavelength corresponded to a change in strain (*Blue Road Research, 1999*).

Analysis of the data collected from the three additional specimens yielded results similar to the initial five control specimens. The strain at failure of the specimens ranged from 3500 to 9400 microstrain, while the strain at the appearance of the first crack was approximately 350 microstrain. These readings confirmed the results that were collected on the first five control specimens. Load and deflection data were also very similar for the three specimens as compared to the initial five beams. Typical failure modes for the control specimens are illustrated in Figure 4.3.

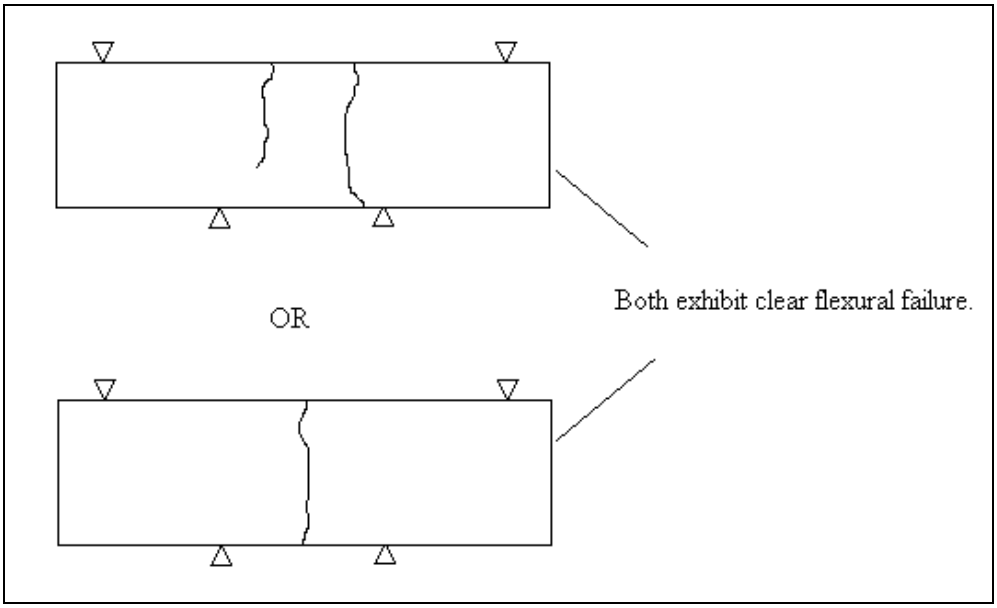

Figure 4.3: Typical control beam failure modes.

4.2 REPLARK® CARBON FRP SYSTEM

Specimens reinforced with the Replark® carbon FRP system exhibited strength increases from 30 to 400 percent. Results from this study seem to indicate that the bond developed between the Replark laminate and the concrete surface was excellent. Debonding of the flexural laminate was not observed. Elongation at failure of the flexural laminates was close to 1 percent (as suggested by the manufacturer).

4.2.1 Flexural Reinforcement Only

Strength increases over the control specimens were 190, 310, and 260 percent, respectively, for one-, two- and three-layer beams. The decrease in ultimate strength between the two- and three-layer beams was possibly the result of a change in failure mode. Both two- and three-layer specimens failed predominately in shear. However, the three-layer specimens did not exhibit flexural cracking. Increasing the number of layers appeared to have little effect on the load at initial cracking.

Replark® reinforced beams did not exhibit any slippage after initial cracking. This behavior was due to adequate bonding both between the laminate and the concrete and between the fibers and the resin matrix within the laminate. Typical specimen behavior is shown in Figures 4.4 and 4.5.

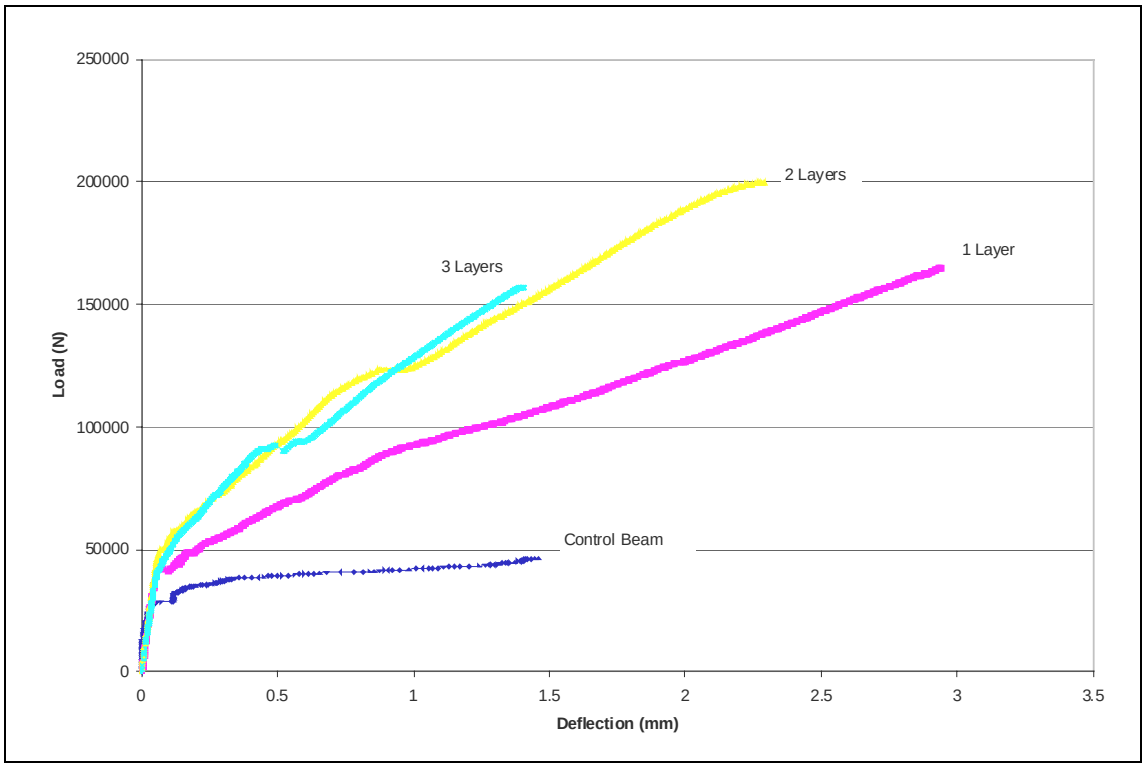

Figure 4.4: Typical load-versus-deflection behavior for specimens reinforced with Replark® for flexure only

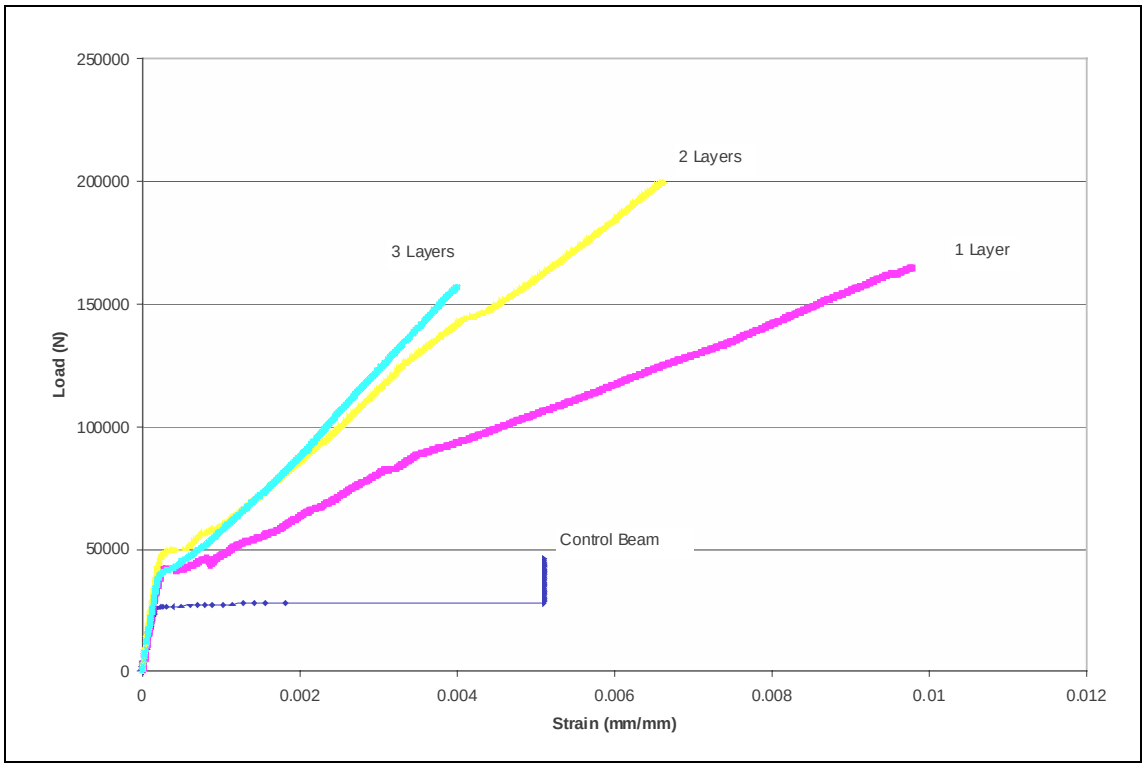

Figure 4.5: Load versus strain for specimens reinforced for flexure only with Replark®

Reinforcement of the specimens caused the mode of failure to change from flexural failure, as in the control beams, to shear or combined failure. In some cases, the laminate, along with a substantial amount of concrete, was pulled out of the beam. This was not considered a debonding failure, as one to three centimeters of concrete were still attached to the surface of the laminate that was pulled off.

4.2.2 Flexural Reinforcement and Shear reinforcement at 90^{o}

Strength gains were significantly higher than for the specimens reinforced for flexure only. Increases over the control specimens were 280, 400, and 340 percent for the one-, two- and three-layer beams, respectively. The shear laminate added approximately 80 to 90 percent additional strength to the flexurally reinforced members. The loads at first crack were also increased by about 10 percent over the flexurally reinforced specimens. Load-versus-deflection and load-versus-strain curves are presented in Figure 4.6 and Figure 4.7.

General trends of the load-versus-strain and load-versus-deflection curves are similar to the members reinforced for flexure only.

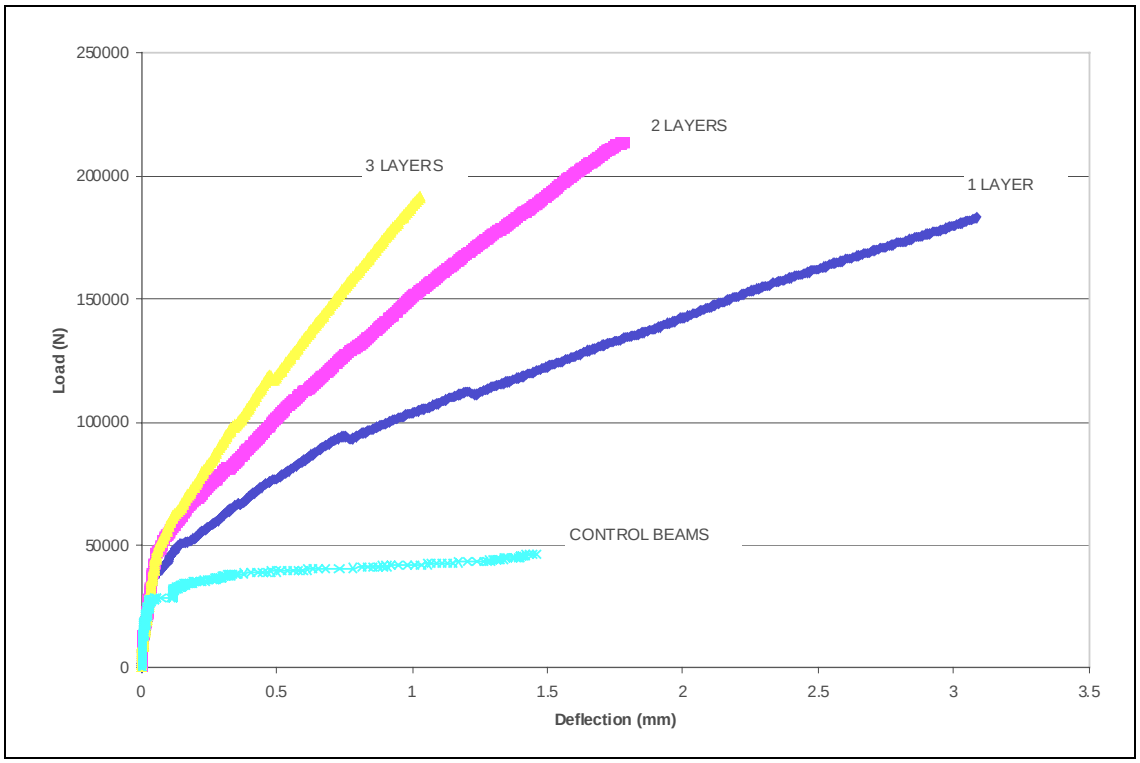

Figure 4.6: Typical load-versus-deflection behavior for specimens reinforced with Replark® for flexure and shear at 90^{o}

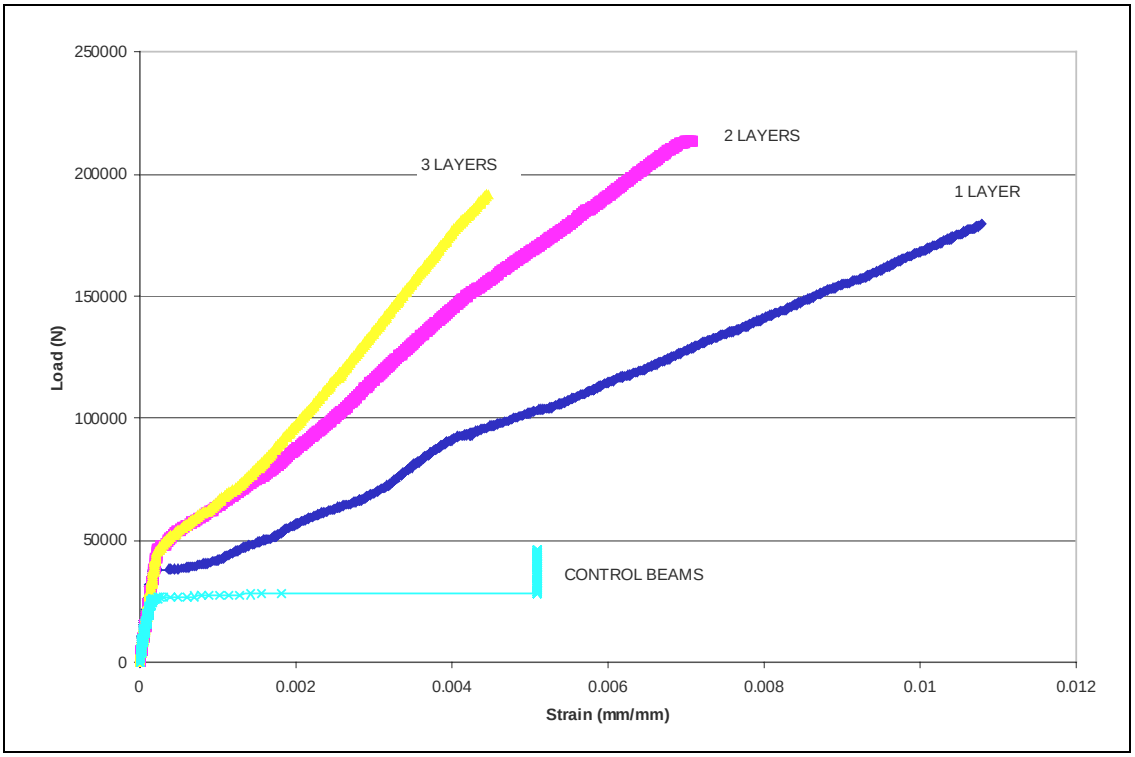

Figure 4.7: Typical load versus strain for specimens reinforced for flexure and shear at 90^{o} with Replark®

Counter-intuitively, it is expected that composite-retrofitted beams would exhibit increased stiffness when compared to control specimens. It is also logical to expect that the greater the laminate thickness, the stiffer the reinforced-concrete member. This should be apparent not only after cracking, but in the linear elastic range as well. As is seen in Figures 4.6 and 4.7, these expectations were not met. The figures indicate that the addition of FRP reinforcement to the reinforced concrete beam had no significant influence on the modulus of elasticity of that beam in the linear region (before cracking of the concrete), but only affected the beam after cracking occurred. These observations suggest that the FRP reinforcement served only to delay the point at which the initial cracking occurs, in terms of load, strain, and deflection, but had no significant effect on the uncracked elastic beam modulus. As addition of steel reinforcement does not significantly enhance the elastic modulus of reinforced concrete beyond that of plain concrete, the small amount of FRP compared to concrete does not noticeably influence the beam modulus. This behavior is typical among all systems presented.

The mode of failure for the one-layer flexurally reinforced specimens was changed from shear to flexure, due to the addition of the shear reinforcement. The two-layer reinforced specimens exhibited shear failure in the concrete as well as cracking at the ends. The vertical cracking was possibly due to wedging action of the ribs of the rebar while the horizontal cracking was likely due to dowel action of the steel reinforcement. The three-layer specimens failed primarily from peeling away of the shear laminate, leading to shear failure.

4.2.3 Shear Reinforcement at 45^{o}

The specimens reinforced for shear at 45^{o} displayed significant increases in stiffness and strength. The load at the appearance of the first crack was also approximately 60 percent higher than that for the control specimens. This increase in load at initial cracking was most likely the result of the confinement provided by the wrapping technique used for laying up the fibers as described in Section 2.3. The reinforcement provided enough flexural strengthening to cause shear failures in the specimen. Each specimen failed with a pulling off or debonding of the shear laminate. The load-versus-deflection diagram is presented in Figure 4.8.

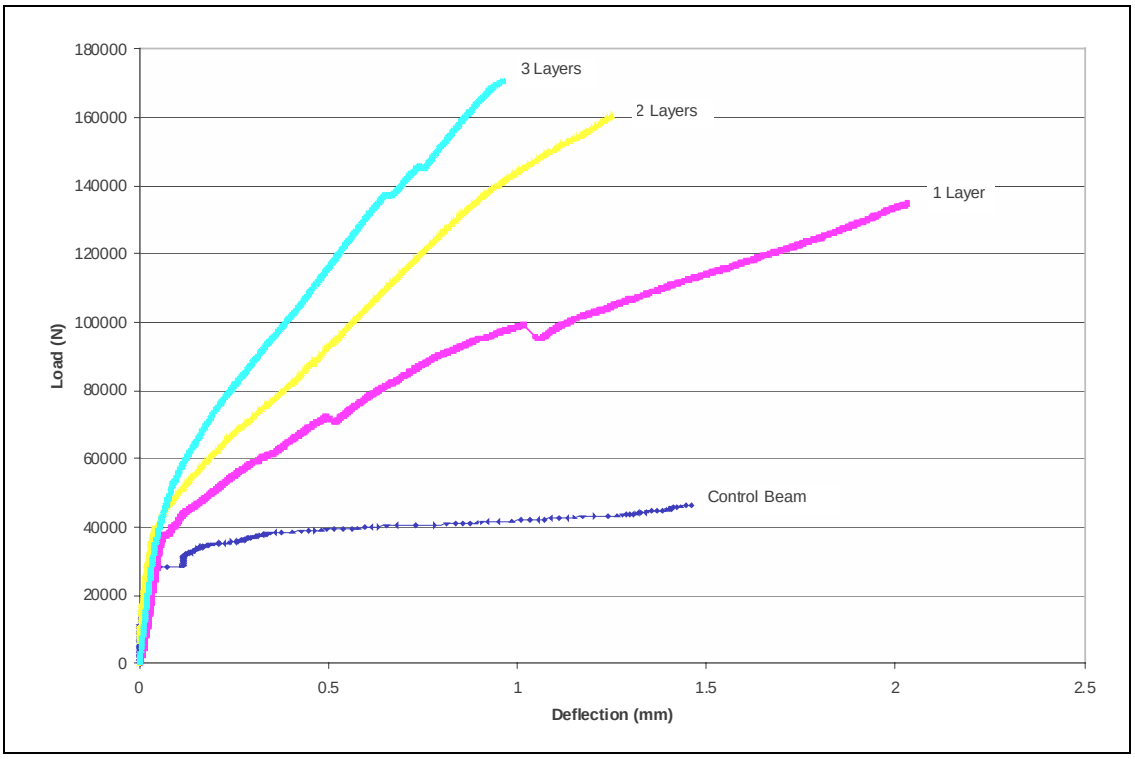

Figure 4.8: Typical load versus deflection for specimens reinforced at 45^{o} for shear with Replark®

Flexural strains were not measured on the 45^{o} shear members. Strain gauges were placed in the direction of the fibers at 45^{o} on the sides of the specimens. This is consistent with the other schemes in which strains are measured in the direction of the fibers. Figure 4.9 shows typical results from these measurements. Shear strains were not measured in the control specimens.

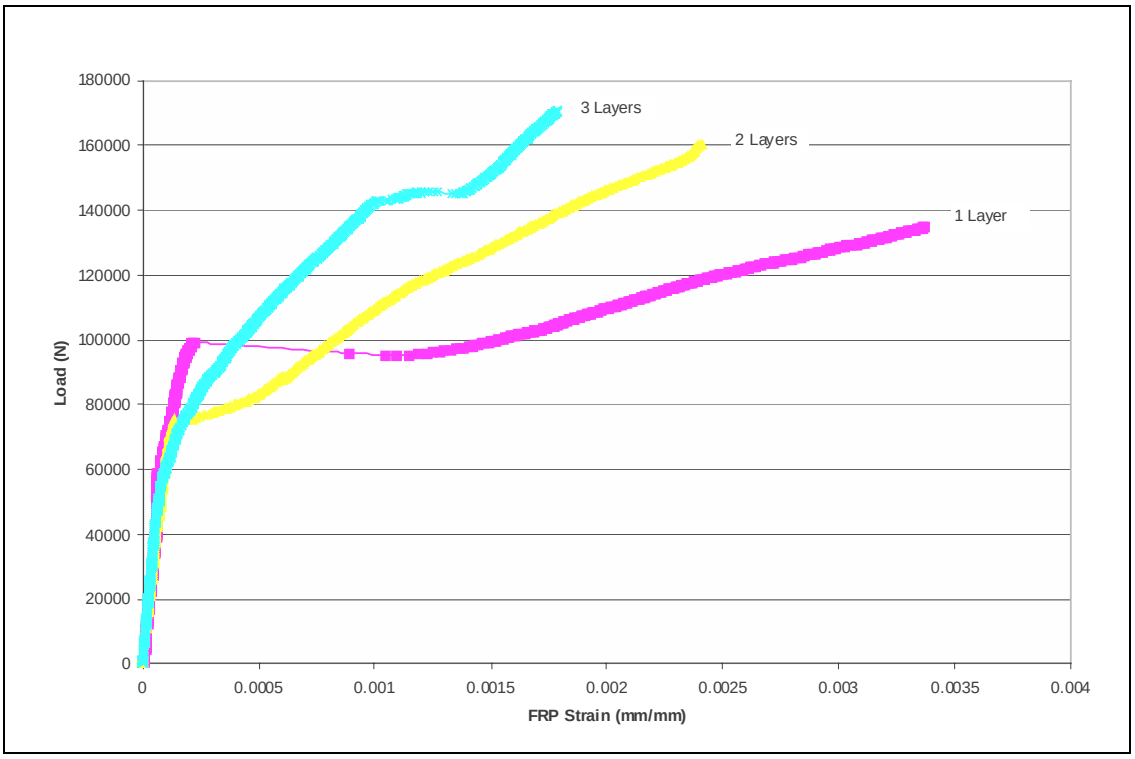

Figure 4.9: Typical load versus shear strain for Replark® specimens reinforced at 45^{o}

An important point observed in Figure 4.9 is the location at which the strain begins to develop in the fibers. For the three-layer specimens, the strain begins to increase significantly at approximately 60,000 N. It is believed that this is due to the substantial flexural stiffness of the specimen provided by the unidirectional and 45-degree laminates, and the orientation of the gauges. Consequently, stresses are immediately transferred to the shear laminate. For the one- and two-layer beams, these strains begin to increase significantly at approximately 100,000 and 78,000 N, respectively. These results reinforce the notion that development of higher flexural stress results in less stress transferred to the shear reinforcement. This also illustrates the tendency of stresses to transfer to the stiffest portion of a member, in this case, first to the flexural area, then to the shear area.

4.2.4 Shear Reinforcement at 90^{o}

An attempt was made to assess the effect of shear reinforcement positioned at 90 degrees relative to the longitudinal axis of the beam. Due to the anisotropy of FRP composites, the strength and elastic properties of these materials vary with direction (*Kachlakev, 1998; Daniel and Ishai, 1994; Jones, 1975*). Substantially higher strength is achieved when the load is applied in the direction of fibers. The strength of FRP in the direction perpendicular to the fiber orientation is mainly provided by the matrix. In the retrofitting scheme in question, i.e., shear at 90 degrees, the fibers are oriented perpendicular to the beam span, and no significant increase of the load-carrying capacity can be expected. However, the 90-degree reinforcement was considered in

order to compliment the scope of the study. Test results confirmed the theoretical expectation of a relatively small contribution to the flexural strength. One-layer beams showed no increase in strength while two- and three-layer specimens exhibited less than a 30 percent increase. Thus, this strengthening scheme was not investigated in the other FRP systems in this study.

Figure 4.10 shows increases in stiffness after cracking. Load at initial cracking increased by approximately 60 percent. For each beam, deflections after the initial cracking were significantly reduced.

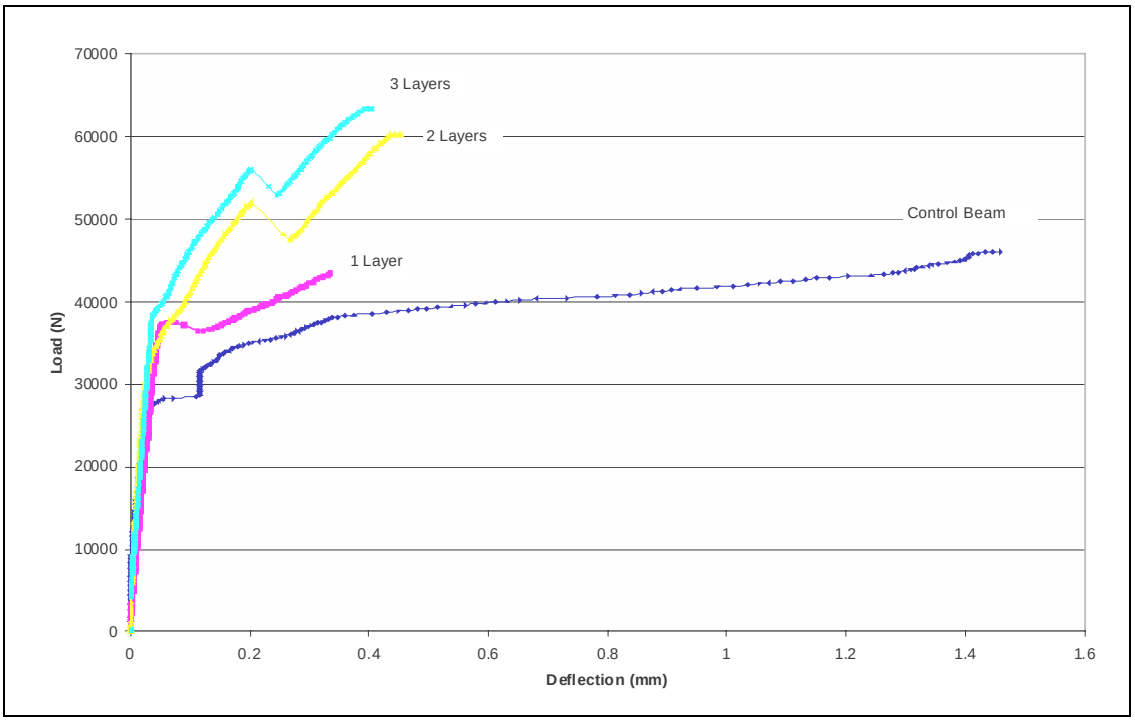

Figure 4.10: Typical load versus deflection for 90^{o} shear reinforced Replark® specimens

Deflection at failure was decreased by over 60 percent in each of the specimens. Consequently, the failure of the beams tended to be more brittle.

4.3 CARBODUR® AND SIKAWRAP® HEX CARBON FRP SYSTEM

Specimens reinforced with Sika products exhibited strength increases from 200 to 440 percent. Bonding of both types of material to the concrete appeared sufficient. Debonding of the flexural laminate was not observed in any of the Carbodur® specimens. Because of the Carbodur® laminate's high strength and thickness (due to the pultrusion manufacturing process), it was not possible to impose laminate failure, given the relatively small dimensions of the specimens.

4.3.1 Flexural Reinforcement Only

The thickness of the Carbodur® material is nearly 10 times that of some of the other systems tested. Thus, only one-layer specimens were fabricated. Strength increases for the flexurally reinforced beams were significant. With one or two layers of the SikaWrap® Hex 103C system, the load at failure was increased by over 200 percent above the control beams. For the Carbodur® beams, the improvement was approximately 280 percent. Presumably, there was some effect on the shear resistance supplied by the flexural reinforcement, or one would expect that all of the beams would have failed at similar loads, since the mode of failure for each beam was changed from flexure to shear.

The beam reinforced with two layers of the SikaWrap® Hex system failed at a similar ultimate load as the one-layer beam. Figure 4.11 seems to indicate that the two-layer specimens failed at a lower load than with one layer. When the average values are compared, however, there is no significant difference. It was initially assumed that this was an example of over-strengthening, causing stress concentrations and premature failure. However, at similar strain values, the two-layered beams exhibited higher sustained loads all across the band. In general, although the ultimate load at failure of the two-layer beam was similar that that of the one-layer beam, the performance of the second one was still considered superior. The beam reinforced with Carbodur®, however, was reinforced with a thicker, stiffer, stronger laminate, and yet exhibited higher ultimate load. It is therefore possible that the decrease in load-carrying capacity of the two-layer laminates is due to bonding problems between layers. In addition, the amount of resin between layers and the penetration of the resin into the fibers also have significant effects on the laminate performance. The Carbodur® did not exhibit these problems, since it is manufactured as a single layer pultruded laminate.

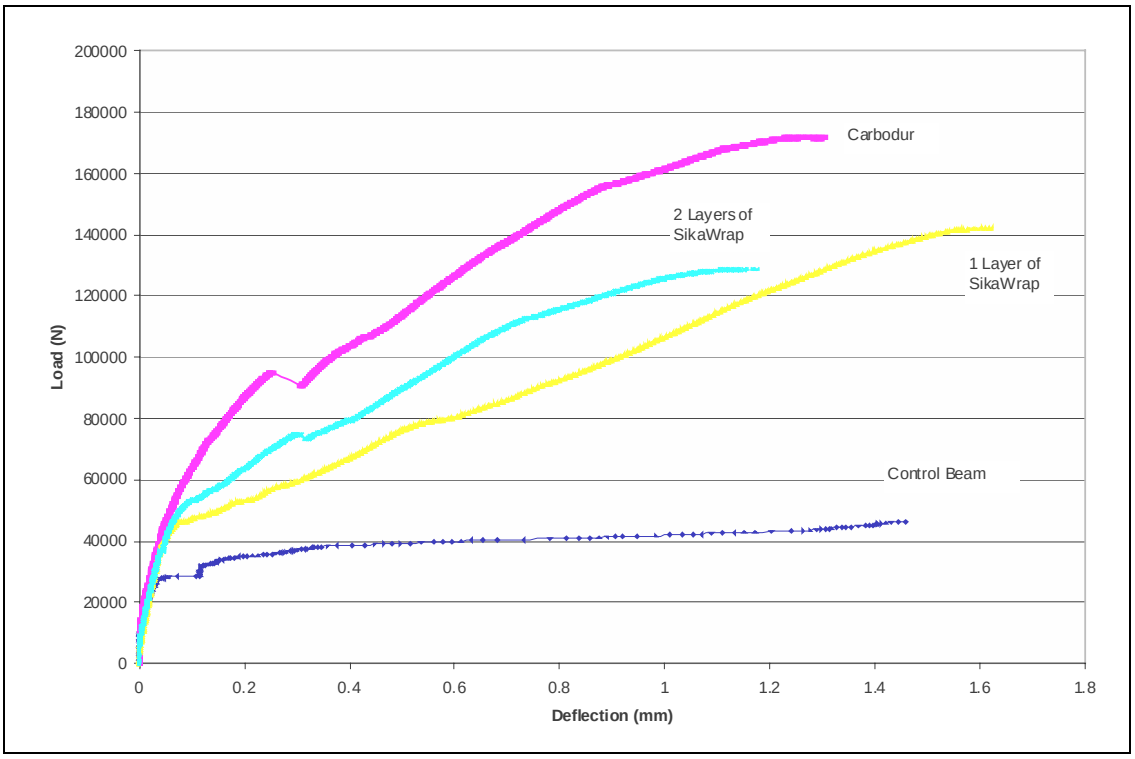

Figure 4.11: Typical load-versus-deflection behavior for specimens reinforced for flexure only with Sika carbon products

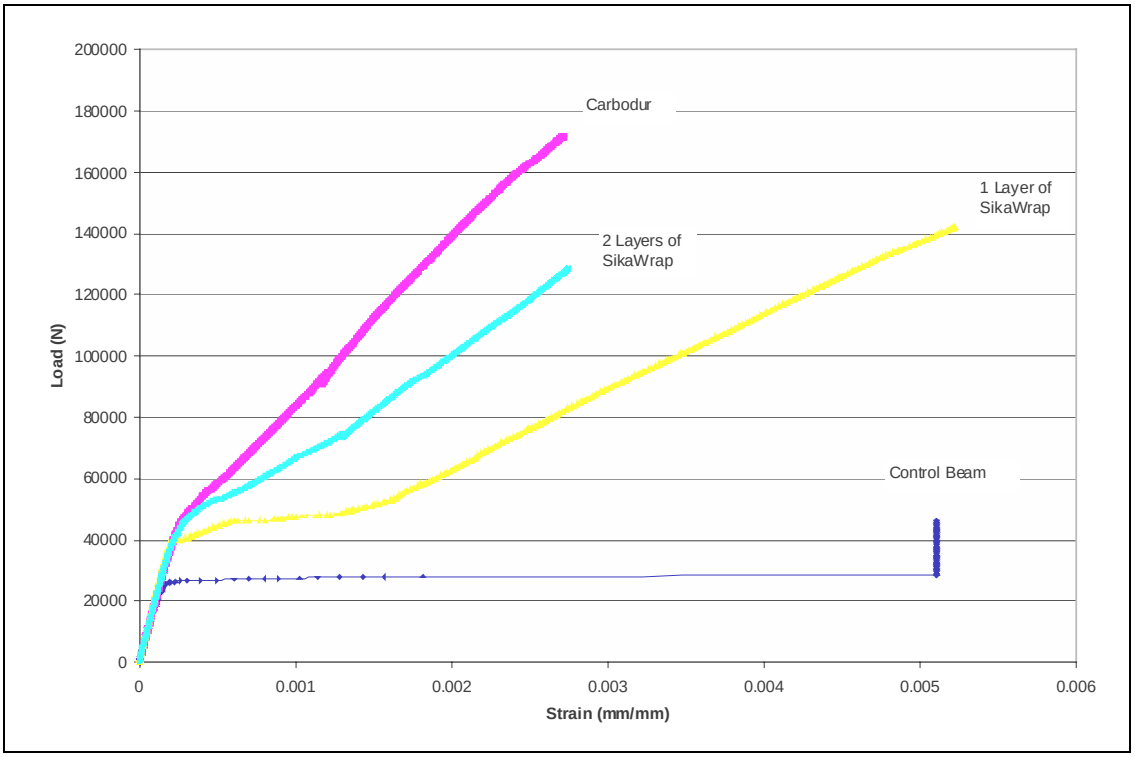

Figure 4.12: Typical load versus strain for specimens reinforced for flexure only with Sika carbon products

The Sikadur® 30 epoxy used to bond the Carbodur® laminate appeared to possess very good bond characteristics. The Carbodur® reinforced specimens developed stresses high enough to cause local concrete cracking at the ends of the beams without debonding. The bond between the SikaWrap® fiber sheet and the concrete was adequate, although there were signs of stress in the epoxy. Separation of the laminate from the concrete was observed in some of the two-layer specimens.

4.3.2 Flexural Reinforcement and Shear Reinforcement at 90^o

Three reinforcement schemes were used for Sika/Hexcel products in this study, employing one and two layers of fiber sheet reinforcement (SikaWrap® Hex 101G) applied for shear and flexural retrofit, and Carbodur® reinforcement for flexural reinforcement and SikaWrap® Hex 101G for shear reinforcement. The SikaWrap® Hex 101G consisted of $\pm 45^o$ oriented E-glass grid, the only commercially available product with off-axis fiber orientation. The behavior of the beams retrofitted with SikaWrap® Hex 101G was primarily dependent on the behavior of the Carbodur® reinforcement. Therefore, the performance of these specimens was compared to the carbon systems, rather than to glass.

The first reinforcing scheme used SikaWrap® Hex 103G carbon FRP as flexural and shear reinforcement. The one- and two-layer specimens showed increases in load at failure of 280 and 440 percent respectively. The bond problems in the flexurally reinforced specimens were not observed in the members with flexure and shear reinforcement.

Another reinforcing scheme studied combined the Carbodur® and SikaWrap® Hex 103C carbon systems. One layer of Carbodur® strip was used as the flexural reinforcement in combination with one and two layers of SikaWrap® Hex 103C for shear reinforcement.

The third retrofit scheme used the Carbodur® system for flexural reinforcement and the SikaWrap® Hex 101G system for shear reinforcement. One layer of reinforcement was used on each of the five specimens tested. Since the fabric had a natural fiber orientation of $\pm 45^o$, it was applied in the same manner as the fabric at 90^o. The specimens showed ultimate strength gains of approximately 400 percent over the control specimens.

Figures 4.13 and 4.14 show the typical load-versus-deflection and load-versus-strain curves for all specimens reinforced for shear and flexure with the Sika/ Hexcel products.

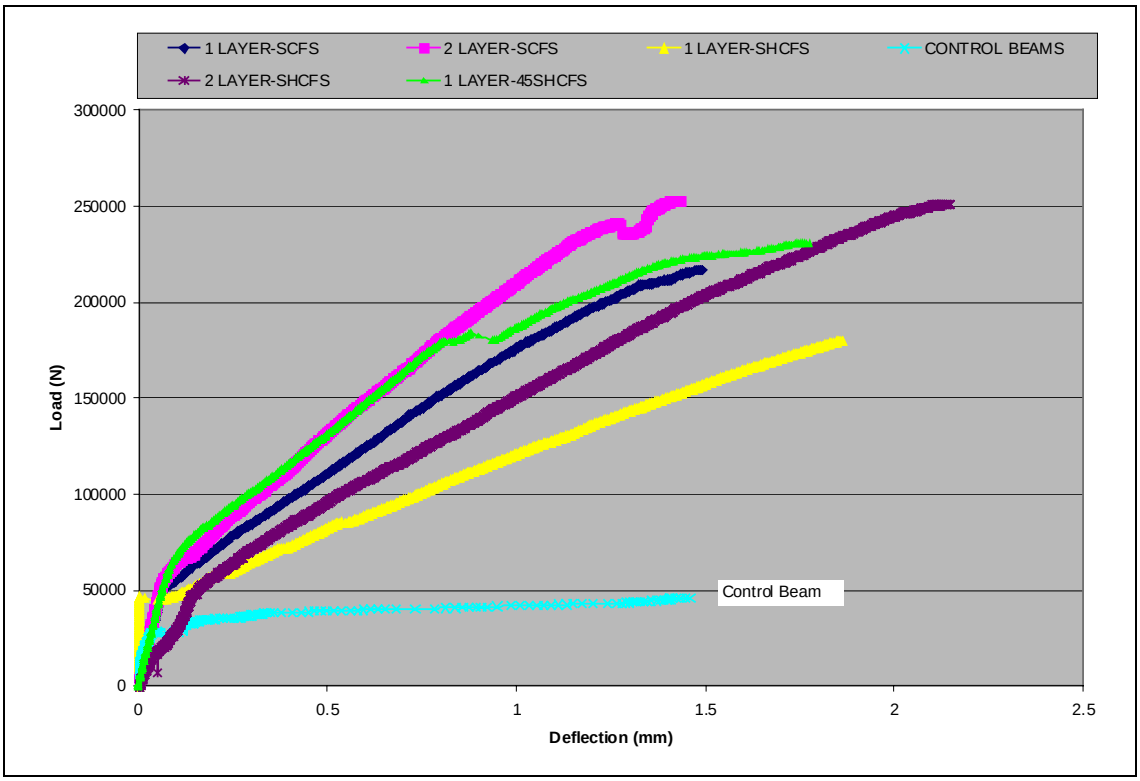

Figure 4.13: Typical load-versus-deflection curves for specimens reinforced with Sika products for shear and flexure

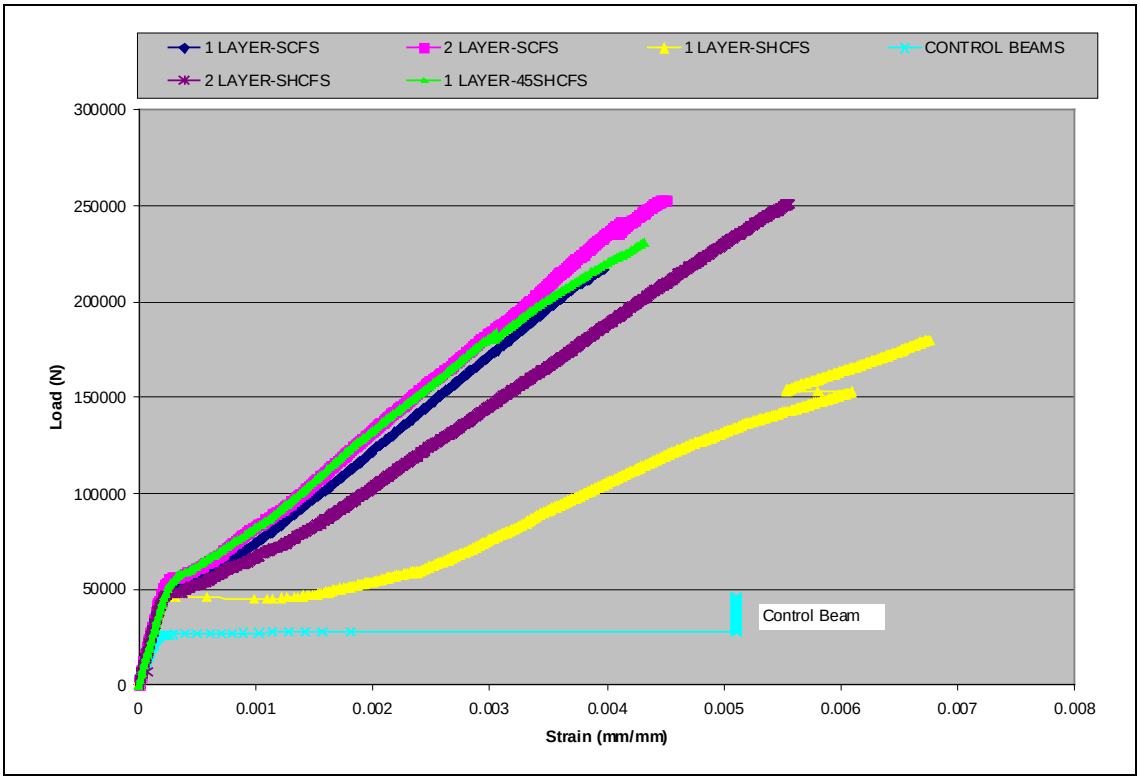

Figure 4.14: Typical stress-versus-strain curves for specimens reinforced with Sika products for shear and flexure

Flexural failure of the concrete and the laminate dominated the failure mode in the one-layer SikaWrap beams. Flexural cracks were observed in the two-layer specimens. However, shear cracking of the concrete and failure of the shear laminate caused ultimate failure. Cracks due to local stresses were also observed at the end of the specimens. Concrete specimens with one layer of Carbodur® for flexure and one layer of SikaWrap® for shear failed primarily from the local stresses at the ends of the flexural laminate. The end of the specimens cracked horizontally and vertically through the location of the rebar as described in Section 4.3.1. The specimens with two layers of SikaWrap® for shear showed the same horizontal cracking of the end of the beam. However, the specimens failed due to pulling off of the shear laminate and shearing of the concrete. The specimens reinforced for shear with the SikaWrap® Hex 101G grid failed primarily due to shear laminate pulling off and shear failure of the concrete.

4.4 TYFO® CARBON FRP SYSTEM

The specimens reinforced with the Tyfo® carbon system exhibited strength gains ranging from approximately 260 percent to over 540 percent over the control samples. The failure modes included shear failure of the concrete with cracking due to concentrated stresses at the ends of the flexural reinforcement, flexural failure of the specimen with the flexural laminate being pulled off, and shear failure combined with pulling off of the shear laminate.

4.4.1 Flexural Reinforcement Only

The ultimate strength of the one-layer specimens was increased by 330 percent over the controls. For the two- and three-layer specimens, strength gains were 280 and 300 percent respectively. Typical load-versus-deflection behavior is shown in Figure 4.15.

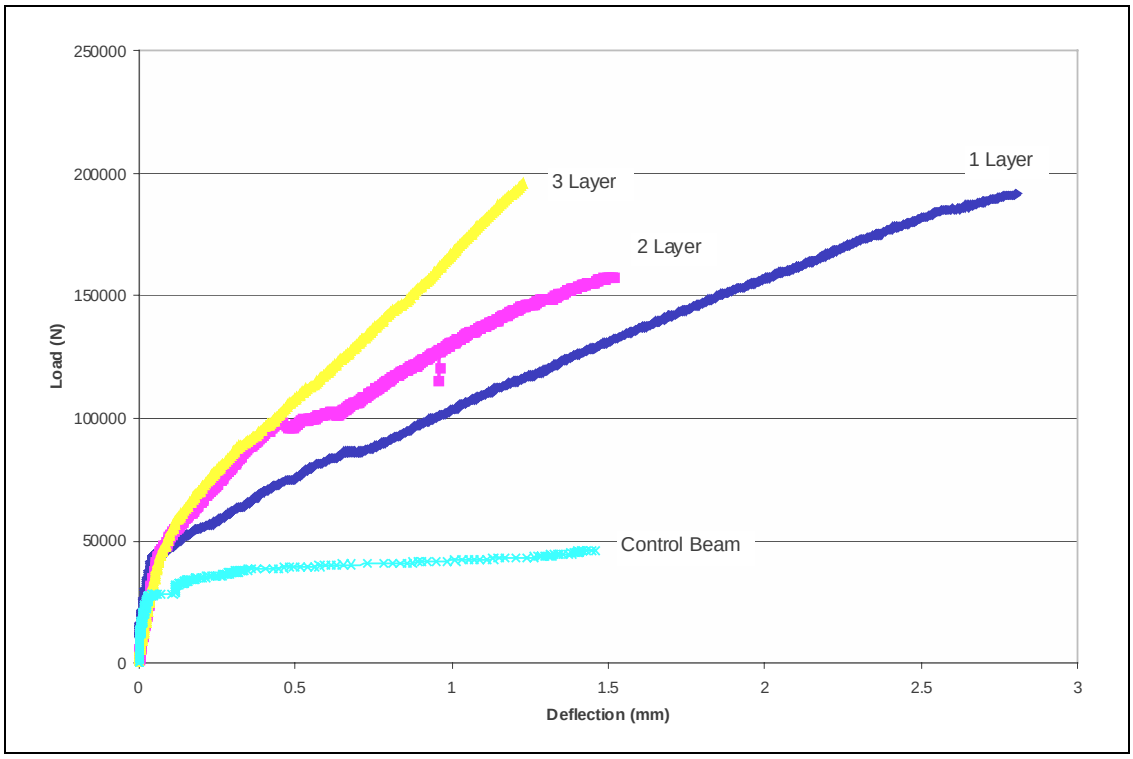

Figure 4.15: Typical load-versus-deflection curves for specimens reinforced with Tyfo® carbon for flexure only

The deflection at failure of the one-layer specimens was 90 percent higher than the control. The bond between the laminate and the concrete surface was apparently sufficient. This is evident from the load-versus-strain curve presented in Figure 4.16. Debonding of the laminate was not observed.

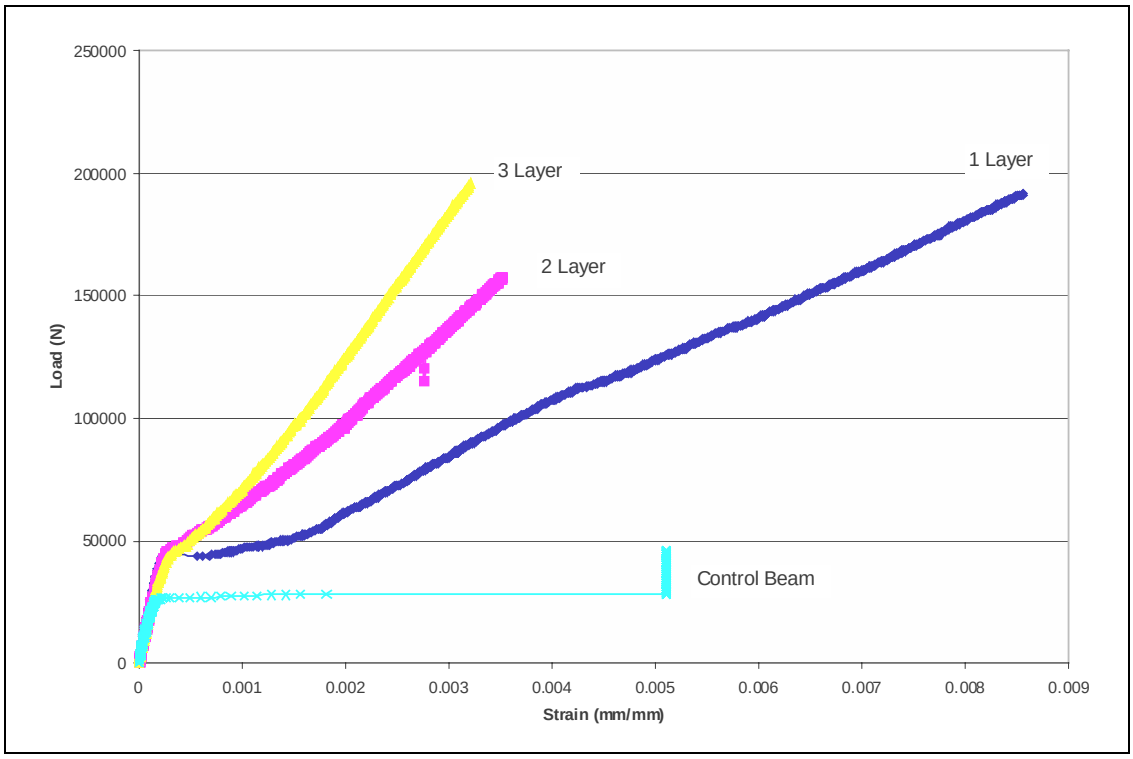

Figure 4.16: Typical load-versus-strain curves for specimens reinforced with Tyfo® carbon for flexure only

The two- and three-layer specimens appeared to be over-reinforced. This behavior was similar to that discussed in Section 4.2.

4.4.2 Flexural Reinforcement and Shear Reinforcement at 90^{o}

Increases in strength over the control specimens were 375, 480, and 545 percent for the one-, two-, and three-layer beams, respectively. Unlike many of the other systems tested, there was no decrease in ultimate sustained load with increasing the thickness of the FRP reinforcement, although there was a significant decrease in the effectiveness of the composite material. It is possible that the reduction in ultimate load of the specimens of the other systems reinforced with thicker laminates, is due to the limited ability of the laminates to bond to the concrete. The ability to bond is controlled by the characteristics of the different epoxies used. When enhancement of the shear capacity is targeted, the manufacturer prescribes using the Tyfo® carbon system with specially developed FRP anchors. However, no such devices were used in this study due to the relatively small size of the beam specimens. Even without the anchors, the performance of the Tyfo®- reinforced concrete members was adequate.

The load at initial cracking was increased by 110, 130, and 155 percent for the one-, two-, and three-layer specimens, respectively. The load-versus-deflection and load-versus-strain behavior of the Tyfo® carbon reinforced specimens is shown in Figures 4.17 and 4.18.

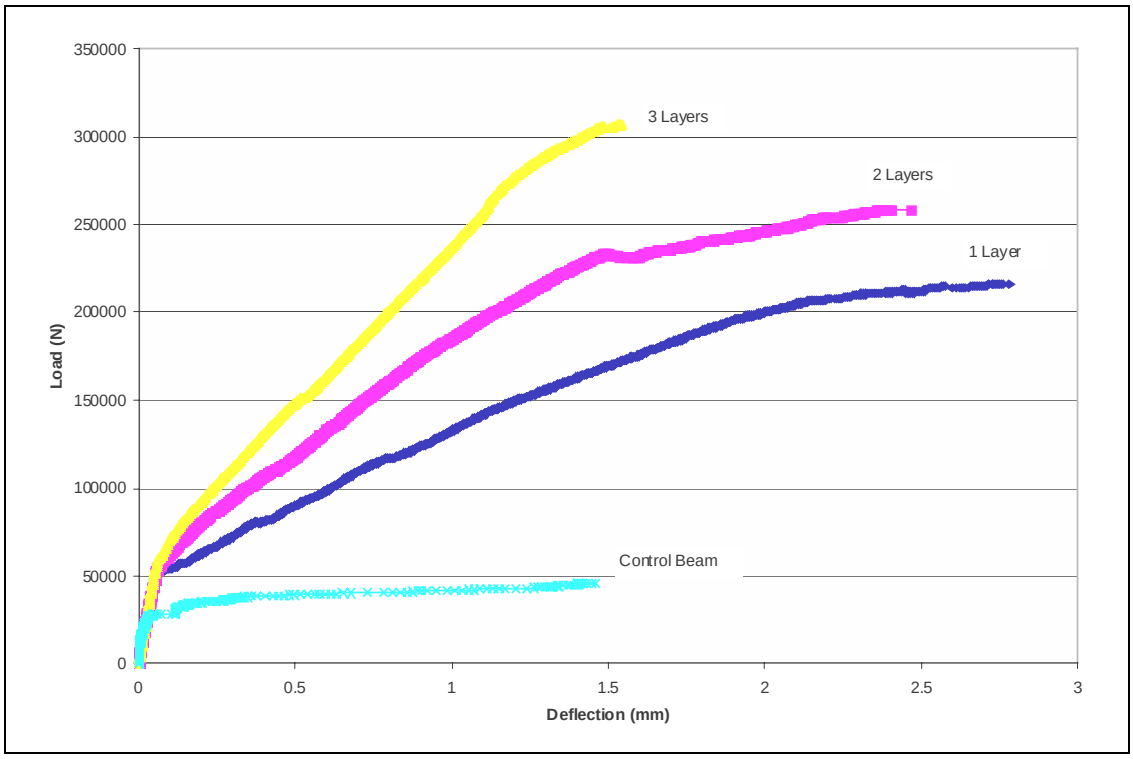

Figure 4.17: Typical load-versus-deflection curves for specimens reinforced with Tyfo® carbon system for shear and flexure

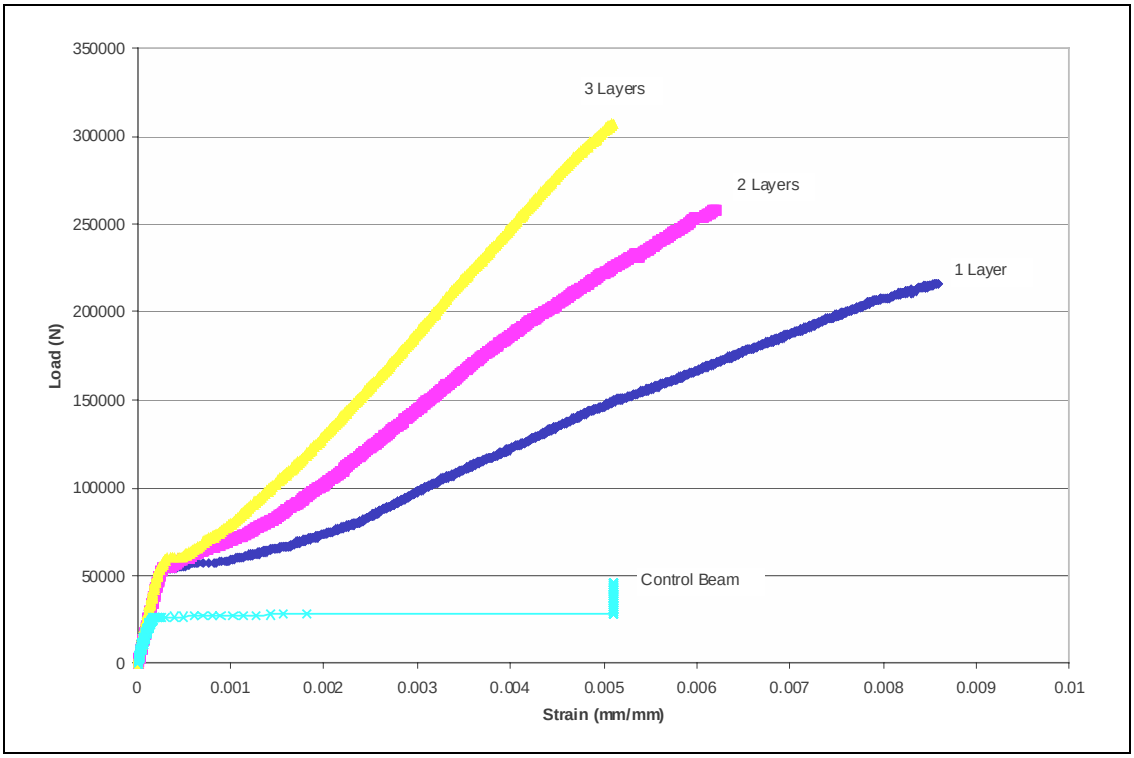

Figure 4.18: Typical load-versus-strain curves for specimens reinforced with Tyfo® carbon system for shear and flexure

Figure 4.17 shows the deflections at failure were significantly increased for the one- and two-layer specimens and approximately the same as the control for the three-layer specimens. This behavior suggests a system that is stiffer in the useful loading range, but behaves with increased ductility at ultimate loads. This shows that the ability of the specimen to crack and deflect prior to failure is not diminished by the addition of FRP reinforcement, but rather it is greatly enhanced, as seen in the one- and two-layer beams.

Figure 4.18 shows the effectiveness of the Tyfo® carbon system. In the one-layer beam, the strain in the flexural laminate is near ultimate capacity at failure without debonding. This suggests excellent bonding between the laminate and the concrete. The two- and three-layer beams developed less strain at failure due to the increased rigidity of the laminates. The properties and limitations of the concrete, rather than FRP reinforcement, governed the failure. The beams failed primarily from shear cracking combined with splitting of the end of the beam due to local stresses.

4.4.3 Shear Reinforcement at 45^{o}

Increases in strength of 270, 310, and 370 percent were observed for the one-, two-, and three-layer beams, respectively. Figure 4.19 illustrates the specimen's ability to carry higher loads with less deflection. However, the deflections at failure are reduced compared to the control specimens.

Figure 4.20 shows the load versus strain in the longitudinal direction of the specimen. This measurement was taken at the top of the FRP laminate, in the center of the tensile face of the specimen, and was not in the direction of the fibers in the laminate. The data suggests that lower strains were developed in laminates with higher rigidity.

Strain measurements were also taken on the shear laminate in the direction of the fibers. Results are shown in Figure 4.21.

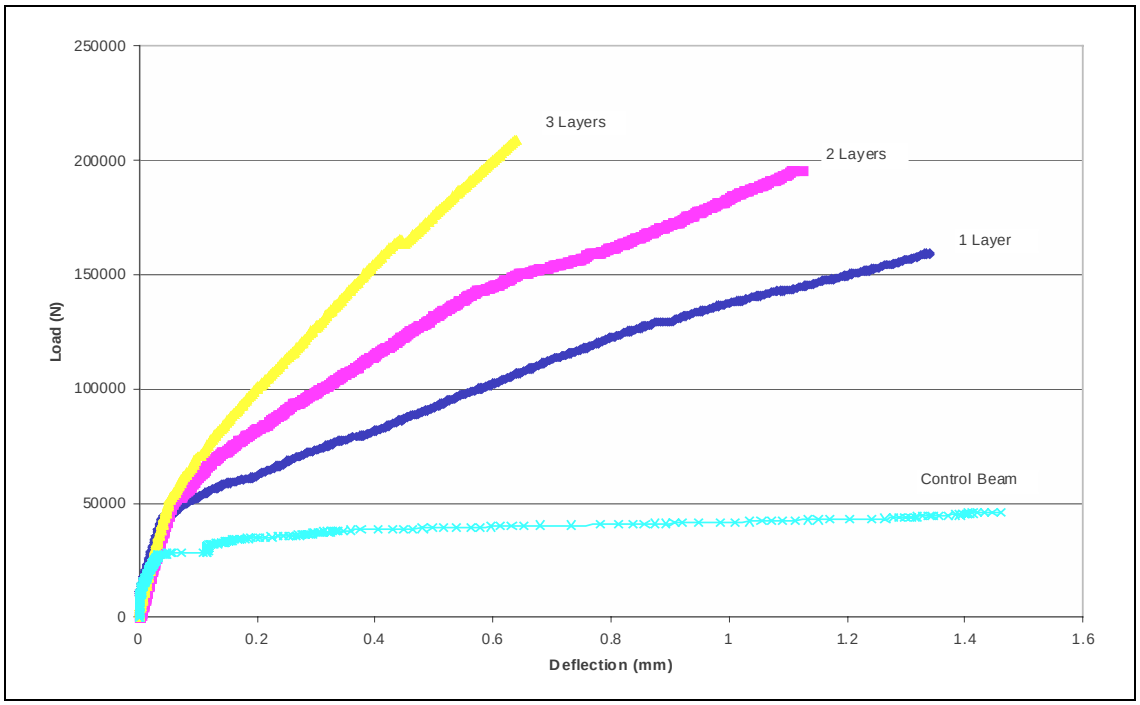

Figure 4.19: Typical load-versus-deflection curves for specimens reinforced with Tyfo® carbon for shear at 45^{o}

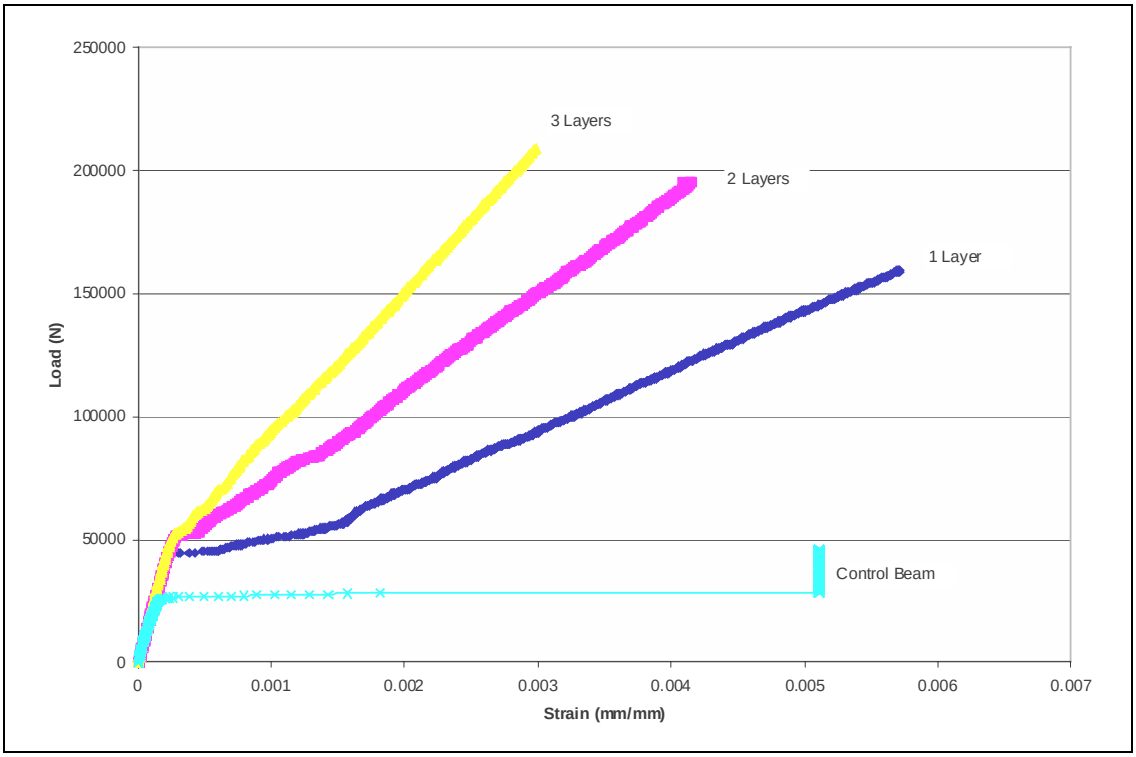

Figure 4.20: Typical load versus flexural strain for specimens reinforced with Tyfo® carbon for shear at 45^{o}

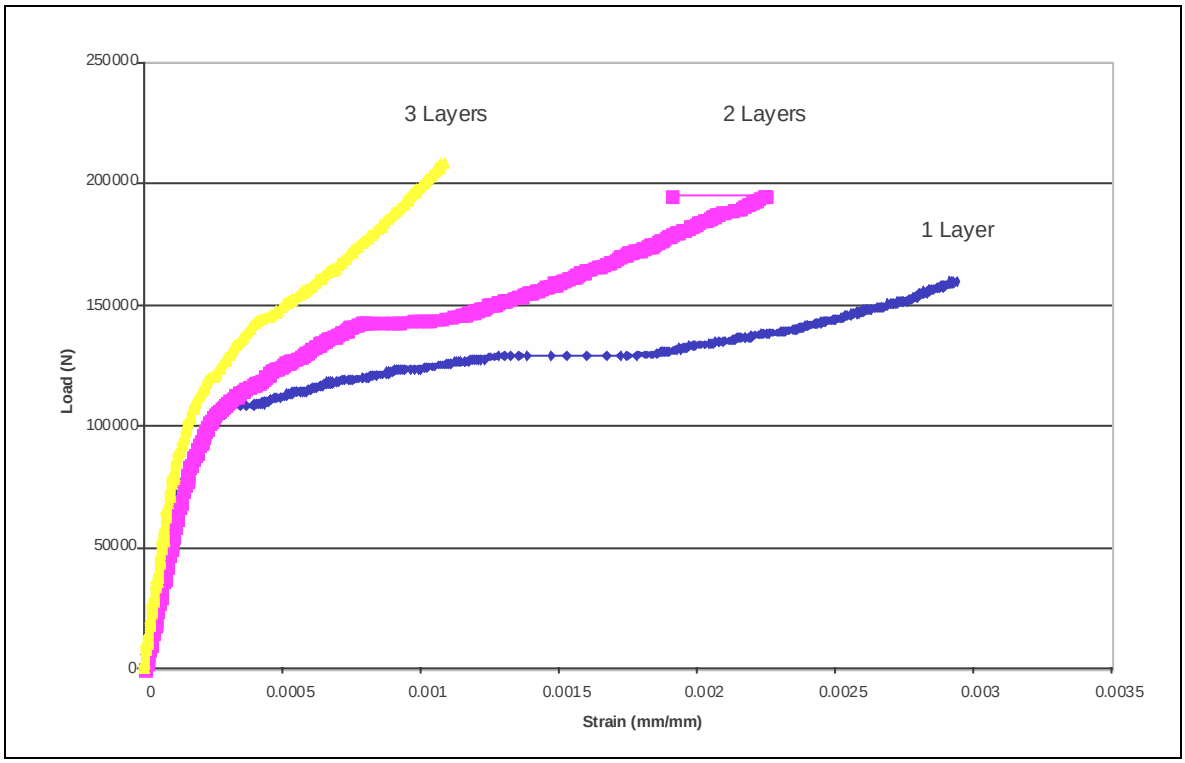

Figure 4.21: Typical load versus strain in fiber direction of shear laminate for specimens reinforced with Tyfo® carbon for shear at 45^{o}

4.5 CMI/REICHHOLD CARBON FRP SYSTEM

Beams reinforced with the CMI/Reichhold carbon FRP system had an increase in strength ranging from 50 to 280 percent. The failure modes included shear failure of the concrete along with laminate debonding, flexural failure of the concrete and laminate, and shear failure combined with cracking at the supports due to local stresses. Shear failure in the specimens was always accompanied by detachment of the shear laminate. Complete fracture of the shear laminate was not observed. The specimen behaviors for different strengthening schemes are discussed further in the following sections.

4.5.1 Flexural Reinforcement Only

The average strength increases were 50, 165 and 170 percent for one, two and three layers of reinforcement, respectively. The addition of a third layer did not seem to improve the performance of the specimens, as illustrated in Figures 4.22 and 4.23. The ultimate strength of the beams reinforced with three layers was approximately the same as for two layers but with lower deflections at failure. Flexural CFRP increased the load at initial cracking by approximately 65 percent when compared to the control specimens. An increase in the number of layers of CFRP reinforcement seemed to have little effect on the load at first crack.

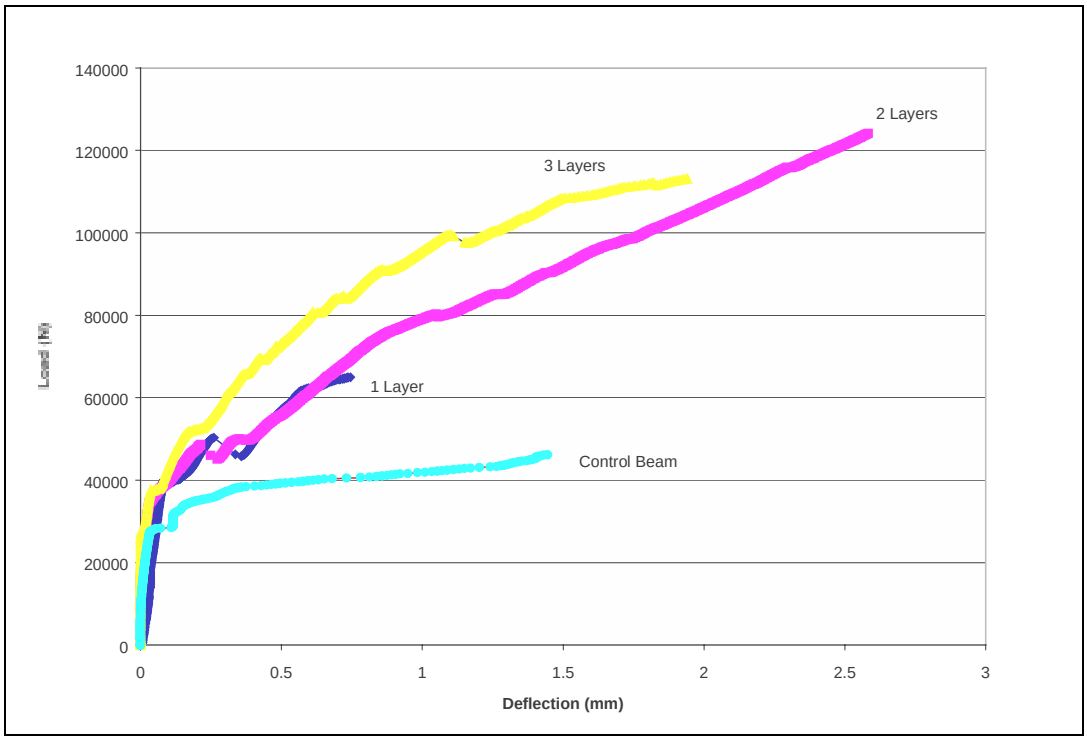

Figure 4.22: Load versus deflection for specimens reinforced for flexure only with CMI/Reichhold

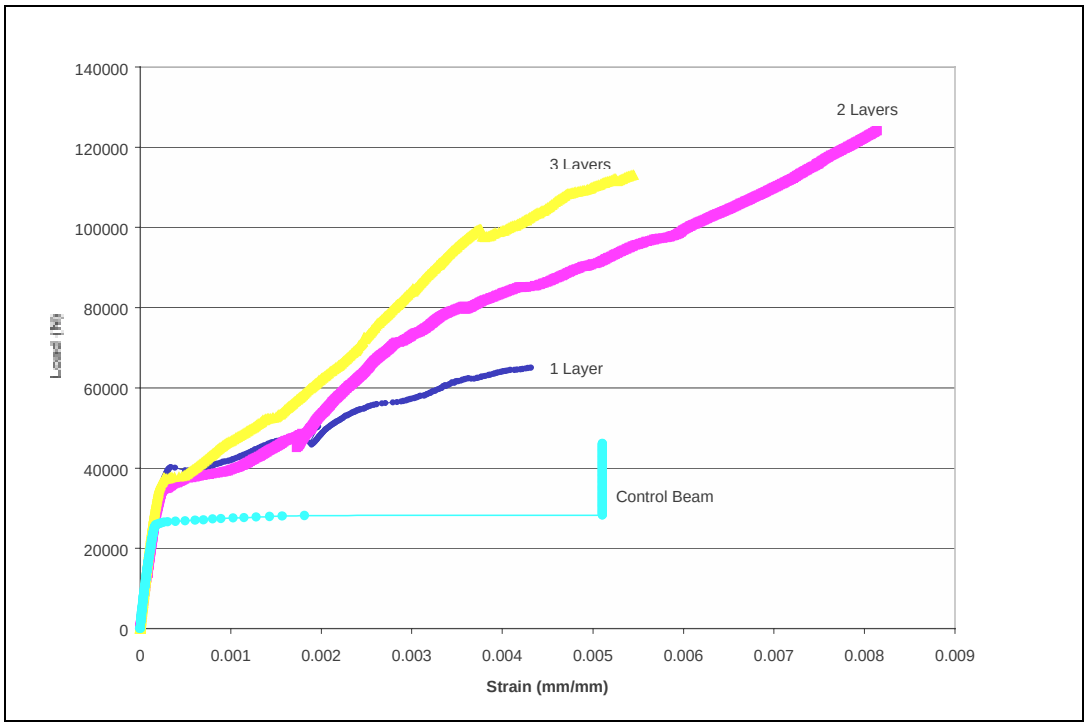

Figure 4.23: Load versus strain for specimens reinforced for flexure only with CMI/Reichhold

The two-layer specimens had an average increase in deflection at failure of 70 percent. Addition of a third layer resulted in a lower deflection at failure than with two layers. The reason for this behavior is over-reinforcement. The failure mode changed from flexural failure to shear failure when adding a third layer.

The specimens reinforced with one and two layers failed primarily in flexure. This typically resulted in the fracture of the laminate across the entire tensile face. Specimens reinforced with three layers failed predominantly in shear. In these cases, the laminate was not fractured.

4.5.2 Flexural Reinforcement and Shear Reinforcement at 90°

The increases in strength averaged 60, 115 and 200 percent for one, two and three layers, respectively. The behavior of the one- and two-layer beams was similar to the specimens reinforced for flexure only. The failure mode was flexural. Therefore, the shear reinforcement did not significantly influence the ultimate strength. The specimens reinforced with three layers had a higher average strength than with flexural reinforcement only. Shear reinforcement caused the three-layer specimens to fail primarily in flexure as opposed to the shear failures observed with three layers of flexural reinforcement only. Typical load-versus-strain and load-versus-deflection curves are shown in Figures 4.24 and 4.25.

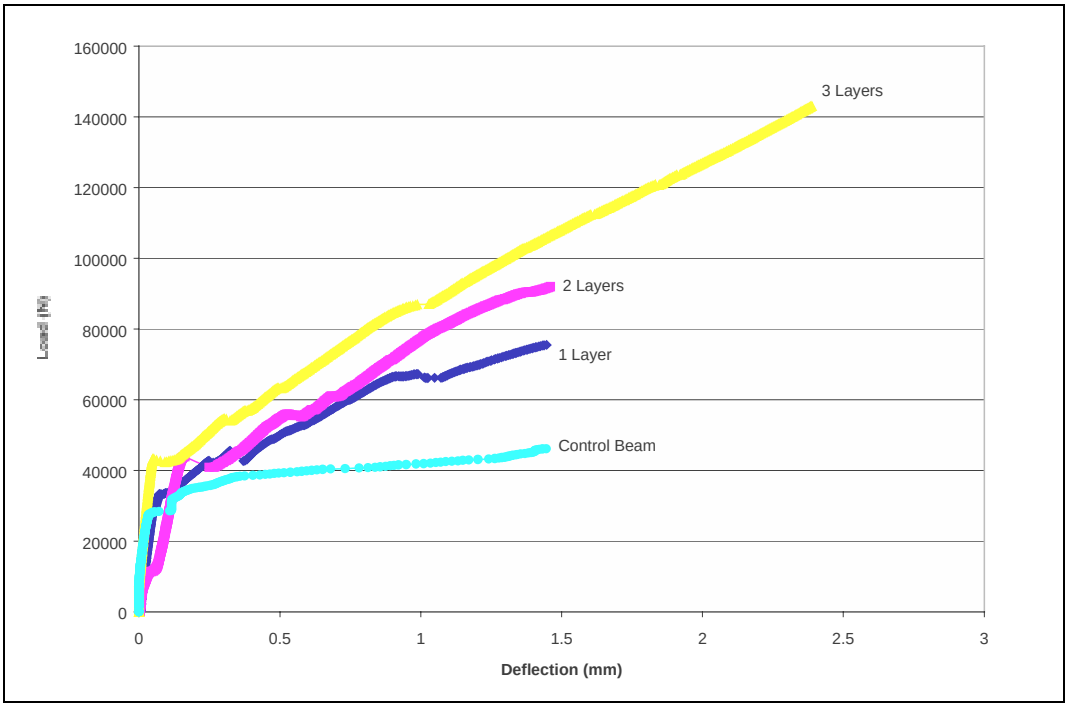

Figure 4.24: Load versus deflection for specimens reinforced with CMI/Reichhold for flexure and shear at 90 degrees

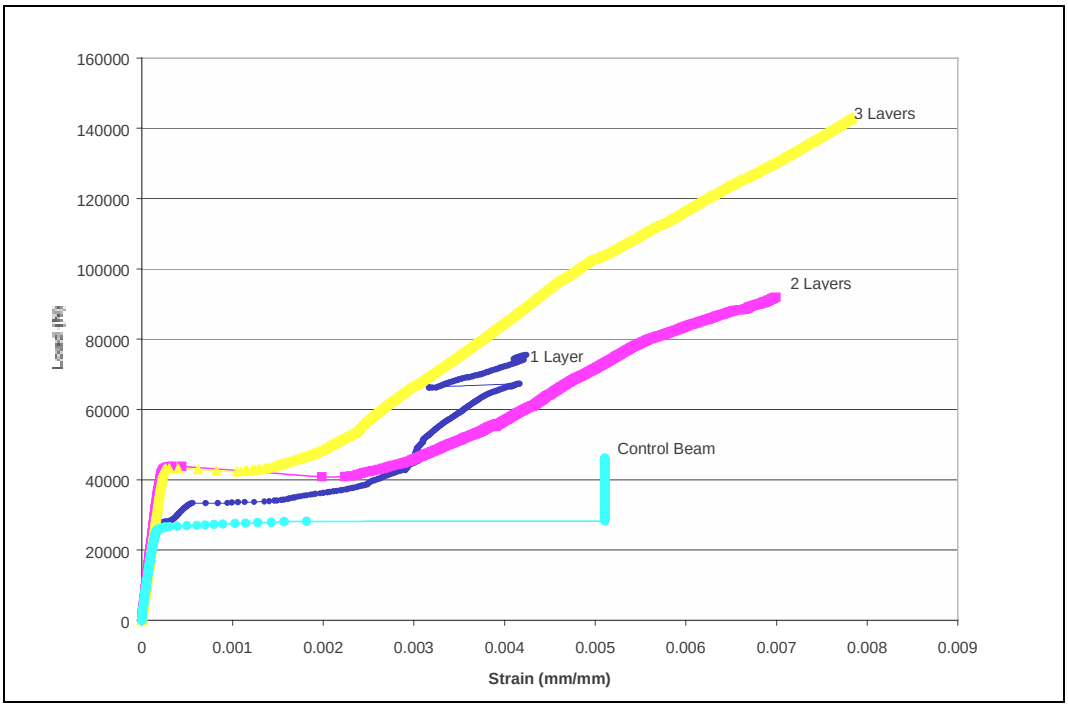

Figure 4.25: Load versus strain for specimens reinforced with CMI/Reichhold for flexure and shear at 90 degrees

Figures 4.24 and 4.25 indicate the performance of the specimens was enhanced as the number of layers increased. The samples reinforced with three layers exhibited significant increases in deflection. The average deflection at failure for three-layer specimens was approximately 30 percent higher than the control. Specimens reinforced with one and two layers did not show significant differences in deflection at failure compared to the control. The load at initial cracking was increased by 40 to 90 percent.

The governing mode of failure was flexural. However, one of the three-layer members failed in shear. The three-layer beams presumably had shear and flexural strengths that were similar.

4.5.3 Flexural Reinforcement and Shear Reinforcement at 45º

The average strength increases were 155, 240 and 280 percent for one, two and three layers of reinforcement respectively. The load at the onset of cracking was increased by 65 to 95 percent. The ultimate strength was higher at each level of reinforcement for this strengthening scheme when compared to beams reinforced for flexure only and for flexure and shear at 90 degrees. This was expected and could not be simply attributed to the angle of shear reinforcement. The 45-degree shear reinforcement overlapped the tensile face of the concrete member. Thus, for each layer of shear reinforcement, two layers of fibers overlapped the flexural reinforcement. For example, the one-layer beams had one layer of flexural reinforcement with fibers aligned with the longitudinal axis plus two layers of flexural reinforcement with fibers oriented at 45 degrees. Therefore, for each layer of reinforcement, additional flexural reinforcement was provided. Direct comparisons of ultimate strength cannot be made with beams reinforced for flexure and

shear at 90 degrees. Typical plots of load versus strain and load versus deflection are shown in Figures 4.26 and 4.27.

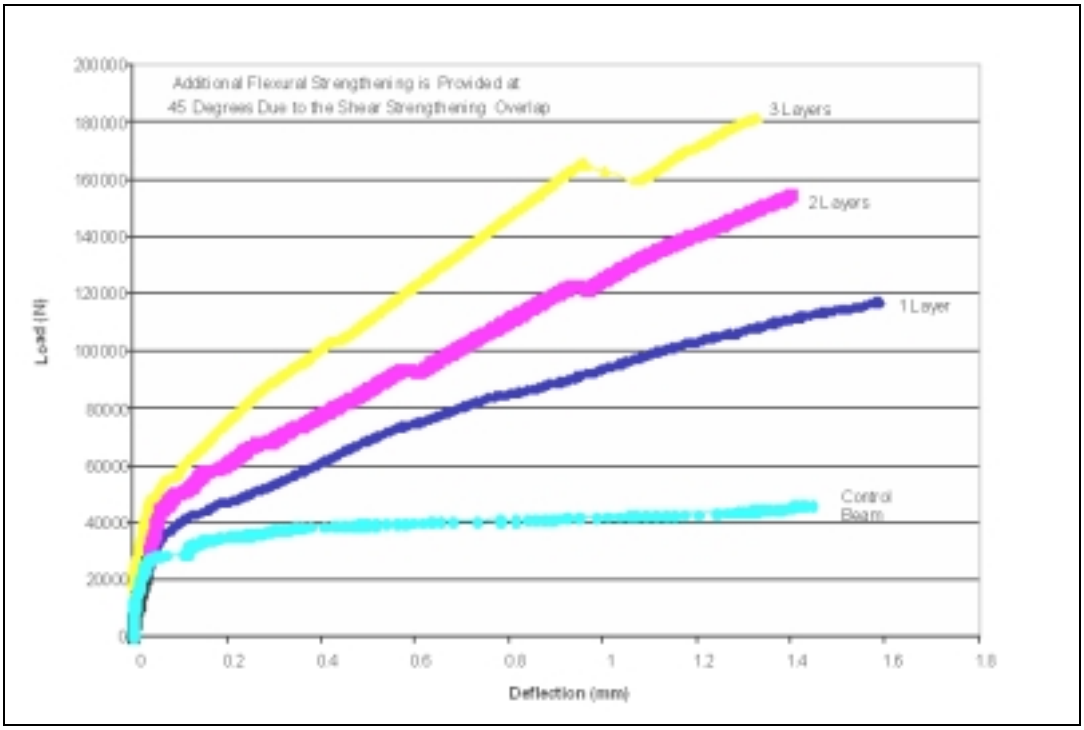

Figure 4.26: Load versus deflection for members reinforced for flexure and shear at 45 degrees with CMI/Reichhold

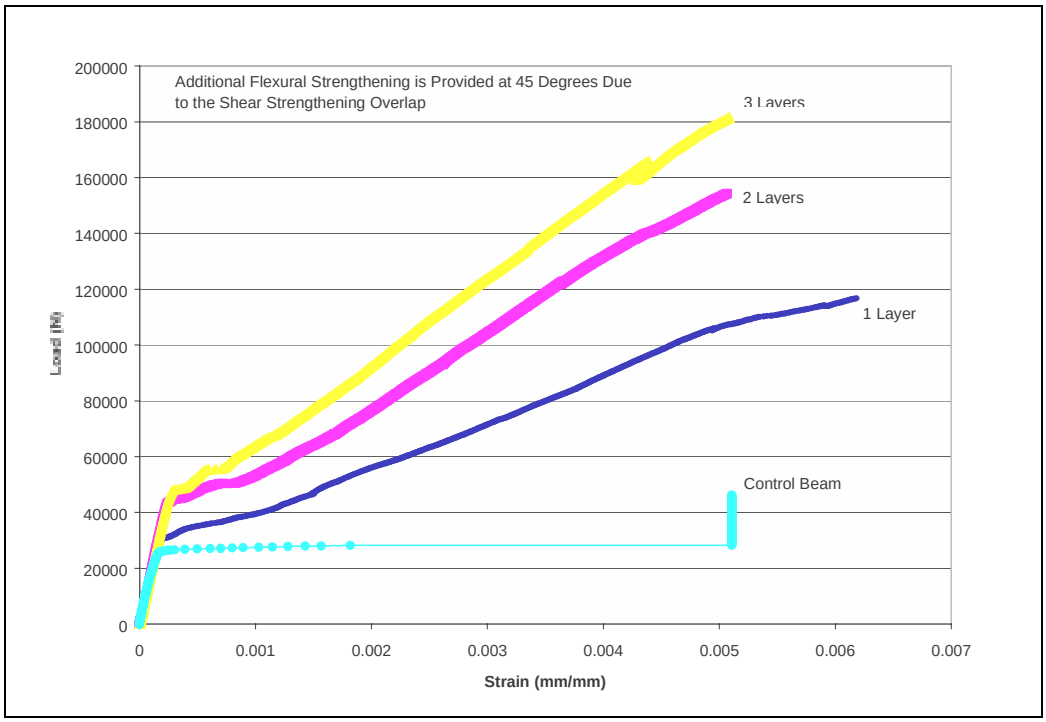

Figure 4.27: Load versus strain for members reinforced with CMI/Reichhold for flexure and shear at 45 degrees

The average deflections at failure were approximately 80 to 95 percent of the control specimens. The decrease in deflection at failure of the beams compared to the control specimens was due to the high axial rigidity.

All of the specimens reinforced for flexure and shear at 45 degrees failed in shear. The shear failures usually resulted in debonding of the shear laminate. In a few cases, the shear laminate was partially fractured but never completely. Failure of the flexural laminate was also observed near the support. This portion of the specimen did not have the extra reinforcement provided by the overlap.

4.5.4 Shear Reinforcement at 45º

The average strength increases were 75, 150 and 170 percent for one, two and three layers of reinforcement, respectively. The load at the onset of cracking increased by about 35 to 85 percent. The load at first crack increased with an increase in the number of layers. However, this was not necessarily the case with other strengthening schemes, and the increase may not be significant. As with specimens reinforced for flexure and shear at 45 degrees, flexural reinforcement was provided at 45 degrees due to the overlap of the shear fibers across the flexural face of the members. Representative load-versus-deflection curves are shown in Figure 4.28. Load-versus-strain curves are not provided, as pure flexural strains were not measured. Shear strains were measured and can be viewed in Chapter 5. However, the strain in the shear laminate is dependent upon where the cracking occurs. This limits the usefulness of making direct graphical comparisons.

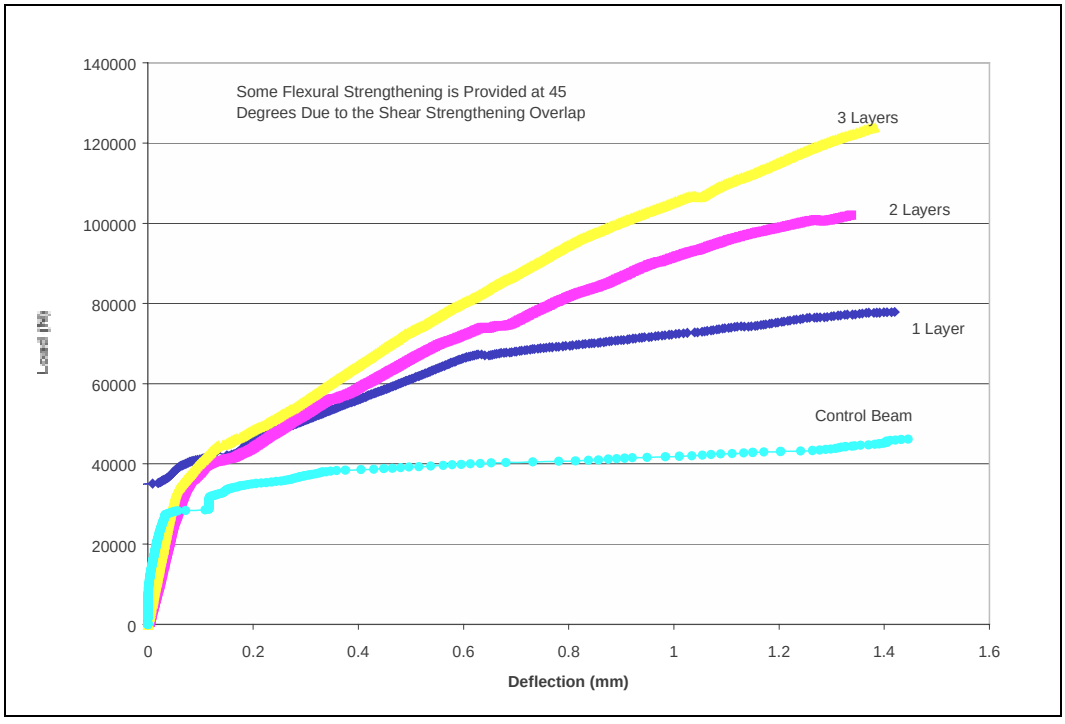

Figure 4.28: Load versus deflection for CMI/Reichhold specimens reinforced for shear at 45 degrees

Figure 4.28 indicates that the deflection at failure was similar for each of the reinforced specimens along with the control specimens. However, for this strengthening scheme, the deflections at failure were inconsistent. These results are tabulated in Chapter 5 of this report. The deflections at failure were inconsistent because the failure modes were inconsistent. This strengthening scheme apparently resulted in beams that had similar shear and flexural strengths. Failure modes varied within the groups of one-, two-, and three-layer specimens. In most cases, the shear laminate debonded and the flexural laminate failed across the flexural face. The flexural failure of the laminate was typically not in the middle third of the beam, presumably because the shear overlap did not cover the entire flexural face.

The failure mode of these specimens was seemingly dependent upon the geometry of the reinforcement scheme. The flexural reinforcement due to the shear overlap varied across the tensile face of the beam. More reinforcement was provided in the center than at the ends of the concrete specimens. Therefore, flexural failures were typically at the edge of the 45-degree reinforcement overlap.

4.6 MBRACE™ CARBON FRP SYSTEM

The dominating failure mode for this system was shear failure with debonding of the laminate. However, flexural failure of the laminate and concrete was also observed. Combinations of shear and flexural failure combined with debonding were also observed. In most specimens, bonding appeared to be insufficient causing premature failure. This was possibly the result of insufficient cure time recommended by the manufacturer or improper procedure used for assembly and application of the product. The MBrace™ resin remained pliable after the suggested cure time.

4.6.1 Flexural Reinforcement Only

Figures 4.29 and 4.30 show the typical behavior of the flexurally reinforced MBrace™ carbon samples.

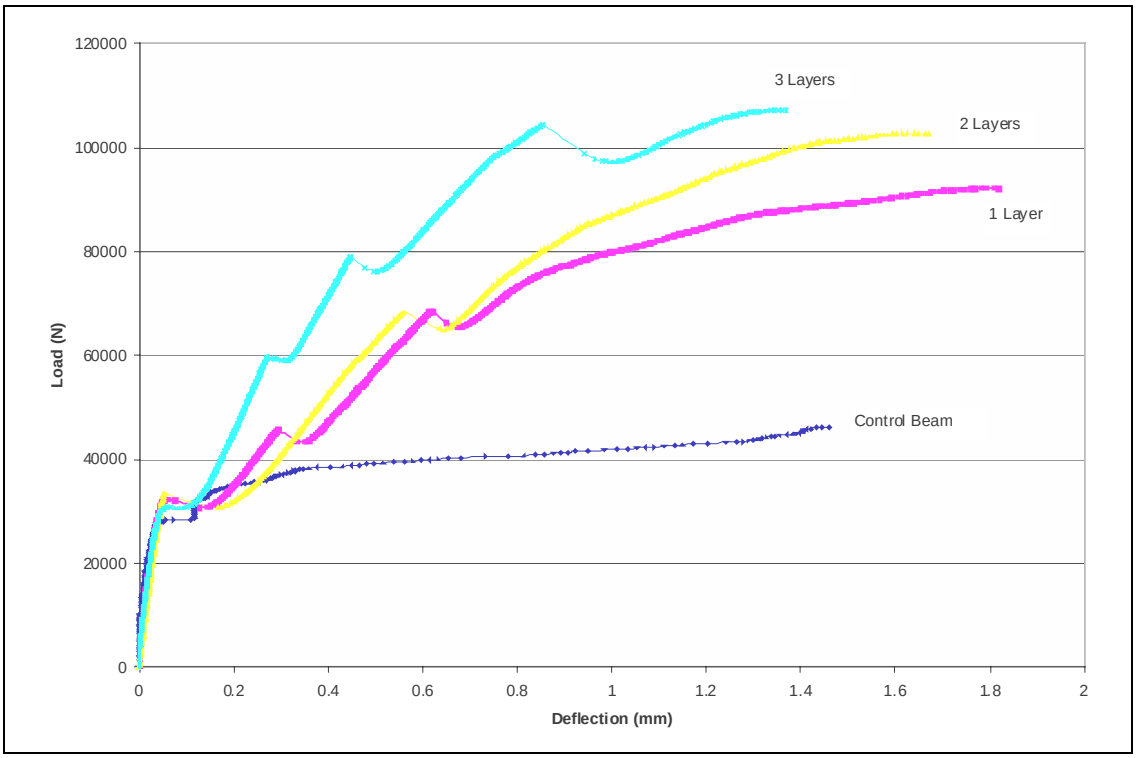

Figure 4.29: Typical load-versus-deflection behavior for flexurally reinforced MBrace™ carbon specimens

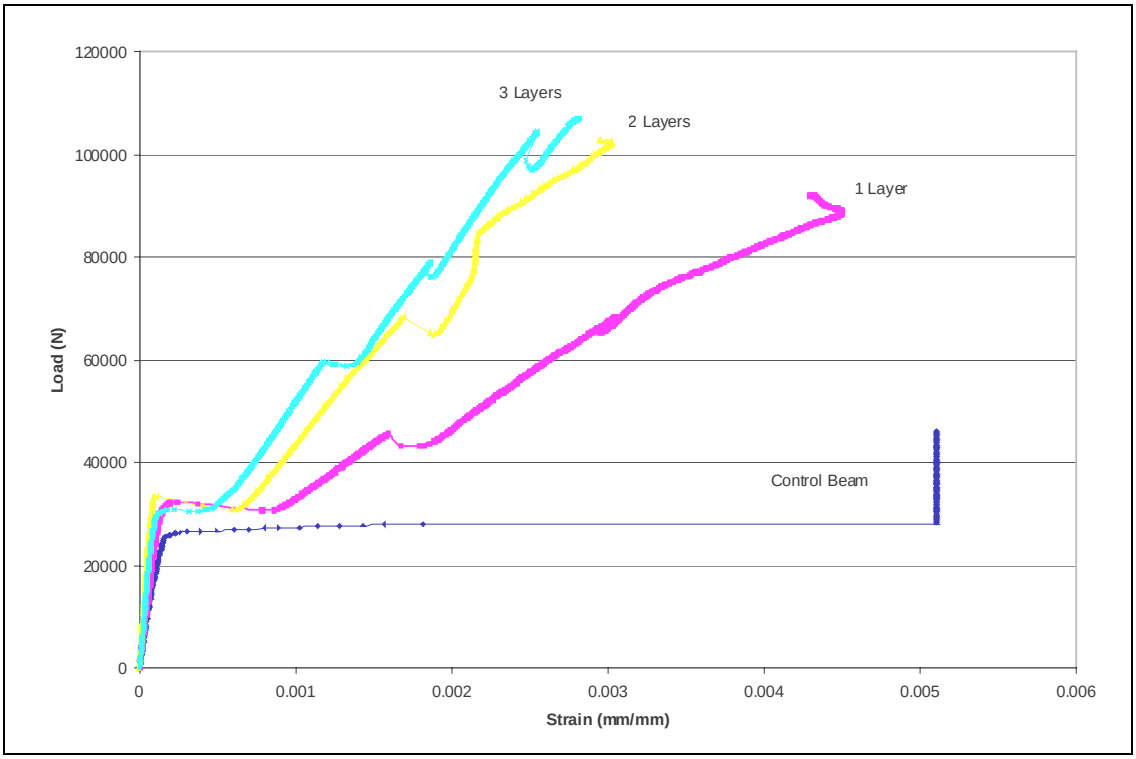

Figure 4.30: Typical load versus flexural strain for flexurally reinforced MBrace™ CFRP specimens

The main differences in behavior of the specimens were most noticeable following cracking. In all cases, a flat portion (increasing deflection and strain at nearly constant load) of the graph occurs following cracking. In Figure 4.29, this occurs between 0.05 and 0.015 mm of deflection. In Figure 4.30 this corresponds to the point of first cracking to a strain of 0.0005 to 0.001 mm/mm, depending on the number of layers. It is believed that this flat portion of the plots is the result of the fibers slipping within the matrix as the tensile stresses are transferred from the concrete to the composite. This phenomenon may have been the result of insufficient cure or an incorrect ratio between the two components of the matrix.

The effect of laminate thickness is illustrated by both figures. As the thickness of the CFRP laminate was increased, the rigidity of the beam also increased; thus less strain was developed in the laminate at a given load (see load-versus-strain graph). The development of strain in the laminate was largely influenced by the adhesive strength of the epoxy. This was due to poor bonding of the laminate and concrete surface.

In the cases of the one- and two-layer specimens, the deflections at failure were greater than the control beams by 0.2 to 0.3 mm. The CFRP also significantly decreased deflections at given loads after cracking, as shown in Figure 4.29.

It is believed that the insufficient bond between the MBrace™ CFRP and concrete was the reason for the inconsistent modes of failure. For the one-layer beams, the bonding between the laminate and the concrete surface was sufficient to cause failure of the beams to change from flexure (in the control specimens) to shear. Thus, the two-layer specimens were expected to also fail in shear, since the addition of another layer should have further increased flexural strength. However, these expectations were not confirmed by the test results. One possible explanation for this behavior is that the ineffectiveness of the resin in bonding the laminate to the beam caused the two-layer specimens to debond before significant stress was developed in the laminate. Another possible explanation is that the bond between the resin and the fibers was inadequate, causing a significant portion of the fibers to slip and become largely ineffective. For the three-layer beams, the mode of failure reverted to shear. Because of the insufficient bond and possible research mistakes, we can not regard the performance of this CFRP system as typical.

4.6.2 Flexural Reinforcement and Shear Reinforcement at 90^{o}

For the one- and two-layer specimens, the strength was increased by 80 percent with the addition of shear reinforcement. The three-layer beams exhibited increases of nearly 150 percent.

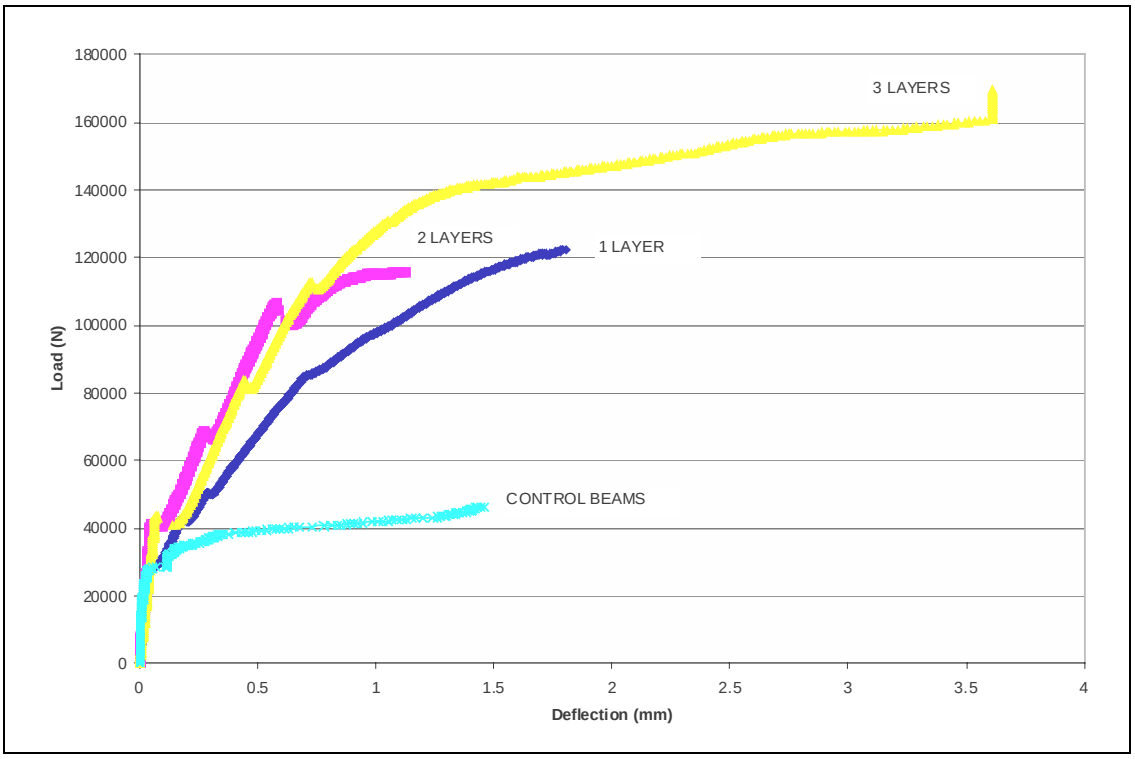

Figure 4.31: Load versus deflection for specimens reinforced with MBrace™ carbon for flexure and shear at 90^{o}

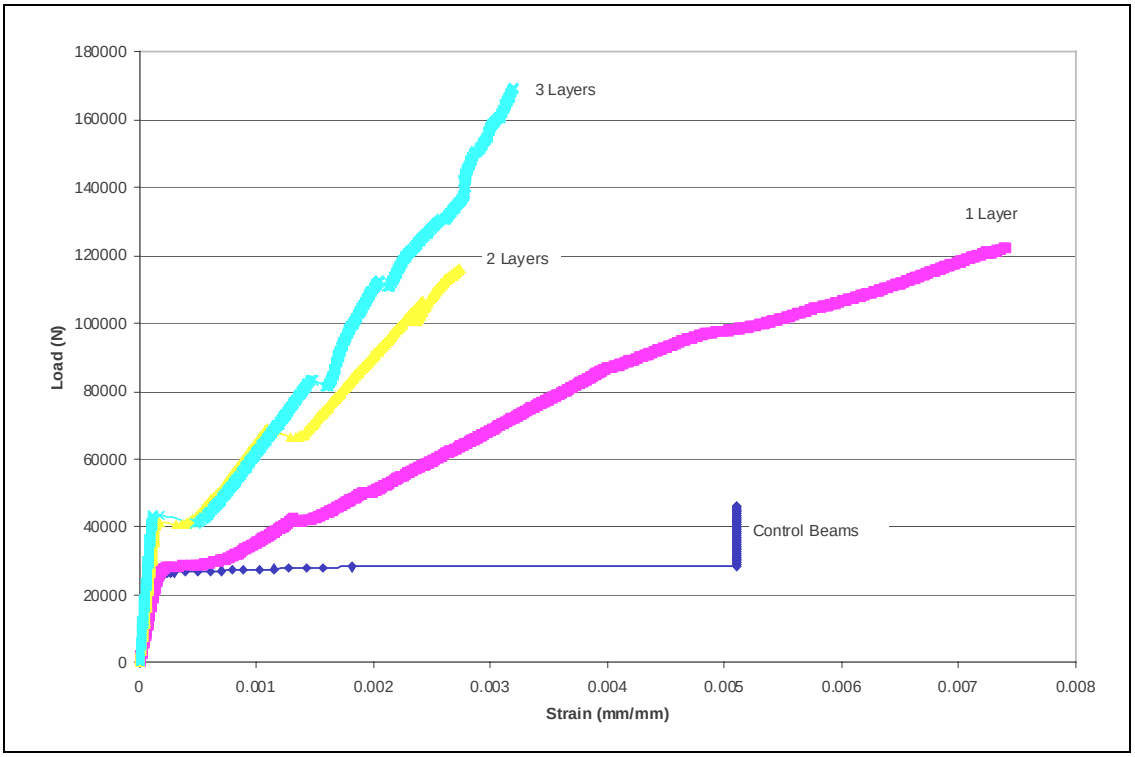

Figure 4.32: Load versus strain for specimens reinforced with MBrace™ carbon for flexure and shear at 90^{o}

As was observed in the members reinforced for flexure only, there was slippage following initial cracking. The addition of the shear laminate seems to have had little effect on the length of the slippage.

The three-layer beams performed in an unexpected manner. For reasons that were not apparent, the deflection at failure of the specimen was very high. Figure 4.32 indicates that the strain at failure for the representative three-layer beam was higher than for the two-layer specimens. However, there was little difference in strain behavior when considering the group averages. This suggests a maximum amount of effective reinforcement, which in this case was likely close to the amount provided by two layers.

The concept of a maximum amount of useful FRP is further illustrated when one considers only the areas of Figures 4.31 and 4.32 between approximately 40,000 and 70,000 N. The measured strains in the two laminates are similar in this region. If the load-versus-deflection curve is analyzed over the same area, one can see that the rate of increase in deflection is similar. Thus, the additional layer of FRP is providing little contribution to the specimen performance.

4.7 MBRACE™ GFRP SYSTEM

Beams reinforced with the MBrace™ glass system showed increased load-carrying capacity compared to the control samples, but significantly less than the carbon systems. Improvement in strength of the MBrace™ glass reinforced beams ranged from 44 to 160 percent over the strength of the control specimens.

4.7.1 Flexural Reinforcement Only

The specimens reinforced for flexure showed strength increases of 44, 116 and 125 percent for the one-, two- and three-layer specimens, respectively. In addition, the load required to cause initial cracking of the beams was increased by 40 percent for the one-layer beams, 55 percent for the two-layer specimens, and 65 percent for the three-layer specimens.

The MBrace™ glass reinforcement reduced deflections of the beams (Figure 4.33). The loads required to cause deflections equal to those at failure of the control specimen were increased by 40 percent for the one layer beams, 75 percent for the two layer specimens, and 95 percent for the three layer specimens.

Figure 4.34 illustrates the load-versus-strain behavior. The strain developed in each of the laminates was dependent on the thickness of the laminate. As expected, thicker laminates developed lower strains at given loads.

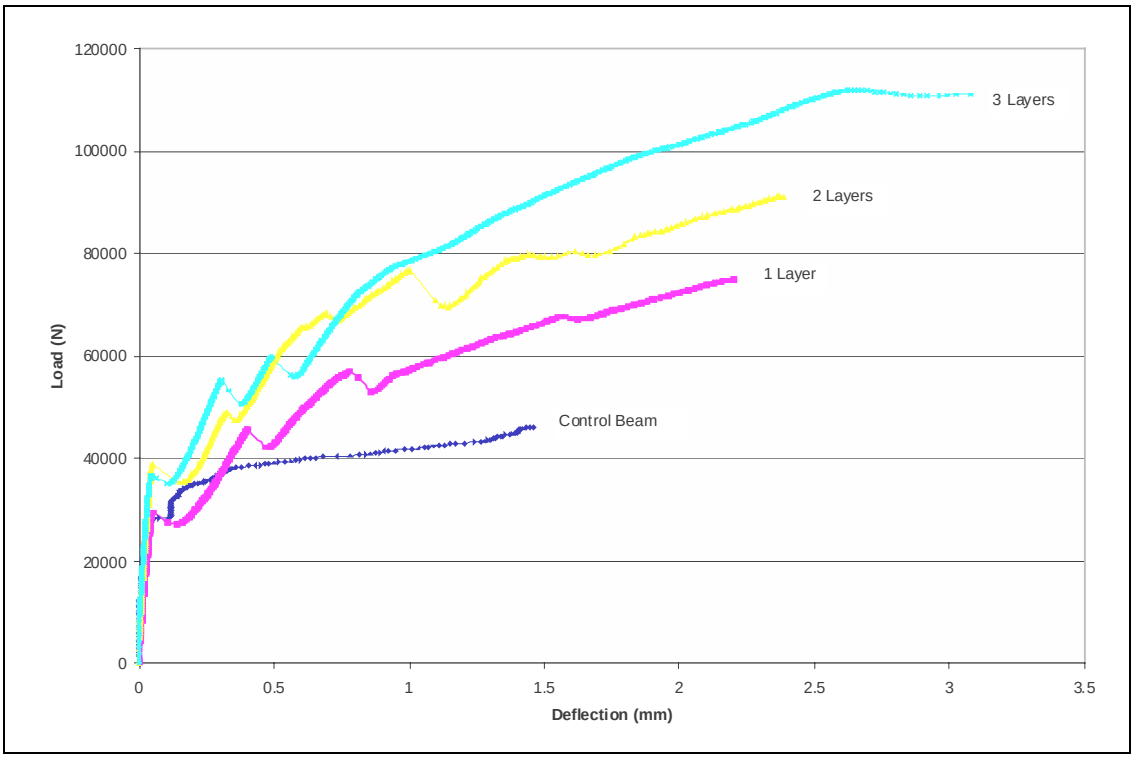

Figure 4.33: Typical load-versus-deflection behavior for specimens reinforced with the MBrace™ glass system for flexure

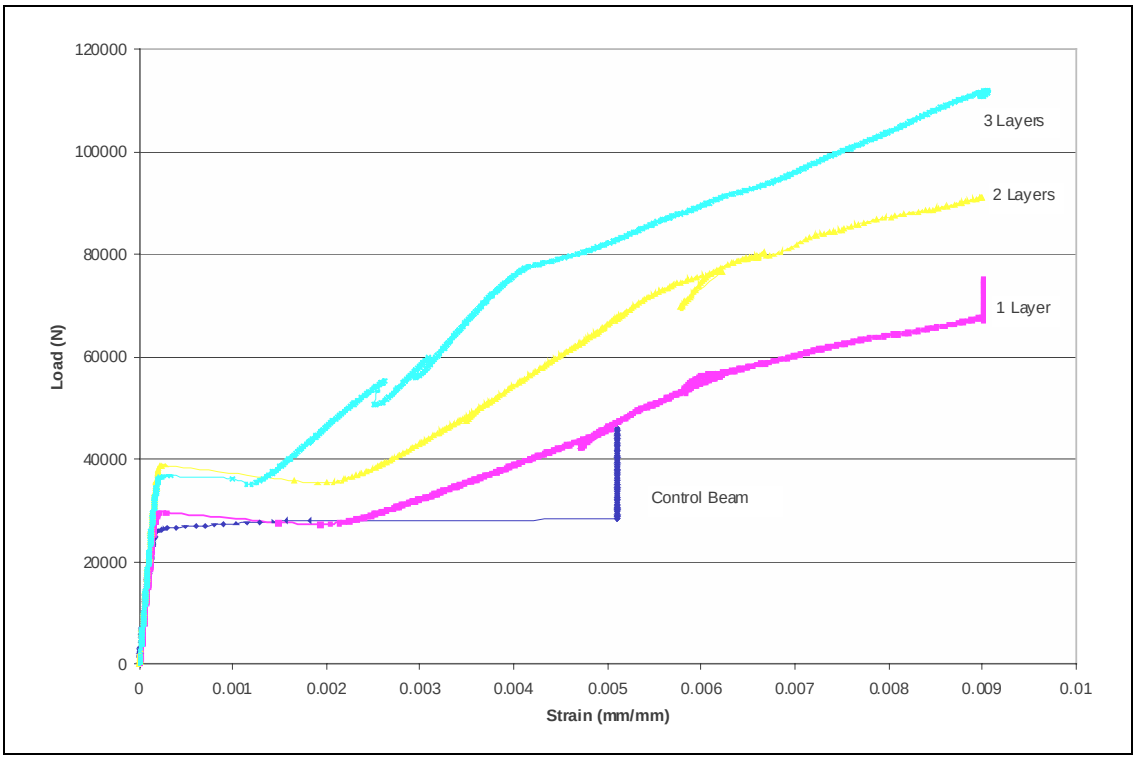

Figure 4.34: Typical load-versus-strain behavior for specimens reinforced with the MBrace™ glass system for flexure

Slippage behavior seen in the MBrace™ carbon laminates was also evident in the glass laminates. This behavior is illustrated in Figure 4.34 between initial cracking to a strain of approximately 0.0012 for the three-layer specimens and approximately 0.002 for the one- and two-layer specimens. This behavior is believed to be dependent on the matrix and is discussed in Section 4.6.

Failure modes of the beams varied. For the one-layer specimens, flexural failure of the concrete and the laminate was typical. The governing mode of failure for the two-layer specimens was shear. For the three-layer specimens, debonding of the laminate led to a combined shear and flexural failure.

4.7.2 Flexural Reinforcement and Shear Reinforcement at 90^{o}

Addition of shear reinforcement had no significant effect on strength. However, the shear reinforcement appeared to control shear cracking. Average strength gains over the control beams were 45, 120 and 160 percent for the one-, two- and three-layer specimens, respectively. In addition to the typical strengthening schemes used in this study, one specimen reinforced with two layers of flexural reinforcement and one layer of shear reinforcement was tested. The specimen showed 120 percent increase in strength over the control. It seems the amount of flexural reinforcement controlled the strength of these specimens. Figures 4.35 and 4.36 show the load-versus-deflection and load-versus-strain behavior.

Figure 4.35 suggests significant changes in behavior with the addition of the shear reinforcement compared to the flexurally reinforced beams. All specimens exhibited similar deflections up to 60,000 N. Beyond that load level, the deflection of the specimens seemed to be influenced by the thickness of the laminate.

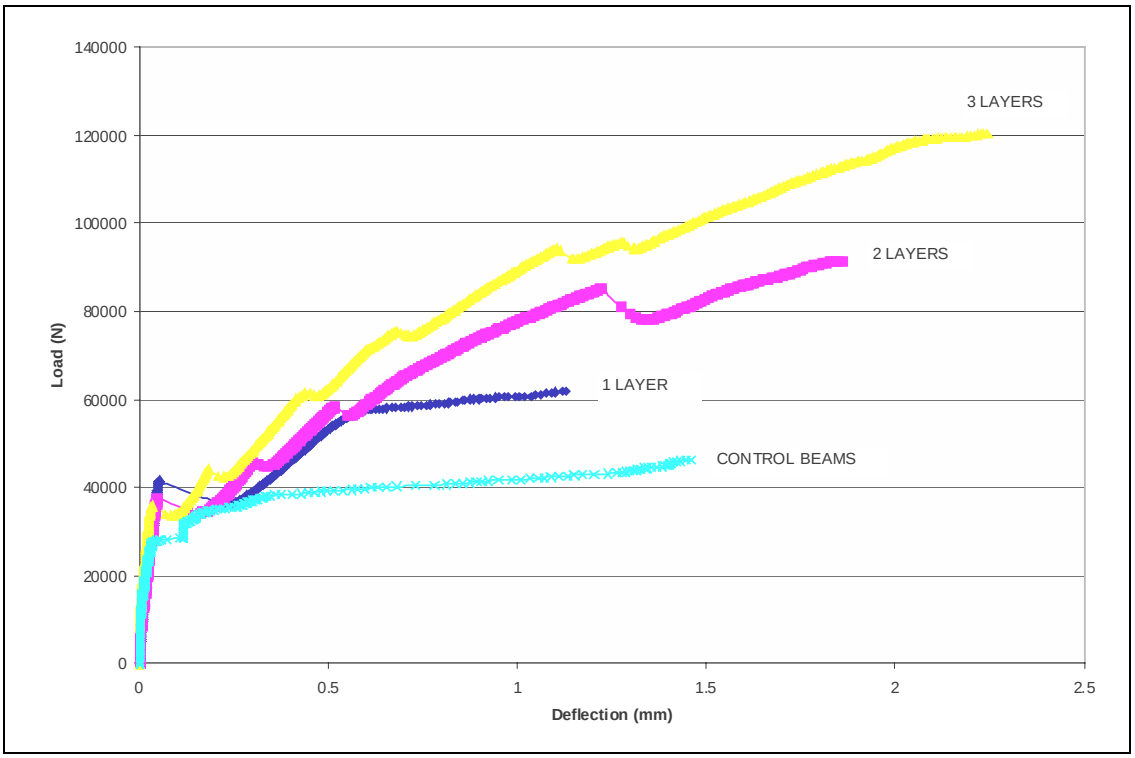

Figure 4.35: Typical load-versus-deflection curves for specimens reinforced with the MBrace™ glass system for flexure and shear

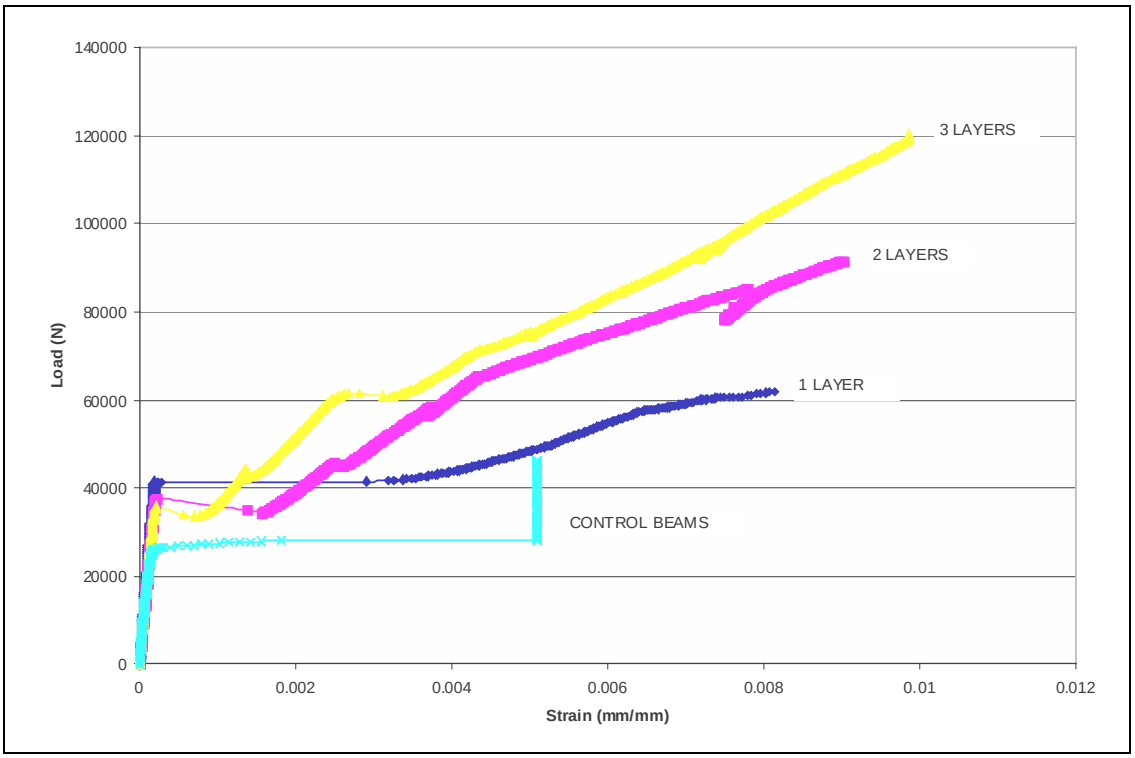

Figure 4.36: Typical load-versus-strain curves for specimens reinforced with the MBrace™ glass system for flexure and shear

The average results from this retrofitting scheme indicated that the strains at failure were close to 0.9 percent. The thicker laminates were able to reach higher strains prior to failure. This behavior was indeed unexpected and not considered typical of systems with proper bonding characteristics.

Failures of both the one- and two-layer beams were similar. Both groups of specimens failed by flexural failure of the laminate. The three-layer beams failed by debonding of the shear laminate and propagation of combined flexure and shear cracking to the compression side of the specimen.

4.8 TYFO® GFRP SYSTEM

Strength gains in the beams reinforced with the Tyfo® GFRP system ranged from 200 to 480 percent, making the system comparable to some of the carbon systems based on strength alone.

4.8.1 Flexural Reinforcement

The specimens reinforced with one layer showed an increase in ultimate strength of 220 percent over the control beams. The performance of the two- and three-layer specimens was similar. Both exhibited strength improvements of approximately 270 percent. The one- and two-layer specimens displayed an increase of approximately 90 percent in the load at initial cracking, while the loads needed to cause cracking in the three-layer specimens were increased by 115 percent.

Deflections at failure of the specimens were increased by 160 percent for the one-layer specimens, 66 percent for the two-layer beams, and 38 percent for the three-layer specimens. The vertical climb in load for the one-layer specimen near the end of the test was due to the LVDT reaching its maximum range (Figure 4.37). The estimated deflection of the specimen was approximately 4 mm, about 180 percent higher than the control specimen.

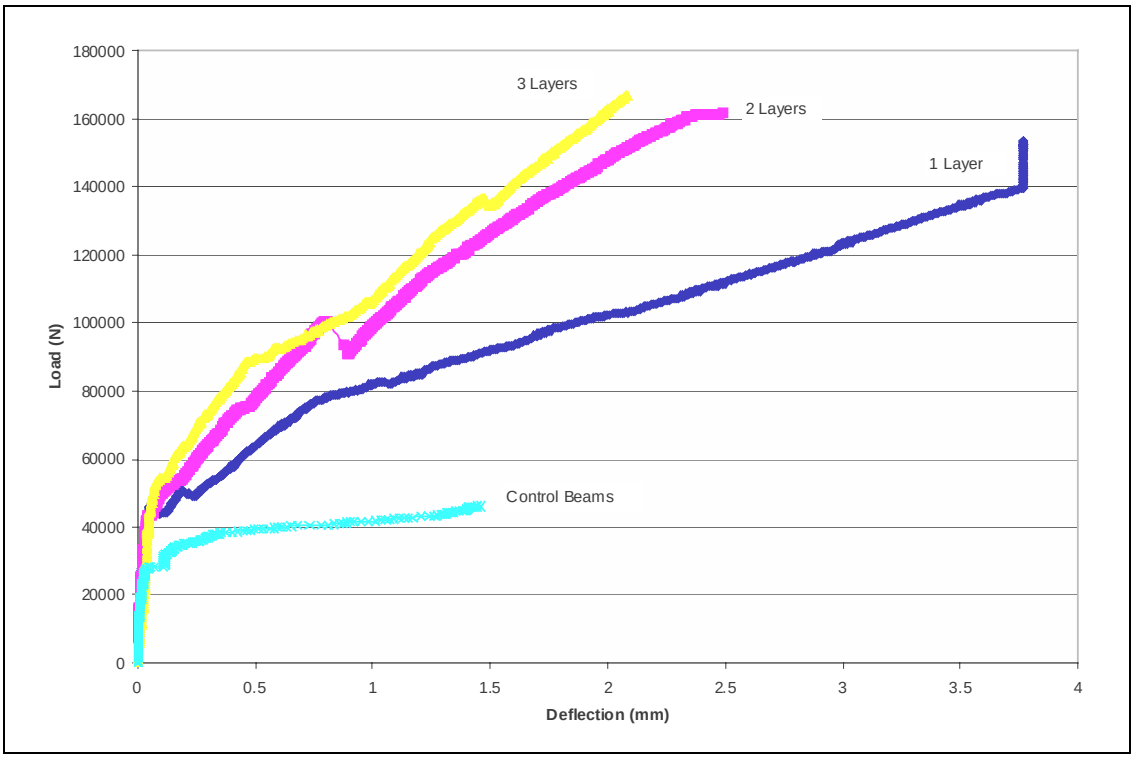

Figure 4.37: Typical load-versus-deflection curves for specimens reinforced with the Tyfo® glass system for flexure only

The one-layer specimens behaved differently from the two- and three-layer specimens. The stress-versus-strain curve appears to be nearly linear, i.e. similar to a typical behavior of FRP laminates alone. The observed behavior suggests that debonding of the laminate occurred at the beam's mid-span. It is logical to assume that when the laminate detached from the concrete surface at mid-span, and was only bonded under the loading points, the beam's behavior was governed by the FRP properties alone. This is also a possible explanation for why the recorded deflection appeared to be linear from approximately 80,000 N to failure of the specimen.

Since the debonding of the laminate that possibly occurred on the one-layer specimen was partial, the behavior of the beams was different from any behavior seen in the other specimens. The laminate, being anchored under the loading points, continued to enhance the performance of the beam, as is evident from both the load-versus-deflection graph and the load-versus-strain graph (Figure 4.38). As the load was increased, the delamination progressed toward the loading points.

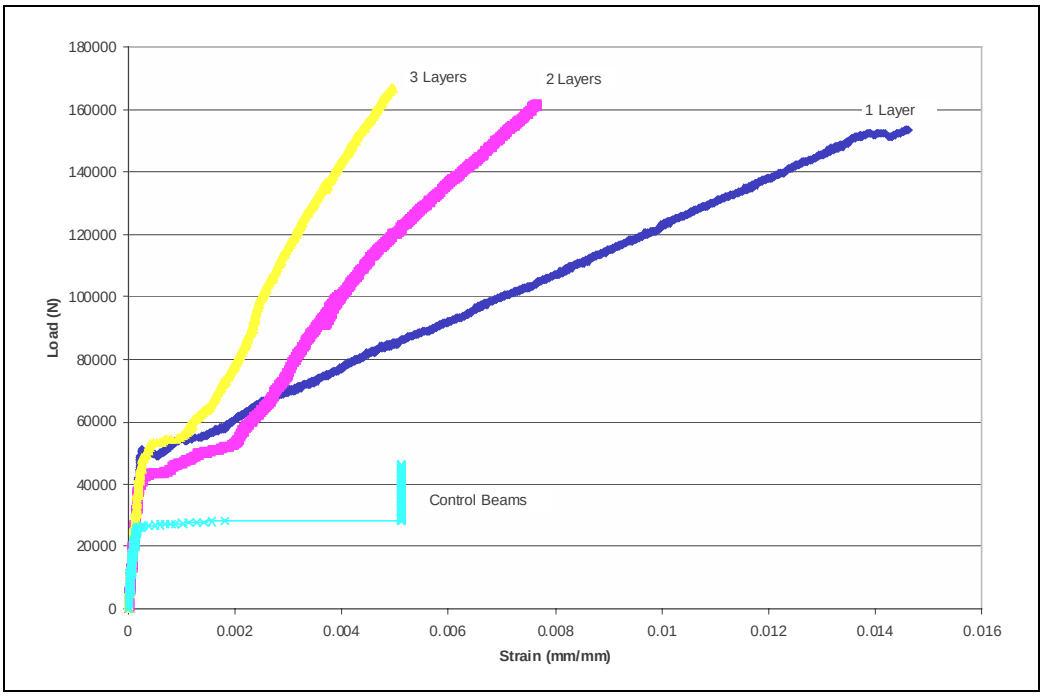

Figure 4.38: Typical load-versus-strain curves for specimens reinforced with the Tyfo® glass system for flexure only

In addition, numerous flexural and shear cracks extended toward the compression face of the concrete specimen. When the cracks reached the compression side of the specimen the laminate broke across and parallel to the fibers, and the specimen failed.

The two- and three-layer specimens did not exhibit the bonding problems observed in the one-layer specimens. Both the two- and three-layer beams failed similarly: shear cracking and cracking at the end of the specimen, due to concentrated stresses at the cut-off points, caused the failure. When the cracks at the ends of the specimen propagated into the shear area, the corners of the specimen broke off.

4.8.2 Flexure and Shear Reinforcement at 90^{o}

The addition of shear reinforcement did not significantly change the strength of the one-layer specimens, but it did result in substantial increases in strength for the two- and three-layer specimens. Figures 4.39 and 4.40 show the load-versus-deflection and load-versus-strain behavior.

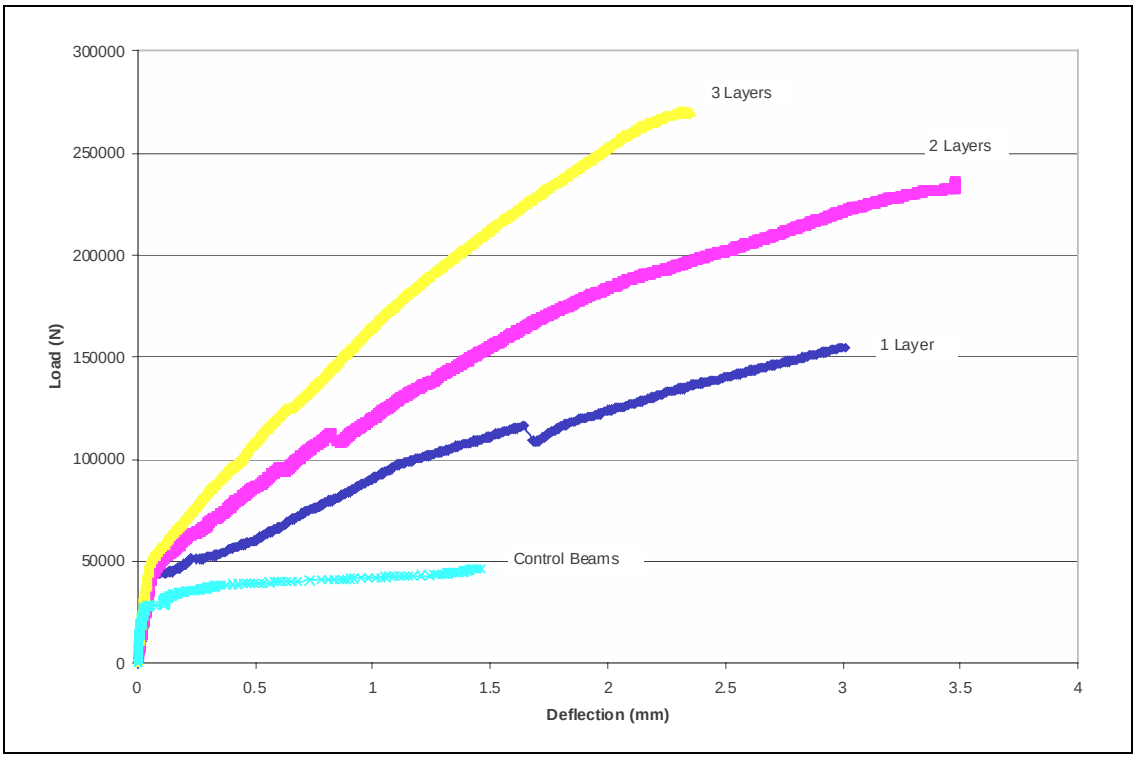

Figure 4.39: Typical load-versus-deflection curves for specimens reinforced with the Tyfo® glass system for flexure and shear

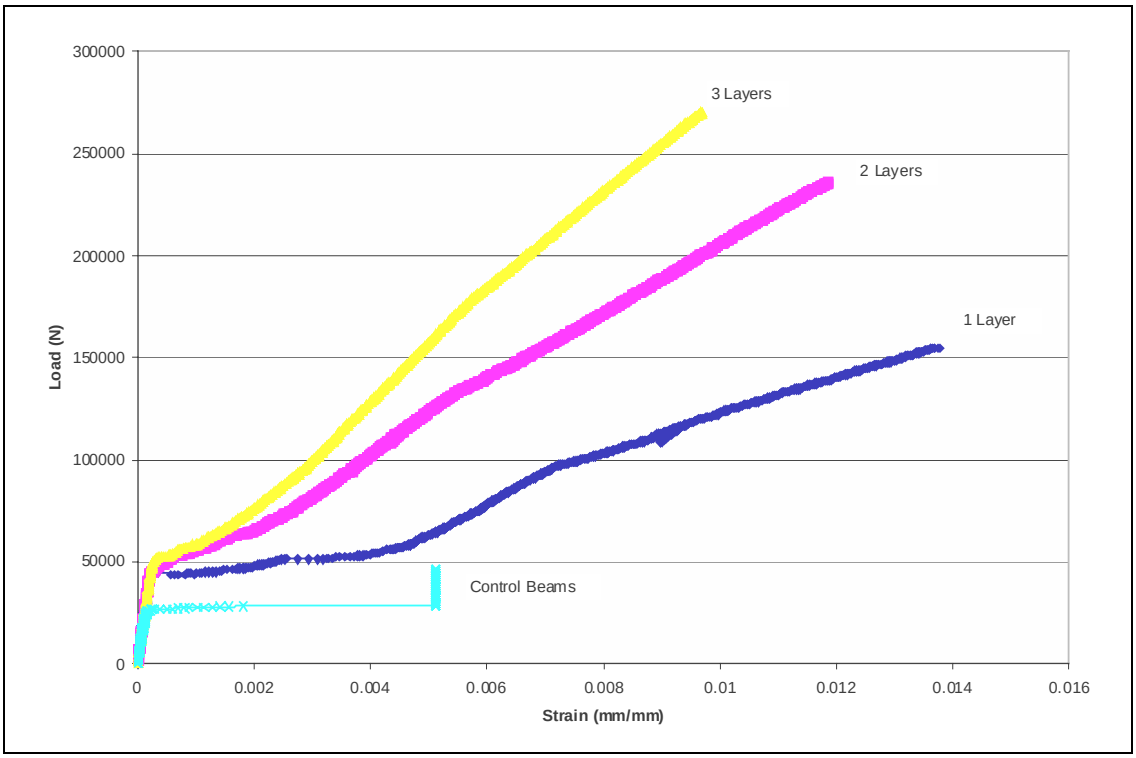

Figure 4.40: Typical load-versus-strain curves for specimens reinforced with the Tyfo® glass system for flexure and shear

As shown in Figure 4.40, the addition of shear laminate allowed the flexural laminates to develop higher strains. The one-layer specimen reached a strain of approximately 1.4 percent before the laminate failed in tension. Due to the increase in laminate thickness, the strains in the two- and three-layer beams were less, with the three-layer specimens being able to develop the least strain in the flexural laminate prior to failure.

The failure modes of the specimens were dependent on laminate thickness. The one-layer specimens did not exhibit any bond problems and failed in tension. The composite remained attached to the concrete surface after failure. The failure typically occurred near the intersection of the shear and flexural laminates. The failures of the two- and three-layer specimens were similar. The main difference was that the two-layer specimens developed more flexural cracks. In addition, cracking due to the concentration of stresses at the cut-off points of the flexural laminate was more pronounced in the three-layer specimens.

4.8.3 Shear Reinforcement at 45^{o}.

The strength increases over the control beams were 200 percent for the one-layer specimens, 330 percent for the two-layer beams, and 300 percent for the three-layer beams. The diminished strengthening effect exhibited by the three-layer beams was likely due to over-reinforcement resulting in a change of failure mode.

As mentioned in Section 4.4.3, the reinforcement of the beams not only supplied an increased shear capacity, but it also significantly increased a specimen's flexural capacity. The typical behaviors of the specimens are shown in Figures 4.41 through 4.43.

Figure 4.42 shows that the strain developed was dependent on the thickness of the laminate. As expected, the thicker laminate developed the least strain.

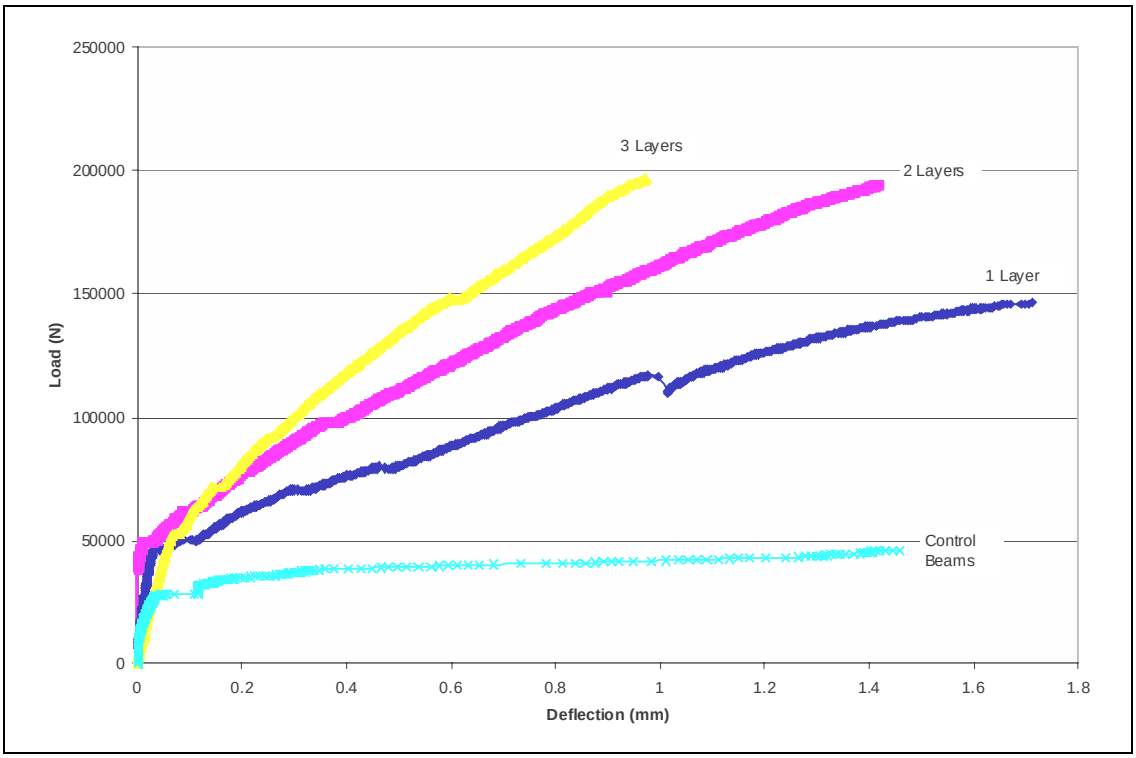

Figure 4.41: Typical load versus deflection for specimens reinforced for shear at 45^{o} with the Tyfo® glass system

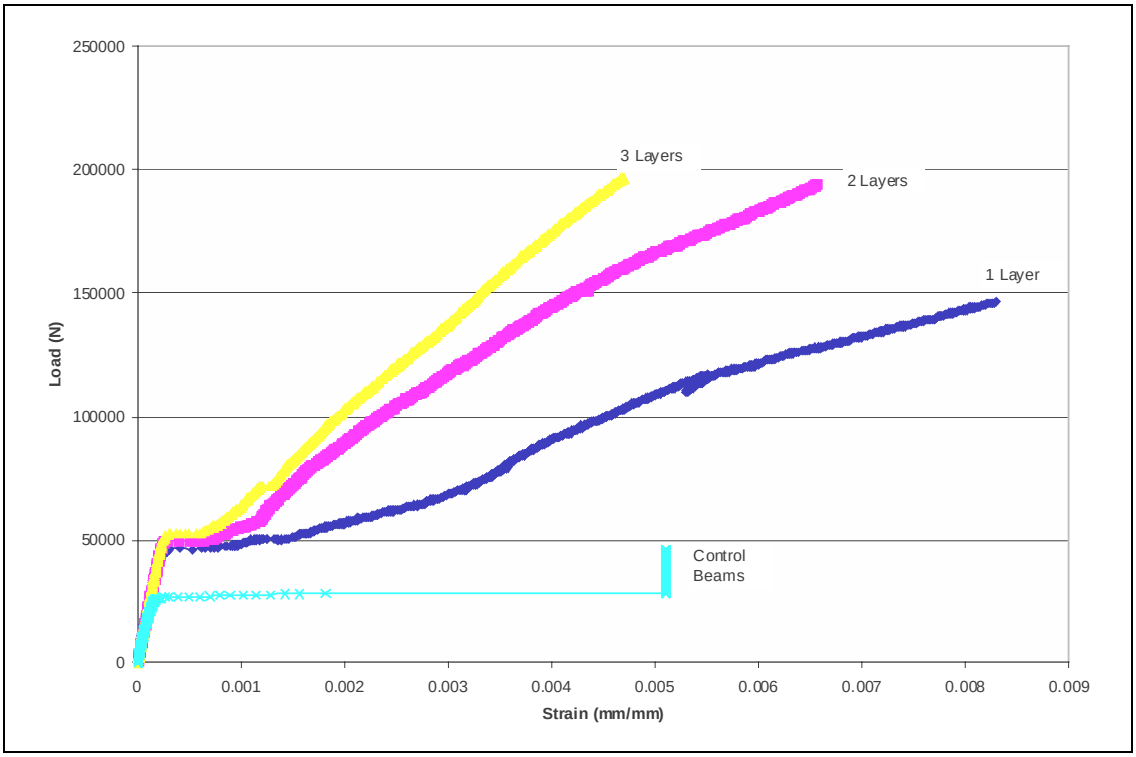

Figure 4.42: Typical load versus flexural strain for specimens reinforced for shear at 45^{o} with the Tyfo® glass system

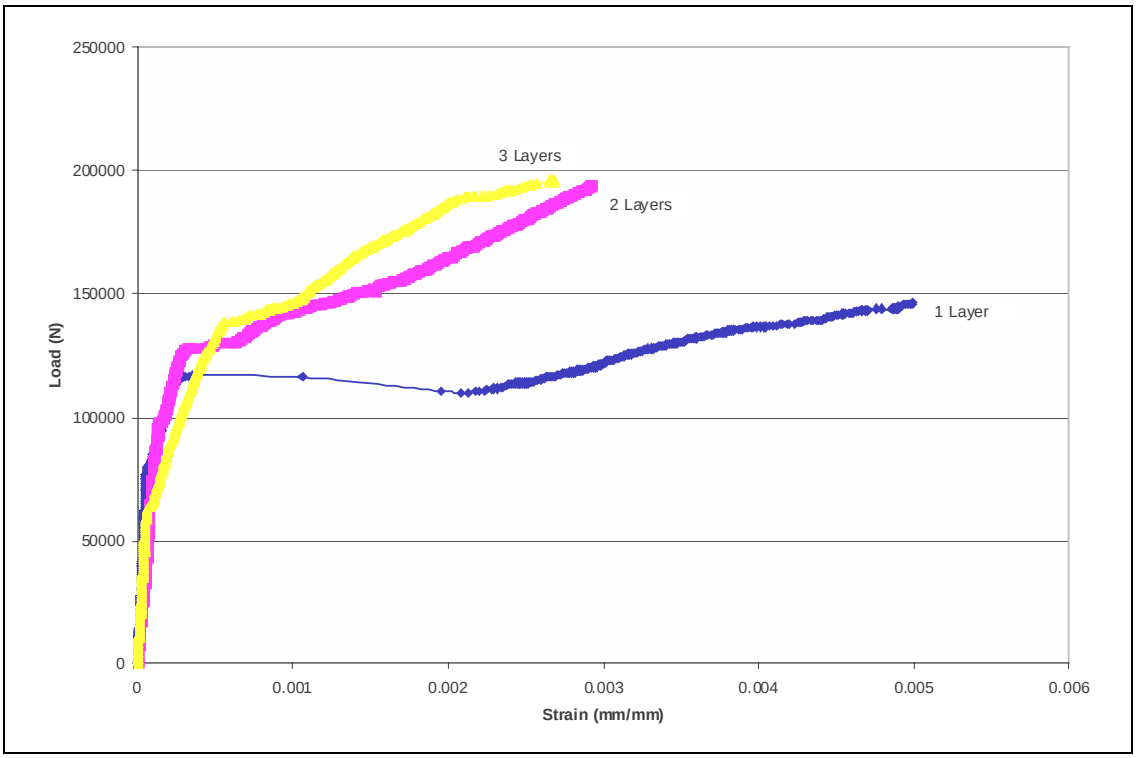

Figure 4.43: Typical load versus strain in shear laminate for specimens reinforced for shear at 45^{o} with the Tyfo® glass system

As shown in Figure 4.43, strains developed in the two- and three-layer specimens were similar. This was likely due to debonding occurring in the shear laminate for each of the specimens with this reinforcing scheme. All of the beams strengthened with this reinforcing scheme failed in shear with debonding of the shear laminate.

4.9 CLARK SCHWEBEL STRUCTURAL GRID

Beams reinforced for flexure exhibited strength gains close to 85 percent above the control samples. Specimens reinforced for flexure and shear displayed strength increases of 80 percent on average. The load at initial cracking was increased by approximately 20 percent in both the flexure and flexure-plus-shear specimens.

In addition to the flexure only, and flexure and shear specimens, five specimens were reinforced for shear only. Due to the specifics of the Clark Schwebel Structural Grid, the beams retrofitted with this system were tested with the shear reinforcement attached to the sides of the specimens only (compared to the other systems in which the shear laminates overlapped at the specimen's tensile face). This strengthening scheme was used as a comparison to the 90^{o} shear reinforced specimens using the Replark® CFRP system. The shear-only specimens exhibited load increases of approximately 20 percent prior to failure.

Figure 4.45 shows that each reinforcement scheme delayed initial cracking. After initial cracking, the behavior of the specimens was dependent on the reinforcing scheme. At similar

load levels, lower strain values were recorded in the flexure specimens than in the flexure-plus-shear specimens.

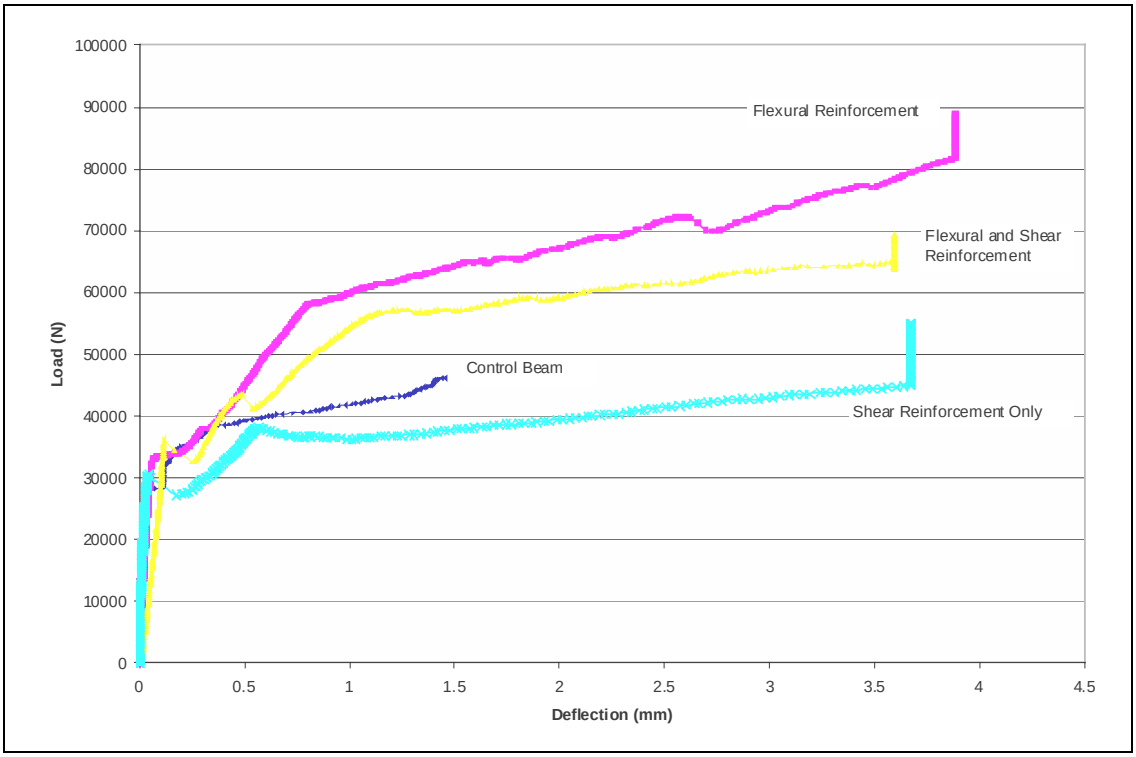

Figure 4.44: Typical load-versus-deflection behavior for specimens strengthened with the Clark Schwebel Structural Grid

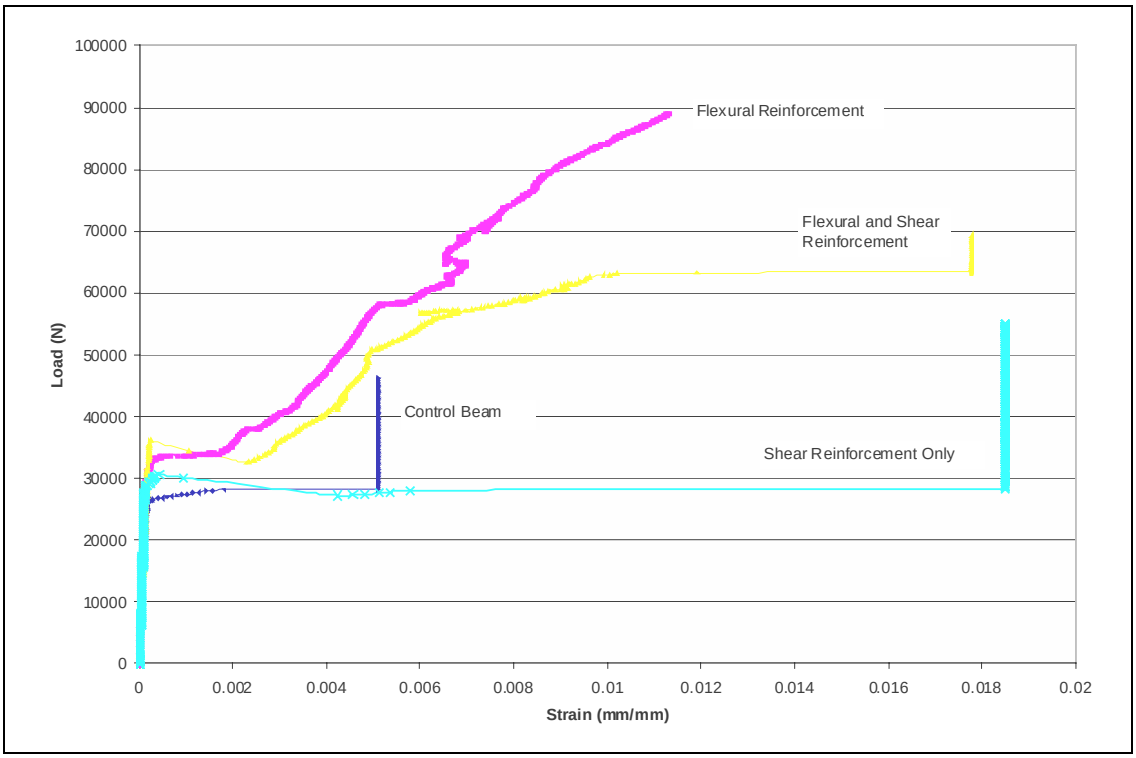

Figure 4.45: Typical load versus strain for specimens reinforced with the Clark Schwebel Structural Grid (Strain in Shear Reinforced and Control was measured on the concrete surface)

Failure modes of the beams varied slightly, although all failed in flexure. The specimens with flexural reinforcement failed after the laminate debonded from the center of the specimen. Similar failure occurred in the flexure-plus-shear specimens. However, in most cases the flexural laminate was not completely fractured. The shear-only specimens failed in flexure.

4.10 OWENS CORNING/REICHHOLD GFRP SYSTEM

Beams reinforced with the Owens Corning/Reichhold glass FRP system had increases in ultimate strength ranging from 30 to 265 percent above the control specimens. The specimen behavior for different strengthening schemes are discussed further in the following sections.

4.10.1 Flexural Reinforcement Only

The average strength increases for the beams reinforced for flexure were 35, 120 and 180 percent for one, two and three layers respectively. The load at initial cracking was increased by approximately 50 percent. The number of layers of FRP reinforcement did not seem to significantly affect the load at initial cracking. Typical load-versus-deflection and load-versus-strain diagrams are given in Figures 4.46 and 4.47.

The ultimate strength increased with additional layers of FRP, as can be seen in Figure 4.46. The deflections and strains at failure are also significantly increased with additional layers.

The specimens reinforced with one layer of reinforcement failed in flexure. This resulted in the fracture of the flexural reinforcement across the concrete tension face. Specimens reinforced with two and three layers failed predominantly in flexure but with some shear failures. The shear failures were accompanied by flexural cracking and debonding of the flexural laminate.

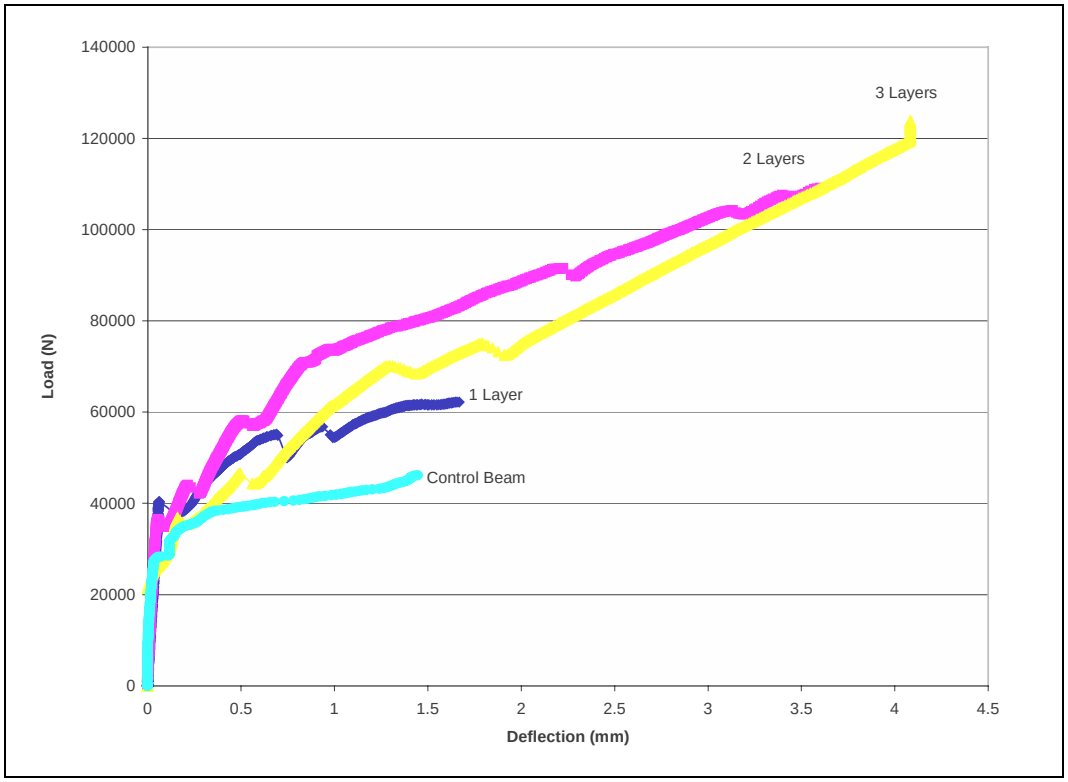

Figure 4.46: Load versus deflection for specimens reinforced for flexure only with Owens Corning/Reichhold

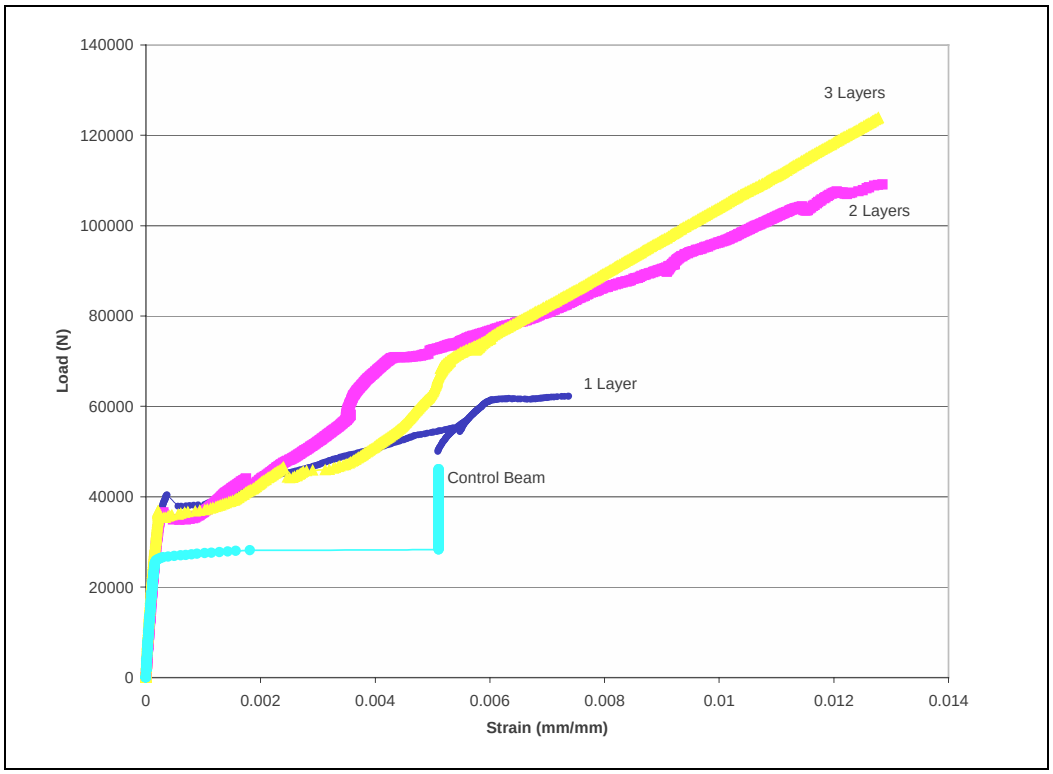

Figure 4.47: Load versus strain for specimens reinforced for flexure only with Owens Corning/Reichhold

4.10.2 Flexural Reinforcement and Shear Reinforcement at 90º

The increases in strength for the beams reinforced for flexure and shear at 90 degrees averaged 30, 145 and 180 percent above the control specimens for one, two and three layers respectively. The behavior for this strengthening scheme was similar to the flexurally reinforced specimens. Figures 4.48 and 4.49 illustrate typical load-versus-deflection and load-versus-strain diagrams.

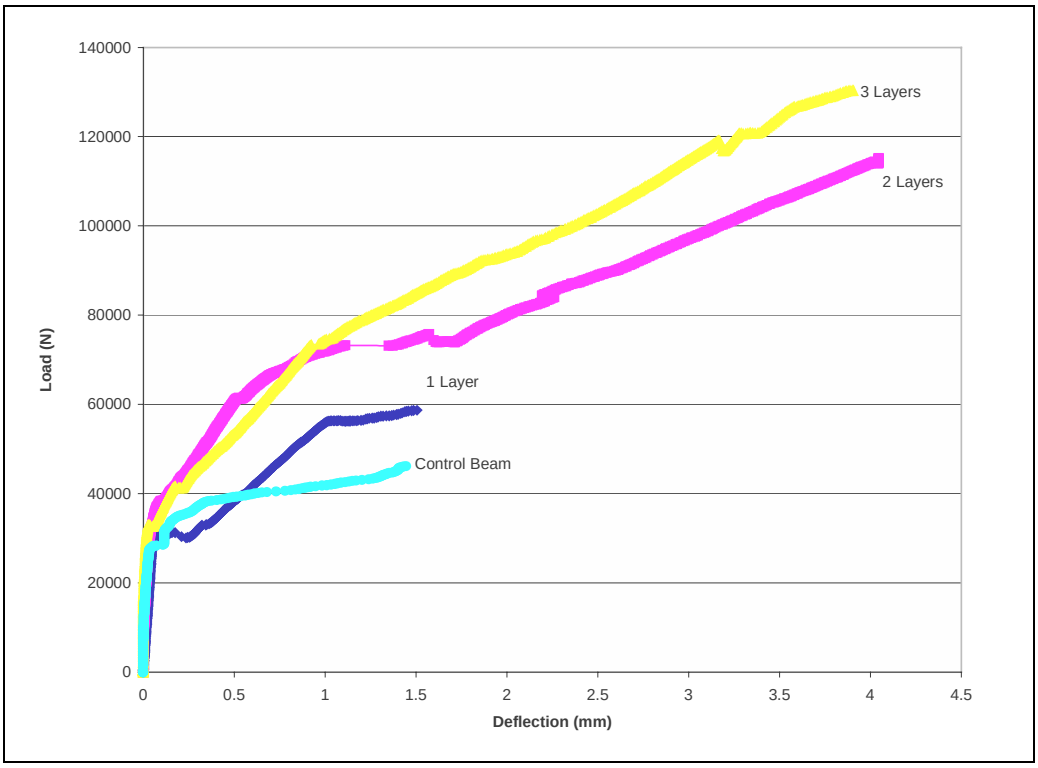

Figure 4.48: Load versus deflection for specimens reinforced for flexure and shear at 90 degrees with Owens Corning/Reichhold

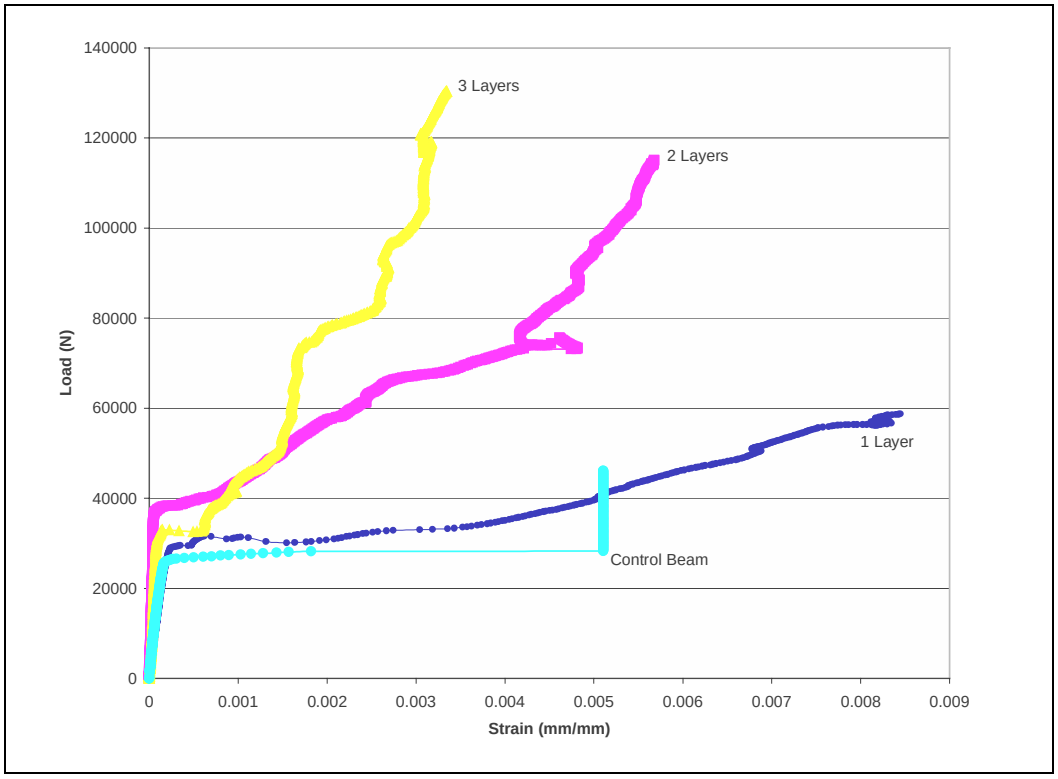

Figure 4.49: Load versus strain for specimens reinforced for flexure and shear at 90 degrees with Owens Corning/Reichhold

Figures 4.48 and 4.49 show the increases in strength for representative specimens for each layer. Beams reinforced with one layer did not significantly increase the load at first crack. However, the two- and three-layer beams increased the load at first crack by approximately 55 percent. Deflection at failure increased substantially for the two- and three-layer specimens but not for the one-layer specimens.

Figure 4.49 illustrates decreasing strain at failure with the addition of more layers. However, the data does not support this conclusion when considering the averages. The strain at failure values were not significantly different between groups.

The failure mode of the one-layer beams was flexural. Beams reinforced with two and three layers exhibited both flexural and combined flexural/shear failures.

4.10.3 Flexural Reinforcement and Shear Reinforcement at 45º

The average ultimate strength increases were 120, 195 and 265 percent for one, two and three layers of reinforcement, respectively. The load at first crack was increased by about 75 percent for one- and two-layer specimens. Three-layer specimens showed an average increase in load at first crack of approximately 95 percent. Direct comparison of ultimate strengths of this strengthening scheme to the others cannot be made due to the shear reinforcement overlap as described in Section 4.7.3. Specimens reinforced for flexure and shear at 45 degrees were the only Owens Corning/Reichhold specimens to exhibit predominantly shear failures. Typical load-versus-deflection and load-versus-strain diagrams are given in Figures 4.50 and 4.51.

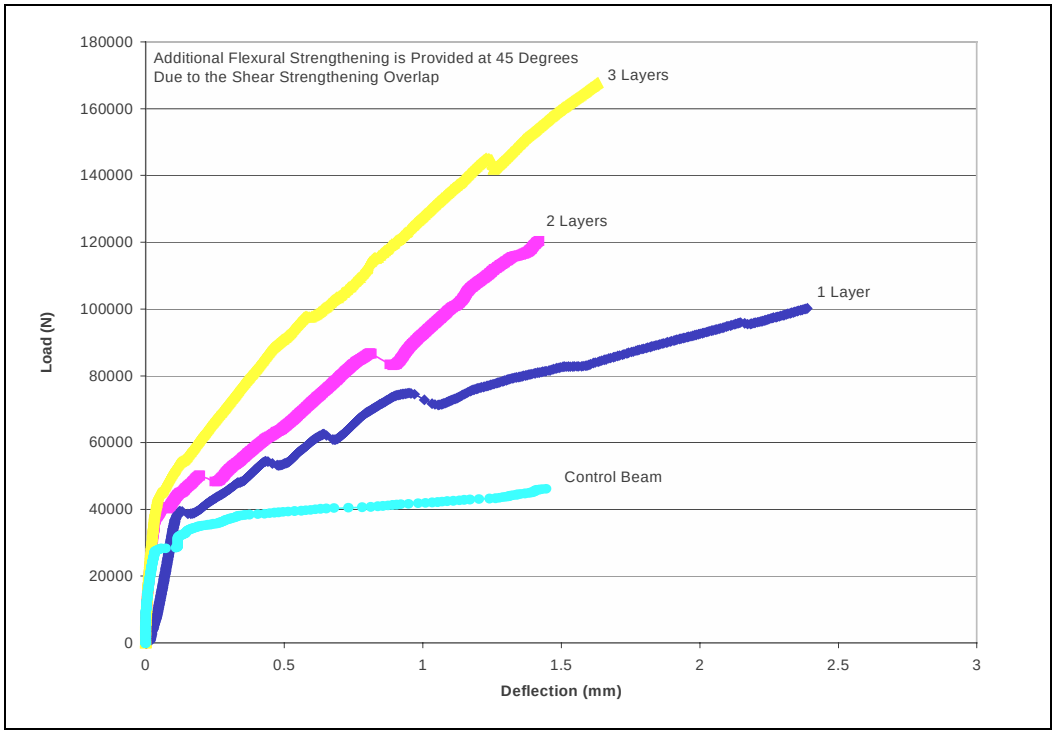

Figure 4.50: Load versus deflection for specimens reinforced for flexure plus shear at 45 degrees with Owens Corning/Reichhold.

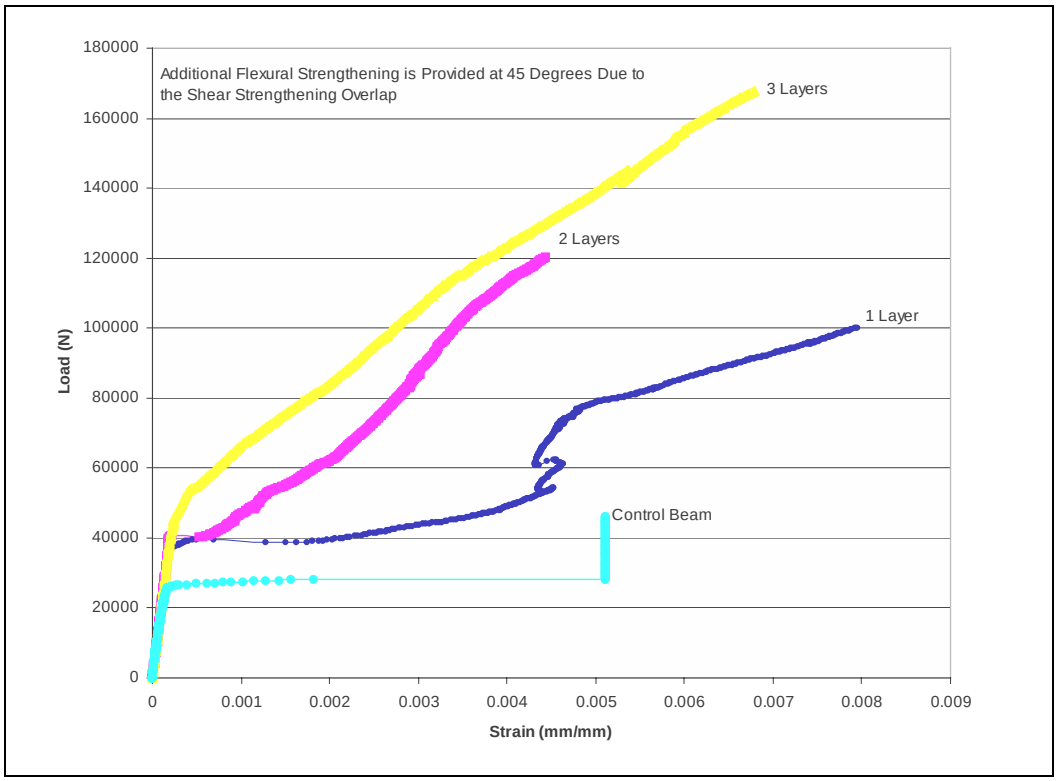

Figure 4.51: Load versus strain for specimens reinforced for flexure plus shear at 45 degrees with Owens Corning/Reichhold.

One-layer specimens exhibited an average increase in deflection at failure of about 45 percent. The two- and three-layer beams showed only a slight increase in deflection at failure. The strain at failure was significantly lower for the two- and three-layer specimens compared to one-layer beams. The reason for the decreased deflection and strain at failure for the two- and three-layer beams is attributed to the failure mode. One-layer specimens failed predominantly in flexure or in a combination of flexure and shear. Two- and three-layer specimens all failed in shear.

4.10.4 Shear Reinforcement at 45º

The average ultimate strength increases were 65, 130 and 135 percent for one, two and three layers of reinforcement, respectively. The load at first crack was increased by approximately 35 to 60 percent for one- and two-layer beams. Three-layer beams did not show a significant average increase over the two-layer specimens. In addition, increasing the number of layers from two to three did not significantly increase the average ultimate strength. The mode of failure shifted from combined to primarily shear. This strengthening scheme seemingly resulted in shear and flexural strengths that were similar. There was no clearly dominant failure mode within the groups of one-, two- and three-layer specimens. Typical load-versus-deflection curves are illustrated in Figure 4.52. Load-versus-strain diagrams are not included, as true flexural strain was not measured.

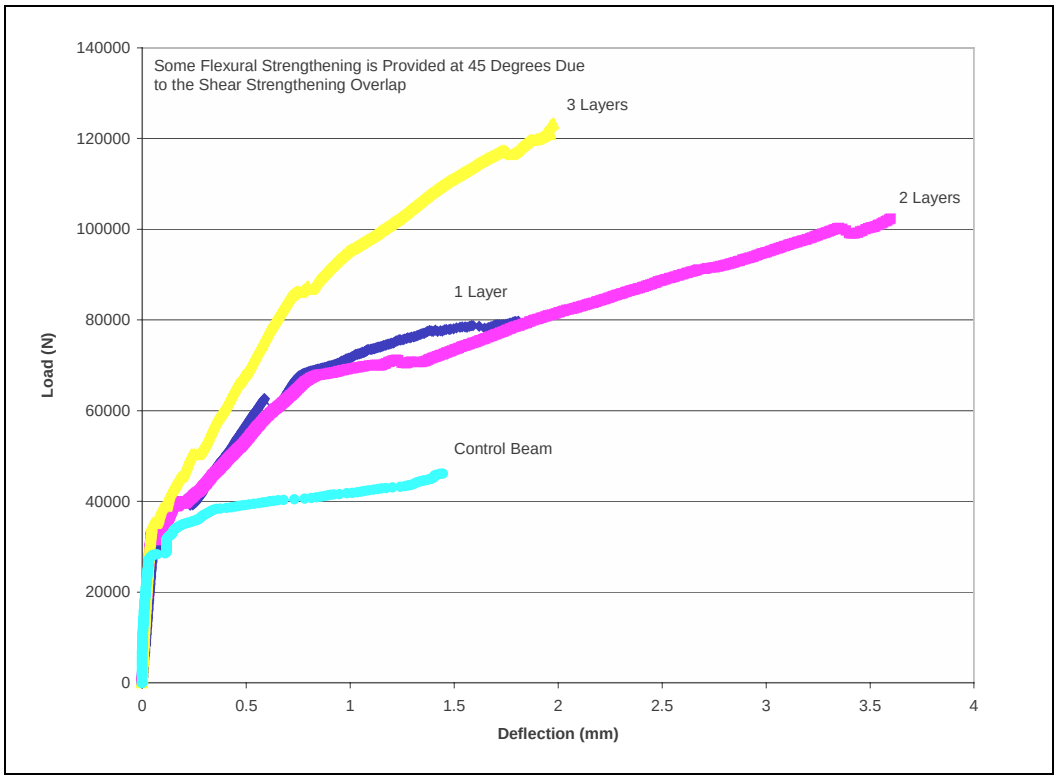

Figure 4.52: Load versus deflection for specimens reinforced for shear at 45 degrees with Owens Corning/Reichhold

Figure 4.52 indicates that the deflection at failure was far superior for two layers of reinforcement. However, due to the variability of failure modes within groups, there was a high variability in deflection at failure. It can be said that when the failure mode was predominantly in shear, the deflection at failure was similar or slightly lower than the control samples. When a flexural failure mode started to dominate, the deflections were greater than the control specimens. The strains in the shear laminates also had a high variability for the same reasons. In addition, shear strains in the laminate were also determined by where the major cracking occurred. Shear strains are tabulated in Chapter 5 of this report.

As discussed previously, the failure modes were highly variable within groups. In several cases, the mode of failure was classified as combined. The combined failures typically consisted of major shear cracking followed by flexural cracking propagating toward the flexural face outside of the middle third of the beam. Shear laminates debonded along with the fracture of the flexural reinforcement. The flexural reinforcement typically led just outside of where the overlap was complete. In this portion of the beam, the flexural reinforcement was less than in the middle of the specimen.

4.11 FRP-CONFINED CONCRETE CYLINDERS

Nineteen standard concrete cylinders were reinforced with both carbon and glass FRP systems. Specimens were tested to ultimate compressive strength. The failure mode of the cylinders was crushing of the concrete followed by tensile failure of the FRP reinforcement. Compressive strength increases ranged between 115 and 300 percent.

4.11.1 Owens Corning/Reichhold GFRP System

Fifteen cylinders were reinforced with an Owens Corning/Reichhold glass FRP system. The average compressive strength increases were 130, 180, 215, 245 and 285 percent for one, two, three, four and five layers of reinforcement, respectively. An increase in the number of layers of reinforcement resulted in an increase in compressive strength. Table 4.3 shows the individual test results for each of the cylinders.

Table 4.3: Ultimate compressive strength results for Owens Corning/Reichhold reinforced cylinders.

Specimen	No. of Layers	Load at Failure (kips)	Ultimate Stress (psi)	% Increase Over Control Specimens
G1A	1	166	5871	130%
G1B	1	149	5270	117%
G1C	1	186	6578	146%
G2A	2	256	9054	201%
G2B	2	220	7781	173%
G2C	2	212	7498	167%
G3A	3	295	10433	232%
G3B	3	262	9266	206%
G3C	3	274	9691	215%
G4A	4	304	10752	239%
G4B	4	291	10292	229%
G4C	4	339	11990	266%
G5A	5	344	12167	270%
G5B	5	386	13652	303%
G5C	5	367	12980	288%

All of the cylinders failed by crushing of the concrete on a horizontal plane somewhere within the specimen. This was followed by a tensile failure of the FRP reinforcement. Figure 4.53 illustrates the appearance of a typical Owens Corning/Reichhold reinforced cylinder after failure.

Figure 4.53: Typical Owens Corning/Reichhold reinforced cylinder after failure.

4.11.2 Fortafil/Reichhold CFRP System

Four cylinders were reinforced with a Fortafil/Reichhold carbon FRP system. The average compressive strength increases were 225 and 300 percent for one and two layers of reinforcement respectively. Table 4.4 shows the individual test results for each of the cylinders.

Table 4.4: Ultimate compressive strength results for Fortafil/Reichhold reinforced cylinders.

Specimen	No. of Layers	Load at Failure (kips)	Ultimate Stress (psi)	% Increase Over Control Specimens
C1A	1	305	10787	240%
C1B	1	274	9691	215%
C2A	2	373	13192	293%
C2B	2	388	13723	305%

The cylinders reinforced with the Fortafil/Reichhold carbon FRP system had the same failure mode as the glass FRP system. Crushing of the concrete occurred followed by a tensile failure of the FRP. A typical Fortafil/Reichhold reinforced cylinder after failure is illustrated in Figure 4.54.

Figure 4.54: Typical Fortafil/Reichhold reinforced cylinder after failure.

5.0 COMPARISON OF STUDY RESULTS

The following sections attempt to compare the different systems in a fair manner. Since it was found to be quite difficult to account for the wide range of thicknesses of the materials used with the different systems, beams with the same number of layers of reinforcement are compared to each other regardless of thickness. Sika Carbodur® – because of its significantly higher thickness, very high elastic modulus, and high fibers-to-resin ratio – is compared to two- and three-layer laminates as well as the one-layer laminates. More explanation for the comparisons made to the Sika Carbodur® system is given in the following section.

5.1 BEAMS STRENGTHENED WITH CARBON FRP SYSTEMS

Carbon fiber polymer reinforcement systems provided the greater increase in strength when compared to the glass FRP systems. For most of the strengthening schemes that were explored, the loads at failure were increased from 100 to 500 percent with typical load-at-failure improvements in the 250 to 350 percent range.

In most cases, the beams reinforced with one layer of carbon FRP sustained deflections as large as or larger than those exhibited by the control beams prior to failure, although the loads required to cause those deflections were substantially higher. For some of the beams with two or more layers of reinforcement the deflection at failure was significantly less than that of the control beams; however the load was many times higher. The lack of ability to deflect prior to failure is due primarily to the higher stiffness of the multi-layer laminates. That type of behavior might lead to the conclusion that CFRP reinforcement enhances the load carrying capacity of the beams at the expense of deformability. As discussed in the previous chapters, the classical definition of ductility is not applicable to FRP-reinforced members due to the linear stress-strain behavior typical for these materials. Based on the energy absorption criteria, most of the CFRP-retrofitted specimens showed greater deformability than plain reinforced concrete samples. This approach is concurrent with the recommendations of the American Concrete Institute (ACI) 318 code, stipulating that structural safety might be achieved either by ductile behavior prior to failure or reserve of strength beyond the ultimate demand.

The Sika Carbodur® reinforced beams were different from most of the beams that were tested in this study, as was mentioned in section 3.1.3. The thickness of the CFRP plate was over seven times the thickness of some of the other CFRP products that were investigated in this study. The elastic modulus of this pultruded laminate is 22.5×10^6 psi, while typical CFRP laminate elastic modulus has a value of $10\text{-}15 \times 10^6$ psi. Furthermore, the Sika Carbodur® has a ratio of reinforcing fibers-to-resin of 68 to 32, while typical FRP composites systems contain 30 to 40 percent fibers. The Sika Carbodur® laminate was never failed, even in the beams reinforced heavily for shear, primarily due to the geometry of the specimens that we tested. It was determined early in this research that the beams reinforced with the Sika product would likely

sustain higher loads compared to the other systems. Thus, it was decided to compare the results from the Sika Carbodur® reinforced beams not only with the one-layer beams, but also to specimens having multiple layers of reinforcement. The SikaWrap® Hex and Fyfe systems, although almost as thick, were not treated in the same manner, because it was assumed that their performance would be closer to that of the other systems in which multiple layers of reinforcement were applied.

The following figures show the results from the one beam of each reinforcement scheme that was selected as the most representative of the group. The tables compare the average results. In addition, the various thicknesses of the laminates that were used are not accounted for; therefore, one might expect the thicker laminates to perform better than the thinner ones. This was not always the case, however. Data that is supplied under the CONTROL heading is the average of the results from the control beams that were tested in this study and is provided as a reference point to which the strengthened specimens can be compared.

5.1.1 Flexural Reinforcement

Six different FRP systems were examined as flexural strengthening systems for the beams in this study. Since some of the materials were similar in appearance, a labeling system was introduced in order to tell the beams apart after the laminate was applied. The following explains the labeling designations that were used:

- CMIRF – Composite Materials Inc. carbon fibers combined with Reichhold Chemicals Inc., resin.
- FCF – Fyfe company's Tyfo® carbon system.
- MBCF – Master Builders' MBrace™ carbon system.
- MCF – Mitsubishi's Replark® carbon system.
- SCF – Sika Carbodur® system. All beams have one layer of Carbodur® laminate.
- SHCF – SikaWrap® Hex 103C system.

The number following each of the designations is the number of laminate layers that were applied to the beam. In each case, the fiber orientation was along the longitudinal axis of the beam, and the laminate was attached to the tension face.

5.1.1.1 One Layer of Flexural Reinforcement.

The Tyfo® FRP system was able to achieve the highest strength increase of the one layer beams. The beams reinforced with this system exhibited higher ductility than any of the beams reinforced with other systems. Results from all of the systems that were tested are presented in Table 5.1 and Figures 5.1 and 5.2.

The Sika Carbodur® system, which is similar in thickness to the Tyfo® FRP system, performed similarly based on strength alone. In addition, this system seemed to delay initial cracking of the beams to a higher load and appeared to be able to control deflection better than the other systems, most likely due to the high stiffness of the laminate.

The SikaWrap® Hex system, the Master Builder's MBrace™ system, and the CMI/Reichhold Chemicals system all seemed to have slight bonding problems. It is possible that this was the result of an insufficient curing time recommended by the manufacturer, environmental conditions at the time of testing, or both.

The Replark® system performed very well, considering the thickness of material that was used. The average load at failure of the beams was approximately 30 percent less than that of the Tyfo® FRP beams, while the average load at initial cracking was only 12 percent less. One should note, however, that the thickness of the CFRP sheet used by Tyfo® FRP system was 7.8 times thicker than the Replark® sheet. Thus, based on load-carrying capacity per unit thickness, Replark® CFRP material was quite possibly the best performing system of all.

Table 5.1: Average results from one-layer flexure-only specimens

	@ initial flexural cracking			**@ failure of the beam**			
Beam	Load (N)	Deflection (mm)	Flexural Strain (x 10^{-4})	Load (N)	Deflection (mm)	Flexural Strain (x 10^{-3})	Type of Failure
CONTROL	22894	0.035	1.396	45850	1.617	NA	Flexure
CMIRF1	39044	NA	2.980	69290	0.897	5.246	Flexural Failure
FCF1	43181	0.062	3.222	196081	2.893	8.210	Shear/Local
MBCF1	30656	0.051	1.940	91931	1.877	5.053	Shear/Debond
MCF1	37808	0.081	2.680	134979	2.687	8.389	Shear
SCF	52989	0.075	3.125	175736	1.145	2.724	Shear/Local
SHCF1	41171	0.055	2.609	141304	1.665	5.289	Shear/Bond problems

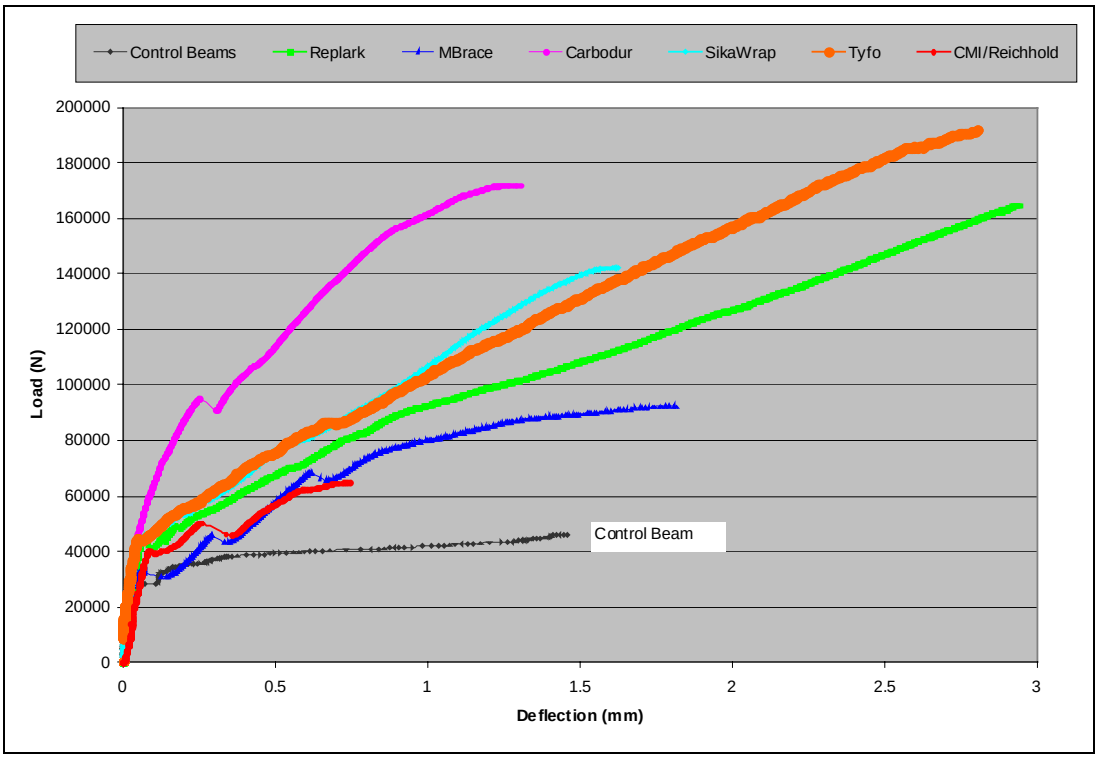

Figure 5.1: Load versus deflection behavior for specimens reinforced with one layer of laminate for flexure only

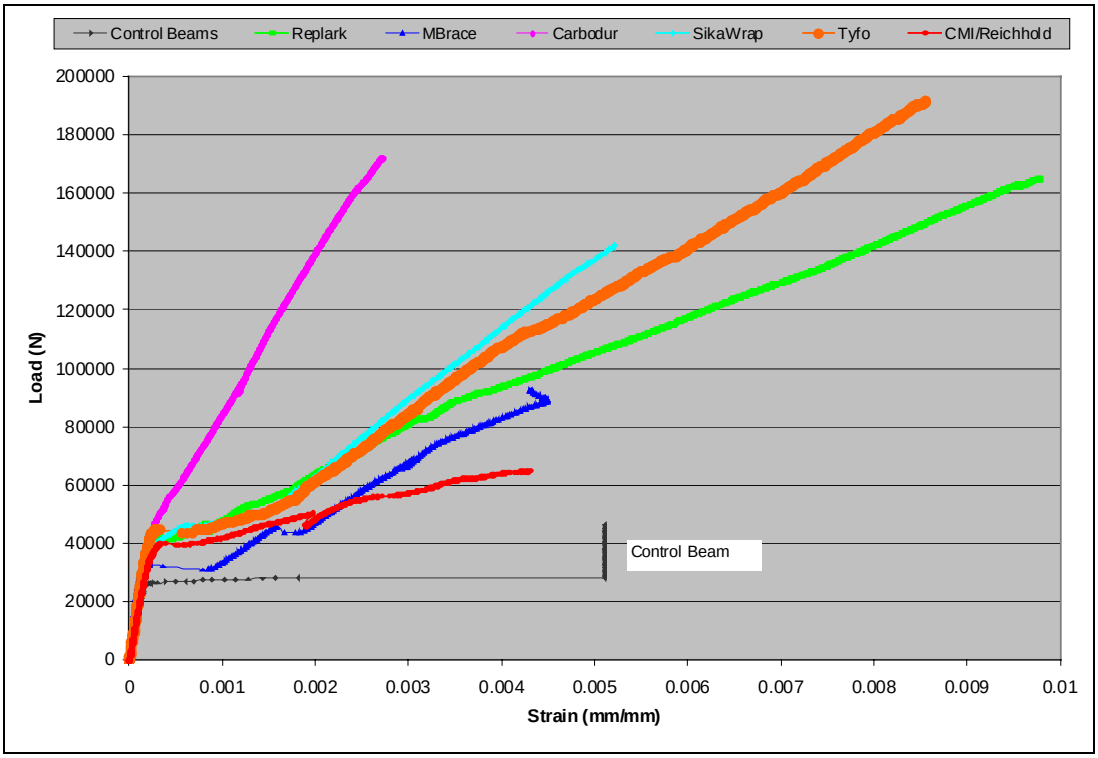

Figure 5.2: Load verus strain behavior for specimens reinforced with one layer of laminate for flexure only

The following observations can be made from the average data presented in Table 5.1. The Carbodur® laminate, which had the highest elastic modulus as given by the manufacturers, developed very little strain. This observation suggests that a high percentage of the laminate's capability remained unutilized, which complies with the general knowledge that the effectiveness of the FRP reinforcement decreases as its rigidity increases. Therefore potential FRP users must acknowledge the fact that load improvement itself is not always the most desirable factor when external reinforcement is considered. The effect of any FRP system will vastly diminish if there is no compatibility between the composite reinforcement and the concrete beam to which it is applied.

Observing the strains at failure of the other systems, one can see that some of the systems that exhibited slight bonding problems failed under similar strains. Some other systems, which had no bonding problems, failed at strains that were a little higher. These similarities in strain are interesting, considering that the materials had different thicknesses and stiffnesses. It may suggest that failure of the FRP reinforced beams was controlled by strains developed within the laminate, and that those strains are controlled by the bonding ability of the resin.

5.1.1.2 Two Layers of Flexural Reinforcement

For the specimens reinforced with two layers of CFRP laminates, the Replark® system performed superior to all of the other systems based on strength alone. The average load at failure of the beams was over 300 percent higher than the control beams.

Load at failure for many of the specimens was reduced with the additional layer of reinforcement, possibly due to the significant thickness of the laminates. This would suggest that the specimens were over-reinforced in flexure, and the addition of material resulted in more sudden failure. The overall reduced strains at failure suggests reduction of CFRP's effectiveness. CMI/Reichhold Chemicals system was the only exception to that phenomenon. For the MBrace™ reinforced beams, this increase in laminate rigidity led to a change in failure mode. The strength of systems that exhibited slight bonding problems in the one-layer case increased with the addition of the second layer of reinforcement. For the SikaWrap® Hex and MBrace™ systems, the increase in their load-carrying ability was negligible when compared to one-layer reinforcement.

Table 5.2: Average results from two-layer flexure-only specimens

	@ appearance of first flexural crack			**@ failure of the beam**			
Beam	Load (N)	Deflection (mm)	Flexural Strain (x 10^{-4})	Load (N)	Deflection (mm)	Flexural Strain (x 10^{-3})	Type of Failure
CONTROL	22894	0.035	1.396	45850	1.617	NA	Flexure
CMIRF2	38271	NA	3.000	121723	2.689	9.13	Flexural Failure
FCF2	47629	0.070	2.807	172916	1.585	3.995	Shear/Local
MBCF2	33845	0.051	0.959	107748	1.718	2.775	Debond/Flexure
MCF2	42981	0.061	2.733	189743	2.240	6.572	Shear
SCF ***	52989	0.075	3.125	175736	1.145	2.724	Shear/Local
SHCF2	41571	0.056	2.515	143355	1.183	3.206	Shear/Slight Bond Prob.

***** Carbodur Beam is one layer only. All others have two layers of fibers.**

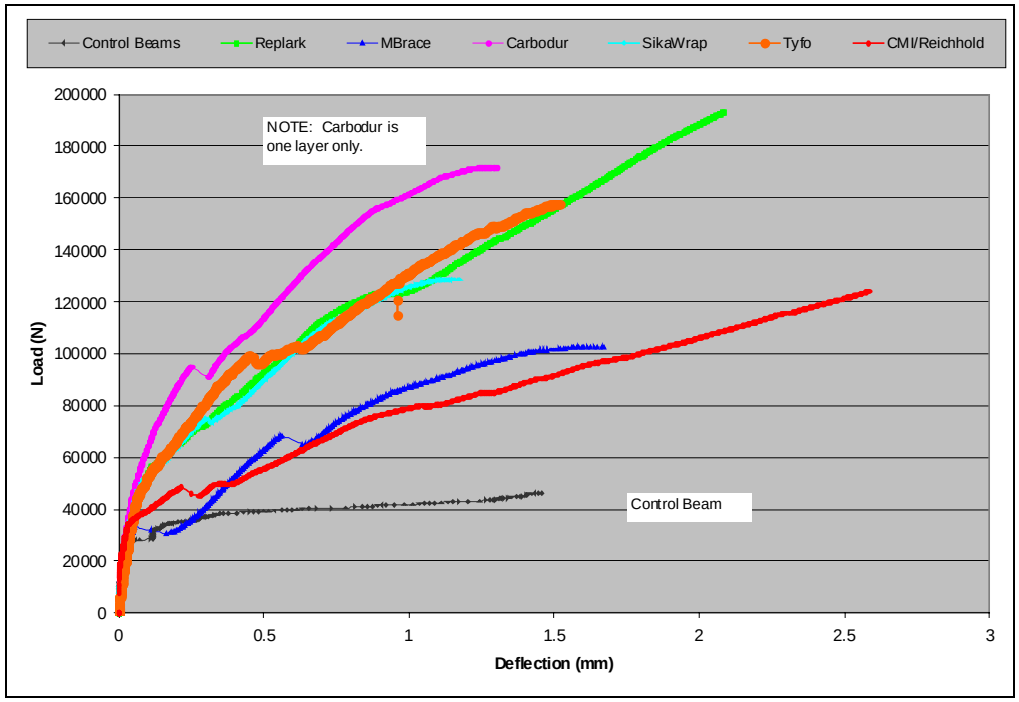

Figure 5.3: Load-versus-deflection behaviors for specimens reinforced with two layers of laminate for flexure only

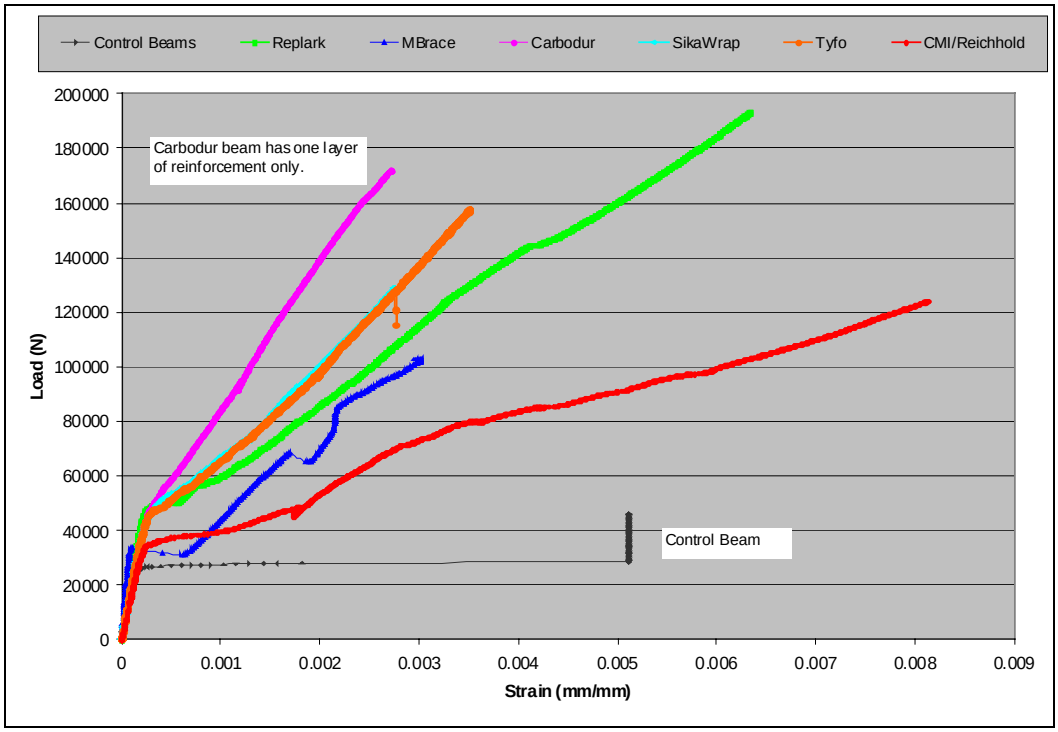

Figure 5.4: Load-versus-strain behaviors for specimens reinforced with two layers of laminate for flexure only

5.1.1.3 Three Layers of Flexural Reinforcement

Beams reinforced with three layers of flexural reinforcement all failed in shear. The strongest specimens were the beams reinforced with the Fyfe Company's Tyfo® system. The slight increase in the strength of the beams between two and three layers was most likely the result of additional shear strength contribution provided by the additional flexural laminate. The difference in strengths of the beams that failed in shear was also the result of the flexural reinforcement contributing to the shear capacity of the beam. This phenomenon is not taken into account in the case of reinforced concrete beams, but will need to be addressed in FRP design.

The thinner laminates that were tested, with the exception of the CMI/Reichhold system, displayed decreases in strength with the addition of the third layer of reinforcement. This finding might suggest there is some point at which the addition of more reinforcement becomes detrimental to the beam's performance. Results of the specimens that were tested are presented in Table 5.3 and Figures 5.5 and 5.6.

Examination of Figure 5.5 reveals that all of the beams failed at approximately the same amount of deflection. Although the loads needed to cause the deflections varied, in every specimen these loads were much higher than those of the control beams. In addition, under the same loading that caused failure of the control beams, the deflections were approximately one tenth those of the control. This is a very clear illustration of the positive effects of the FRP laminate on controlling deflections, even under ultimate loading.

Table 5.3: Average results from three-layer flexure-only specimens

	@ initial flexural cracking			**@ failure of the beam**			
Beam	Load (N)	Deflection (mm)	Flexural Strain (x 10^{-4})	Load (N)	Deflection (mm)	Flexural Strain (x 10^{-3})	Type of Failure
CONTROL	22894	0.035	1.396	45850	1.617	NA	Flexure
CMIRF3	37949	NA	0.265	123918	1.757	5.798	Shear Failure
FCF3	46148	0.066	2.775	181069	1.343	3.008	Shear/Local
MBCF3	33066	0.050	1.317	101357	1.153	2.551	Shear
MCF3	43159	0.063	2.462	164656	1.493	4.004	Shear
SCF***	52989	0.075	3.125	175736	1.145	2.724	Shear/Local

***** Carbodur Beam is one layer only. All others have three layers of fibers.**

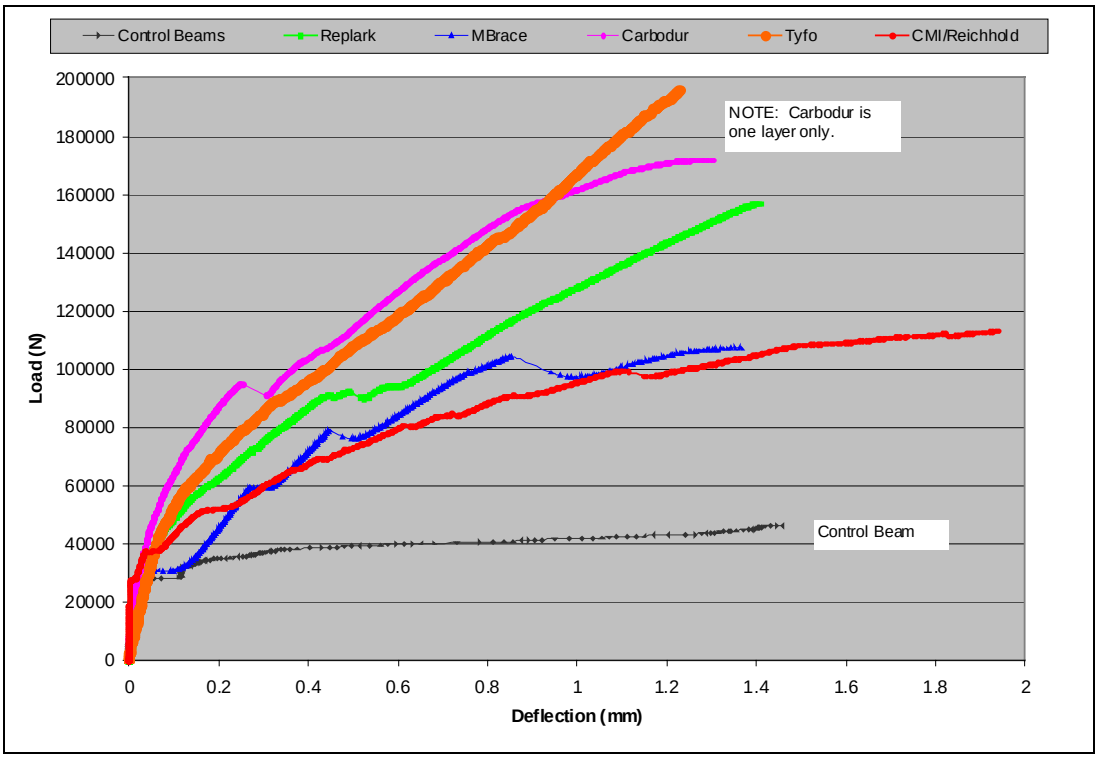

Figure 5.5: Load versus deflection behaviors for specimens reinforced with three layers of laminate for flexure only

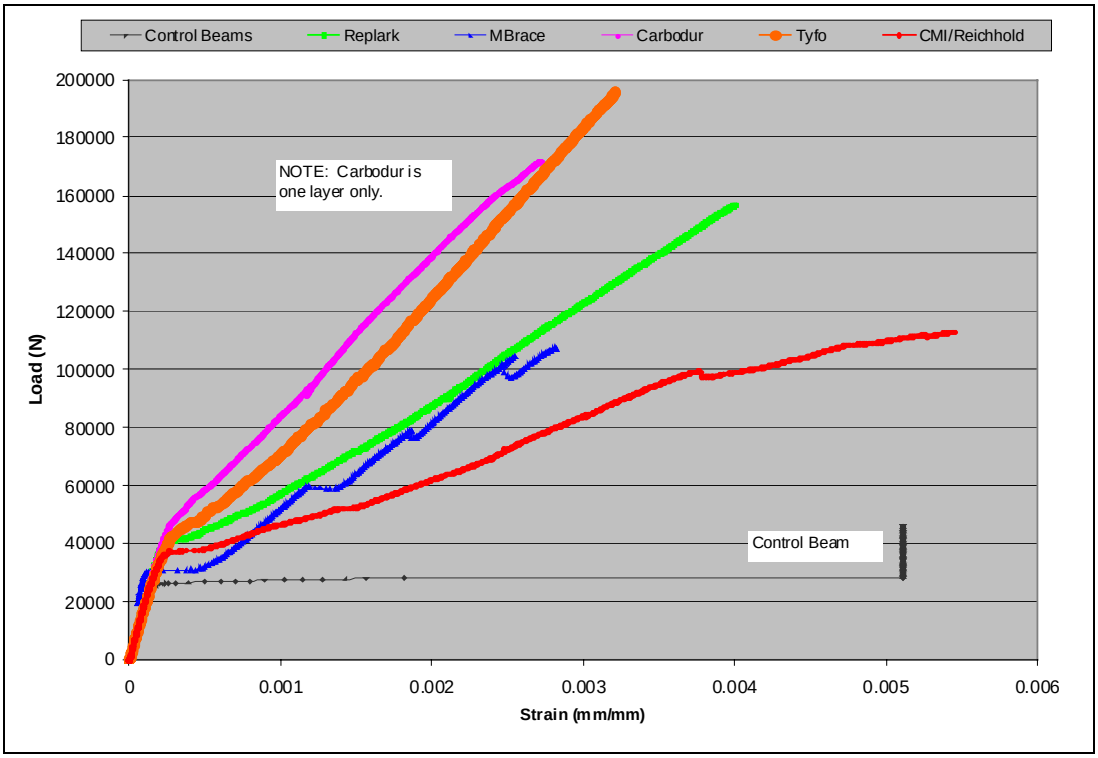

Figure 5.6: Load versus strain behavior for specimens strengthened with three layers of laminate for flexure only

5.1.2 Flexure plus Shear Reinforcement

Eight different reinforcing scenarios were explored using combinations of shear and flexural reinforcement. The designation for each reinforcing scheme is as follows:

- CMIRFS – Composite Materials Inc. carbon fibers combined with Reichhold Chemicals Inc., resin. The 90 designation refers to shear fibers oriented at 90 degrees to the longitudinal axis. The 45 designation refers to a shear fiber orientation of 45 degrees to the longitudinal axis of the beam. The beams with 45 degree fiber orientation also have significantly more flexural reinforcement, since the shear fibers are wrapped across the tensile face of the beam as well as the sides.
- FCFS – Fyfe company's Tyfo® carbon system. Shear fibers are at 90 degrees to the longitudinal axis of the beam.
- MBCFS – Master Builders' MBrace™ carbon system. Shear fibers are at 90 degrees to the longitudinal axis of the beam.
- MCFS – Mitsubishi's Replark® carbon system. Shear fibers are at 90 degrees to the longitudinal axis of the beam.
- SHCFS – SikaWrap® Hex 103C system. Shear fibers are at 90 degrees to the longitudinal axis of the beam.
- SCFS – All beams have one layer of Sika Carbodur® laminate for flexural reinforcement and SikaWrap® Hex 103C for shear reinforcement (number of shear layers given by number after SCFS) with fibers oriented at 90 degrees to the longitudinal axis of the beam.
- 45SHCFS – All beams have one layer of Sika Carbodur® laminate for flexural reinforcement and one layer of SikaWrap® Hex 101G for shear reinforcement. Shear fibers are oriented at ± 45 degrees to the longitudinal axis of the beam.

The 45SHCFS beams, although strengthened with glass FRP for shear, are included in this section due to the fact that the flexural CFRP laminate governed the majority of the beams' behavior. For all of the beams the number following the designation is the number of layers of shear laminates, and for all beams except those reinforced with the Carbodur® system, this is also the number of layers of flexural reinforcement.

The CMIRFS – 45 beams are strengthened in flexure in two ways. First flexural laminate was applied on the beams, followed by application of 45 degree-orientated layers positioned on the sides of the beam. These layers started at one end of the beam and ran up the side, across the tensile face, and down the opposite side at the other end of the beam. Therefore, beams that are considered as three-layer beams actually have nine layers of laminate at the midspan due to the overlapping shear layers.

5.1.2.1 One Layer of Flexural and Shear Reinforcement

Sika Carbodur® laminate for flexural reinforcement and one layer of SikaWrap® Hex 101G for shear reinforcement exhibited the greatest load carrying capacity of all compared specimens. It appears that the ± 45 degree glass laminate provided better control of the shear cracking prior to debonding.

Of the other systems, the Tyfo® FRP system performed superior to the other of the thicker systems (individual layer thickness about 1 mm). The Replark® system performed the best of the thinner systems (individual layer thickness about 0.1 mm). The CMI/Reichhold Chemicals and MBrace systems showed similar enhancement of the performance of the beams. In general, all of the systems displayed large improvements in performance over the control beams. Average results for the beams are presented in Table 5.4.

Table 5.4: Average results for one layer flexure and shear reinforced specimens

	@ initial flexural cracking			**@ failure of the beam**				
Beam	Load (N)	Deflection (mm)	Flexural Strain (x 10^{-4})	Load (N)	Deflection (mm)	Flexural Strain (x 10^{-3})	Strain** in Shear (x10^{-4})	Type of Failure
CONTROL	22894	0.035	1.396	45850	1.617	NA	NA	Flexure
CMIRFS1-90	32396	NA	2.770	72952	1.328	5.350	NA	Flexural Failure
CMIRFS1-45	37936	NA	2.350	117827	1.509	6.055	47.26	Shear Failure
FCFS1	48741	0.087	3.158	217583	2.805	9.074	7.477	Flexure
MBCFS1	34267	0.047	2.059	130411	1.809	7.318	NA	Flexure
MCFS1	42910	0.061	2.792	175491	2.490	9.650	10.959	Flexure
SHCFS1	46384	0.074	2.613	174784	1.717	6.575	NA	Flexure
SCFS1	53189	0.073	2.545	206276	1.216	3.652	NA	Local/Shear
45SHCFS	51664	0.060	2.599	226955	1.704	4.063	111.675	Debond/Shear

**** Shear strains are measured in direction of shear fiber orientation (either 90^o or 45^o)**

Many FRP manufacturers suggest strain at failure in the vicinity of 1 to 1.8 percent, depending upon the type of fibers being used. However, the laminates that were tested typically failed at significantly lower strain levels. Replark® and Tyfo® FRP systems displayed strains at failure closer to the manufacturers suggested levels, i.e., 0.96 and 0.9 percent, respectively. The other systems failed at a strain level close to 0.60 to 0.75 percent. Behavior of all the one-layer beams are presented in Figures 5.7 and 5.8.

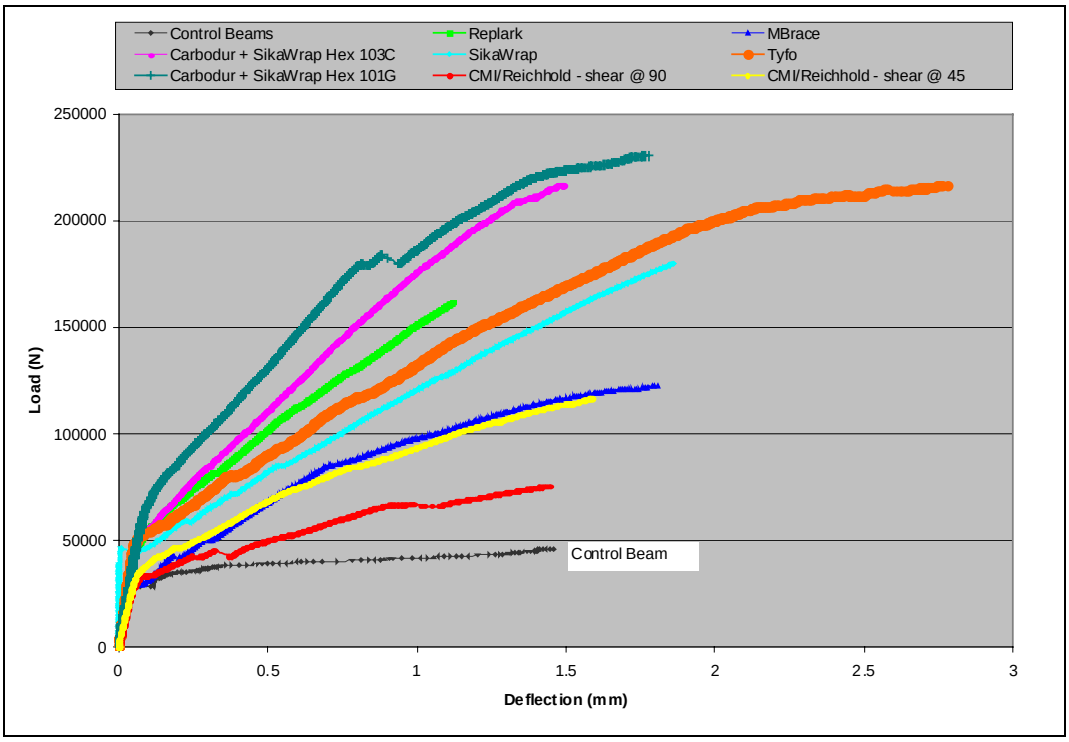

Figure 5.7: Load versus deflection behavior for specimens strengthened with one layer of laminate for shear and flexure

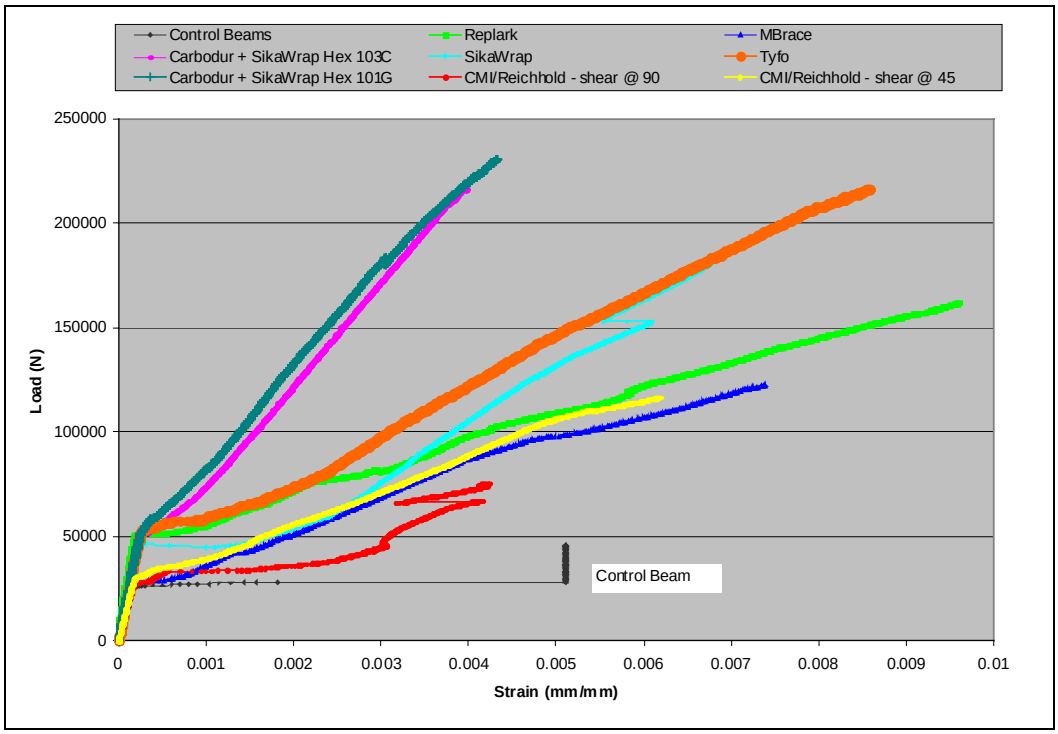

Figure 5.8: Load versus flexural strain behavior for specimens strengthened with one layer of laminate for shear and flexure

5.1.2.2 Two Layers of Flexure and Shear Reinforcement

Tyfo® CFRP system outperformed the others in terms of strength for the two-layered samples. Typical failure occurred due to concentrated local stresses at the ends of the flexural laminate. With the exception of the MBrace™ system and the CMI/Reichhold system, all of the strengthened beams showed improvements of nearly 380 percent in terms of load at failure over the strength of the control beams. These systems all failed due to cracking from stress concentration at the end of the flexural fibers and shear cracking combined with pulling off of the shear laminates.

The MBrace™ and CMI/Reichhold beams strengthened for shear at 90 degrees failed in a combination of flexure and shear. Average results from the beams are given in Table 5.5.

Table 5.5: Average results for two layer flexure and shear specimens

	@ initial flexural cracking			**@ failure of the beam**				
Beam	Load (N)	Deflection (mm)	Flexural Strain (x 10^{-4})	Load (N)	Deflection (mm)	Flexural Strain (x 10^{-3})	Strain** in Shear (x10^{-4})	Type of Failure
CONTROL	22894	0.035	1.396	45850	1.617	NA	NA	Flexure
CMIRFS2-90	43568	NA	0.338	99090	1.570	6.343	NA	Flexural Failure
CMIRFS2-45	44877	NA	0.278	154768	1.267	5.249	3.271	Shear Failure
FCFS2	53189	0.078	2.750	264843	2.615	6.286	12.077	Shear/Local
MBCFS2	41873	0.056	1.729	143052	1.730	3.936	NA	Flex/Shear/Deb.
MCFS2	44258	0.070	2.724	227893	2.570	7.848	10.501	Shear/Local
SHCFS2	46704	0.064	2.577	247420	2.103	5.622	NA	Lam. Split/Shear/Local
SCFS2	51708	0.058	2.743	233520	1.335	4.129	NA	Debond/Shear/Local

**** Shear strains are measured in direction of shear fiber orientation (either 90^o or 45^o)**

From Figures 5.9 and 5.10, it is apparent that the behavior of several of the reinforced specimens was similar. From the load-versus-deflection curves one can see that the behavior of Sika's Carbodur®, Fyfe's Tyfo®, and Mitsubishi's Replark® systems performed quite similarly up to 100,000 N. The load-versus-strain figure shows that the strain behavior of the SikaWrap® and Tyfo® systems were nearly identical. The similar strain behavior of the Tyfo® and SikaWrap® systems could be expected, since the two systems are similar in most respects. The reasons for the deflection behavior of the other systems is more uncertain to determine. It is likely that the deflection behavior of the specimen is highly influenced by its geometry up to a point, and beyond that point, the behavior is influenced by the mechanical properties of the laminate.

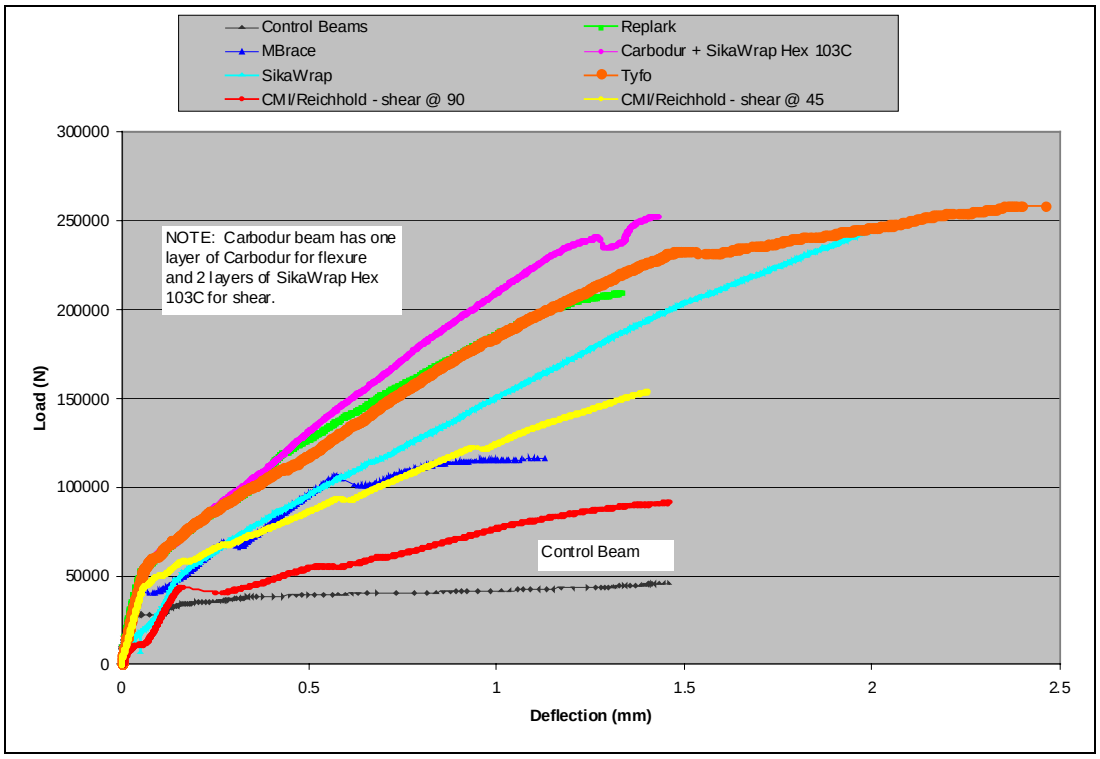

Figure 5.9: Load versus deflection behavior for specimens strengthened with two layers of laminate for flexure and shear

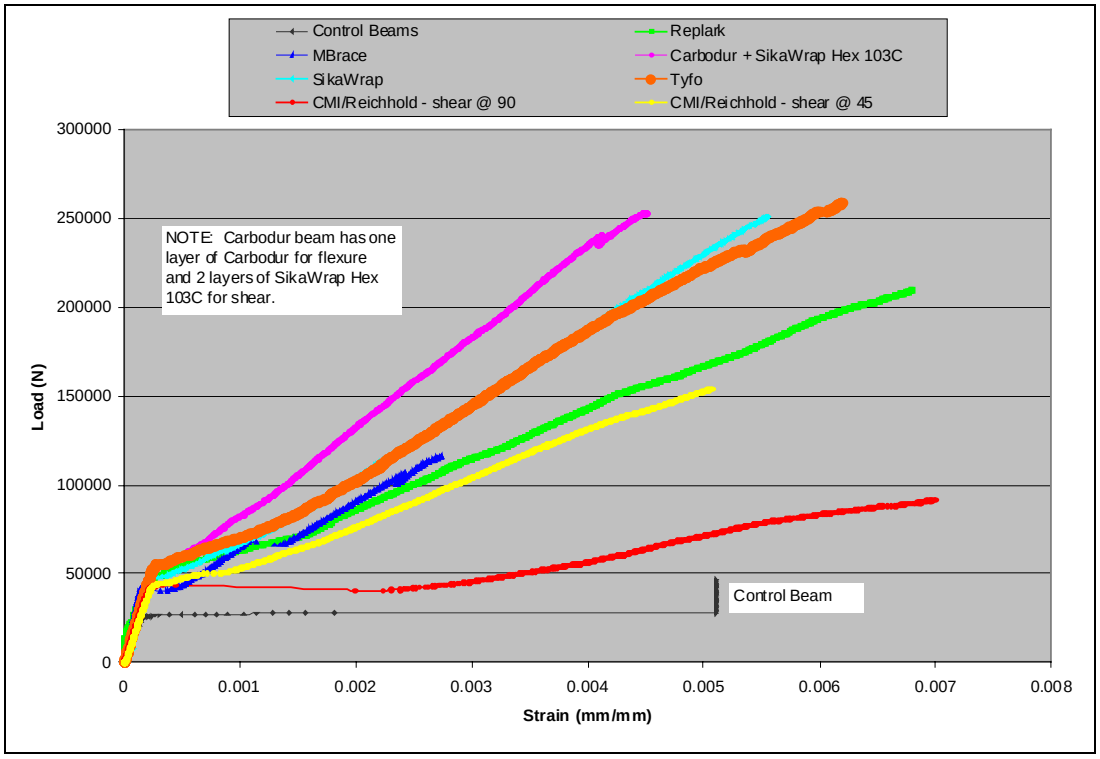

Figure 5.10: Load versus strain behavior for specimens reinforced with two layers of laminate for flexure and shear

5.1.2.3 Three Layers of Flexural and Shear Reinforcement

The Fyfe Tyfo® reinforced beams were the strongest beams tested in this study, with an average improvement in strength of 545 percent.

The Replark® system was the only system in which the strength dropped as the laminate was increased from two to three layers. This was likely due to the increased laminate stiffness, causing debonding of the shear laminate at a lesser load. Considering the similarity of the strains in the shear laminate at failure of both the Fyfe and Replark® specimens, it is possible that debonding of the laminate may be strain controlled, and may be independent of the laminate stiffness. It has been shown, however, that the strain that developed in the laminate for a given load is highly dependent on laminate stiffness (*Kachlakev et.al, 1998; Triantafillou, 1998, Kachlakev and Barnes, 1999*).

Table 5.6: Average results for three-layer flexure and shear specimens

	@ initial flexural cracking			**@ failure of the beam**				
Beam	Load (N)	Deflection (mm)	Flexural Strain (x 10^{-4})	Load (N)	Deflection (mm)	Flexural Strain (x 10^{-3})	Strain** in Shear (x10^{-4})	Type of Failure
CONTROL	22894	0.035	1.396	45850	1.617	NA	NA	Flexure
CMIRFS3-90	40853	NA	0.263	138551	2.133	7.277	NA	Flexural Failure
CMIRFS3-45	43196	NA	0.258	175554	1.366	4.988	2.527	Shear Failure
FCFS3	59492	0.064	3.011	295605	1.690	4.966	8.255	Shear/Local/Deb.
MBCFS3	43555	0.076	1.137	169549	3.614	3.198	NA	Debond/Shear
MCFS3	48243	0.058	2.520	201085	1.179	4.767	8.376	Shear/Debond

**** Shear strains are measured in direction of shear fiber orientation (either 90^o or 45^o)**

Figures 5.11 and 5.12 show the load versus deflection and load versus strain behaviors for the three-layer specimens, respectively. These figures indicate that the CMIRFS - 45 specimens performed nearly as well as the Replark® system. It is important to recall, however, that these specimens actually had six overlapping layers of laminate at the midspan in addition to the three layers of flexural reinforcement, while the Replark® system had only the three layers of flexural reinforcement at midspan.

Most of the systems failed due to debonding of the shear laminate. It is likely that if some type of anchoring were provided, the specimens could have handled higher loads. However, even after debonding of the shear laminate, the specimens were still able to carry approximately three times the load that caused failure of the control beams. This reserve of load carrying capacity might be a very important consideration from a safety standpoint.

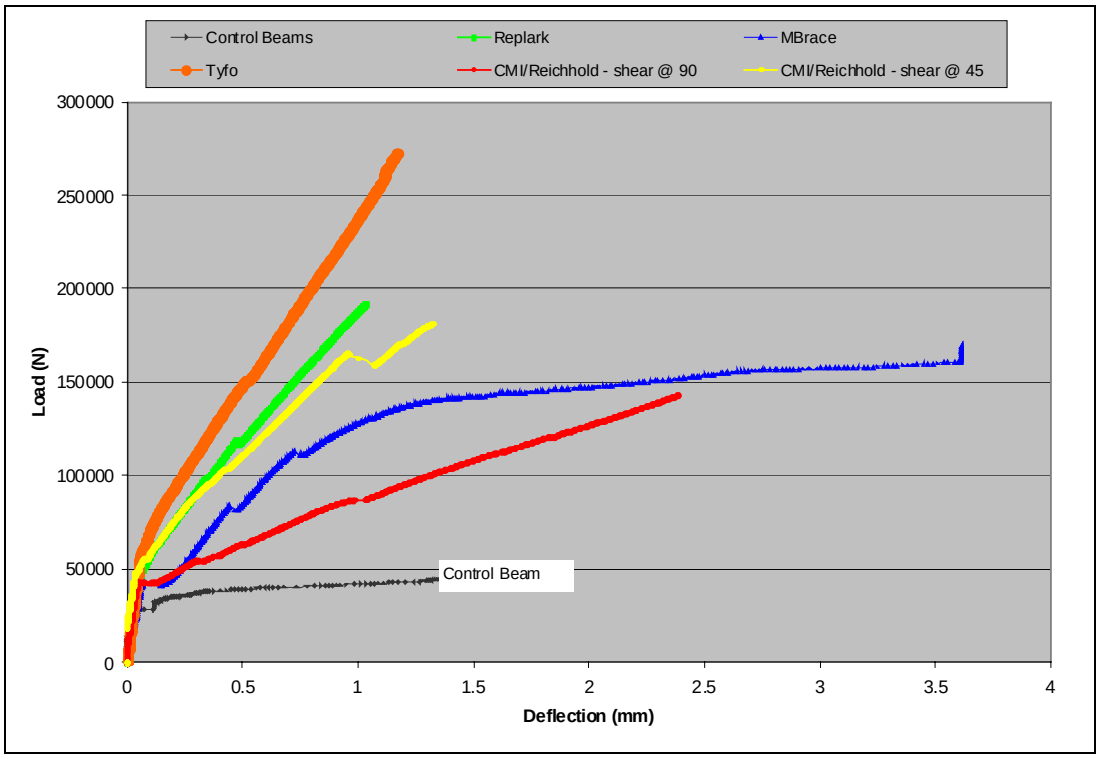

Figure 5.11: Load versus deflection behavior for specimens reinforced with three layers of laminate for flexure and shear

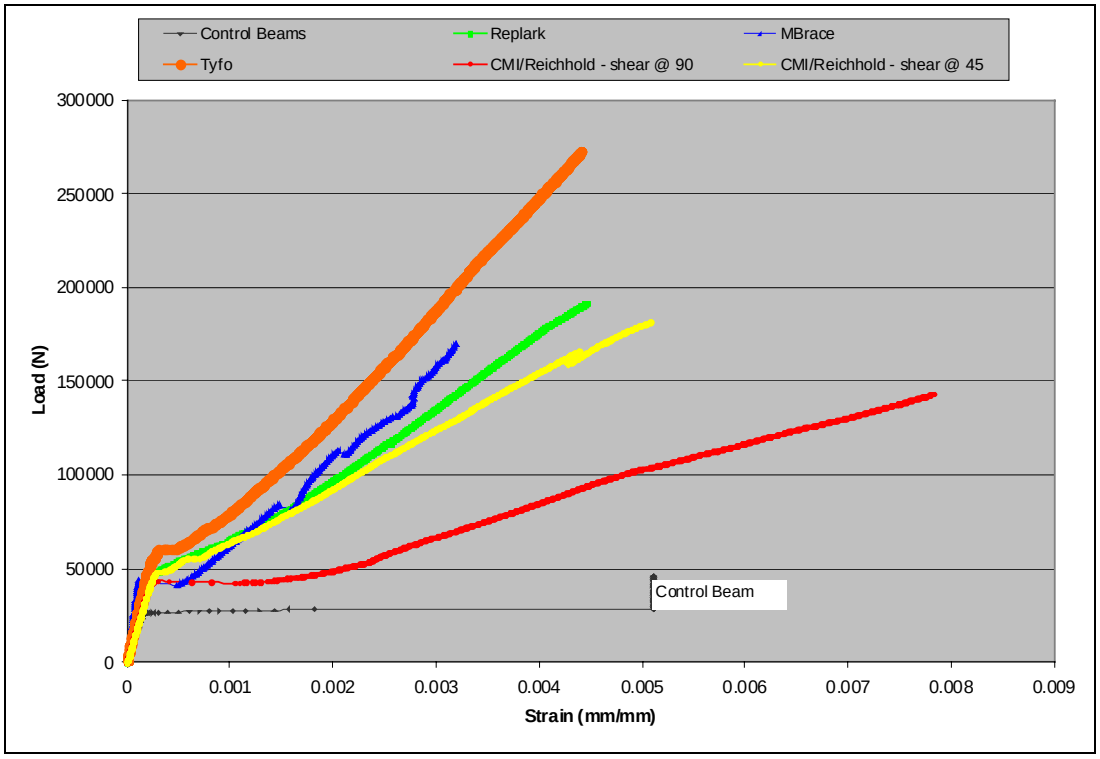

Figure 5.12: Load versus strain behavior for specimens reinforced with three layers of laminate for flexure and shear

5.1.3 Shear Reinforcement at 45^o

Although the original intention of this reinforcing scheme was to strengthen the beams for shear only in order to provide an adequate development length, the shear reinforcement was wrapped across the tension face of the beams, thus providing additional flexural strengthening as well. The adopted approach was intentional, since the control beams failed in flexure. Had no flexural strengthening been provided, the reinforced beams would have possibly failed in flexure too, with little insight being gained on the effects of this type of reinforcing scheme.

The beam designations used for these beams were as follows:

- CMIRS - 45 – Composite Materials Inc. carbon fibers combined with Reichhold Chemicals Inc., resin.
- 45FCS – Fyfe company's Tyfo® carbon system.
- 45MCS – Mitsubishi's Replark® carbon system.

The number following either CMIRS, 45FCS, or 45MCS designates the number of layers of shear laminate that were applied to the beam.

5.1.3.1 One Layer of Shear Reinforcement at 45^o.

The beam strengthened with the Tyfo® system was the strongest of the specimens that were tested with this reinforcing scheme. Strength increases over the control beams were 100 and 270 percent for the load at initial cracking and the load at failure, respectively. Table 5.7 shows the average results from each of the systems that were tested. Based on strain at failure, the Replark CFRP was the most effective system. The CMI/Reichhold composite laminate exhibited the most desirable behavior, failing in flexure with no signs of debonding.

Figure 5.13 shows the tremendous ability for this reinforcing scheme to control the deflections of the beams. It appears that the Tyfo® FRP system outperformed the other specimens based on ultimate load at failure, likely because of its significant thickness. It must be pointed out that the load sustained at failure cannot be regarded as proof that any system is superior to the others. The effectiveness of the FRP reinforcement and the mode of failure are often more important factors from an engineering standpoint than the load capacity increase alone.

Table 5.7: Average results from one-layer shear at 45^o specimens

	@ initial flexural cracking				**@ failure of the beam**				
Beam	Load (N)	Deflection (mm)	Flexural * Strain (x 10^{-4})	Strain** in Shear (x10^{-4})	Load (N)	Deflection (mm)	Flexural * Strain (x 10^{-3})	Strain** in Shear (x10^{-4})	Type of Failure
CONTROL	22894	0.035	1.396	NA	45850	1.617	NA	NA	Flexure
CMIRS1-45	31431	0.079	NA	0.332	80047	1.353	NA	28.91	Flexural Failure
45FCS1	45779	0.047	2.469	0.695	168281	1.159	5.689	30.06	Shear/Debond
45MCS1	36165	0.062	NA	0.536	129174	1.909	NA	38.09	Shear/Debond

*** Flexural strain does not correspond to a fiber orientation but was measured in the longitudinal direction of the beam.**

**** Shear strains were measured in direction of shear fiber orientation (45^o) on the sides of the beams.**

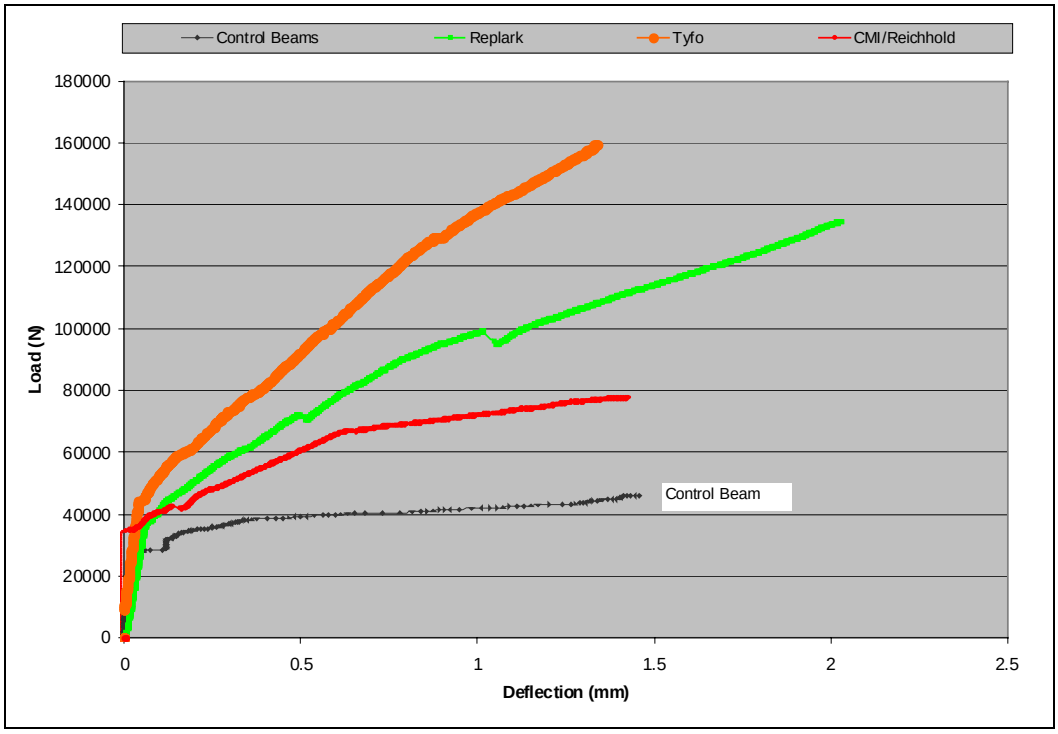

Figure 5.13: Load versus deflection behavior for specimens reinforced with one layer of laminate for shear at 45^{o}

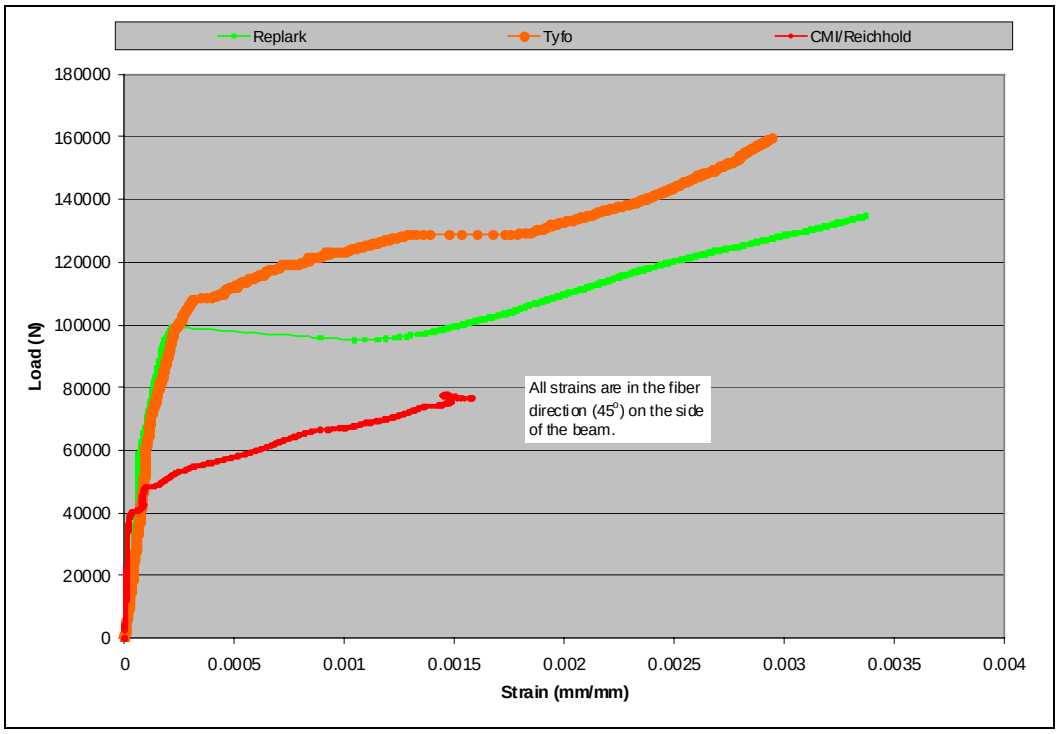

Figure 5.14: Load versus strain in shear laminate for specimens reinforced with one layer of laminate for shear at 45^{o}

Of interest is the fact that although the laminates had different thicknesses and stiffnesses, the strains at which the shear laminate debonded from the beams for each of the one-layer specimens seemed to be fairly close, at approximately 0.34 % or 3400 microstrain. This similarity could be due to the adhesive limitations. Had anchors been used in attaching the shear laminate, it is likely that the strains would have been more dependent on laminate stiffness.

5.1.3.2 Two Layers of Shear Reinforcement at 45^o

The Tyfo® FRP system again proved to have the largest load carrying capacity increase of the systems. The Replark® system performed remarkably well, considering that the thickness of the fibers used was approximately one-fifth the thickness of the Tyfo® FRP fibers. Both systems showed strength improvement of over 250 percent when compared to the control beams. Based on the strain developed at failure, the Replark® CFRP system proved to be the most efficient one. Table 5.8 shows the average results for all of the systems.

Table 5.8: Average results of 2 layer shear at 45^o specimens

	@ initial flexural cracking				@ failure of the beam				
Beam	Load (N)	Deflection (mm)	Flexural * Strain (x 10^{-4})	Strain** in Shear (x10^{-4})	Load (N)	Deflection (mm)	Flexural * Strain (x 10^{-3})	Strain** in Shear (x10^{-4})	Type of Failure
CONTROL	22894	0.035	1.396	NA	45850	1.617	NA	NA	Flexure
CMIRS2-45	36034	0.099	NA	0.425	114592	1.926	NA	29.20	Shear Failure
45FCS2	47816	0.060	2.705	0.734	189040	0.984	3.799	18.72	Shear/Debond
45MCS2	38480	0.049	NA	0.593	160622	1.389	NA	25.44	Shear/Debond

*** Flexural strain does not correspond to a fiber orientation, but was measured in the longitudinal direction of the beam.**

**** Shear strains were measured in direction of shear fiber orientation (45^o) on the sides of the beams.**

For all of the systems, the load at which initial cracking occurred and the load at failure was increased with the additional layer of shear reinforcement. In the CMI/Reichhold system, the mode of failure was also changed from flexure to shear. The strains at failure of this system were similar regardless of the number of layers. This similarity might suggest that only a certain amount of the laminate was being developed and that the ultimate load sustained by the specimen was governed by the limitations of the concrete more than properties of the FRP system. The CMI/Reichhold CFRP system was the only one in this group that did not exhibit debonding prior to failure.

Figures 5.15 and 5.16 display the typical behaviors for the specimens reinforced for shear at 45^o and show the strong dependence of the behaviors of the specimens on the material properties and bonding ability of the systems.

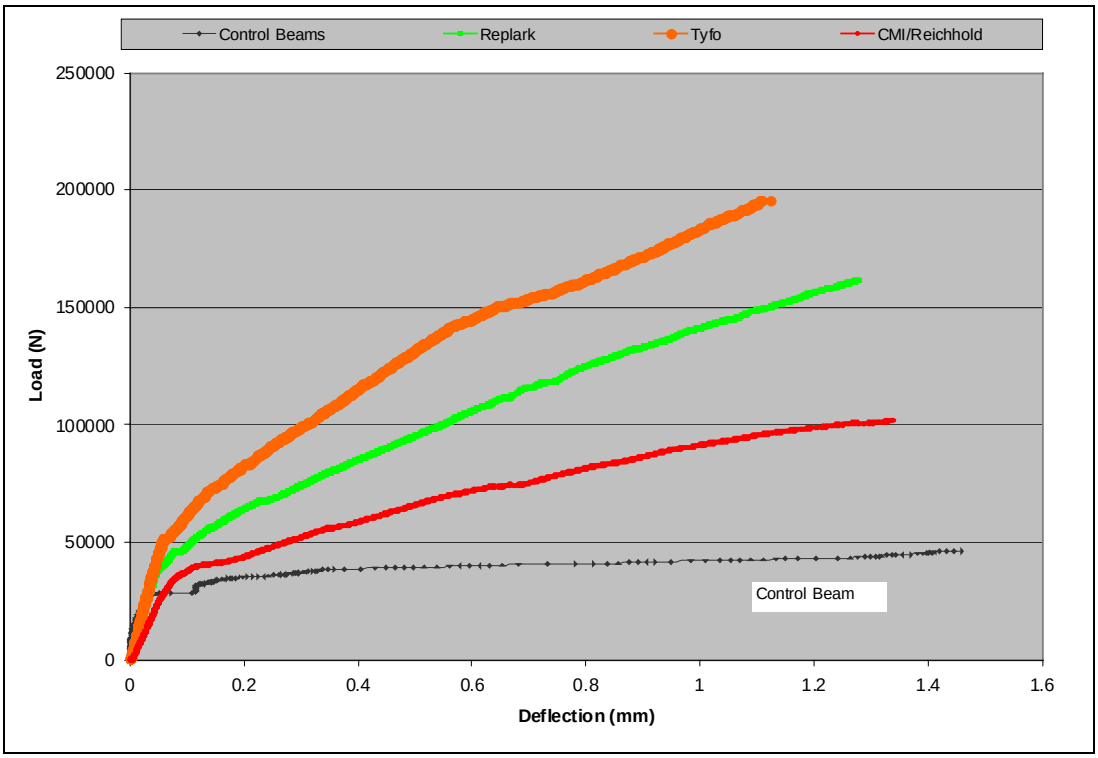

Figure 5.15: Load versus deflection behavior for specimens reinforced with two layers of laminate for shear at 45^{o}

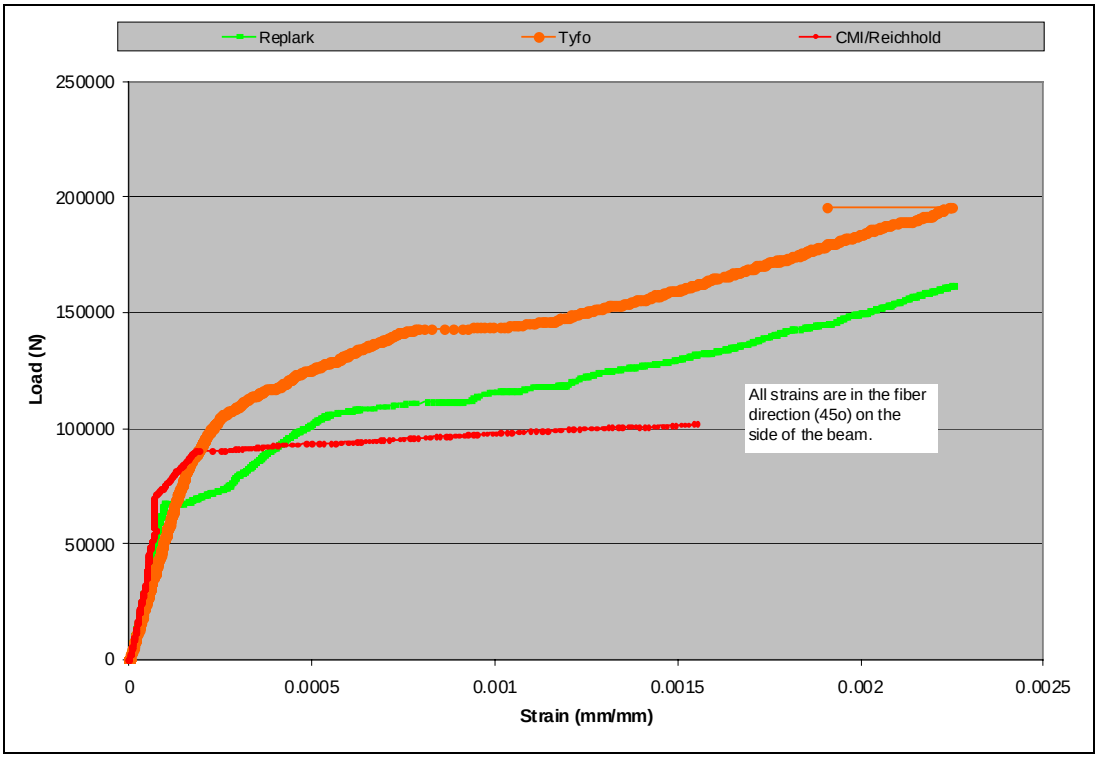

Figure 5.16: Load verus strain in shear for specimens reinforced with two layers of laminate for shear at 45^{o}

5.1.3.3 Three Layers of Reinforcement for Shear at 45^o

With the addition of a third layer of material, cracking at the ends of the beams was observed. It is possible that the tensile force developed at the cut-off points of the FRP laminates exeeded the tensile limits of the concrete. This behavior was evident in all systems being tested, but it was extremely pronounced in Fyfe's CFRP, possibly due to its greater thickness compared to the other FRP systems in the group. It seems that the CMI/Reichhold CFRP laminate was the least affected by this phenomenon, suggesting that it was the most effective of all systems. As previously mentioned, the highest load at failure sustained by the Fyfe system cannot be regarded as proof of better performance due to the greater thickness of this composite and the unpredictable failure mechanism governed by local stress concentrations. This cracking was likely the result of insufficient rebar development length.

Table 5.9: Average results from three-layer shear at 45^o specimens

	@ initial flexural cracking				**@ failure of the beam**				
Beam	Load (N)	Deflection (mm)	Flexural * Strain (x 10^{-4})	Strain** in Shear (x10^{-4})	Load (N)	Deflection (mm)	Flexural * Strain (x 10^{-3})	Strain** in Shear (x10^{-4})	Type of Failure
CONTROL	22894	0.035	1.396	NA	45850	1.617	NA	NA	Flexure
CMIRS3-45	42935	0.097	NA	0.512	123639	1.383	NA	26.92	Shear Failure
45FCS3	56343	0.057	3.075	0.529	216284	0.736	3.192	12.09	Local Stresses
45MCS3	45559	0.045	NA	0.620	170145	0.969	NA	18.95	Shear/Debond

*** Flexural strain does not correspond to a fiber orientation, but was measured in the longitudinal direction of the beam.**

**** Shear strains were measured in direction of shear fiber orientation (45^o) on the sides of the beams.**

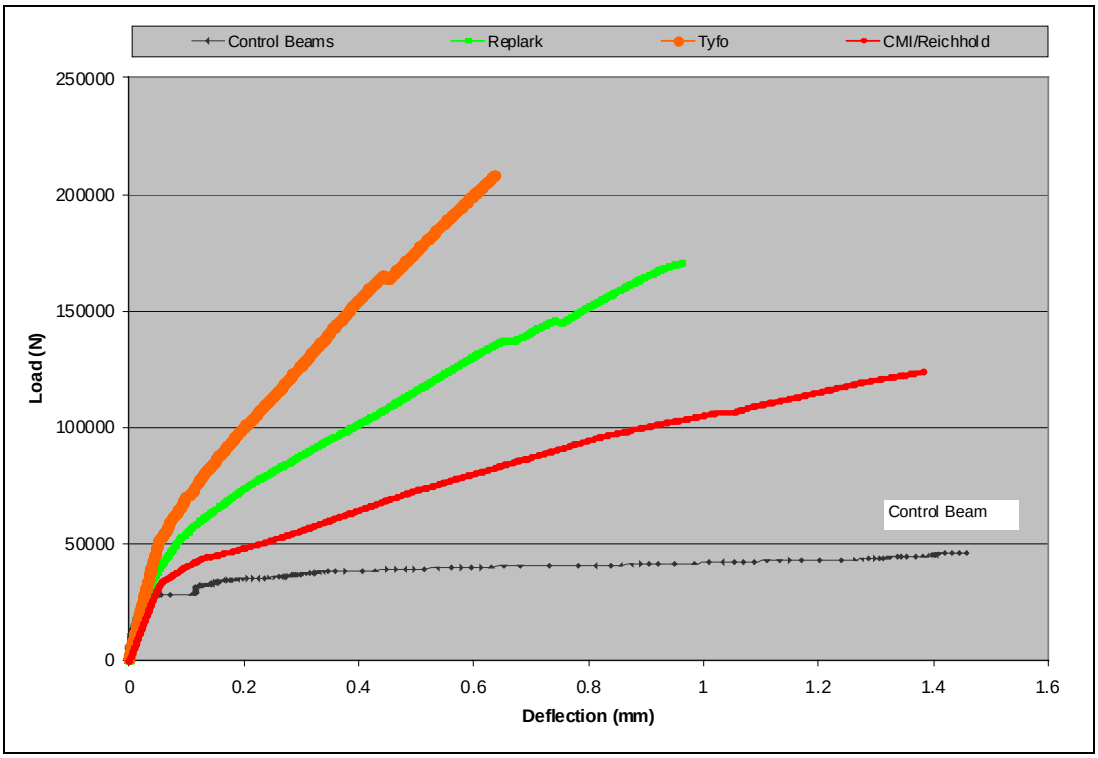

Figure 5.17: Load versus deflection behavior for specimens reinforced with three layers of laminate for shear at 45^{o}

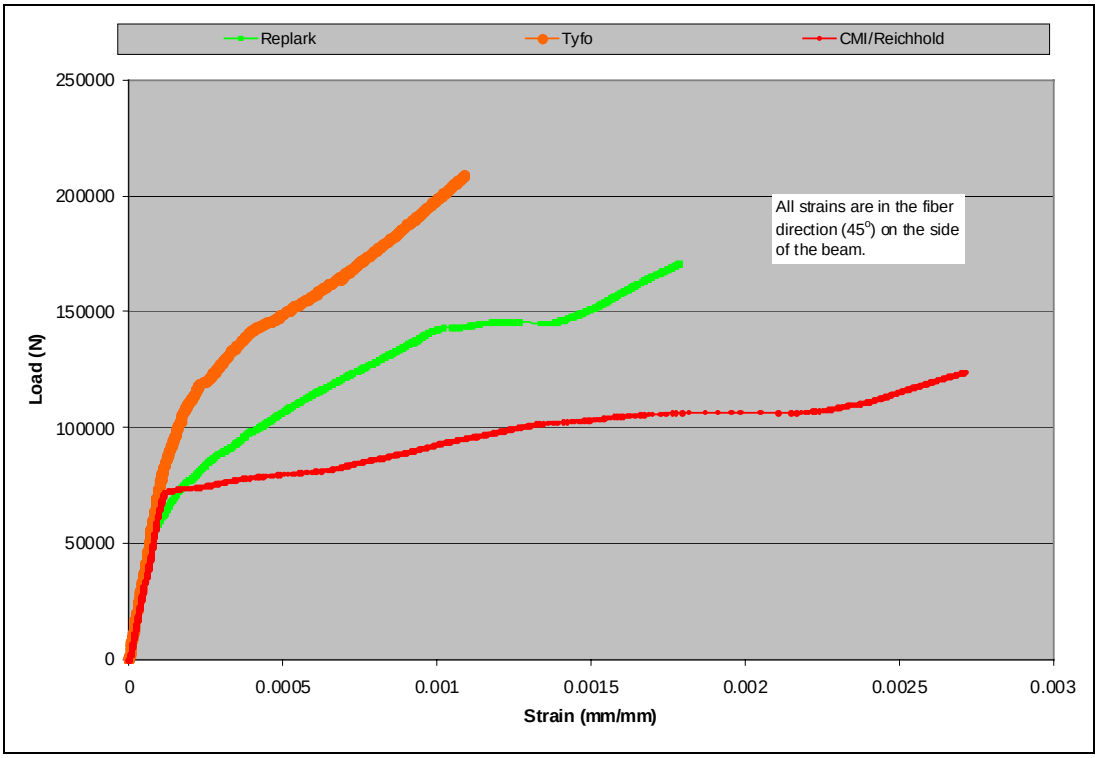

Figure 5.18: Load versus strain in shear laminate for specimens reinforced with three layers of laminate for shear at 45^{o}

All of the figures show the dependence of the specimen behavior on the thickness and stiffness of the laminates. All of these specimens failed in shear combined with debonding of the shear laminate.

5.2 BEAMS STRENGTHENED WITH GLASS SYSTEMS

Beams reinforced with glass laminates exhibited strength increases at failure ranging from 30 to 475 percent, with an average increase of 175 percent for all strengthening schemes and laminate thicknesses. In addition, glass reinforced beams tended to exhibit larger deflections and strains but less ultimate load at failure than the carbon reinforced beams, primarily due to the material properties of the laminate.

Most of the beams with one layer of glass reinforcement failed in flexure. Similar behavior was observed with some of the two- and three-layer specimens with shear reinforcement. The rest of the specimens failed in shear or combinations of shear and flexure. This behavior indicates that the E-glass systems might be a better choice in situations where smaller structural deficiencies must be corrected in an environment that is not detrimental to the glass fibers. The ability for the glass to develop strains at failure approximately two times greater than carbon systems also seemed to result in more predictable failure mode and pseudo-ductile behavior.

5.2.1 Flexural Reinforcement

Four different glass reinforcement systems were explored as flexural reinforcement. The following designations were used to denote each system:

- CSGF – Clark Schwebel Structural Glass Grid attached with Reichhold Chemicals Atlac® 580-10 vinyl ester resin.
- FGF – Fyfe Company's Tyfo® glass system.
- MBGF – Master Builders' MBrace™ glass system.
- OCRF – Owens Corning glass fibers combined with Reichhold Chemicals resin.

The number that follows the designation is the number of laminate layers. For the Clark Schwebel system only one-layer beams were tested.

5.2.1.1 One Layer of Flexural Reinforcement

Typically, the beams from this group failed in flexure or a combination of flexure and shear. In all of the beams the laminate failed in tension. Based on ultimate load alone, the Tyfo® FRP - wrapped beams appeared to be the strongest. This was to be expected, since the glass fiber sheet used by this system was significantly thicker than the others that were tested. However, in these specimens the tensile failure of the laminate was coupled with splitting of the laminate parallel to the fibers. Both the Tyfo® FRP system and the Clark Schwebel system seemed to have slight bonding problems, likely due to the laminate thickness. Owens Corning/Reichhold and MBrace GFRP systems showed predictable behavior by failing in flexure. Also, these two systems developed the highest

strains at failure. Results from the one-layer beams are presented in Table 5.10 and Figures 5.19 and 5.20.

Table 5.10: Average results from one layer flexure beams

	@ initial flexural cracking			**@ failure of the beam**			
Beam	Load (N)	Deflection (mm)	Flexural Strain (x 10^{-4})	Load (N)	Deflection (mm)	Flexural Strain (x 10^{-3})	Type of Failure
CONTROL	22894	0.035	1.396	45850	1.617	NA	Flexure
CSGF	36078	0.057	2.815	84970	3.885	10.173	Flexure/Debond
FGF1	44667	0.109	3.203	148265	3.749	13.975	Flex/Shear/Deb.
MBGF1	32626	0.044	1.937	66200	1.519	6.306	Flexure
OCRF1	35473	0.089	3.140	61341	1.529	8.394	Flexural Failure

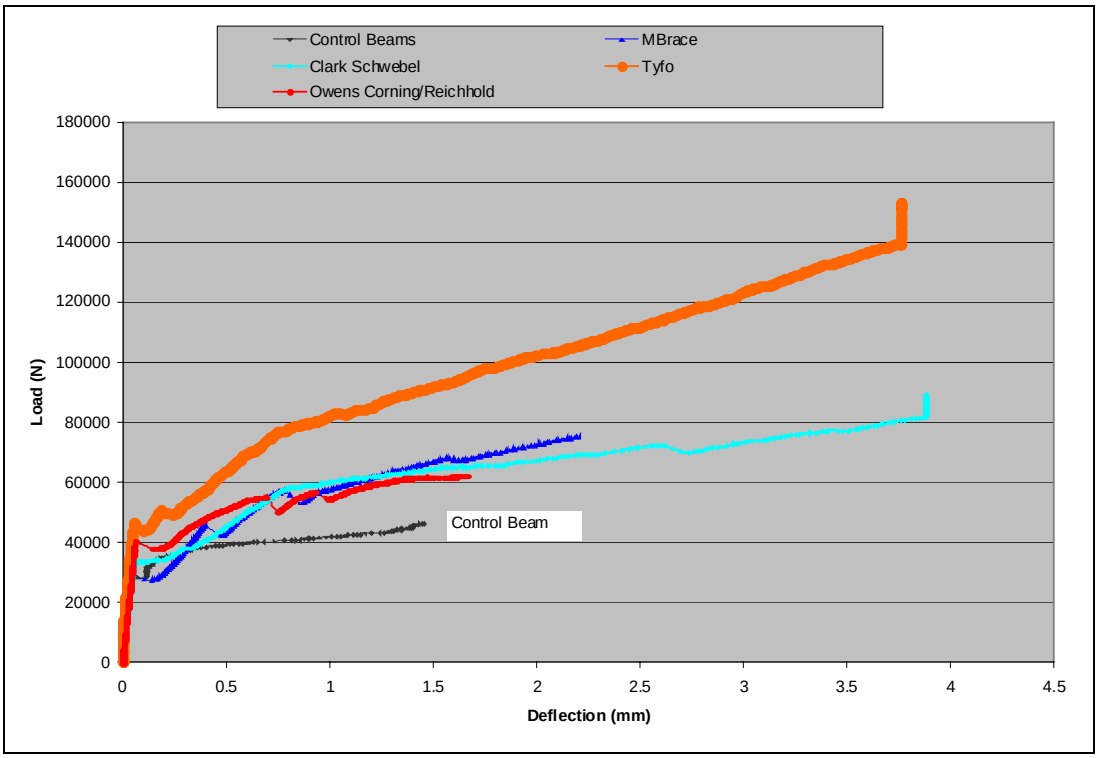

Figure 5.19: Load versus deflection behavior for specimens reinforced with one layer of glass laminate for flexure

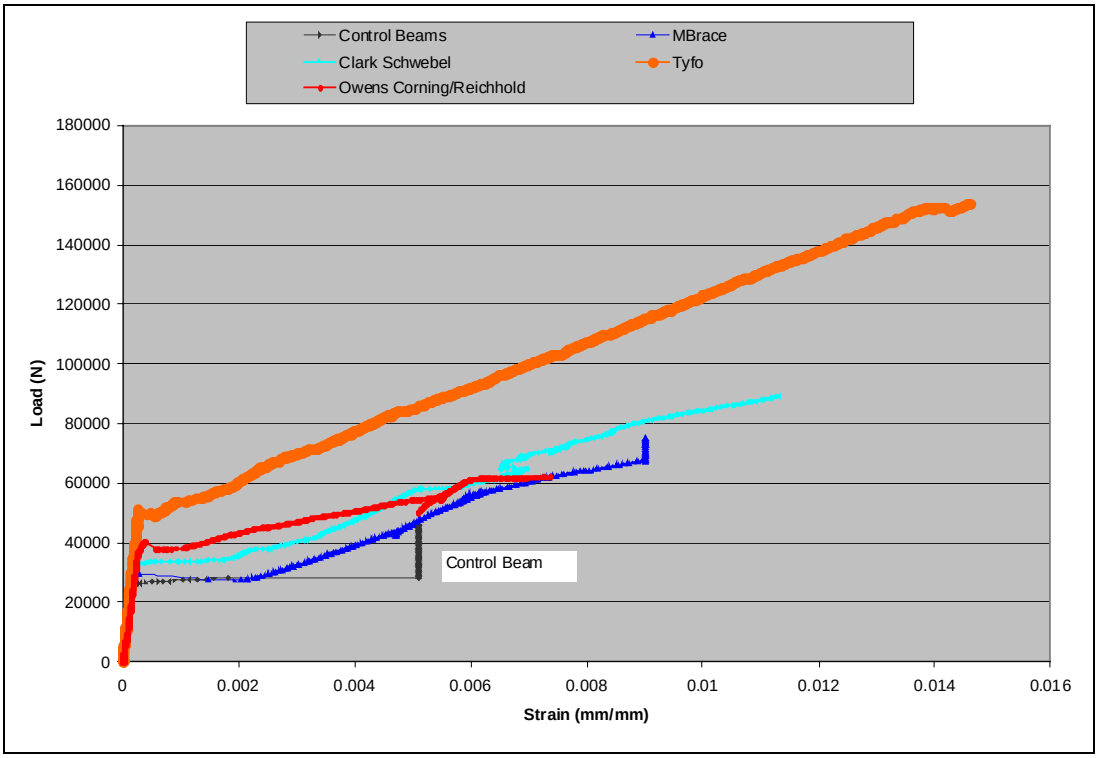

Figure 5.20: Load versus strain behavior for specimens reinforced with one layer of glass laminate for flexure

Except for the behavior of the Tyfo® FRP beam, the behavior of the systems appeared to be very similar. This would suggest that the behavior of the strengthened beam was highly dependent on the thickness of the FRP, geometry and material properties of the beam.

5.2.1.2 Two Layers of Flexural Reinforcement

Similar to one-layer reinforcement, the beams strengthened with the Tyfo® FRP system exhibited the largest load increase. Failure of the beams occurred due to a combination of cracking at the ends of the beams – from concentration of stresses at the ends of the laminate – and shear cracking.

The addition of the second layer of reinforcement changed the behavior of the other systems. The MBrace™ beams failed in shear, while the OCRF beams failed due to combinations of shear and flexural cracking. The largest strains developed by the OCRF beams suggested their high efficiency in utilizing the FRP properties. Beam results are presented in Table 5.11 and Figures 5.21 and 5.22.

Table 5.11: Average results from two layer flexure specimens

	@ initial flexural cracking			**@ failure of the beam**			
Beam	Load (N)	Deflection (mm)	Flexural Strain (x 10^{-4})	Load (N)	Deflection (mm)	Flexural Strain (x 10^{-3})	Type of Failure
CONTROL	22894	0.035	1.396	45850	1.617	NA	Flexure
FGF2	44480	0.062	3.509	172547	2.787	9.11	Shear/Local
MBGF2	36007	0.049	2.234	99004	2.704	8.694	Shear
OCRF2	35151	0.058	2.970	100006	4.030	12.030	Flexural/Shear Failure

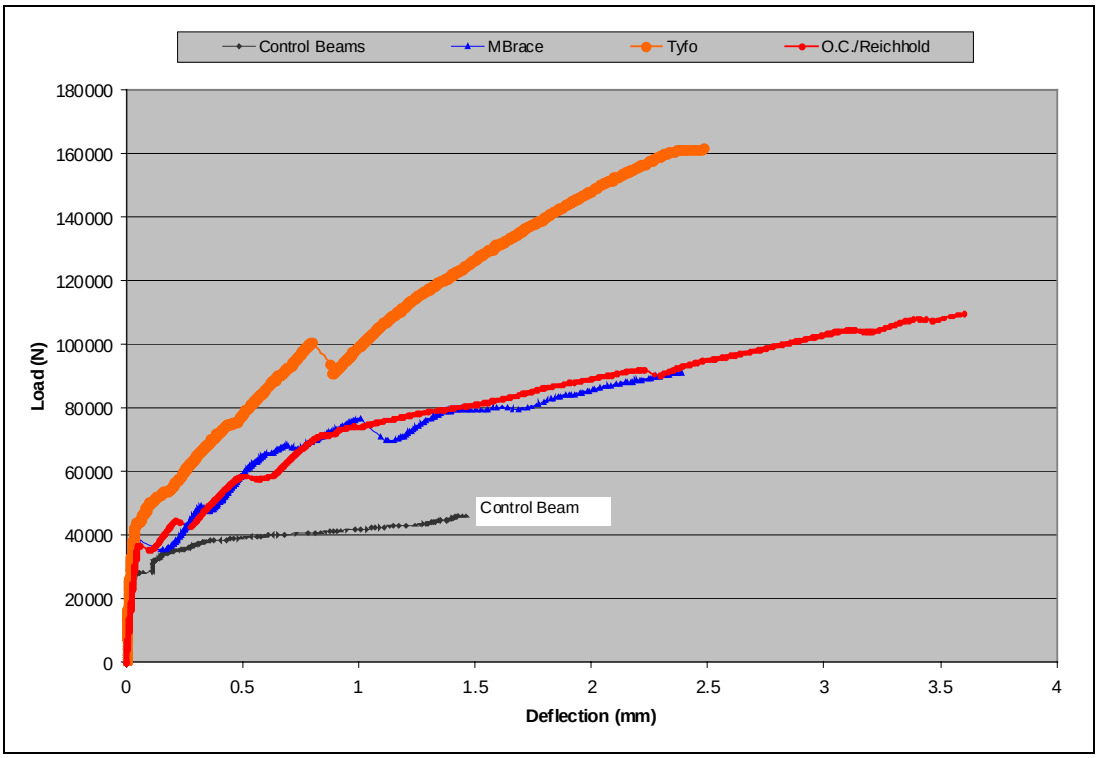

Figure 5.21: Load versus deflection behavior for specimens reinforced with two layers of laminate for flexure

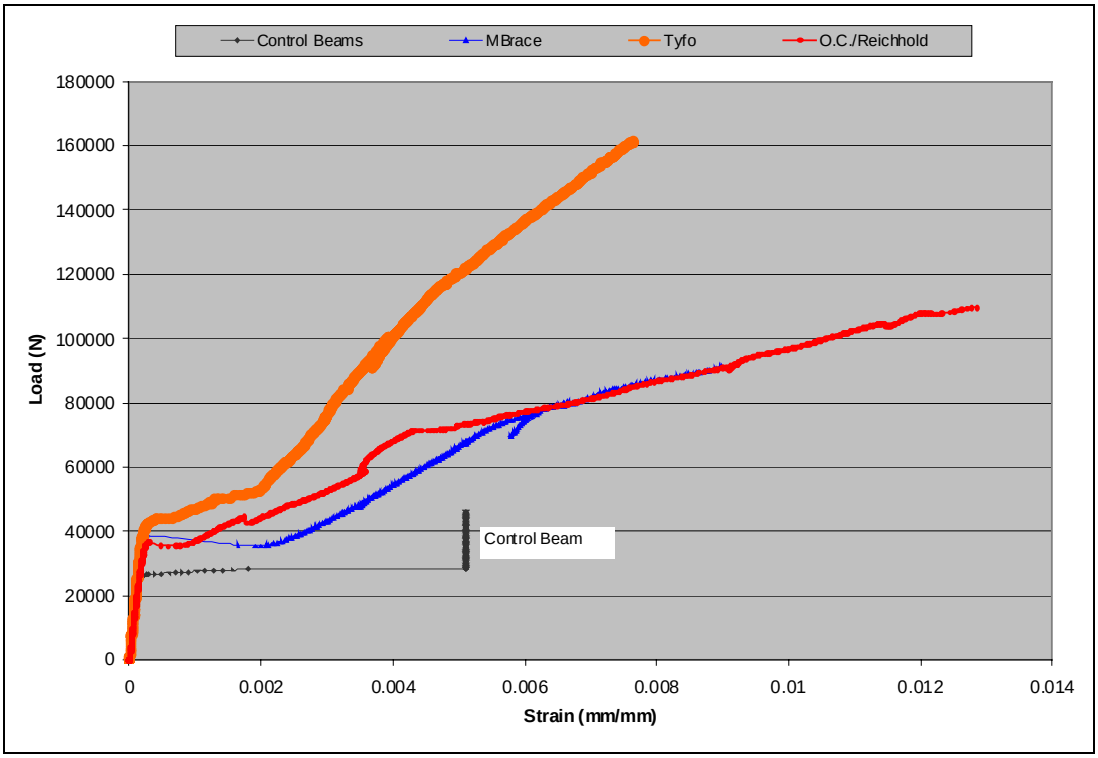

Figure 5.22: Load verus strain behavior for specimens reinforced with two layers of laminate for flexure

From Figures 5.21 and 5.22, one can observe that the MBrace™ and OCRF beams behaved quite similarly. The slight differences between the two are quite possibly the result of the differences in failure modes and bond characteristics of the resins that were used to attach each laminate to the beam. The similar behavior again suggests a strong dependence on the properties of the specimen prior to reinforcement, especially since the properties of the two laminates are substantially different.

5.2.1.3 Three Layers of Flexural Reinforcement

The Tyfo® FRP system appeared to be the most load-carrying of the glass systems. The addition of a third layer of laminate increased the average load sustained prior to initial cracking of the concrete by approximately 12 percent. However, a reduction of the ultimate load at failure was observed, likely due to the stiffening effects of the additional layer and the resulting change of failure mode.

The failure modes of the beams reinforced with the other two systems were changed with the additional layer of reinforcement. The MBrace™ beams failed in a combination of shear and flexure, and the OCRF reinforced specimens failed in flexure. The changes in failure mode were likely the direct result of the increased stiffness of the laminate. Due to the increased stiffness of the laminate, the failure was controlled by the limitations of the adhesive layer. Thus, the laminate debonded prior to developing its full potential. It is likely that the use of anchors in the thicker reinforced members could eliminate the debonding problem and would result in more effective utilization of the GFRP properties and more desirable failure modes. The MBrace™ and OCRF systems seemed to behave less similar with three layers of reinforcement than they did with less reinforcement. It is possible that these differences were due to the specimens' behavior being influenced more by the properties of the adhesive layer when thicker laminates were applied. Table 5.12 and Figures 5.23 and 5.24 show the results from the three-layer specimens.

Table 5.12: Average results from three layer flexure specimens

	@ initial flexural cracking			**@ failure of the beam**			
Beam	Load (N)	Deflection (mm)	Flexural Strain (x 10^{-4})	Load (N)	Deflection (mm)	Flexural Strain (x 10^{-3})	Type of Failure
CONTROL	22894	0.035	1.396	45850	1.617	NA	Flexure
FGF3	50040	0.078	3.075	170136	1.854	5.34	Shear/Local
MBGF3	38302	0.046	2.543	103291	2.212	9.249	Flex/Shear/Deb.
OCRF3	35092	0.075	2.440	127821	4.270	15.350	Flexural Failure

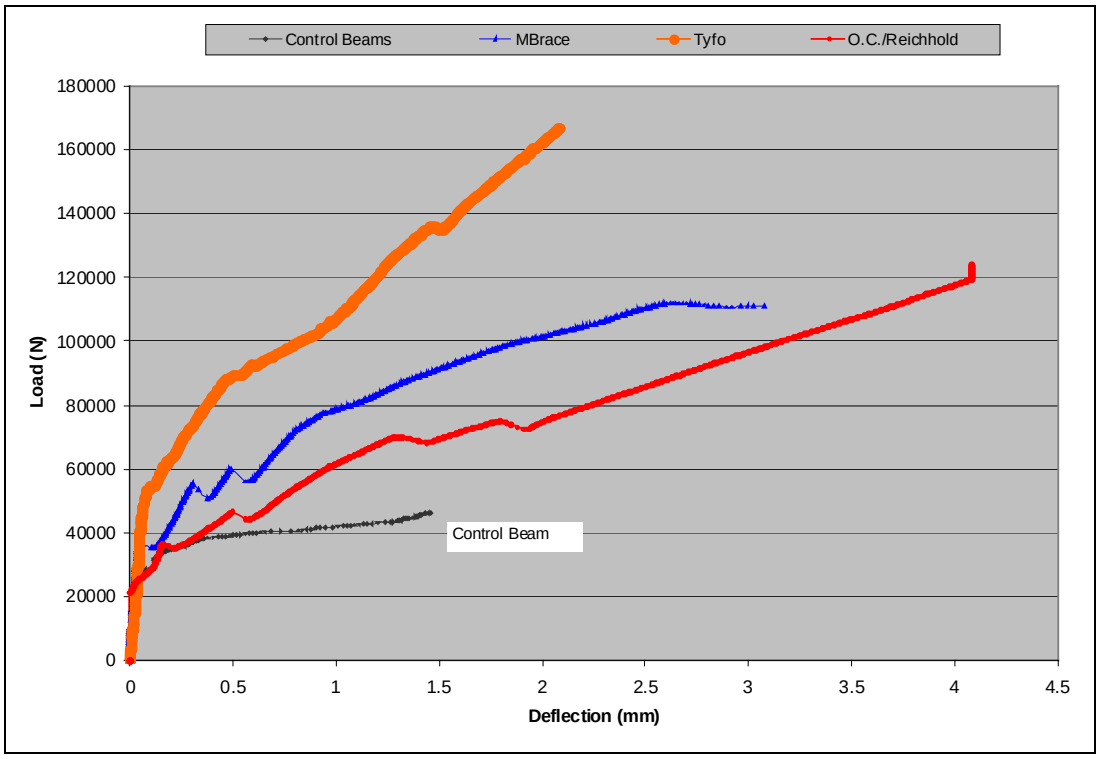

Figure 5.23: Load versus deflection behavior for specimens reinforced with three layers of laminate for flexure

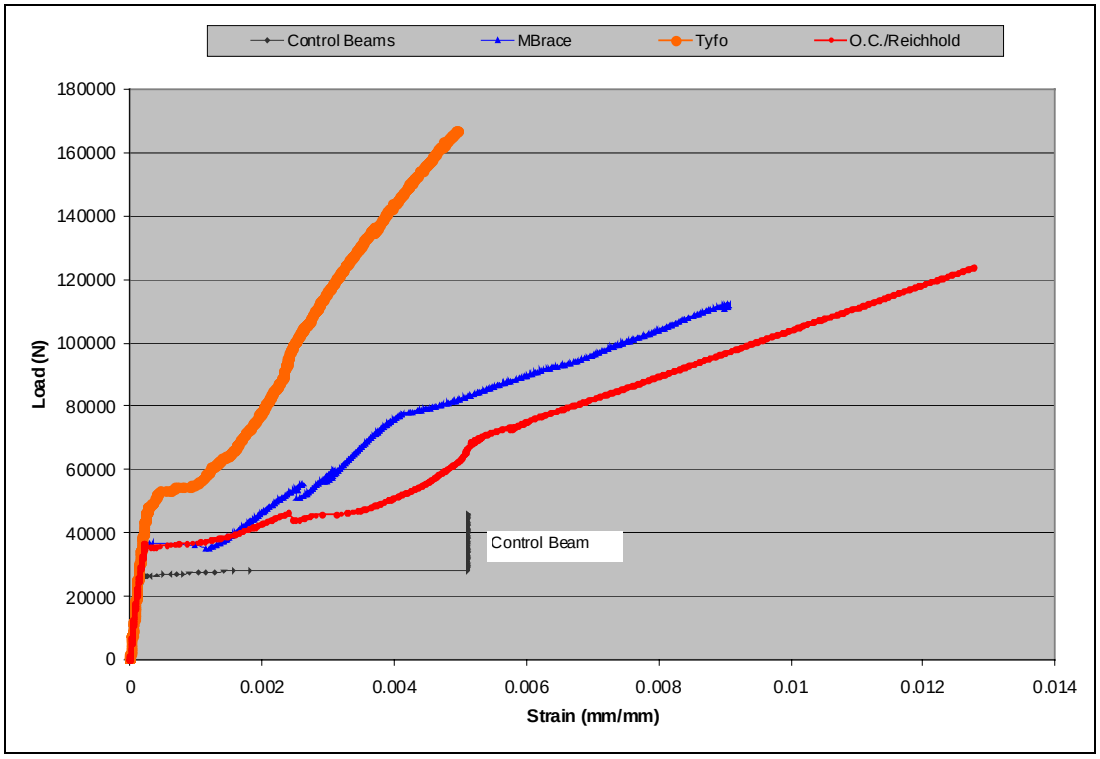

Figure 5.24: Load versus strain behavior for specimens reinforced with three layers of laminate for flexure

5.2.2 Flexure plus Shear Reinforcement

Five different reinforcing schemes with four different materials were studied involving beams reinforced for shear and flexure with glass fibers. The following designations were used to distinguish between the specimens:

- CSGFS – Clark Schwebel Structural Glass Grid. Grid on the shear sides of the beam was not wrapped around the tensile face to form U-shaped stirrup as was done with most of the other systems.
- FGFS – Fyfe Company's Tyfo® glass system.
- MBGFS – Master Builders' MBrace™ glass system.
- OCRFS – 90 – Owens Corning glass system with flexural reinforcement along the longitudinal axis of the beams (as in the previous section) and shear reinforcement oriented at 90^o to the longitudinal axis of the beam (same as FGFS and MBGFS).
- OCRFS – 45 – Owens Corning glass system with flexural reinforcement along the longitudinal axis of the beam plus shear laminate oriented at 45^o on the sides of the beam and wrapped across the tensile face (same as beams in section 5.2.3).

The 1, 2, or 3 that follows the designation is the number of laminate layers of both the shear and flexure. It should be noted that the OCRF – 45 beams have a significant amount of additional flexural reinforcement due to the overlapping layers of shear laminates at the midspan of the beam. For these beams, the three-layer beams actually have nine layers overlapping at the midspan at various angles relative to the beam axis.

5.2.2.1 One Layer of Flexure and Shear Reinforcement

The Tyfo® - and OCRFS-45 reinforced beams showed the largest load carrying capacity of the group. The MBrace™, Clark Schwebel, and OCRFS-90 beams performed similarly to each other, despite differences in material properties of the laminates. Table 5.13 and Figures 5.25 and 5.26 show the specimen results.

Table 5.13: Average results from one layer flexure and shear specimen

	@ initial flexural cracking			**@ failure of the beam**				
Beam	Load (N)	Deflection (mm)	Flexural Strain (x 10^{-4})	Load (N)	Deflection (mm)	Flexural Strain (x 10^{-3})	Strain** in Shear (x10^{-4})	Type of Failure
CONTROL	22894	0.035	1.396	45850	1.617	NA	NA	Flexure
OCRFS1-90	26741	0.054	1.90	60368	1.400	8.52	NA	Flexure
OCRFS1-45	39830	0.061	1.85	100278	2.349	8.787	98.44	Flexure/Shear
FGFS1	44853	0.078	3.649	155688	3.050	13.92	NA	Flexure
MBGFS1	43793	0.053	2.522	66561	0.989	9.048	NA	Flexure
CSGFS1	39281	0.074	2.299	73870	3.532	18.64	NA	Flexure/Debond

**** Shear strains are measured in direction of shear fiber orientation (either 90^o or 45^o)**

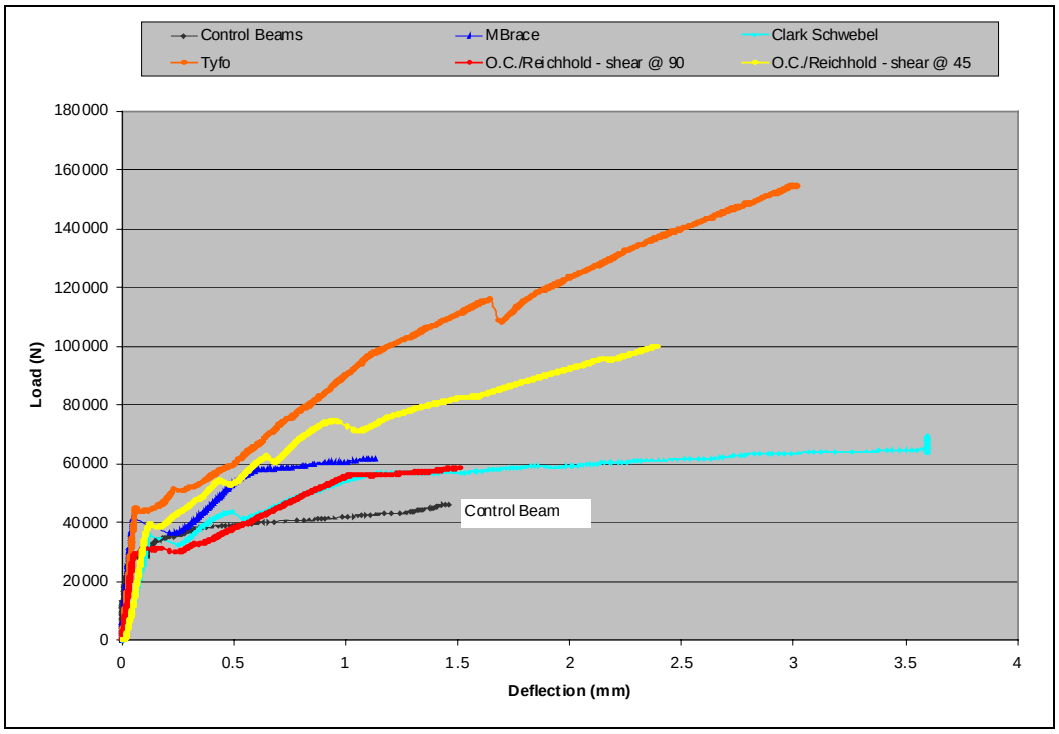

Figure 5.25: Load versus deflection behavior for specimens reinforced with one layer of glass laminate for shear and flexure

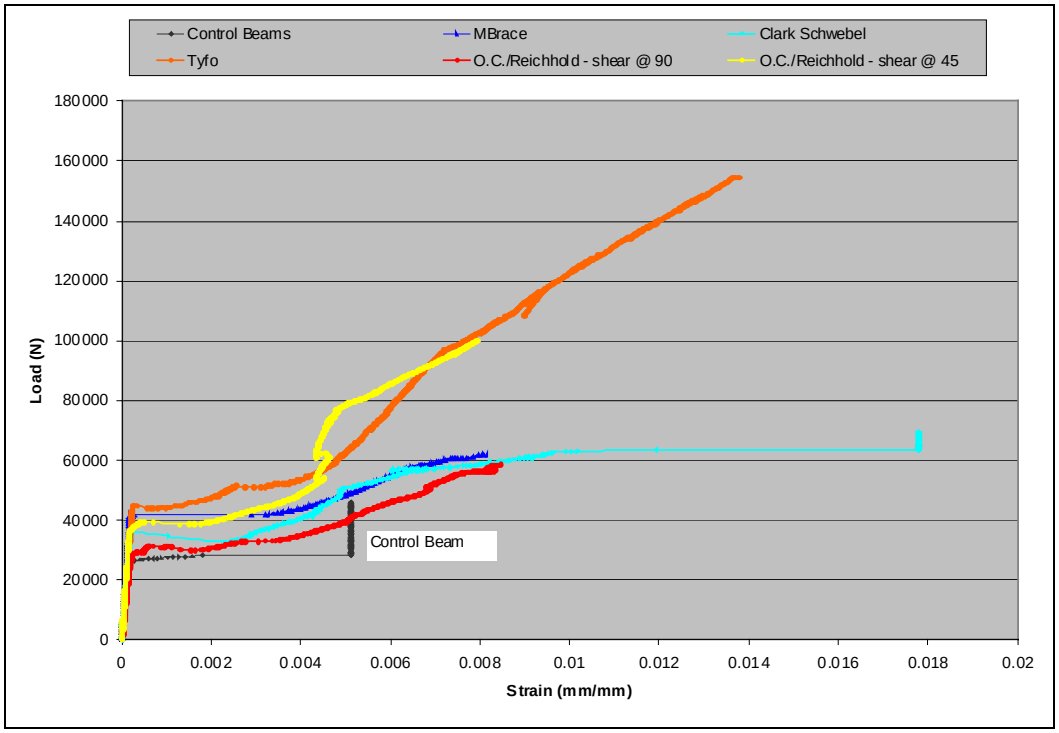

Figure 5.26: Load versus strain behavior for specimens reinforced with one layer of glass laminate for shear and flexure

5.2.2.2 Two Layers of Reinforcement for Flexure and Shear

Similar to the previous results, the Tyfo® FRP reinforced beams displayed the largest load carrying ability and the least desirable mode of failure. The mode of failure of these beams was dominated by shear with debonding of the shear laminate. The OCRFS-45 beams also failed in shear at a lower load level than the one-layer specimens. The MBrace and OCRFS-90 beams performed similarly with both systems failing in flexure.

Table 5.14: Average results from two layer flexure and shear specimens

	@ initial flexural cracking			**@ failure of the beam**				
Beam	Load (N)	Deflection (mm)	Flexural Strain (x 10^{-4})	Load (N)	Deflection (mm)	Flexural Strain (x 10^{-3})	Strain** in Shear (x10^{-4})	Type of Failure
CONTROL	22894	0.035	1.396	45850	1.617	NA	NA	Flexure
FGFS2	45779	0.066	3.394	228885	2.989	11.677	NA	Shear/Debond
MBGFS2	39458	0.058	2.644	101886	2.489	9.366	NA	Flexure
OCRFS2-90	36169	0.054	1.920	111873	3.700	9.490	NA	Flexural Failure
OCRFS2-45	40153	0.057	2.060	134451	2.545	6.176	35.120	Shear Failure

**** Shear strains are measured in direction of shear fiber orientation (either 90^o or 45^o)**

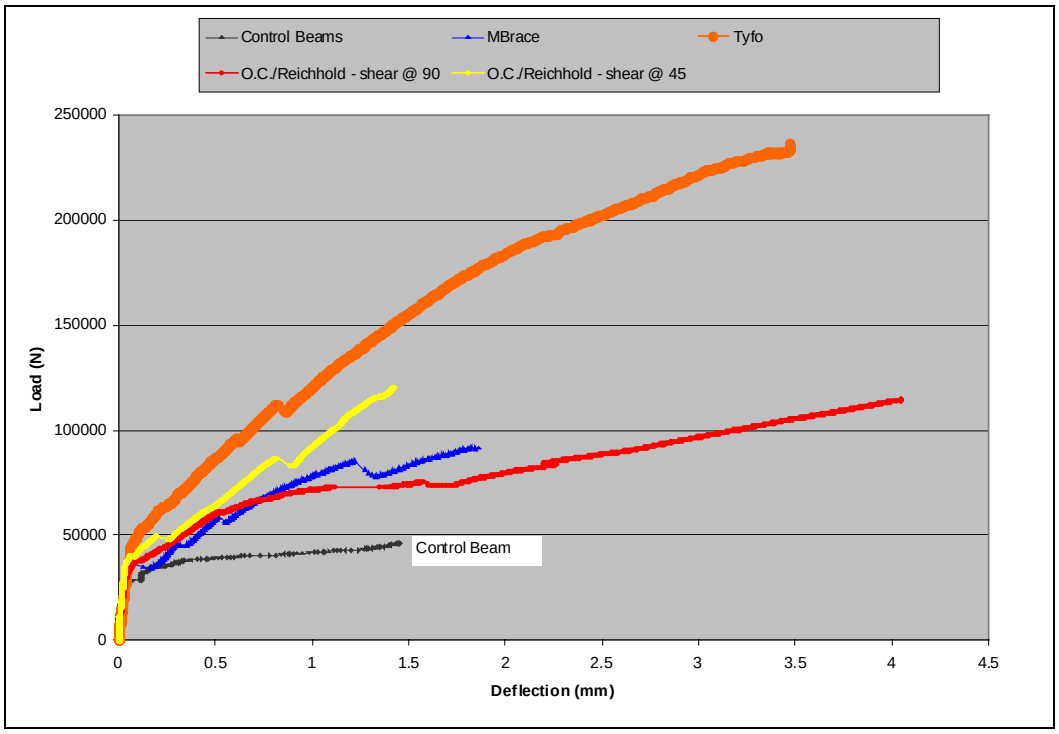

Figure 5.27: Load versus deflection behavior for specimens reinforced with two layers of glass laminate for flexure and shear

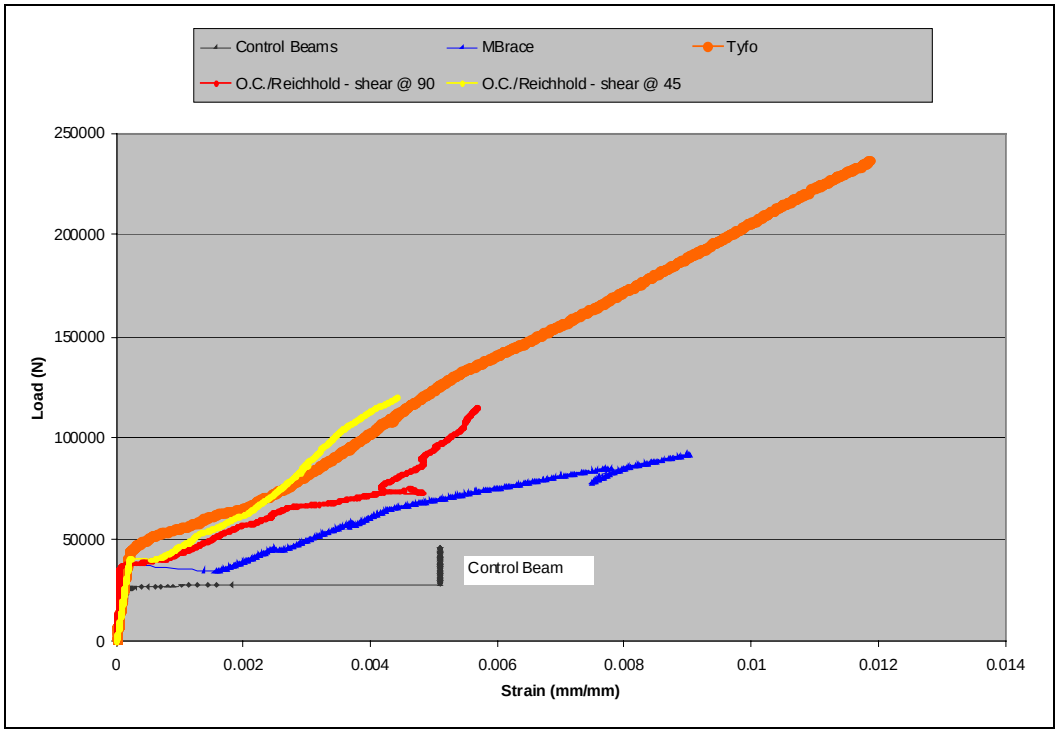

Figure 5.28: Load versus strain behavior for specimens reinforced with two layers of glass laminate for flexure and shear

5.2.2.3 Three Layers of Reinforcement for Flexure and Shear

As expected, the three-layer beams performed similarly to the two layer beams. The Tyfo® FRP system was the strongest and appeared to resist deflections the best. The average improvement over the control beams for load at failure was over 475 percent. This system surpassed many of the specimens that were reinforced with carbon in terms of strength and was the strongest of the glass specimens that were tested.

In addition to the shear cracking and debonding of the shear laminate that was seen in the two-layer Tyfo® FRP beams, the three-layer beams also showed signs of stress concentrations at the ends of the laminate. The propagation of the cracking at the end of the beam into the area where the shear cracking had already occurred led to the eventual failure of the beams.

The MBrace™ and OCRFS-90 systems behaved nearly identically, despite different material properties. The fibers used in the two systems had nearly identical elastic moduli, but the thicknesses of the materials were different. This may suggest that some portions of the laminates remain ineffective, due to possible debonding from the concrete surface, limitations of the substrate, or both.

Table 5.15 and Figures 5.29 and 5.30 show the results from the three-layer glass specimens. The unusual strain pattern of the OCRF-90 beam in Figure 5.30 was likely the result of cracking in the beam outside of the area in which the strain gauge was placed on the laminate. The appearance of the cracks resulted in stress relaxation. As a result, significant additional stress was transferred to the surrounding areas, increasing the strains in the laminate.

Table 5.15: Average results from three layer flexure and shear specimens

	@ initial flexural cracking			**@ failure of the beam**				
Beam	Load (N)	Deflection (mm)	Flexural Strain (x 10^{-4})	Load (N)	Deflection (mm)	Flexural Strain (x 10^{-3})	Strain** in Shear (x10^{-4})	Type of Failure
CONTROL	22894	0.035	1.396	45850	1.617	NA	NA	Flexure
FGFS3	52633	0.064	3.451	265212	2.182	9.248	NA	Shear/Local/Deb.
MBGFS3	35962	0.034	2.224	120318	2.245	9.867	NA	Flexure/Shear
OCRFS3-90	35709	0.031	2.040	128810	3.793	9.580	NA	Flexural/Shear Failure
OCRFS3-45	44651	0.055	2.320	167954	1.829	5.898	35.460	Shear Failure

**** Shear strains are measured in direction of shear fiber orientation (either 90^o or 45^o)**

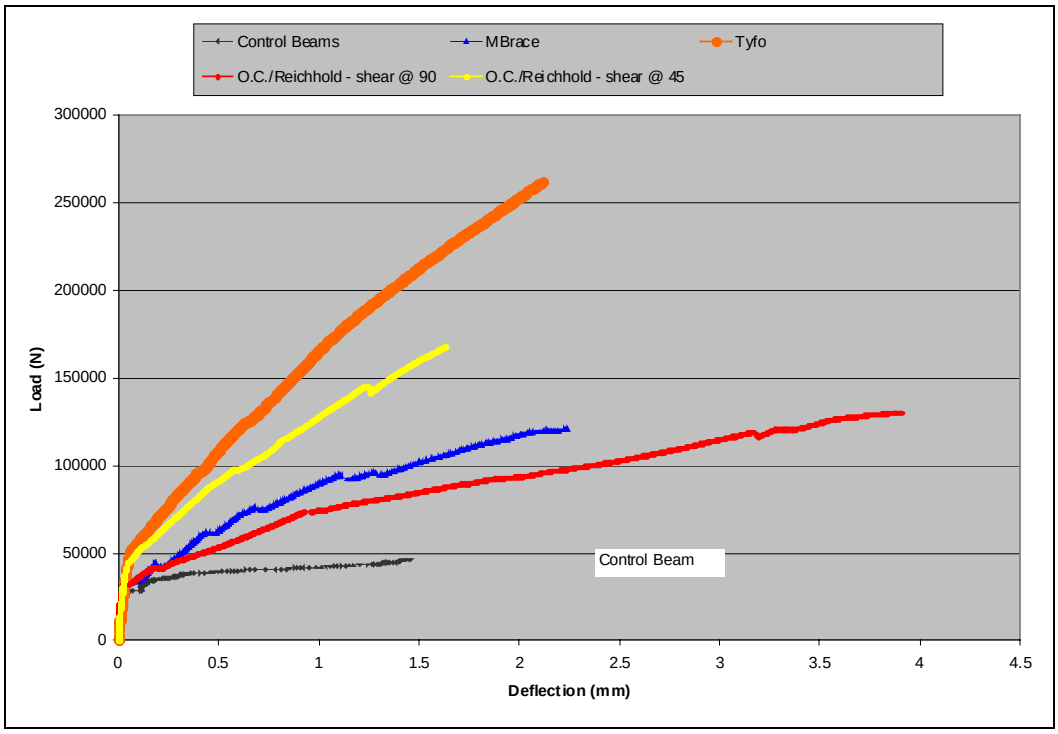

Figure 5.29: Load versus deflection behavior for specimens reinforced with three layers of glass laminate for flexure and shear

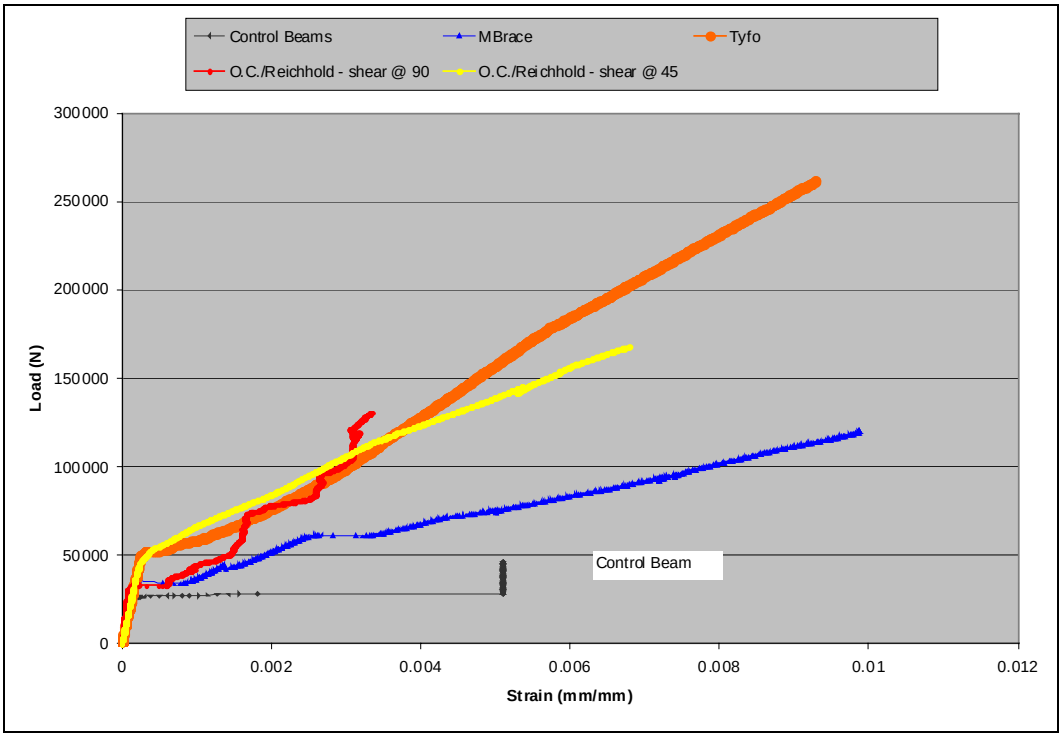

Figure 5.30: Load versus strain behavior for specimens reinforced with three layers of glass laminate for flexure and shear

5.2.3 Shear Reinforcement at 45^o

The original intention of this reinforcing scheme was to strengthen the beams for shear only. However, in order to supply an adequate distance for the fibers to develop, the shear reinforcement was wrapped across the tension face of the beamsm resulting in a significant amount of flexural reinforcement as well.

The beam designations used for these beams were as follows:

- 45FGS – Fyfe's Tyfo® glass system.
- OCRS-45 – Owens Corning glass fibers combined with Reichhold Chemicals vinyl ester resin.

The 1, 2, or 3 following the designation was the number of layers of shear laminate that were applied to each side of the beam. The three layer beams actually had six overlapping layers of shear laminate at the midspan, three from each side of the beam.

Because only two systems were studied and the results of the two were significantly different, it was decided to change the format of this section and combine all of the varying layers.

In each of the different layers of laminates, the Tyfo® FRP - reinforced beams provided the largest load increase. This was expected because of the greater thickness of this system (single layer of the Tyfo glass sheet is 1.3 mm thick). All of the Tyfo beams failed due to a combination of shear cracking and debonding of the shear laminate from the sides of the beams. Two interesting aspects of the Tyfo® FRP system can be observed from the averages presented in Table 5.16:

- Regardless of the number of layers of reinforcement, the flexural strains that were recorded at the first signs of cracking were nearly identical. The loads were also fairly close.

- The strains in the shear laminate at the initial cracking, the deflections at failure, and both the flexural and shear strains at failure, seemed to be dependent on the thickness of the laminate.

These same observations did not apply for the Owens Corning system. This could have been partially due to the changing failure modes throughout the different layers of the system. It is also possible that the system exhibited some bonding problems that we were not aware of during testing. The OCRS-45 specimens did seem to be more dependent on the amount of shear reinforcement that was provided than the amount of flexural reinforcement. This can be seen by the gradual change of failure mode from flexure to shear as more layers were added. However, had the study accounted for the difference in thickness of the two systems, their behavior could be regarded as very similar.

Table 5.16 and Figures 5.31 and 5.32 show the results from all of the shear at 45^o specimens.

Table 5.16: Average results from 45^{o} glass specimens

	@ initial flexural cracking				@ failure of the beam				
Beam	Load (N)	Deflection (mm)	Flexural * Strain (x 10^{-4})	Strain** in Shear (x10^{-4})	Load (N)	Deflection (mm)	Flexural * Strain (x 10^{-3})	Strain** in Shear (x10^{-4})	Type of Failure
CONTROL	22894	0.035	1.396	NA	45850	1.617	NA	NA	Flexure
45FGS1	49297	0.100	2.858	0.704	138813	1.779	7.824	48.01	Shear/Debond
OCRS1-45	30850	0.066	NA	0.448	74765	1.738	NA	30.51	Flexural Failure
45FGS2	48185	0.024	2.833	0.530	197749	1.482	6.509	29.71	Shear/Debond
OCRS2-45	36739	0.050	NA	0.611	105424	2.637	NA	39.84	Flex/Shear Failure
45FGS3	53745	0.068	2.820	0.469	184223	0.936	4.140	19.95	Shear/Debond
OCRS3-45	34321	0.069	NA	0.499	108637	1.619	NA	38.52	Shear Failure

*** Flexural strain does not correspond to a fiber orientation, but was measured in the longitudinal direction of the beam.**

**** Shear strains were measured in direction of shear fiber orientation (45^{o}) on the sides of the beams.**

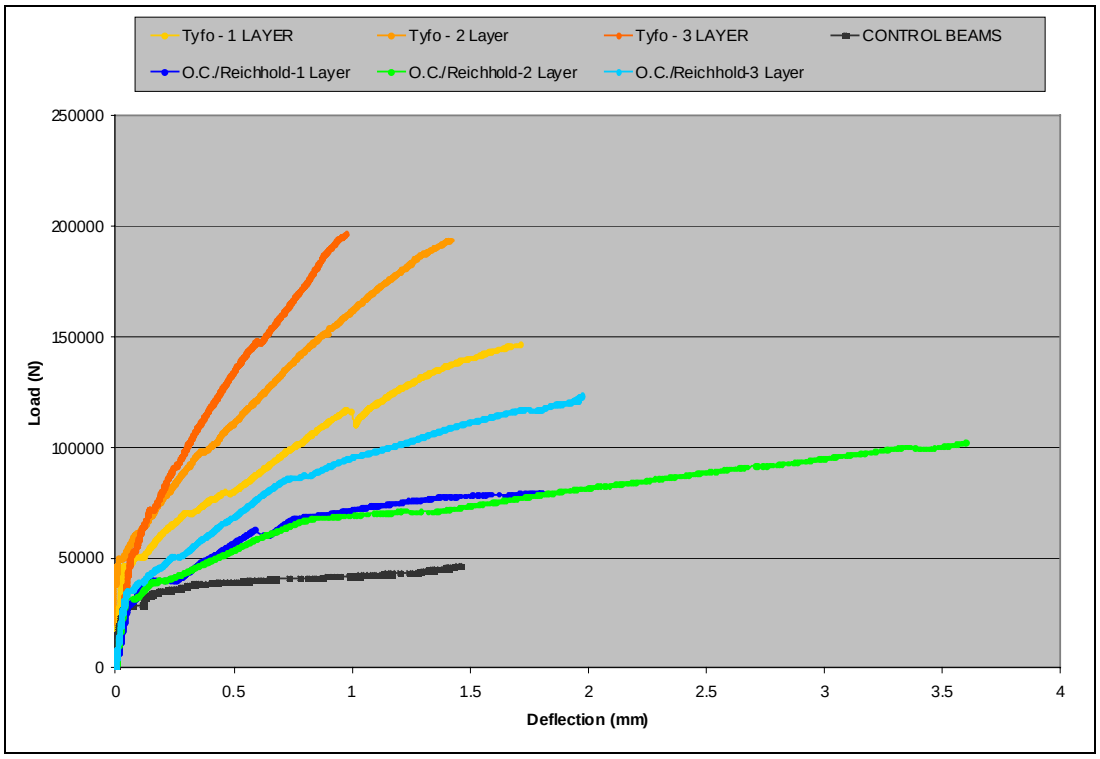

Figure 5.31: Load versus deflection behavior for specimens reinforced with glass laminates for shear at 45^{o}

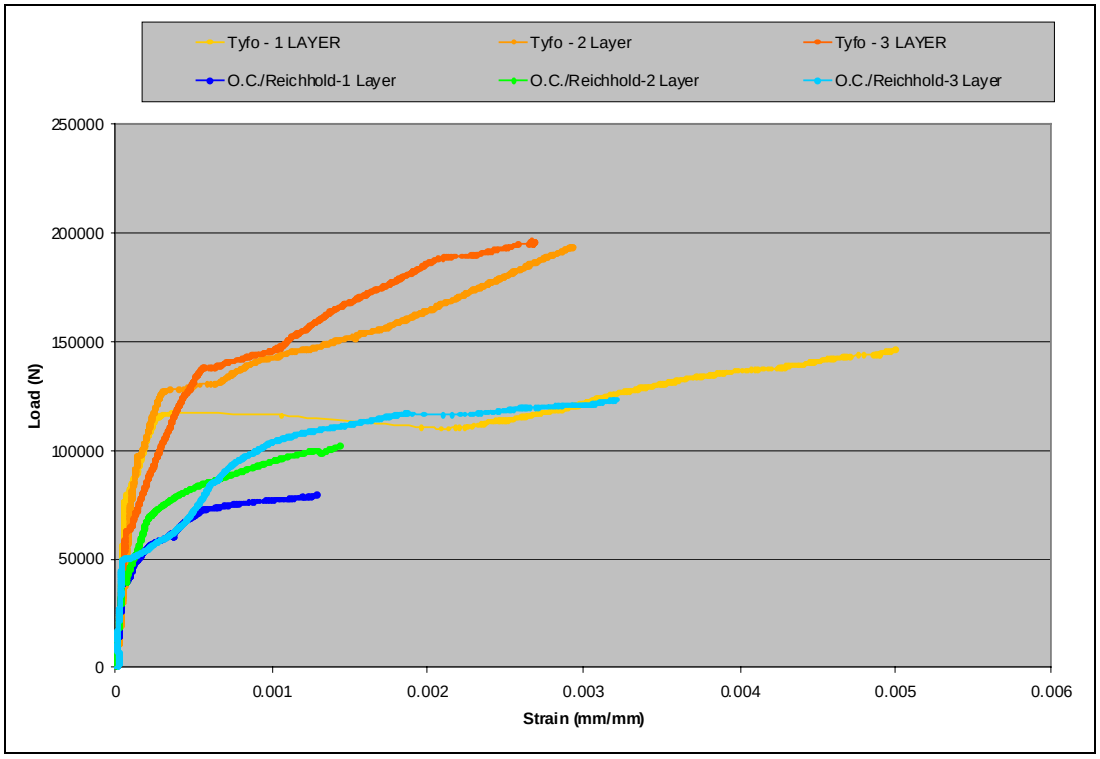

Figure 5.32: Load versus shear strain behavior for specimens reinforced with glass laminates for shear at 45^{o}

6.0 CONCLUSIONS AND RECOMMENDATIONS

The main objective of this study was to investigate the interaction between FRP composites and concrete by addressing the most important variables in terms of FRP properties. Type of fibers, thickness of the laminates, fiber orientation and FRP strengthening configuration were studied while keeping the type of concrete, steel reinforcement and geometry of the samples constant. The study compared the performance of most commercially available FRP systems used for strengthening concrete structures. Additionally, new glass and carbon-based strengthening FRP systems were researched.

The intent of the data collection and analysis was to gather extensive information on the performance of FRP-reinforced concrete, rather than to investigate the structural behavior of FRP-reinforced members. Appearance of first crack on the concrete, ultimate loads sustained by the concrete specimens with the corresponding strains and deflection, and the failure modes were of main interest. The reader must be aware that the conclusions made herein are not necessarily valid for full-size, reinforced concrete beams. The behavior of such structural members might be affected by variables not intended for investigation in this study. However, the conclusions made herein would be an important asset to the future development of design guidelines for reinforced concrete members using FRP laminates.

From analysis of the data that is presented in Chapters 4 and 5, the following conclusions were made:

1. The study demonstrated the effectiveness of FRP reinforcement on small-size concrete beams. All of the FRP strengthened specimens showed significant increases in flexural and shear strength. The typical increase of the sustained load at appearance of first crack ranged from 20 to 200 percent compared to the unstrengthened specimens.

2. The ultimate strength increase at failure ranged from 18 to 545 percent, depending upon the FRP-application scheme. Most reinforcing schemes exhibited a gain in the ultimate load at failure ranging from 200 to 300 percent.

3. The specimens in this study showed no significant increase in stiffness prior to initial cracking of the concrete. The average, uncracked modulus for the control specimens was approximately 22,700 N/mm^2, while the average uncracked modulus for all of the strengthened specimens in this study was approximately 23,150 N/mm^2. This behavior was expected, because the elastic modulus of a typical FRP composite is much closer to concrete than to the modulus of steel. Therefore, the FRP-reinforced

specimen should behave in such a way that would indicate no significant increase of the beam modulus prior to concrete cracking.

4. The load at initial cracking for FRP reinforced specimens showed a significant increase over the control specimens. The application of a relatively high tensile strength material with elastic modulus similar to that of concrete on the surface of the beams delayed concrete cracking, a strain dependent phenomenon. This behavior was counterintuitive.

5. The FRP-strengthened specimens exhibited greater deflections prior to initial cracking of the concrete. This finding indicates that externally applied FRP laminates might improve the behavior of reinforced concrete beam at low loads and possibly during earthquakes. However, this conclusion cannot be regarded as definitive, because the behavior of full-size members during earthquakes is a more complex phenomenon, not intended for investigation in this study.

6. Following initial cracking, the behavior of the specimens was more heavily influenced by the properties of the FRP laminate. This was evident when comparing the stiffness of the cracked FRP- retrofitted specimens to that of the control specimens. The study concluded that the stiffness after cracking increases as the number of layers of FRP on the specimens increases.

7. The results of this study suggest that the increase of the load-carrying capacity and the performance of the FRP-reinforced beams were strongly dependent on the reinforcing scheme (FRP configuration). The failure modes showed dependency on the stiffness and strength of the FRP reinforcement and the scheme used to strengthen them.

8. The typical failure mechanisms observed in this study were flexural failure of the beam and/or the laminate, shear (diagonal tension) failure of the specimen, failure due to local stresses developed at the ends of the FRP laminate, and debonding (separation of the concrete and the FRP laminate). Combinations of the above failure modes were not uncommon. However, typically one failure mode was governing the behavior of the specimen. When analyzing failure modes the researcher must consider the mechanism that dominates the failure, rather than accompanying failures.

9. It seems that debonding occurred most often in specimens reinforced with thicker and stiffer FRP laminates. In such cases, the beam behavior was affected less by the properties of the FRP composite and more by the shear resistance of concrete and/or the shear (tensile) strength of the adhesive layer.

10. The results indicate that the effectiveness of the FRP composite decreases as the rigidity (elastic modulus x FRP thickness) of the laminates increases. Mostly shear mode of failure was governing the behavior of specimens reinforced with thick and very stiff FRP laminates, thus reducing the ultimate load at failure and diminishing the effectiveness of the composite reinforcement. In these specimens, a lower strain

is generally developed in the flexural FRP reinforcement. These results strongly indicate that over-reinforcement of the specimens is detrimental to their behavior, which is primarily dependent upon the shear resistance of the reinforced concrete beams.

11. Traditional designs do not account for the shear capacity contribution of the flexural reinforcement when calculating shear capacity of a member. Typically, it is expected that specimens with no shear reinforcing would fail at approximately the same load whenever the shear mode of failure was dominant. In several situations, when the mode of failure of the beam had already been changed to shear by the addition of one layer of FRP reinforcement, addition of second and third layers of FRP caused the load at failure to increase. In some cases, however, the additional layers of FRP reinforcement caused the load at failure to be reduced. The observed behavior is probably due to change in the local stress distribution and fracture mechanism. The results also suggest that there is an optimum amount of reinforcement, which if exceeded would result in deteriorated performance.

12. The capacity of the shear reinforcement on most of the specimens was limited by the strength of the bond between the laminate and the concrete. The strains that were developed in the shear laminate were far below those strains that caused failure in the flexural laminates. This behavior was most likely due to the geometry of the specimens (relatively short span). In most of the beams strengthened for shear, the mode of failure was either failure of the flexural laminate, debonding of the shear laminate, or the concentration of stresses at the end of the flexural laminate causing cracking of the end of the specimen. This last type of failure is likely due primarily to the geometry of the specimens that were tested and might be less common on full size beams. Calculations of the capacity of shear laminates must account for the various bond strengths of the resins used with the different systems. If anchors are used to attach the shear laminates, it is likely that far more benefit can be gained from the shear reinforcement.

13. The strains measured at failure were significantly smaller than those suggested by the manufacturers. It is likely that such a discrepancy was due to the different ways in which the FRP was tested. While most manufacturers reported strains at failure from direct tensile tests, the data in this study were gathered by flexural beam tests. Bond line deficiencies could also have contributed to the composites not reaching their strain capacities. Considering all systems, typical strains at failure were approximately 40 to 70 percent of those reported by the manufacturer. Of the carbon reinforced specimens that were tested, the Fyfe Tyfo® and Mitsubishi Replark® systems exhibited strain values at the higher end of this range. For the beams strengthened with glass, the Fyfe Tyfo® system performed the closest to what the manufacturer suggested.

The differences in the strain at failure need to be accounted for in any design standards that are produced, since the strain at failure is typically guiding the design philosophy and calculations.

14. The majority of the beams behaved with significant increases in post-cracking stiffness. The deflection of these beams at failure was similar to that of the unreinforced beams; however, the load needed to cause the deflection was typically much higher. In addition, some of the beams exhibited increased ductility, or were able to sustain higher deflections before failure. Deflection at failure for these beams was as much as three times that of the deflection for unreinforced beams. It is believed that the increased ductility was a result of the greater energy absorption capacity of the beams provided by the FRP composites. These results contradict what once was widely believed that, because of the high stiffness of most FRP composites, the ductility of FRP reinforced beams is reduced causing sudden brittle failure. However, it seems that the generally accepted definition of ductility (ratio of the strain at yield to the strain at failure) is not applicable to composites because of their linear stress-strain curves. We believe that adoption of the energy principles is a better approach of explaining the ductility of FRP-reinforced structural members.

15. Of all of the specimens that were tested, those retrofitted with 45-degree strengthening scheme exhibited the lowest deflections.

16. Cylinders wrapped with glass and carbon FRP showed significant increases in compressive strength when compared to the control specimens. Increases in compressive strength ranged between 120 and 300 percent.

17. Comparison of the performance of the glass and carbon cylinder FRP reinforcement shows that the systems provide similar compressive strength increases when the thickness is taken into account.

The following observation was made during this study:

Based on visual inspection at the time of material application, the wet lay-up systems appeared to bond better with the concrete surface. This was especially evident on beams where the shear laminate was wrapped around a beam edge. However, analysis of the test data suggested that the bond between concrete and FRP was not a function of the application method, but rather depended on the preparation of the substrate and correct usage of the application steps suggested by the manufacturers. Typically the wet lay-up systems are bonded to the concrete by the resin used to saturate the fibers, while a primer layer is usually applied on the concrete surface, prior to the resin layer when dry lay-up FRP systems are used.

7.0 REFERENCES

Al-Sulaimani, G., Sharif, A., Basundul, I., Baluch, M., and Ghaleb, B., "Shear Repair for Reinforced Concrete by Fiberglass Plate Bonding", *ACI Structural Journal*, V.91, July-August 1994.

Blaschko M., Niedermeier, R., and Zilch, K., "Bond Failure Modes of Flexural Members Strengthened with FRP", *2nd International Conference on Composites in Infrastructure"*, Tucson, Arizona, 1998.

Blue Road Research, *E-mail interview with John Seim*. March 15, 1999.

Cercone, L., and Korff, J., "Putting the Wraps on Quakes", *Civil Engineering*, July 1997.

Chajes, M., Januszka, T., Mertz, D., Thomson, T. and Finch, W., "Shear Strengthening of Reinforced Concrete Beams Using Externally Applied Composite Fabrics", *ACI Structural Journal*, V.92, May-June 1995.

Challal, O., Nollet, M.-J., and Saleh, K., "Use of CFRP Strips for Flexural and Shear Strengthening of RC Members", *2nd International Conference on Composites in Infrastructure"*, Tucson, Arizona, 1998.

Cjan, K.S., and Tan, T.H., "Repair and Strengthening with Adhesive-Bonded Plates", *Repair and Strengthening Concrete Members with Adhesive Bonded Plates, the American Concrete Institute*, SP-165, 1996.

Clark Schwebel, "Structural Grids", *Manufacturer Publication*, Anderson, South Carolina, 1997.

Composite Materials, Inc. " Technical Data Specifications", *Manufacturer Publication*, 1998.

Demers M., Hebert, D., Gauthier, M., Labossiere, P., and Neale, K., "The Strengthening of Structural Concrete with An Aramid Woven Fiber/Epoxy Resin Composite", *Proceedings from the 2nd Conference on Advanced Composite Materials in Bridges and Structure*, CSCE, Montreal, Canada, 1996.

Dolan, C., Rider, W., Chajes, M., DeAscanis, M., "Prestressed Concrete Beams Using Non-Metallic Tendons and External Shear Reinforcement", *Fiber-Reinforced Plastic Reinforcement for Concrete Structures*, SP-138, the American Concrete Institute, 1992.

Dussek, I.J., "Strengthening of Bridge Beams with Similar Structures by Means of Epoxy-Resin-Bonded External Reinforcement", *Transportation Research Record 785*, Transportation Research Board, Washington, D.C., 1980.

Finch, W., Chajes, M., Mertz, D., Kaliakin, V., and Faqiri, A., "Bridge Rehabilitation Using Composite Materials", *3rd Materials Conference, "Infrastructure Repair Methods"*, ASCE, 1995.

Forca Tow Sheet Manual, *Publication of the Tonen Corporation*, Tokyo, Japan, April 1996.

Fortafil Fibers, Inc., "Technical Specifications", *Manufacturer Publication*, 1993.

Fyfe Company, "Specifications for Composite Beam Retrofitting", *Manufacturer Publication*, July 1997.

Hexcel Corporation, "Civil Engineering and Construction Systems: Repair and Retrofit Solutions for the Construction Industry", *Manufacturer Publication*, 1998.

Hutchinson, A., and Rahimi, H., "Flexural Strengthening of Concrete Beams with Externally Bonded FRP Reinforcement", *Proceedings from the 2nd Conference on Advanced Composite Materials in Bridges and Structure*, CSCE, Montreal, Canada, 1996.

Juvandes, L., Figueiras, J.A., and Marques, A., "Performance of Concrete Beams Strengthened with CFRP Laminates", *2nd International Conference on Composites in Infrastructure"*, Tucson, Arizona, 1998.

Kachlakev, D., "Strengthening Bridges Using Composite Materials", *Report # FHWA-OR-98-08*, March 1998.

Kachlakev, D., Lundy J., and Barnes, W., "Shear and Flexural Strengthening of Reinforced Concrete Beams Using FRP Laminates", *Proceedings, International Conference on Advanced Composites*, Editors Abdel-Hady, F. and Gowayed, Y., Hurghada, Egypt, December 15-18, 1998.

Kachlakev, D.I., and Barnes, W.A., "Flexural and Shear Performance of Concrete Beams Strengthened with Fiber Reinforced Polymer Laminates", *Fiber Reinforced Polymers for Reinforced Concrete Structures*, SP-188, the American Concrete Institute, Farmington Hills, Michigan, November 1999.

Klaiber, F.W., Dunker, K.F., and Sanders, W.W., "Strengthening of Single-Span Steel Beams Bridges", *Journal of Structural Engineering, American Society of Civil Engineers*, Vol. 108, No. 12, 1982.

Limberger, E., and Vielhaber, J., "Experimental Investigations on the Behavior of CFRP-Prepreg Strengthened Structural RC Elements", *Proceedings from the 2nd Conference on Advanced Composite Materials in Bridges and Structure*, CSCE, Montreal, Canada, 1996.

Malek, A., Saadatmanesh, H., and Ehsani, M., "Prediction of Failure Load of R/C Beams Strengthened with FRP Plate Due to Stress Concentration at the Plate End", *ACI Structural Journal*, March-April, 1998.

Marshall, O.S. and Busel, J.P., "Composite Repair/Upgrade of Concrete Structures", *4th Materials Conference, "Materials for the New Millennium"* Editor K. Chong, American Society of Civil Engineers, Washington, D.C., November, 1996.

Master Builders, Inc., "MBrace Composite Strengthening System: Carbon Fiber and E-glass Reinforcement to Extend the Life of Concrete Structures", *Manufacturer Publication*, 1997.

McConnell, V.P., "Infrastructure Update", *High Performance Composites*, May/June, 1995.

Mitsubishi Chemical Corporation, "Replark System: Material Properties & Standard Application Procedures", *Manufacturer Publication*, November, 1997.

Owens-Corning, "Technical Data Sheet", *Manufacturer Publication*, 1998.

Reichhold Chemicals, Inc., "Technical Data Sheet", *Manufacture Publication*, 1993.

Reichhold Chemicals, Inc., "Technical Data Sheet", *Manufacture Publication*, 1996.

Rostasy, F., Hankers, C, and Ranish, E-H, "Strengthening of R/C and P/C-Structures with Bonded Plates", *Advanced Composite Materials in Bridges and Structures*, CSCE, Sherbrooke, Canada, 1992.

Saadatmanesh, H., Alberecht, P., and Ayyub, B.M., "Experimental Study of Prestressed Composite Beams", *Journal of Structural Engineering, American Society of Civil Engineers*, Vol. 115, No. 9, 1989.

Saadatmanesh, H., and Ehsani, M., "RC Beams Strengthened with GFRP Plates. I: Experimental Study", *Journal of Structural Engineering,* ACSE, V.117, No.11, 1991.

Saadatmanesh, H., and Ehsani, M., "RC Beams Strengthened with GFRP Plates. II: Analysis and Parametric Study", *Journal of Structural Engineering*, ACSE, V.117, No.11, 1991.

Sato, Y., Ueda, T., Kakuta, Y., Tanaka, T., "Shear Reinforcing Effect of Carbon Fiber Sheet Attached to Side of Reinforced Concrete Beams", *Proceedings from the 2nd Conference on Advanced Composite Materials in Bridges and Structure,* CSCE, Montreal, Canada, 1996.

Seible, F., Hegemeir, G. and Karbhari, V., "Advanced Composite for Bridge Infrastructure Renewal", *Forth International Bridge Engineering Conference, Proceedings*, Vol. 1, August 29-30, 1995, San Francisco, California.

Sharif, A., Al-Sulaimani, G., Basundul, I., Baluch, M., and Ghaleb, B., "Strengthening of Initially Loaded Reinforced Concrete Beams Using FRP Plates", *ACI Structural Journal*, the American Concrete Institute, March 1994.

Sika Corporation, "Sika Construction Products Catalog", *Manufacturer Publication*, Lyndhurst, New Jersey, 1997.

Sika Corporation, “Sika Construction Products Catalog”, *Manufacturer Publication,* Lyndhurst, New Jersey, 1998.

Sika Corporation, “Sika Carbodur Structural Strengthening System: Application Guide for SikaWrap®”, *Manufacturer Publication,* Lyndhurst, New Jersey, 1998.

Swamy, R., Lynsdale, C., Mukhopadhyaya, P., “Effective Strengthening with Ductility: Use of Externally Bonded Plates of Non-Metallic Composite Materials”, *Proceedings from the 2nd Conference on Advanced Composite Materials in Bridges and Structure,* CSCE, Montreal, Canada, 1996.

Swanson, S.R., Introduction to Design and Analysis with Advanced Composite Materials. New Jersey: Prentice-Hall, 1997.

Triantafillou, T.C., and Plevris, N., “Post-Strengthening of R/C Beams with Epoxy-Bonded Fiber Composite Materials”, *Proceedings of ASCE Specialty Conferences, “ Advanced Composite Materials in Civil Engineering Structures”,* Editor S. Iyer, Las Vegas, Nevada, 1991

Triantafillou, T., “Shear Strengthening of reinforced Concrete Beams Using Epoxy-Bonded FRP Composites”, *ACI Structural Journal,* V.95, March-April 1998.

APPENDICES

APPENDIX A: BEAM DESIGNATION LEGEND

BEAM DESIGNATION LEGEND

CON	- Control Beam. Number following CON is sample number
CSGF	- Clark-Schwebel Glass Structural Grid reinforcing for flexure only(F). Number following CSGF is sample number.
CSGFS	- Clark-Schwebel Glass Structural Grid reinforcing for flexure and shear(FS). Number following CSGFS is sample number.
CSGS	- Clark-Schwebel Glass Structural Grid reinforcing for shear only (S). Number following CSGS is sample number.
FCF	- Fyfe Carbon system (Tyfo) reinforcing for flexure only. Number following FCF is number of layers of reinforcement. Number following dash is sample number.
FCFS	- Fyfe Carbon system (Tyfo) reinforcing for flexure and shear. Number following FCFS is number of layers for both shear and flexural laminates. Number following dash is sample number.
45FCS	- Fyfe Carbon system (Tyfo) reinforcing for shear at 45 degrees. Since fibers are also wrapped across tension side, they provide significant flexural strengthening as well. Number following 45FCS is number of layers. Number following dash is sample number.
FGF	- Fyfe Glass system (Tyfo) reinforcing for flexure only. Same as FCF, but glass rather than carbon.
FGFS	- Same as FCFS, but glass system rather than carbon.
45FGS	- Same as 45FCS, but glass system rather than carbon.
MBCF	- Same as FCF, but Master Builders Carbon system (M-Brace).
MBCFS	- Same as FCFS, but Master Builders Carbon system (M-Brace).
MBGF	- Same as FGF, but Master Builders Glass system (M-Brace).
MBGFS	- Same as FGFS, but Master Builders Glass system (M-Brace).
MBG2F1S	- Two layers of Master Builders Glass system (M-Brace) for flexure, and one layer for shear.
MCF	- Same as FCF, but Mitsubishi Carbon System (Replark).

MCFS - Same as FCFS, but Mitsubishi Carbon System (Replark).

45MCS - Same as 45FCS, but Mitsubishi carbon system (Replark).

90MCS - Mitsubishi carbon system (Replark) reinforcing shear only. Fibers run vertically (@ 90 degrees to longitudinal axis of beam) on side and tension side of beam similar to a U-shaped stirrup. No flexural strengthening is provided (other than transverse strength of the laminate). Number following 90MCS is number of layers. Number following dash is sample number.

SCF - Sika (Carbodur) carbon system reinforcing for flexure only. All are one layer only. Number following SCF is sample number.

SCFS - Sika (Carbodur) for flexure (one layer only) and Sika/Hexcel (SikaWrap) for shear reinforcing. Number following SCFS is number of layers of shear reinforcement. Number following dash is sample number.

SHCF - Sika/Hexcel (SikaWrap) carbon system reinforcing for flexure only. Number following SHCF is number of layers. Number following dash is sample number.

SHCFS - Sika/Hexcel (SikaWrap) carbon system reinforcing for flexure and shear. Number following SHCFS in number of layers of both shear and flexural laminate. Number following dash is sample number.

45SHCFS - One layer of Sika (Carbodur) for flexure and one layer of Sika/Hexcel (SikaWrap) ±45 degree glass grid for shear. Glass shear reinforcement is provided in similar to 90 MCS (U-shaped stirrup), but fibers run at ±45 degrees. Glass grid does not extend into center of beam, therefore it does not provide any increase in flexural strengthening.

APPENDIX B: TYPICAL FAILURE MODES

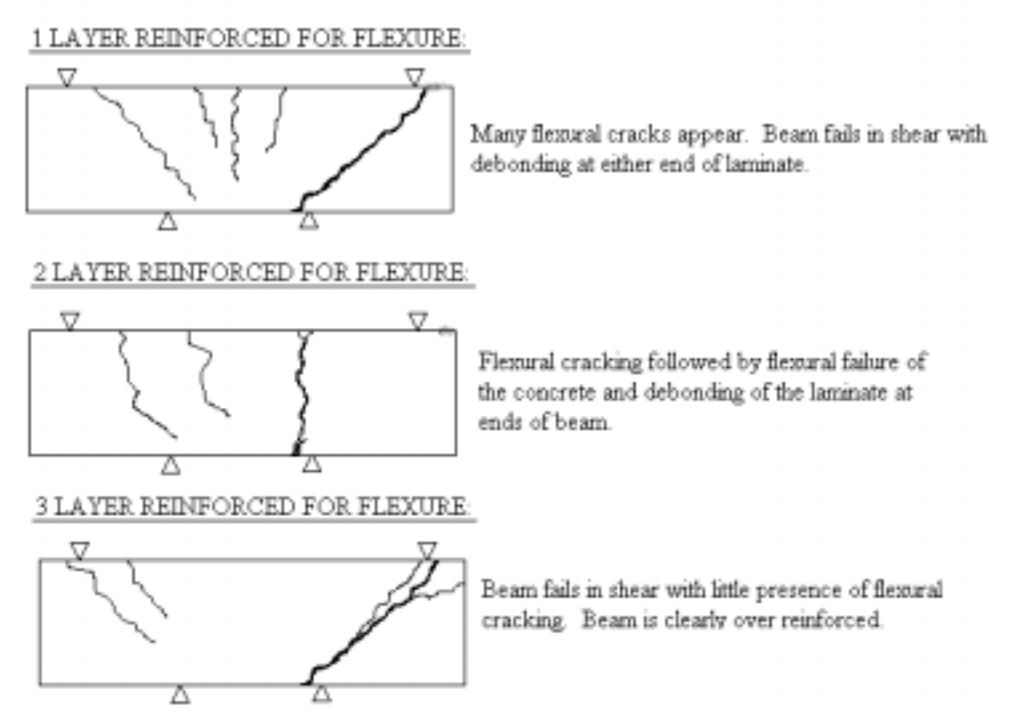

Figure B.2.1.3: Typical failure modes and crack patterns for flexurally reinforced MBrace™ carbon beams.

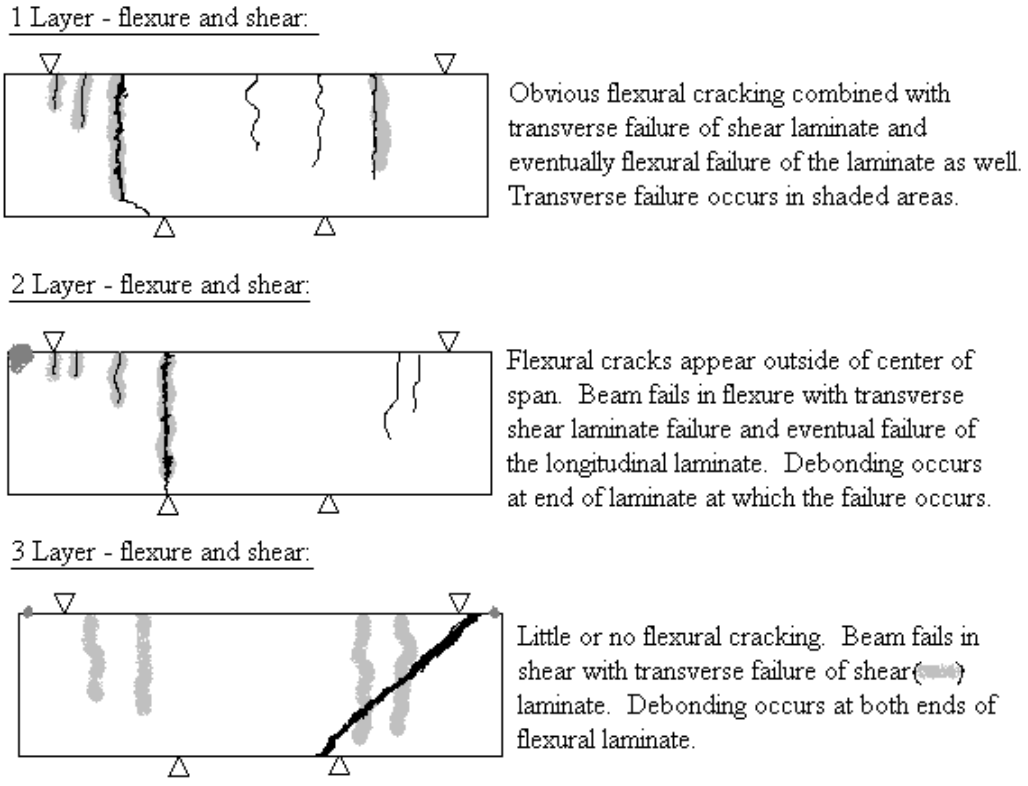

Figure B.2.2.3: Typical failure modes for MBrace™ carbon flexure and shear at 90° reinforced beams.

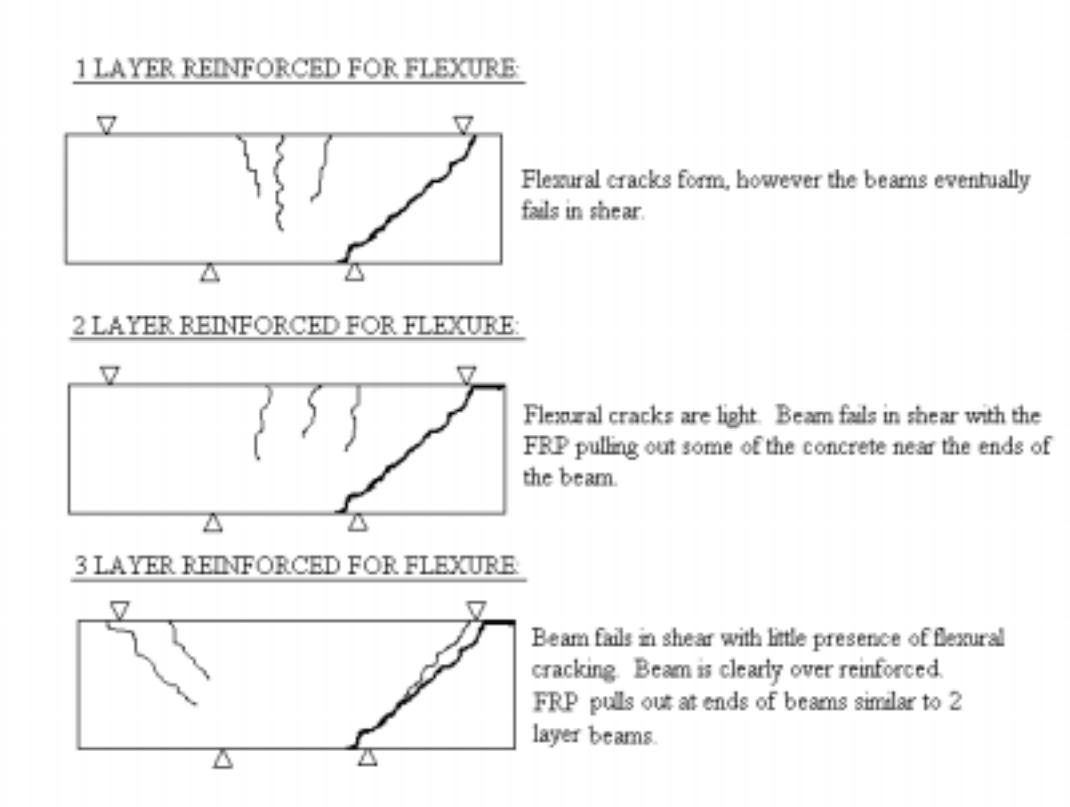

Figure B.3.1.3: Typical failure modes for Replark® beams reinforced for flexure only.

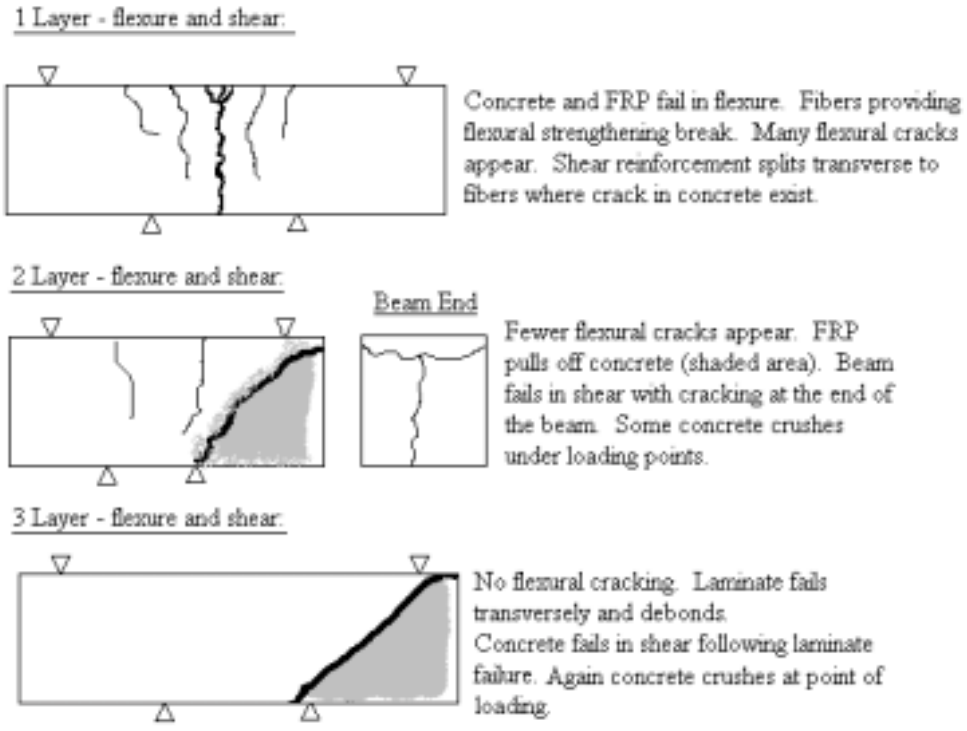

Figure B.3.2.3: Typical failure mode and crack patterns for beams reinforced with Replark® for flexure and shear at 90º.

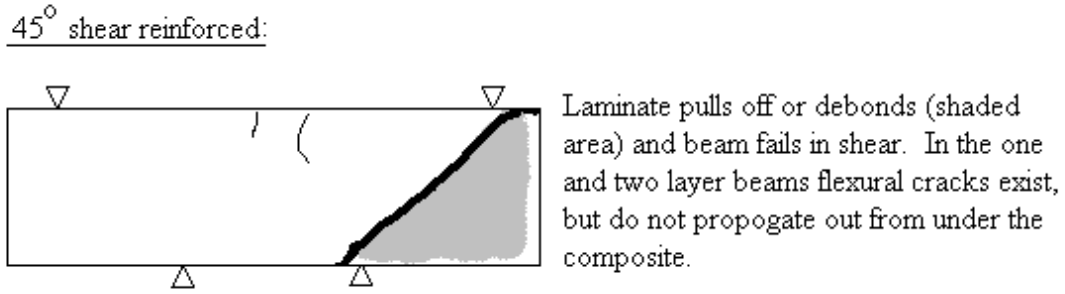

Figure B.3.3.3: Typical crack pattern and failure mode for beams reinforced at 45° for shear with Replark.

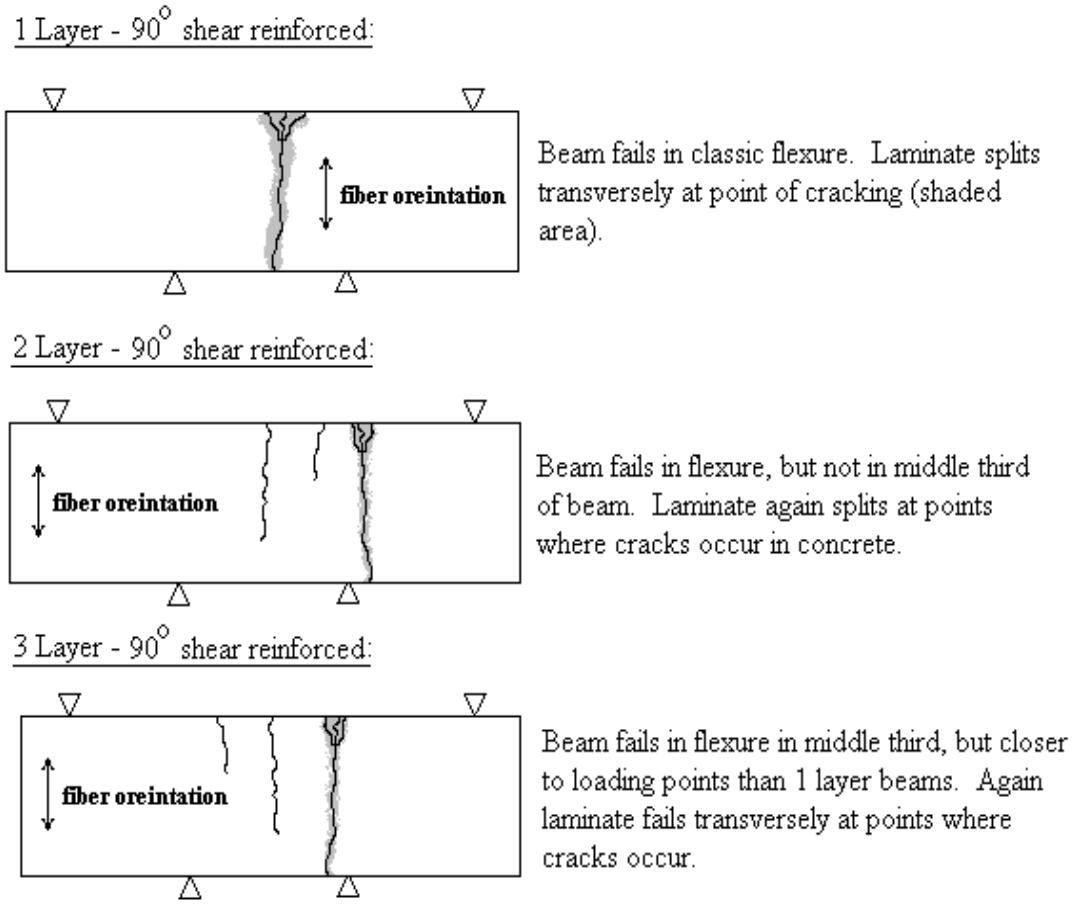

Figure B.3.4.2: Typical crack patterns and failure mode for beams reinforced with Replark® for shear at 90°.

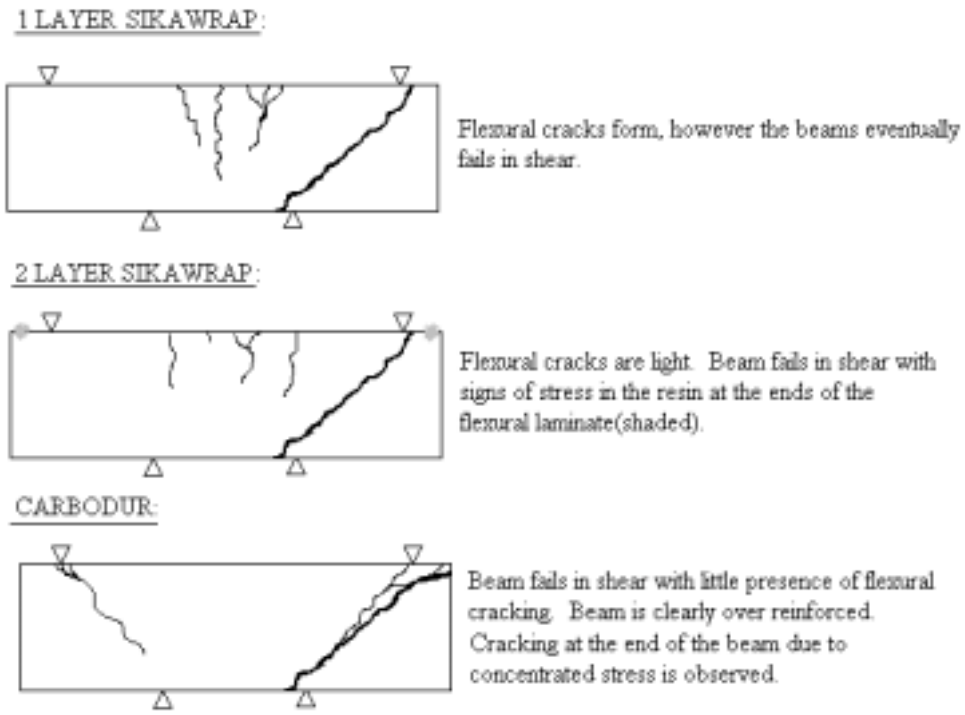

Figure B.4.1.3: Typical cracking and failure modes for beams reinforced for flexure only with Sika carbon products.

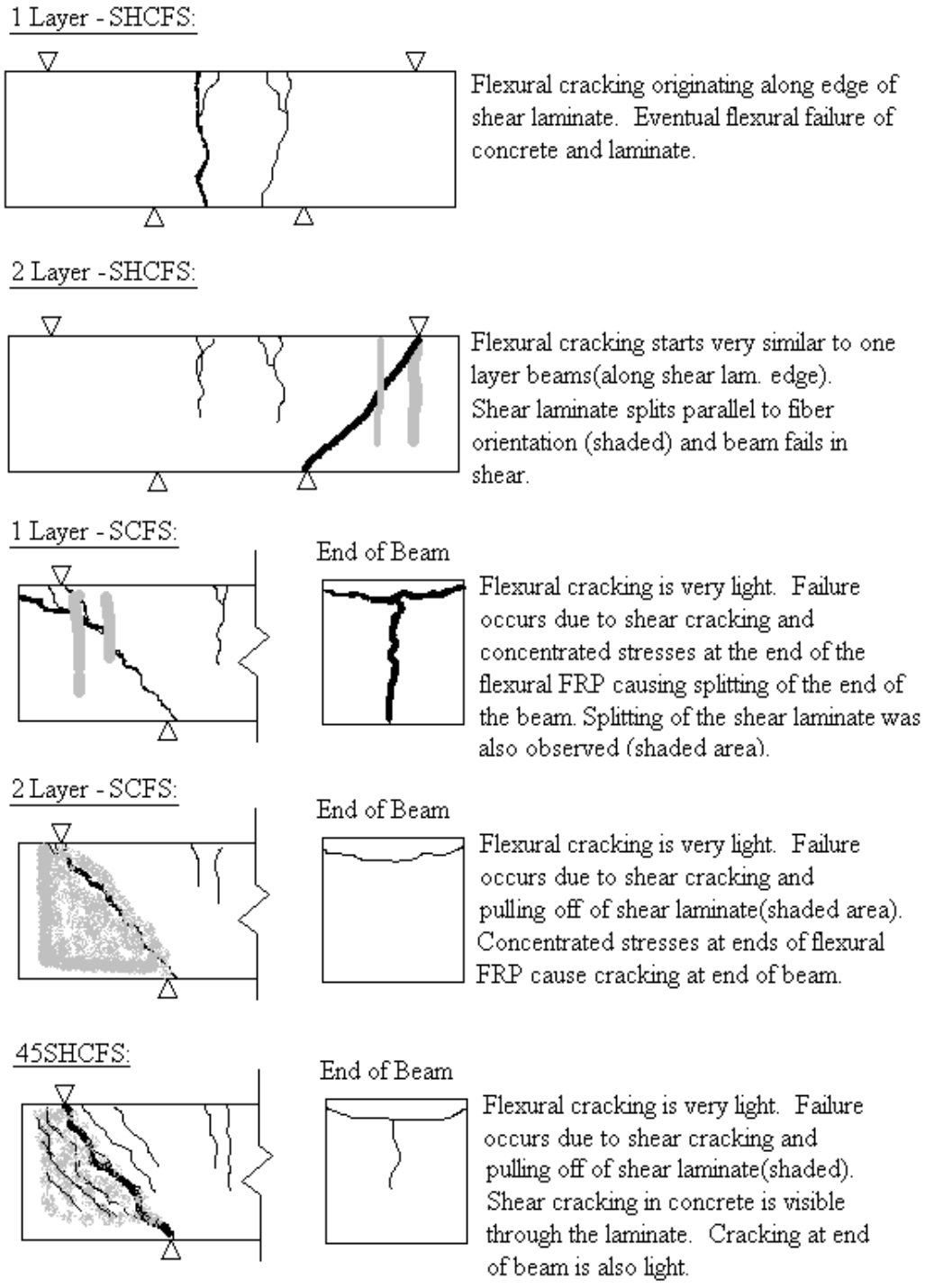

Figure B.4.2.3: Typical cracking and failure modes for beams reinforced for shear and flexure with Sika products.

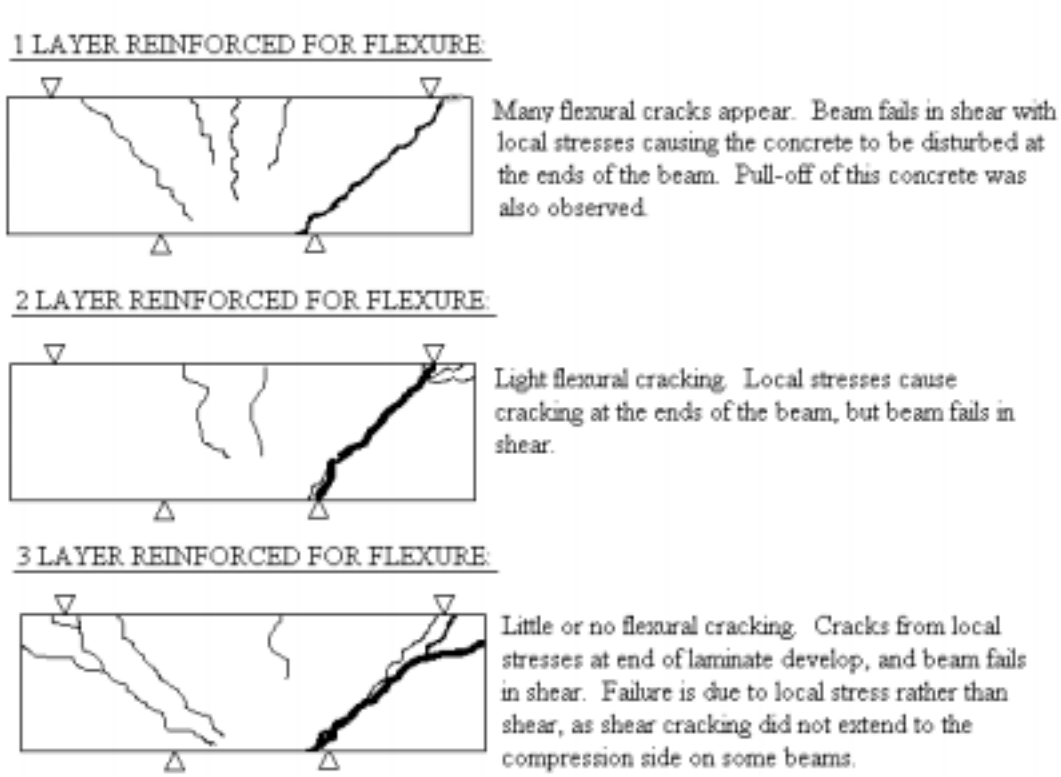

Figure B.5.1.3: Typical cracking and failure modes for beams reinforced for flexure with Tyfo® carbon FRP.

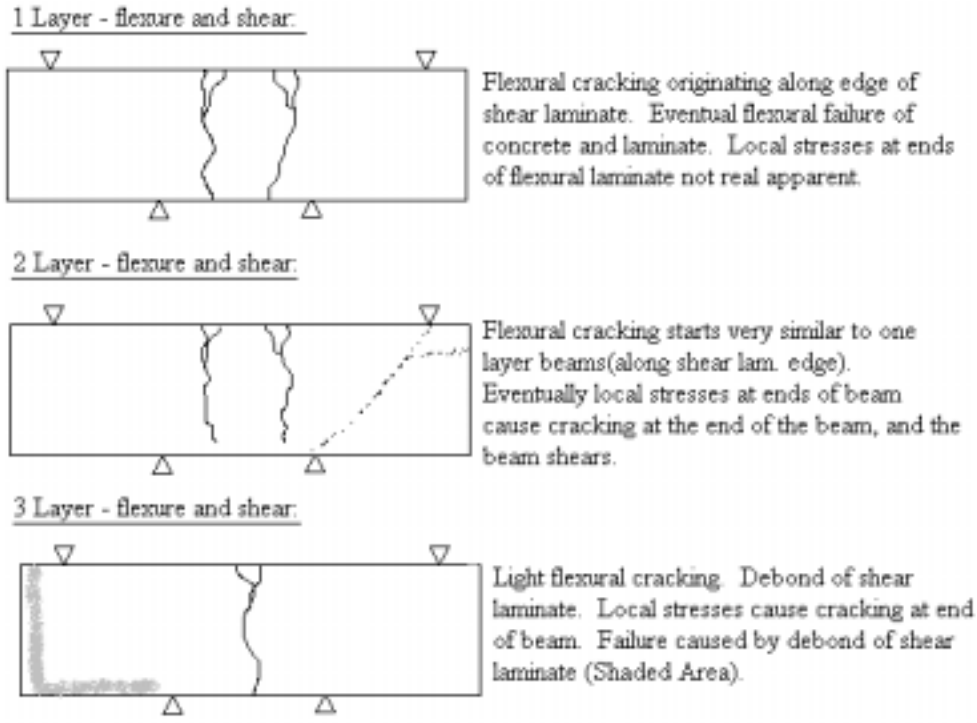

Figure B.5.2.3: Typical crack patterns and failure modes for beams reinforced with Tyfo® carbon for flexure and shear.

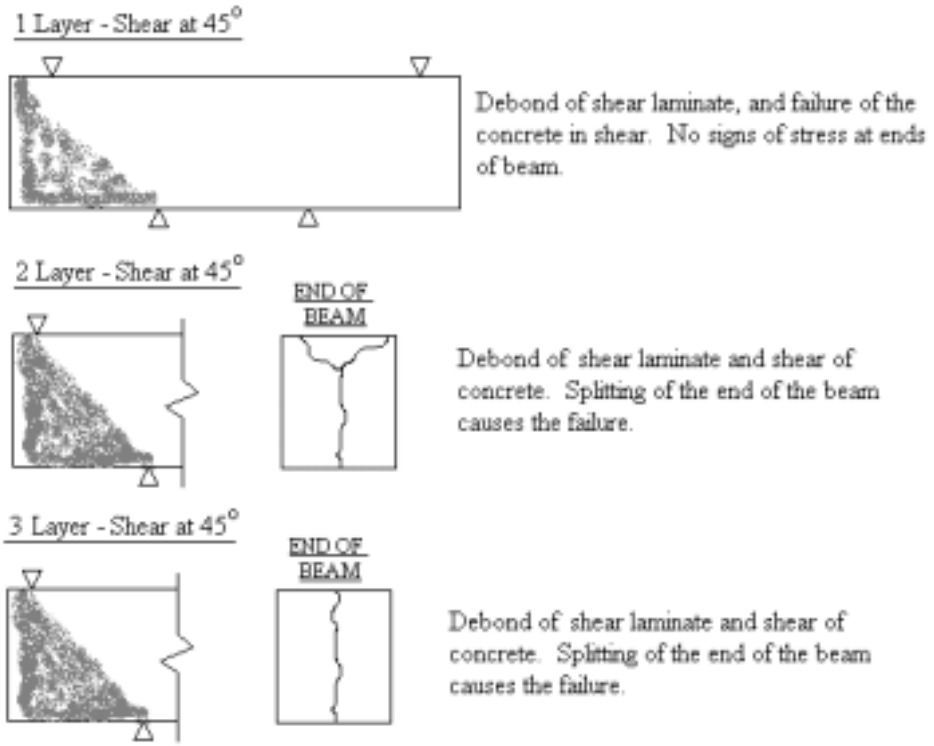

Figure B.5.3.4: Typical cracking and failure modes of beams reinforced with Tyfo® carbon for shear at 45°.

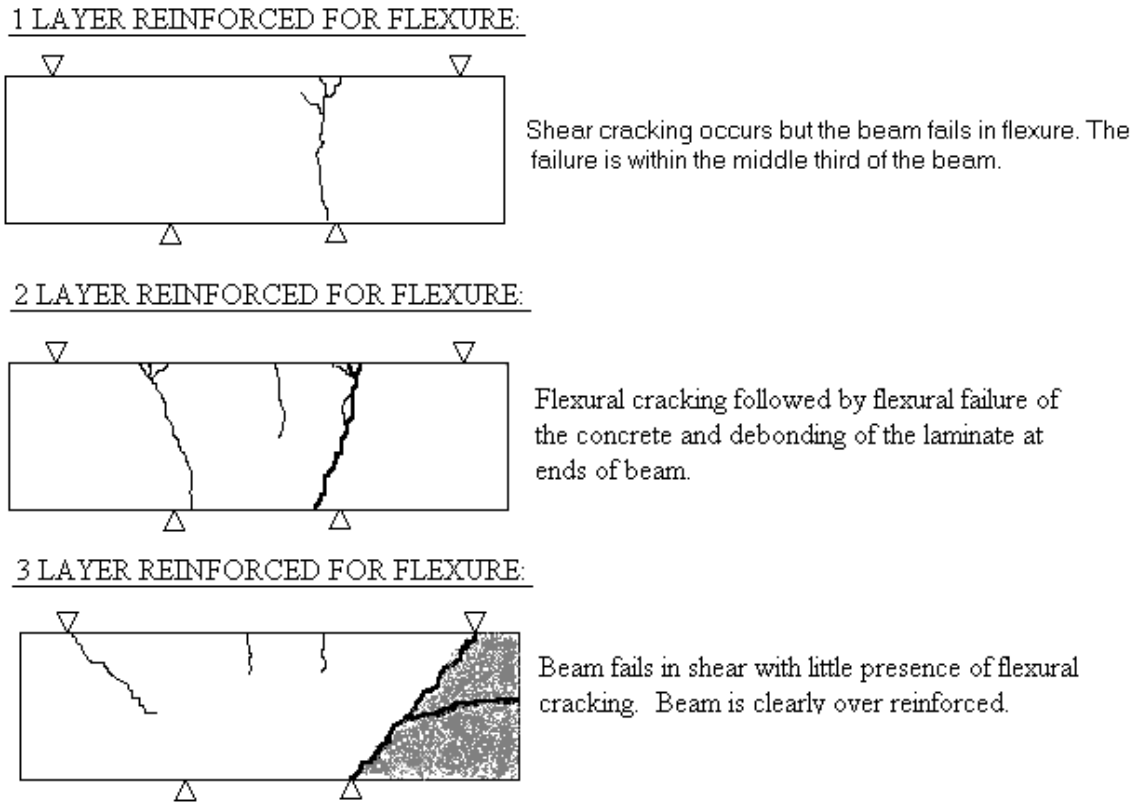

Figure B.6.1.3: Typical failure modes for CMI/Reichhold beams reinforced for flexure.

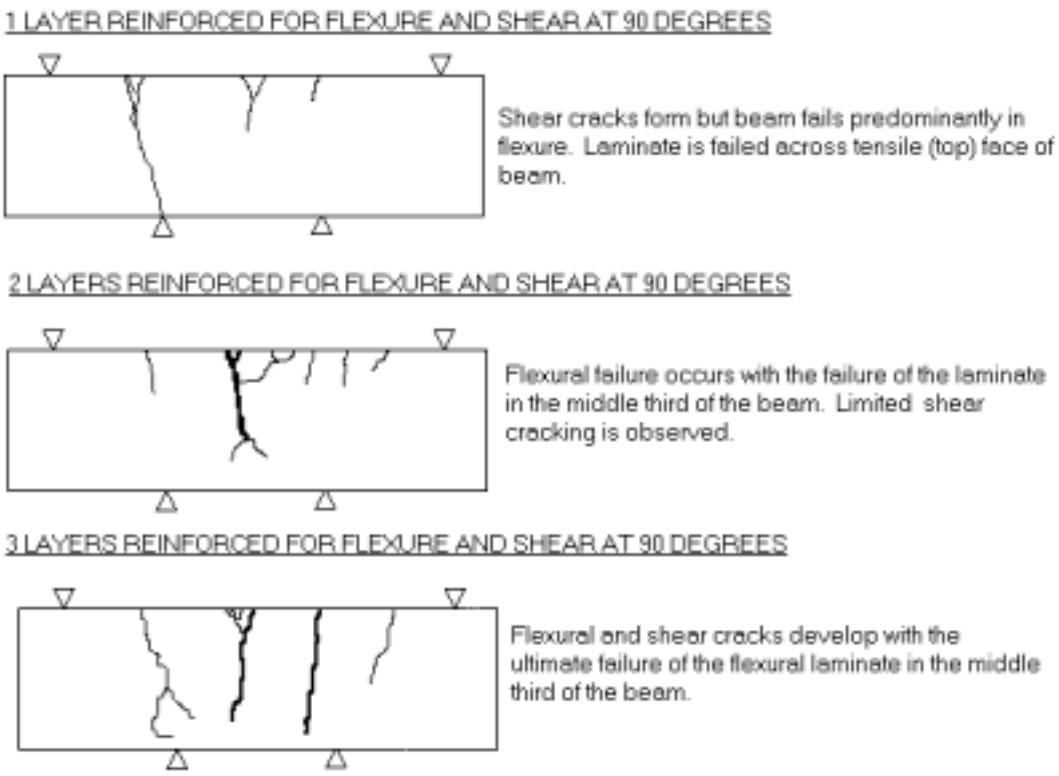

Figure B.6.2.3: Typical failure modes for CMI/Reichhold beams reinforced for flexure and shear at 90 degrees.

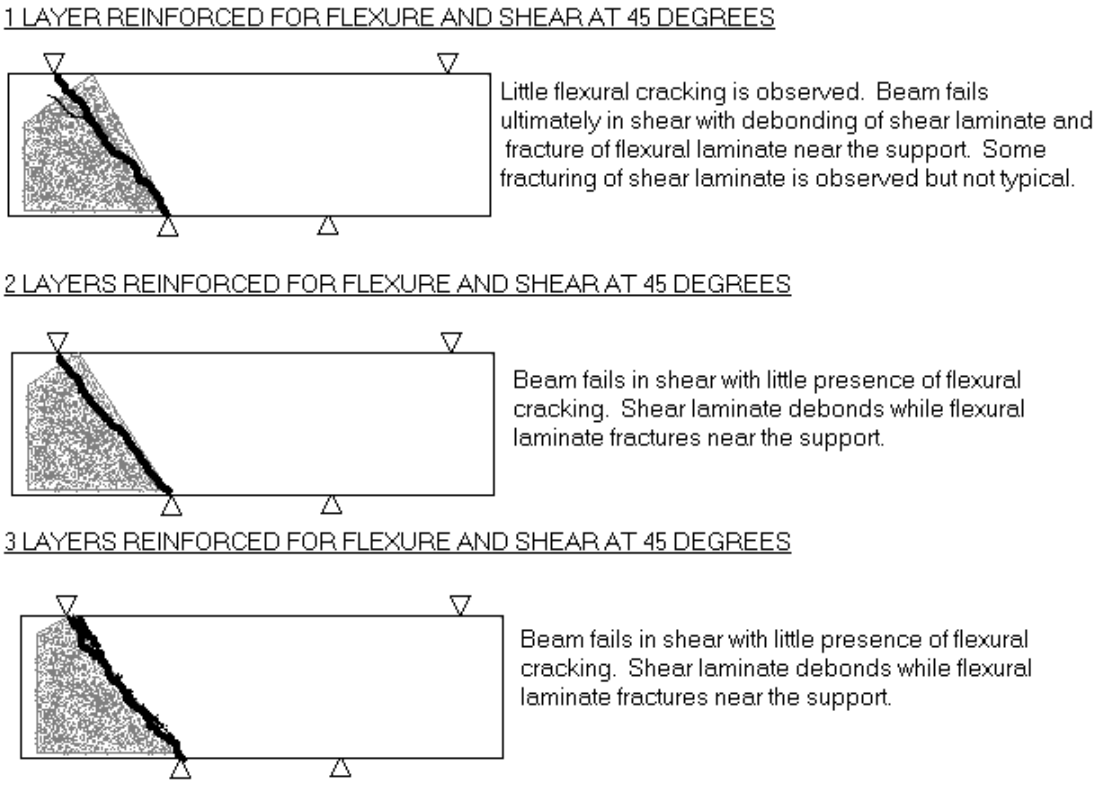

Figure B.6.3.3: Typical failure modes for CMI/Reichhold beams reinforced for flexure and shear at 45 degrees.

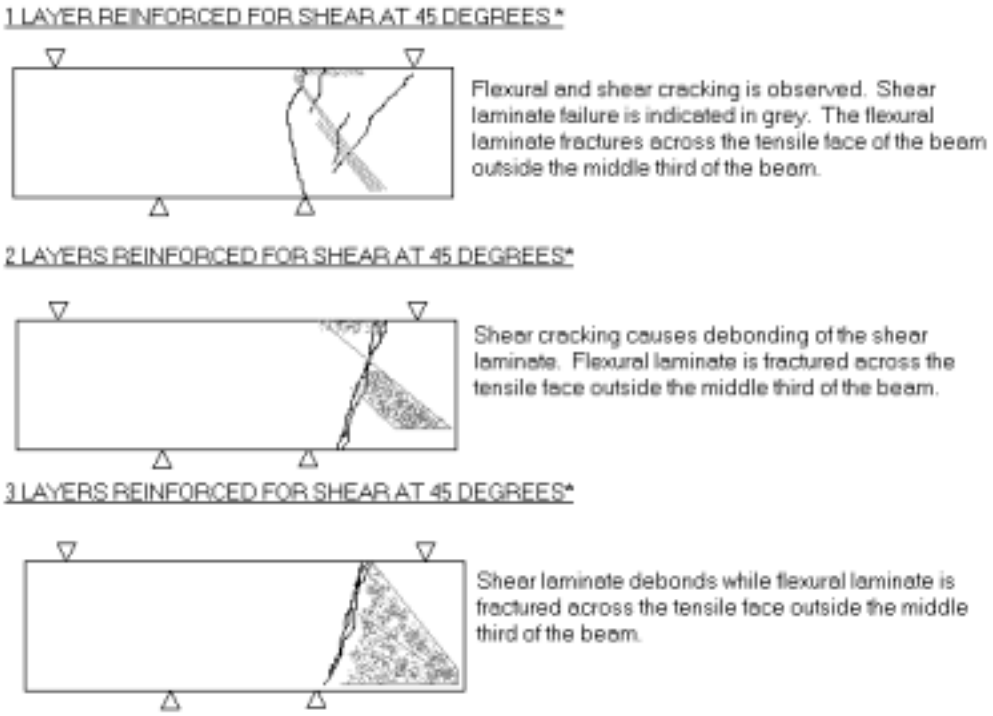

Figure B.6.4.2: Typical failure modes for CMI/Reichhold beams reinforced for shear at 45 degrees.

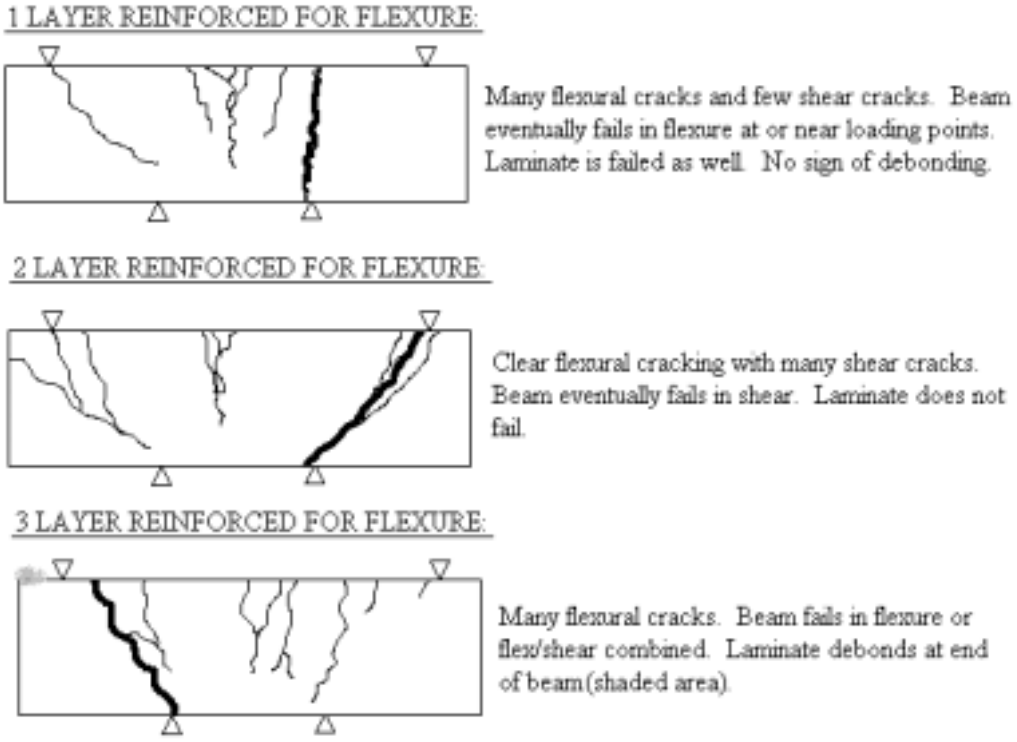

Figure B.7.1.3: Typical crack patterns and failure modes for beams reinforced for flexure with the MBrace™ glass system.

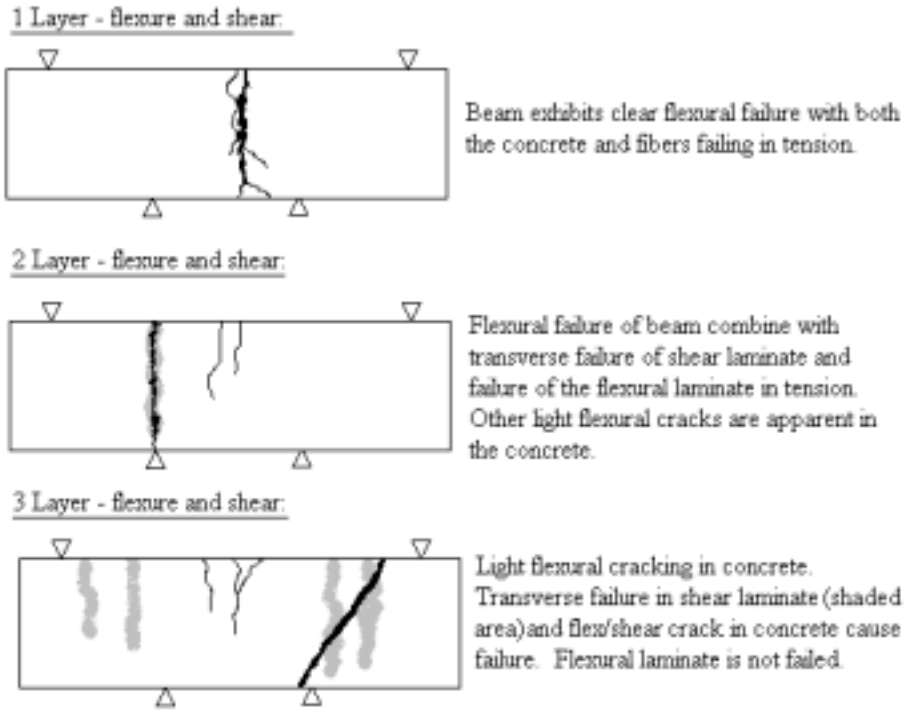

Figure B.7.2.3: Typical cracking and failure modes for beams strengthened with the MBrace™ glass system for shear and flexure.

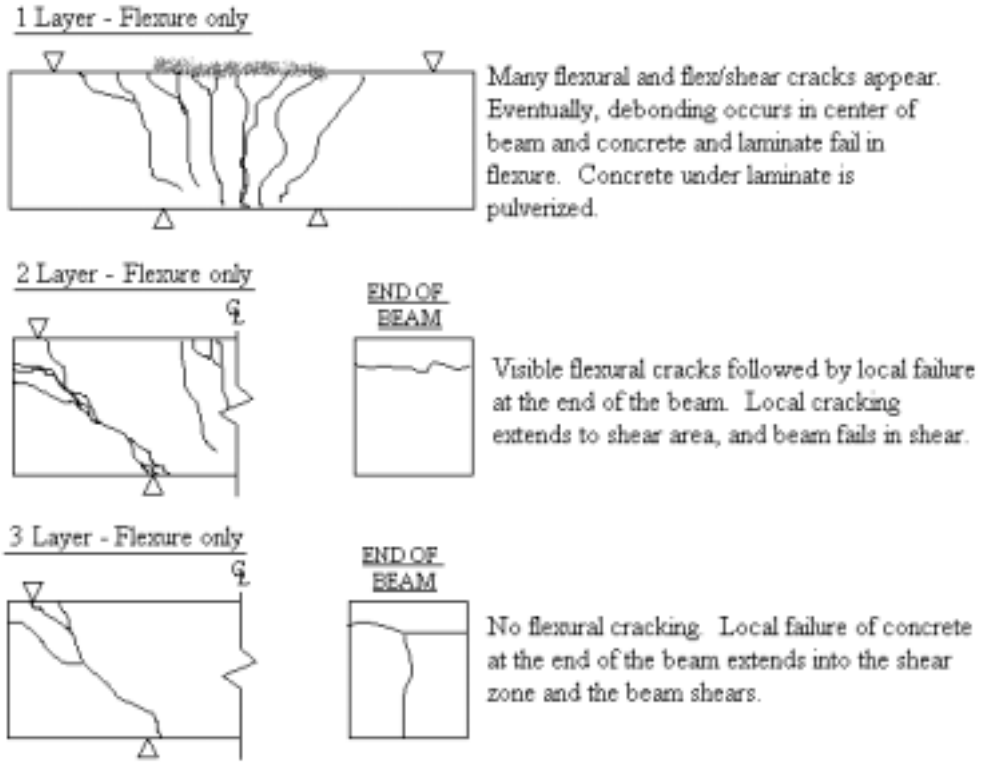

Figure B.8.1.3: Typical cracking and failure modes for beams reinforced with the Tyfo® glass system for flexure only.

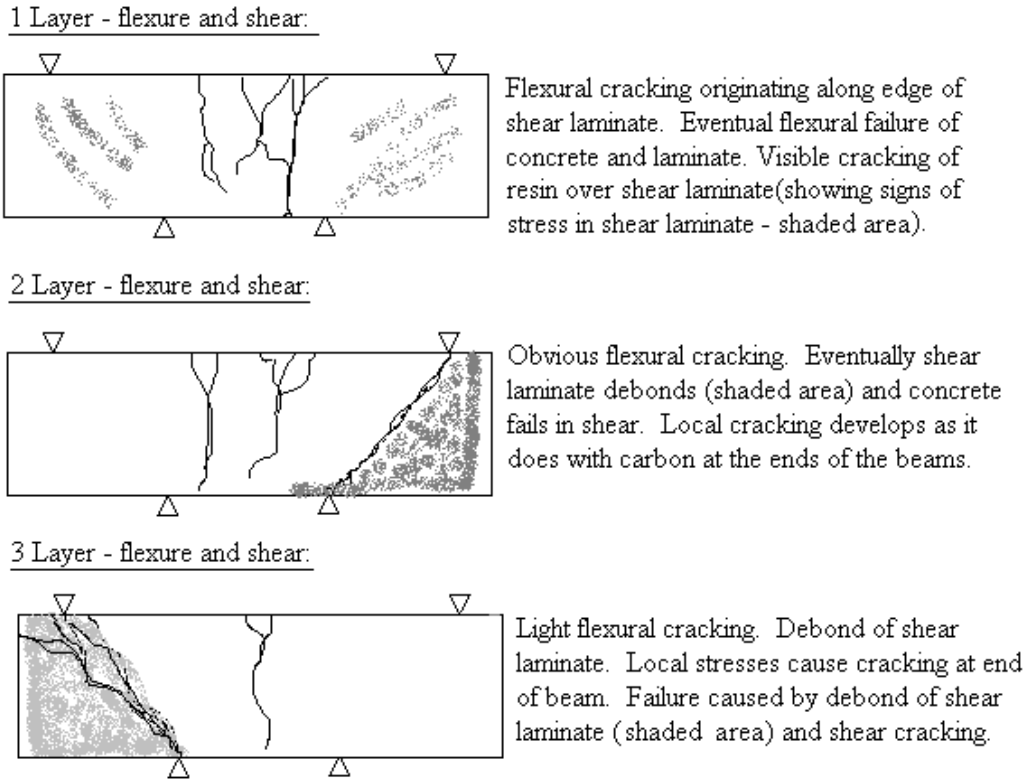

Figure B.8.2.3: Typical cracking and failure modes for beams reinforced with the Tyfo® glass system for flexure and shear.

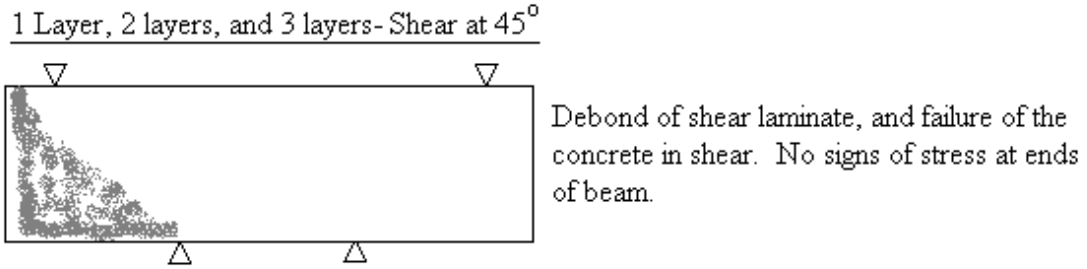

Figure B.8.3.4: Typical failure mode of beams strengthened with the Tyfo® glass system for shear at 45°.

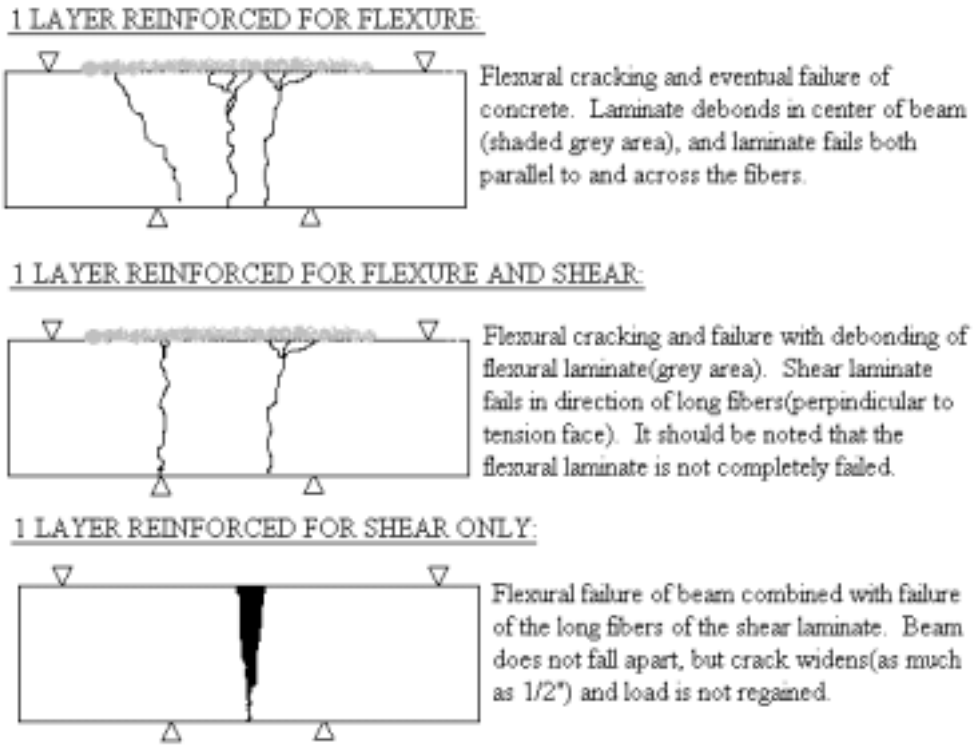

Figure B.9.3: Typical failure modes and cracking for beams reinforced with the Clark Schwebel Structural Grid.

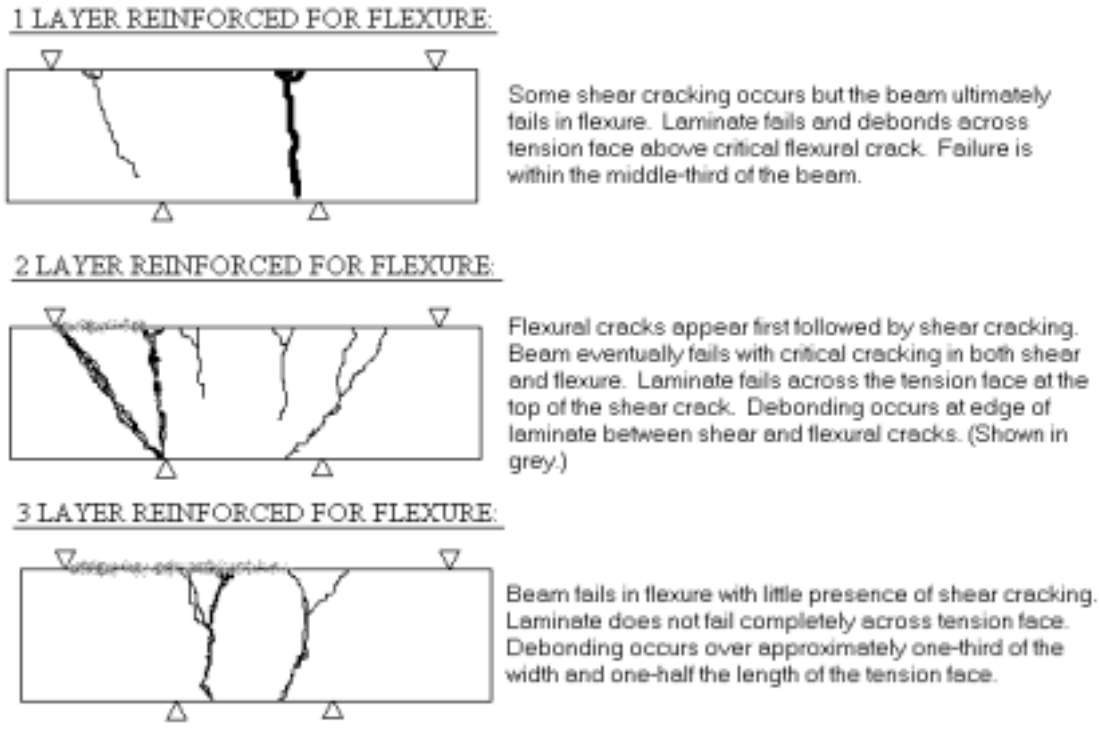

Figure B.10.1.3: Typical failure modes for beams reinforced for flexure with Owens Corning/Reichhold.

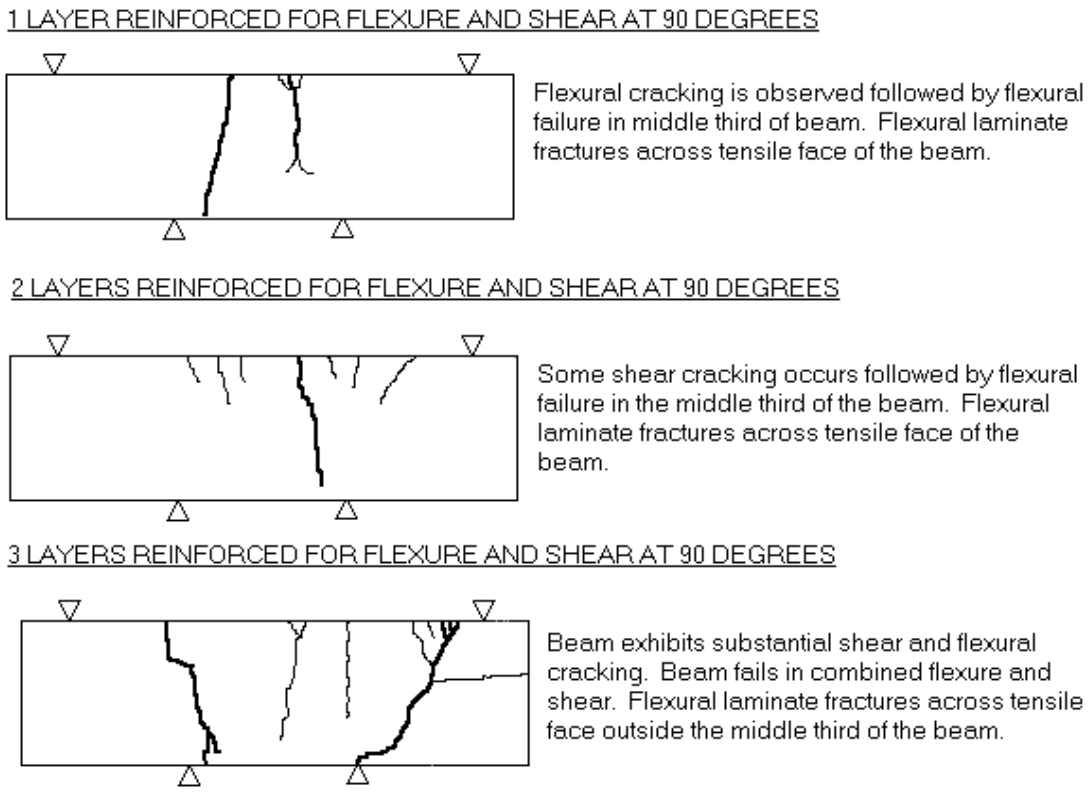

Figure B.10.2.3: Typical failure modes for Owens Corning/Reichhold beams reinforced for flexure plus shear at 90 degrees.

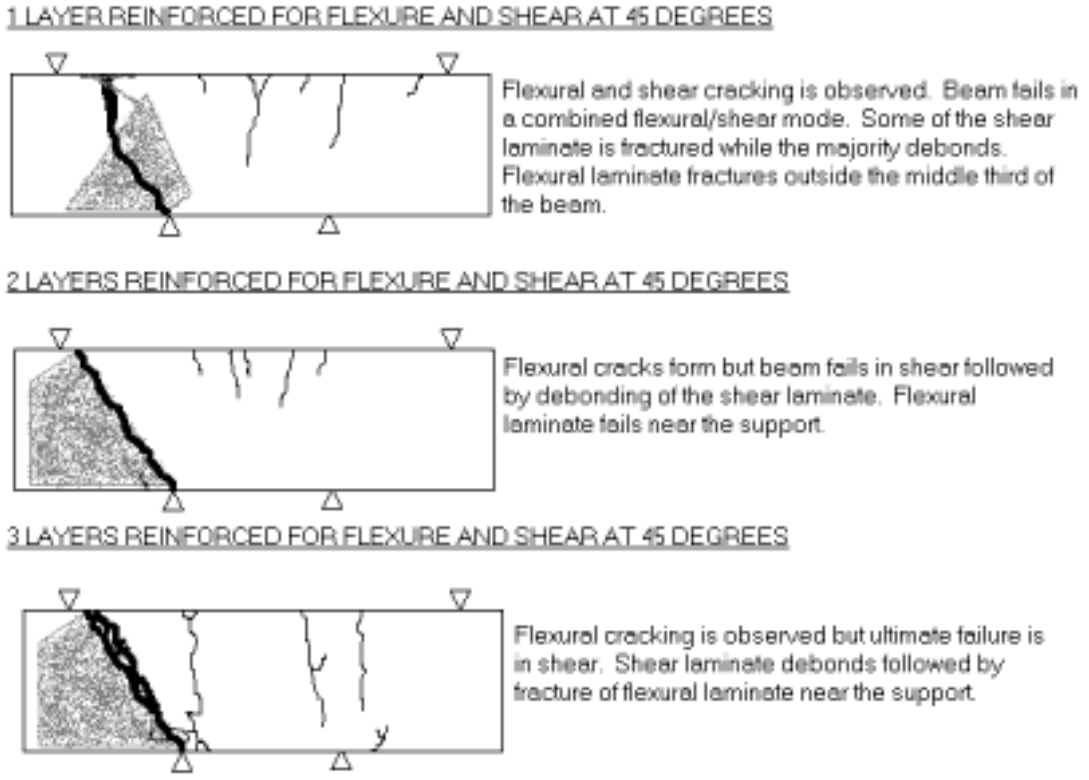

Figure B.10.3.3: Typical failure modes for Owens Corning/Reichhold beams reinforced for flexure and shear at 45 degrees.

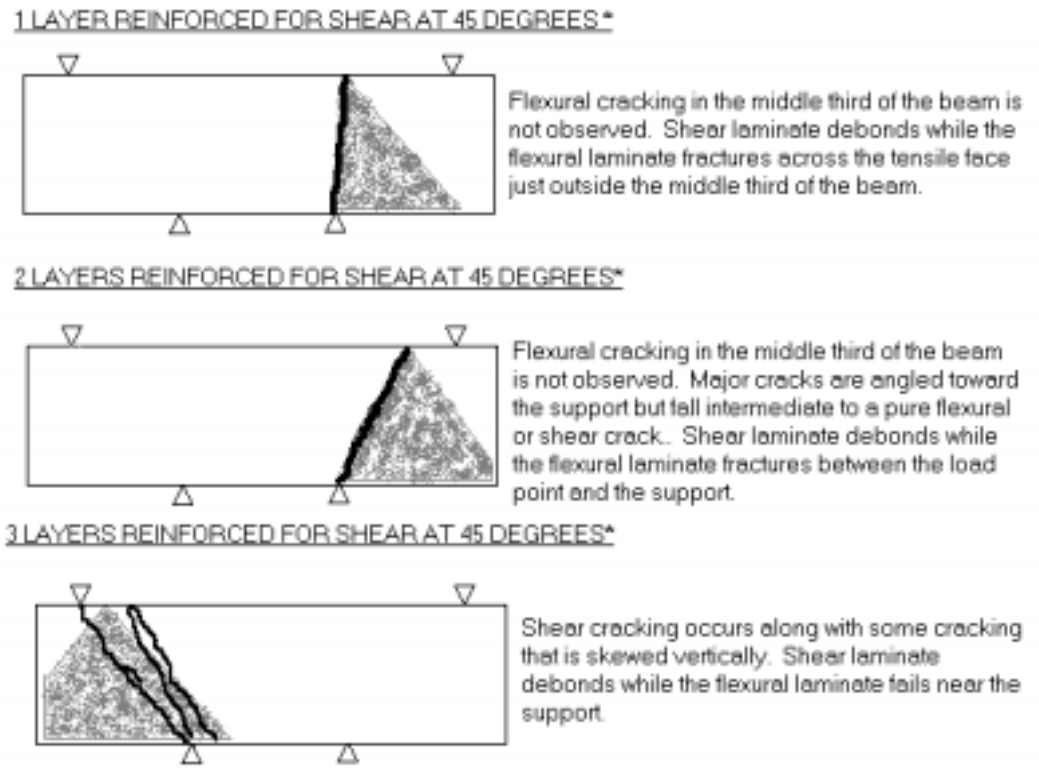

Figure B.10.4.2: Typical failure modes for Owens Corning/Reichhold beams reinforced for shear at 45 degrees.